TERAPIA CELULAR–GÉNICA DE ESCLEROSIS MÚLTIPLE EN UN MODELO MURINO

MARIÉN COBO PULIDO

1 de Diciembre del 2011

Editor: Editorial de la Universidad de Granada
Autor: Marién Cobo Pulido
D.L.: GR 1164-2012
ISBN: 978-84-695-1024-7






Esta tesis ha sido realizada por Marién Cobo Pulido en el Centro Pfizer-Junta de Andalucía-Universidad de Granada de Genómica e Investigación Oncológica, y financiado por un contrato del Fondo de Investigaciones Sanitarias (Instituto de Salud Carlos III) y un contrato financiado por la Fundación Pública Andaluza Progreso y Salud (Consejería de Salud. Junta de Andalucía).

Fdo. Marién Cobo Pulido

AUTORIZACIÓN PARA LA PRESENTACIÓN DE LA TESIS

FRANCISCO MARTÍN MOLINA, INVESTIGADOR PRINCIPAL DEL CENTRO PFIZER-UNIVERSIDAD DE GRANADA-JUNTA DE ANADALUCÍA DE GENÓMICA E INVESTIGACIÓN ONCOLÓGICA, Y PER OLOF ANDERSON, INVESTIGADOR CONTRATADO POR EL PROGRAMA MIGUEL SERVET EN EL MISMO CENTRO,

CERTIFICAN: Que la presente tesis titulada TERAPIA CELULAR-GÉNICA DE ESCLEROSIS MÚLTIPLE EN UN MODELO MURINO, ha sido realizada bajo su dirección por MARIÉN COBO PULIDO, en el programa de doctorado en Inmunología (P42.56.1) y superando el Máter en "Inmunología Molecular y Celular" impartido por la Universidad de Granada.

Revisado el presente trabajo, los directores consideran que tiene la calidad científica necesaria para ser defendido ante el Tribunal que se designe al efecto.

Y para que conste y surta sus efectos en el expediente correspondiente, expedimos la presente certificación en Granada, 24 de Octubre del 2011.

Dr. Francisco Martín Molina

Dr. Per Olof Anderson

ÍNDICE

A. INTRODUCCIÓN

1. Esclerosis Múltiple.

1.1. Definición.

La Esclerosis Múltiple (EM) es una enfermedad autoinmune sistémica que afecta al sistema nervioso central (SNC). En ella se produce una desmielinización que es focalizada al principio, y se vuelve difusa conforme progresa la enfermedad, originando placas en la materia blanca y gris del SNC que cursan con un daño neurodegenerativo y crónico [1].

La EM es una enfermedad muy heterogénea en las manifestaciones clínicas de los pacientes que la padecen.

Existen diferentes formas de la enfermedad:

- *Remitente-recurrente (EMRR.*): Caracterizada por la aparición aguda de síntomas que varían desde horas a días, comenzando por neuritis óptica (inflamación del nervio óptico) que causa deterioro en la visión. En esta fase los síntomas disminuyen o desaparecen espontáneamente, existiendo recaídas o remisiones que aparecen de forma imprevisible. Las Resonancias Magnéticas de pacientes en esta fase muestran que el daño producido en el SNC es permanente, incluso cuando los síntomas han remitido.

- *Secundaria progresiva (EMSP):* La enfermedad cambia a lo largo de los años produciéndose un progreso lento con o sin recaídas. La mayoría de los enfermos en EMRR terminan desarrollando EMSP.

- *Primaria progresiva (EMPP):* Alrededor de un 15% de pacientes presentan un avance crónico desde el comienzo de los síntomas. A menudo comienza con debilidad en las piernas y alteraciones en el andar o en la vejiga urinaria. Es la más severa de las presentaciones de EM.

Aunque la etiología es desconocida, en ella están involucrados mecanismos autoinmunes donde células del propio sistema inmunológico (S.I.), reconocen y destruyen las vainas de mielina que envuelven a los axones de las neuronas del sistema nervioso central (SNC). La enfermedad predomina en el norte de Europa y América y en el este de Australia, así como en el sexo femenino más que en el masculino. Por ello se baraja la hipótesis de la implicación de

infecciones virales, polución, factores alimenticios, de hormonas sexuales o genéticos en su origen [2, 3].

En las primeras fases de la enfermedad predomina la actividad inflamatoria y ésta va disminuyendo progresivamente aumentando la neurodegeneración, la cual va acumulándose a lo largo de la enfermedad. En función de que áreas del SNC se vean dañadas aparecerán unos síntomas u otros. Los más frecuentes son cansancio, visión borrosa o doble, temblor y debilidad en manos y piernas, vértigo y pérdida del equilibrio, incontinencia urinaria, dificultad al caminar y en coordinación y en los casos más severos parálisis [4]. Estos síntomas están relacionados con el daño sufrido por los axones, que impide una correcta transmisión del impulso nervioso [5]. Además de por las manifestaciones clínicas, el diagnóstico se realiza a través de la combinación de RMN (resonancia magnética nuclear) y de exámenes del fluido cerebroespinal.

1.2. Sistema inmunológico en Esclerosis Múltiple.

La EM es considerada una enfermedad autoinmune en la cual, células T antígeno-específicas del SNC, inician una cascada inflamatoria que resulta en daño axonal. El desarrollo de células T en el timo se produce a partir de progenitores sujetos a selecciones positivas y negativas, procesos que darán lugar a una autotolerancia por parte del S.I. mediante la presentación antigénica por parte de las moléculas MHC (complejo principal de histocompatibilidad). A pesar de estos procesos, células T capaces de reconocer autoantígenos, incluyendo antígenos del SNC, como la proteína básica de la mielina (MBP), escapan del timo y se encuentran en la circulación en individuos sanos [6, 7]. Para prevenir los mecanismos autoinmunes otro linaje de células T $CD4^+$ se forma en el timo, denominadas células T reguladoras naturales (nTregs), que expresan el factor de transcripción FoxP3. Estas nTregs previenen la activación de células T autorreactivas. Alteraciones en el número o actividad de estas células están involucradas en procesos autoinmunes [8].

Parece ser que la EM tiene lugar cuando las células T $CD4^+$ y $CD8^+$ que reconocen estos autoantígenos se activan en respuesta a algún estímulo ambiental y entran en el SNC, induciendo la destrucción de la mielina y el proceso inflamatorio[9].

Las funciones de las células T $CD4^+$ son fundamentales en el SI, ya que promueven la respuesta $CD8^+$, ayudan a los linfocitos B y previenen los procesos autoinmunes. Todas estás funciones las puede llevar a cabo tras diferenciarse a células T $CD4^+$efectoras a través de estimulación del TCR (receptor de células T).

El proceso de diferenciación depende de las citoquinas presentes, de manera que IFNγ junto a IL2 induce células T helper 1 (Th1), las cuales participan en la defensa del organismo ante patógenos intracelulares; IL-4 e IL-2, inducen células Th2 encargadas de proteger frente a parásitos; y TGFß, con IL-6 e IL-21, induce células Th17, que protegen frente a patógenos extracelulares y hongos [10-12]. Finalmente, bajo la influencia de IL-10, IL-21, IL-27, de la vitamina D3 y de la dexametasona, las células T $CD4^+$ pueden adquirir funciones reguladoras convirtiéndose en células reguladoras inducidas (iTregs), pudiendo controlar la respuesta inmunológica mediante la producción de IL-10 [13].

Las células Th1 y Th17, juegan un papel importante en al patogénesis de EM, encontrándose en el SNC y promoviendo el ataque a mielina [14]. Las células Th1 producen IFNγ, el cual produce un reclutamiento de macrófagos, mientras que las células Th17, producen citoquinas pro-inflamatorias (IL-17A, IL-17F) que activan a los neutrófilos [10]. Esta acumulación de células T, B, macrófagos y mediadores inflamatorios, activa células propias del SNC, como los astrocitos y la microglía, los cuales promueven los procesos inflamatorios/autoinmunes [9].

Entre los diferentes mecanismos por los que el proceso inflamatorio produce deterioro del SNC están los daños producidos por las células T $CD4^+$ y T $CD8^+$ mediante perforina, FasL, TRAIL y granzymaB (figura 1). Sin embargo es la secreción de citoquinas y quimocinas pro-inflamatorias lo que tiene un efecto más relevante en la patología de EM. Además de producir efectos citotóxicos directos, estos factores producidos por las células T autoreactivas provocan la entrada de macrófagos, granulocitos y microglía. Estas células son capaces de destruir directa o indirectamente a través de mediadores del sistema del complemento. Otros mecanismos involucrados en el daño son la producción de especies reactivas de nitrógeno y oxígeno, y la presencia de receptores de la familia del TNF [15-18].

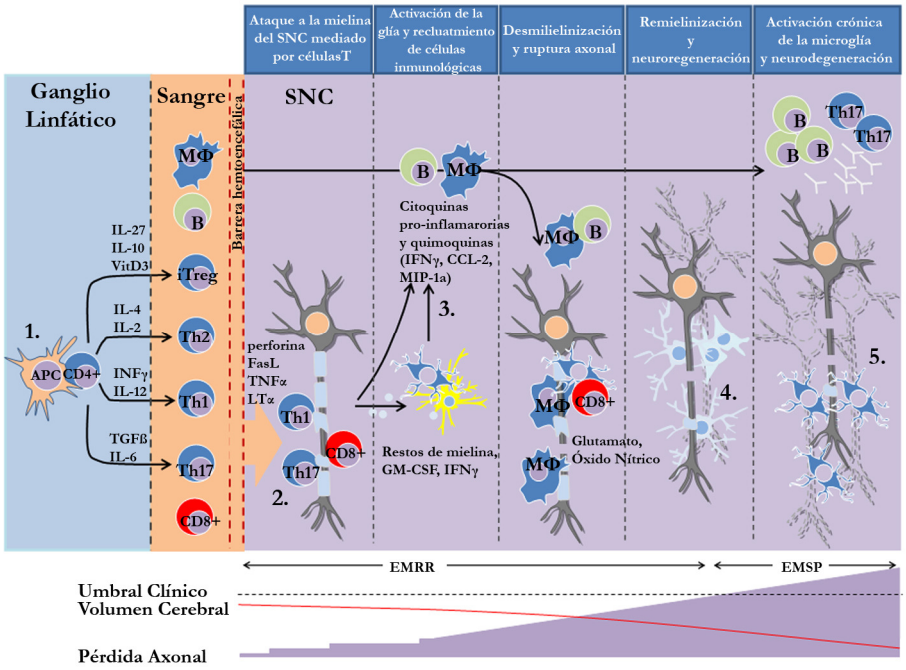

- **Figura 1: Procesos involucrados en daño en el SNC en EM. 1.** Las células T CD4⁺ vírgenes durante la activación pueden diferenciarse a diferentes células T efectoras con distinta función. Las citoquinas juegan aquí un papel decisivo. **2.** Las células T antígeno-específicas del SNC se activan en la periferia y se infiltran en el SNC. Las células T CD4⁺ Th1, Th17 y T CD8⁺, atacan en sitios específicos (focalizados) y destruyen las vainas de mielina que recubren los axones, mediante Fasl, LT-α (Lymphotoxin-α), perforina y Granzyma B. **3.** Los restos de mielina y las citoquinas pro-inflamatorias provenientes de células T activan y reclutan astrocitos y microglía en el lugar de daño. La astroglía coopera con las células T secretando citoquinas y quimoquinas, para reclutar más células inmunológicas en el SNC, incluyendo macrófagos y neutrófilos. **4.** La remielinización de los axones dañados comienza en la fase aguda de la EM. Sin embargo, la reparación no es completa. La transición de EMRR a EMSP se produce cuando la capacidad compensatoria del SNC es excedida, superando el umbral de daño axonal que el SNC es capaz de reparar. Esto conlleva una pérdida irreversible axonal con el desarrollo permanente de síntomas neurológicos. **5.** La forma de EMSP se caracteriza por una activación difusa de la microglía y por un bajo número de células T en el parénquima. Por otro lado, las meninges contienen numerosas células T y células B secretoras de anticuerpos.

1.3. Neurorregeneración del SNC dañado en EM.

La forma de EMRR se caracteriza por períodos agudos de daño seguidos de una recuperación funcional. Cuando el ataque inflamatorio cesa, empieza la etapa de remitencia, y esta fase puede depender de la apoptosis de células

efectoras y la presencia de células reguladoras [19]. La resolución del ataque autoinmune/inflamatorio, la remielinización de los axones dañados y la redistribución de los canales de sodio permite la recuperación total o parcial de los síntomas [20]. Sin embargo, conforme la enfermedad avanza, la reparación de los axones dañados se hace más compleja debido a la presencia de inhibidores del proceso de remielinización, y/o a daños axonales más severos [21, 22].

Cuando esto ocurre los pacientes no recuperan la movilidad perdida durante el ataque y los síntomas se van acumulando entrando en la fase progresiva de la enfermedad (EMSP) [1]. Entre las diferentes teorías de por qué fallan los mecanismos de remielinización en los enfermos de EM, se encuentran, la teoría del fallo en el reclutamiento de OPCs (células progenitoras de oligodendrocitos), y la teoría de la inhibición de la diferenciación de progenitores neuronales por factores existentes en el ambiente de la lesión. En la primera parece ser que fallan los mecanismos de proliferación, migración y repoblación en la áreas de remielinización [23], [24]. La segunda teoría se basa en la existencia en las lesiones de diferentes factores que inhiben la diferenciación de los precursores. En este sentido se han descrito diversos componentes de la mielina y de la matriz extracelular (acido hialurónico), como potentes inhibidores [25, 26] actuando a través de los receptores NgR1 (receptor 1 de Nogo-66). Además PSA-NCAM (poly-sialated neural cell adhesión molecule), expresado en axones dañados, y Lingo1 y jagged1 en astrocitos, son también potentes inhibidores de la diferenciación de OPCs hacia oligodendrocitos remielinizantes.

1.4. Terapia actual para EM.

El Interferón beta (IFN-ß), se ha utilizado como tratamiento principal durante años para la EM, ya que al tener diferentes efectos sobre el S.I., como el de alterar la presentación antigénica, la proliferación de células T y el patrón de expresión de quimoquinas y citoquinas, se puede considerar como un agente inmunomodulador en determinados ambientes inmunológicos. El tratamiento con IFN-ß es más efectivo en EMRR que en EMSP, ya que actúa reduciendo el ritmo de aparición de la fase remitente [27].

Los tratamientos con anticuerpos monoclonales (Natalizumab, Daclizumab Zenapax, Ocrelizumab, etc) actúan bloqueando moléculas expresadas en al superficie de determinadas células del SI (linfocitos T y B activados, NKs o monocitos), impidiendo su migración al SNC, su proliferación o disminuyendo la población de linfocitos B [28]. Otros tratamientos como el Copaxone (Glatiramer acetato) tienen un efecto inmunomodulador, favoreciendo la proliferación de linfocitos Th2 y de células Tregs (T reguladoras) ($CD4^+CD25^+FoxP3^+$) [29, 30]. También se utiliza Mitroxantona, el cual es un agente antineoplásico con efecto inmunomodulador, inhibiendo las células B y reduciendo el número de células T, y es efectivo tanto en EMRR, como en EMSP [4, 31]. En la actualidad, todos los tratamientos aprobados son sólo efectivos en EMRR, siendo sólo parcialmente efectivosen al comienzo de EMSP y sin efecto alguno en enfermos crónicos que cursan la forma EMPP. En EMRR los principales procesos que ocurren son autoinmunes, por lo que aquí son efectivas las terapias encaminadas a inhibir los procesos inflamatorios/autoinmunes. Sin embargo en las formas progresivas, al existir un daño neuronal importante, la terapia debe de incluir factores que favorezcan la remielinización y/o impidan la degeneración neuronal. Por otro lado las terapias aprobadas para EM conllevan una serie de efectos secundarios como la depresión, leucoencefalopatía multifocal y reacciones hipersensibles [31]. Por todo esto se hace necesaria una búsqueda de otras terpias más seguras y eficientes, sobre todo para EMSP.

1.5. Encefalomielitis autoinmune experimental.

La encefalomielitis autoinmune experimental (EAE) es un modelo animal de EM. Fue descubierto por Rivers et al en 1930 [32], al encontrar encefalomielitis con zonas de desmielinización, cuando estudiaban las posibles complicaciones neurológicas que se producían en monos tras la combinación de vacunas virales con extractos de cerebro de conejos. Estos estudios dieron paso a un modelo murino (EAE) donde estudiar Esclerosis Múltiple. En la actualidad se utiliza una combinación de adyuvantes y antígenos de la mielina (en lugar de

lisados completos de cerebro) para activar células T autorreactivas e inducir EAE.

Debido a la heterogeneidad de la EM, no existe un único modelo animal para esta enfermedad. En función del antígeno administrado, de la especie animal (ratón, rata o primate) o de la cepa, se pueden obtener diferentes modelos.Los antígenos utilizados para el establecimiento del modelo de enfermedad son:

- Antígenos de la mielina, MOG (myelin oligodendrocyte glycoprotein), MBP (myelin basic protein), PLP (proteolipoprotein), MAG (myelin associated glycoprotein), MOBP (myelin associated oligodendrocyte basic protein, OSP (oligodendrocyte specific protein), Nogo-A, CNPasa (2´3´-cyclic nucleotide 3´-phosphodiesterare).
- Antígenos de la glía, GFAP (glial fibrillary acidic protein) , αß-cristalina y la proteína S-100.
- Antígenos neuronales, neurofilamentos L y M, neurofascina, contactina-2 y ß-sinucleina.

En función del antígeno usado y de la cepa de ratón los mecanismos inmunológicos implicados en el establecimiento de la enfermedad pueden variar, lo que permite estudiar diferentes tipos o fases de la enfermedad[33]. (Tabla 1).

Cepa de ratón	Antígeno	Aplicación
C57BL/6	MOG, OSP, Nogo	Estudiar patogénesis mediada por linfocitos TCD4+ Th1/Th17; daño en el SNC mediado por linfocitos T CD8+; validación preclínica de posibles tratamientos
SJL/J	MOG, PLP, OSP, Nogo, MOBP	Estudiar los mecanismos que ocurren en la fase remitente en EMRR, desmielinización mediada por anticuerpo, mecanismos autoinmunes o validación preclínica de posibles tratamientos
Biozzi ABH	MOG, MBP, αß-cristalina	Estudiar los mecanismos implicados en la fase de remitencia y desmielinización mediada por anticuerpo y validación preclínica de posibles tratamientos.
B10.PLy PL/J	MBP y MOG	Estudiar las células Tregs, la autotolerancia de linfocitos T y validación preclínica de posibles tratamientos
C3H/Hej	PLP	Estudiar el daño del CNS mediado por las células TCD8+ y autotolerancia de linfocitos T.

Tabla 1: Diferentes modelos murinos para el estudio de diferentes formas o fases de la EM. Mediante la elección de una cepa y un antígeno determinados, podemos estudiar diferentes procesos implicados en la enfermedad.

1.6. Comparación entre EM y EAE.

EAE es el modelo animal más relevante para mimetizar la EM. La mayoría de tratamientos aprobados se han desarrollado en este modelo. Es el modelo prototipo de autoinmunidad mediada por células y parte de diferentes características comunes con EM como son:

i) infiltración de células T CD4 (Th1, Th17) y células citotóxicas T $CD8^+$ en el SNC,

ii) el reclutamiento y activación de macrófagos en el SNC,

iii) la activación de células B que genera anticuerpos específicos contra la mielina,

iv) la existencia de de autoantígenos del SNC (MBP, MOG, PLP),

v) daño axonal y desmielinización cortical,

vi) y componentes genéticos.

A pesar de ser EAE uno de los modelos que mejor imita los procesos que ocurren en EM, muchos de los tratamientos estudiados en él no son efectivos, como son Linomida, mielina oral o anti-CD4, que aumentan los síntomas de la enfermedad, como el IFNγ y el anti TNFα. Otros como IFNß, IVIG (Inmunoglobulina intravenosa), ciclofosfamida, ciclosporina y minociclina tienen efecto tanto en EAE como en EM [34]. Algunos tratamientos actuales de EM como Copaxone, Mitroxantona y Natalizumab se desarrollaron en modelo de EAE [35, 36], por ello existen una serie de diferencias entre ambos a tener en cuenta.

Las mayores diferencias entre EAE y EM son:

i) EAE se induce a través de diferentes cepas susceptibles a este daño en el SNC, o con antígenos específicos del SNC, usando un fuerte adyuvante, mientras que la EM es un proceso espontáneo (de etiología desconocida hasta el momento).

ii) En EAE se suelen utilizar cepas endogámicas mientras que la EM ocurre en una población genéticamente heterogénea [34, 37],

Los estudios realizados en EAE proponían un modelo de enfermedad inflamatoria mediada por respuesta Th1, pero según este modelo existen una serie de contradicciones encontradas en EM. En las lesiones en EAE, predominan infiltrados perivasculares de linfocitos T CD4+, mientras que en EM existe una variedad de lesiones que no siempre cumplen esta característica, encontrándonos con otro tipo que presenta una inflamación mínima o que predomina la oligodendrogliopatía. Además en los pacientes de EM se ve un predominio de células T CD8+ y de macrófagos frente a CD4+[38].

2. Péptido Intestinal Vasoactivo, VIP.

2.1. Descripción.

El péptido intestinal vasoactivo (VIP) es un neuropéptido de 28 aminoácidos, aislado originalmente del duodeno porcino y caracterizado como un potente vasodilatador [39]. Pertenece a la familia de las secretinas y posee alta homología con otros péptidos como son PACAP (pituitary adenylyl cyclase-activating polypeptide), glucagón o PHI/PHM (peptide histidina isoleucine/methionine) y su estructura primaria es idéntica en numerosas especies (humano, ratón, mono, oveja, vaca, rata, cerdo y cabra) [40]. Está ampliamente distribuido en diferentes tejidos y órganos como el cortex cerebral, glándula pituitaria y adrenal, terminaciones nerviosas del sistema respiratorio, tracto gastrointestinal, sistema inmunológico y sistema reproductivo. En el sistema inmunológico es sintetizado por diferentes tipos celulares como son los linfocitos B y T $CD4^+$ (sólo los Th2 tras estimulación antigénica), T CD8+ y en timo los linfocitos doble positivos, basófilos , neutrófilos y eosinófilos [41].

2.2. Estructura.

El péptido de 28 aminoácidos (aas) es el resultado del procesamiento post-trancripcional de su mRNA, el cual da lugar a un primer precursor de 170 aas llamado preproVIP. Este precursor además de dar lugar a VIP, da lugar también a otro péptido de 27 aas llamado PHM en humanos y a PHI en roedores [42] (figura 2).

Su estructura se determinó por RMN y posee una región N-terminal desordenada de unos 6 residuos, seguida de una hélice α de 17 residuos y los restantes en C-terminal de forma helicoidal.[43]

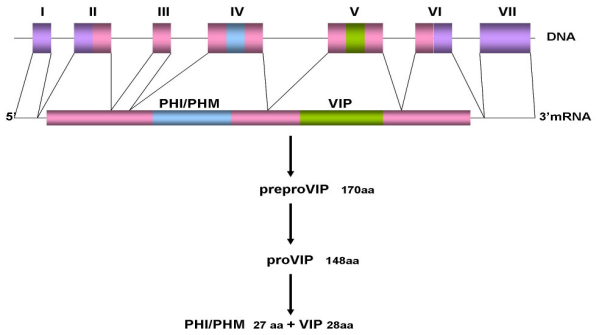

Figura 2: Estructura de VIP. El gen de VIP da lugar a los precursores peptídicos preproVIP y proVIP, que más tarde darán lugar a VIP y a PHI/PHM.

2.3. Receptores de VIP.

VIP posee alta afinidad por sus dos receptores VPAC1 y VPAC2, y algo menos por el receptor de PACAP, PAC1, todos ellos ampliamente distribuidos en diferentes tejidos, en neuronas en SNC y periferia. Está presente en linfocitos y en las inervaciones con los órganos linfoides. Estos receptores pertenecen al grupo II de los receptores acoplados a proteínas G (GPCRs) [44, 45]. Aunque los 3 receptores pueden actuar por ambas vías, VPAC1 y VPAC2 normalmente están acoplados a la estimulación de la adenilato ciclasa (AC) y ruta de transducción vía proteína quinasa A (PKA) con liberación de cAMP, mientras que PAC1 está acoplado preferentemente a proteína quinasa C (PKC) [46].

Los receptores VPAC se expresan en macrófagos y células T, y en menor cantidad en células dendríticas, basófilos y neutrófilos. VPAC1 se expresa constitutivamente en macrófagos y en células T estimuladas y no estimuladas. VPAC2 no se expresa en células T en reposo, pero tras la activación del TCR se estimula su producción, mientras que la expresión de VPAC1 disminuye. A través de sus receptores, VIP modula la diferenciación de las células T CD4+.

La unión de VIP a VPAC2 en células T, favorece la diferenciación a células Th2, la producción de citoquinas como IL-4, IL-5 e IL-13, y bloquea la diferenciación a Th1. También en células T, pero a través de VPAC1, favorece la diferenciación de Th17. En cambio, en células presentadoras de antígeno (APCs), la unión de VIP a VPAC2 induce un fenotipo regulador capaz de inducir el cambio de células T a Tregs con la consiguiente expresión de TGF-ß e IL-10 y disminución de las Th17[47].

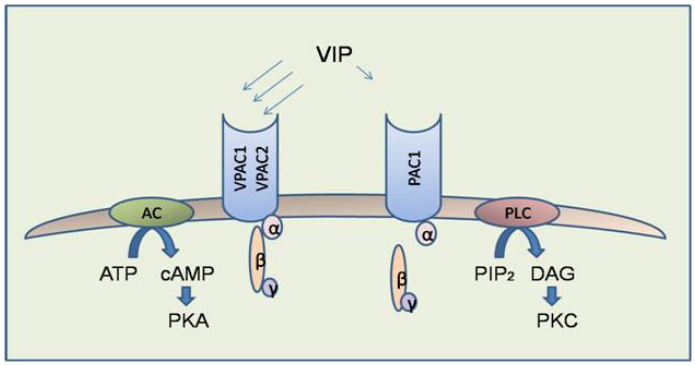

Figura 3: Receptores utilizados por VIP. Pueden estar asociados a vías dependientes o independientes de cAMP.

2.4. Funciones/actividad de VIP.

Originariamente se caracterizó como vasodilatador responsable de bajar la tensión sanguínea [39]. Pero hoy en día se conocen otras funciones como la de mediador de adhesión, migración, producción de citoquinas, proliferación y supervivencia de diversos tipos celulares. Los macrófagos, linfocitos T, basófilos, células glandulares, epiteliales o de músculo liso son capaces de responder a VIP. Todo esto le permite actuar como modulador tanto de la respuesta inmunológica innata como adaptativa, predominado su activad anti-inflamatoria. Las diferentes funciones de VIP dependen no sólo del ambiente o tipo celular sobre el que actúe, sino también a través de que receptor lo haga.

2.4.1. Papel de VIP como agente anti-inflamatorio e inmunomodulador.

Ante la presencia de un patógeno externo, un primer ataque es llevado a cabo por los macrófagos, los cuales inician la inflamación mediante la producción de agentes pro-inflamatorios como son, TNFα, IL-12, IL-1, IL-6, y NO (óxido nítrico), seguido de la producción de agentes anti-inflamatorios como IL-10 o TGFß. En este entorno VIP es capaz de inhibir la respuesta inmunológica innata llevada a cabo por los macrófagos, la microglía y células dendríticas activados, que secretan diferentes factores pro-inflamatorios (citoquinas, quimoquinas, y especies reactivas de oxígeno)[48, 49], inhibiendo NFkB (figura 4) [50], y estimulando la producción de IL-10 y IL-1Ra [51, 52].

VIP actúa sobre la respuesta adaptativa reduciendo la capacidad coestimuladora de las células presentadoras de antígeno, induciendo preferentemente una respuesta tipo Th2 e inhibiendo la respuesta Th1[53]. VIP induce CD86 en macrófagos en reposo y CDs inmaduras, promoviendo la respuesta tipo Th2 [54].

VIP es capaz de inducir mecanismos de inmunosupresión mediante la generación de células Tregs, a través de la inducción de células dendríticas tolergénicas [55]. Para ello actúa inhibiendo la expresión de moléculas coestimuladoras como son CD40, CD80 y CD86, por lo que en la presentación antigénica dan lugar a poblaciones T anérgicas o Tregs [56-58]. En macrófagos activados inhibe la expresión de CD80 y CD86 sin afectar a MHC-II ni a CD40, y en microglía inhibe la expresión de CD86 y CD40[59].

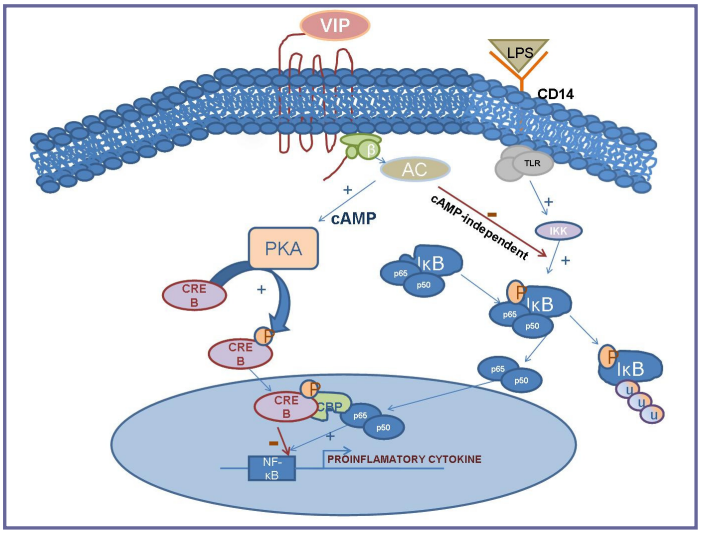

Figura 4: Esquema de la ruta de actuación de VIP. Inhibición de expresión de citoquinas proinflamatorias, mediante inhibición de NFkB, desencadenada por la unión de VIP a sus receptores, mediante vías de actuación dependientes e independientes de cAMP.

2.4.2. Papel de VIP en neuroprotección.

En las enfermedades neurodegenerativas, las células primeras causantes del daño son las de la microglía, las cuales actúan como células presentadoras del antígeno, activando la respuesta inmunitaria adaptativa, así como secretoras de moléculas pro-inflamatorias y reactivas de oxígeno, causantes directos del daño

a células como oligodendrocitos en el SNC. VIP actúa como factor neurotrófico, siendo capaz de inhibir la producción de estos mediadores pro-inflamatorios por la microglía y los macrófagos inactivando estos tipos celulares, e inhibiendo por tanto la neurodegeneración inducida por beta-amieloide [60].

Además actúa directamente sobre los astrocitos estimulando la secreción de factores neuroprotectores como son ADNP (activity-dependet neuroprotective protein), ADNF (activity-dependent neurotrophic factor) y BDNF (brain-derived neurotrophic factor) [40, 61-63].

2.5 Aplicación de VIP en modelos murinos de enfermedades autoinmunes.

A nivel de administración sistémica del péptido, se han realizado estudios en diferentes modelos murinos de enfermedades autoinmunes e inflamatorias, donde se han encontrado tanto inhibición de la respuesta Th1 y/o generación de células Tregs, demostrando un efecto terapéutico, en modelos de choque séptico, artritis reumatoide, diabetes autoinmune, uveoretinitis autoinmune, enfermedad inflamatoria intestinal y esclerosis múltiple [64-71].

Aunque los tratamientos con el VIP péptido son muy prometedores existen una serie de desventajas. La principal es la susceptibilidad de ser degradado por peptidasas. VIP es un péptido tan inestable que para tener un efecto terapéutico se hace necesaria la administración diaria de una concentración elevada, para que llegue una dosis terapéutica al sitio de acción de éste. Además estas dosis no son efectivas en todos los grados de enfermedad, por ejemplo en el modelo de artritis reumatoide inducida por colágeno, sólo se tenía efecto hasta el grado 4 (0 a 16)[71]. Por ello en nuestro laboratorio se ideó una estrategia de terapia génica, mediante la administración de un vector lentiviral expresando VIP para su aplicación en un modelo de artritis reumatoide inducida por colágeno (CIA). Con esta estrategia fuimos capaces de prevenir y revertir totalmente la enfermedad, incluso en grados elevados de ésta [72]. En el caso de EAE, sólo se ha observado beneficio terapéutico consistente de administración sistémica de VIP en uso preventivo o en el inicio de la enfermedad [66, 73, 74].

3. Células madre mesenquimales MSC.

3.1. Origen y características

Las células madre mesenquimales (MSCs), son células madre adultas no hematopoyéticas, caracterizadas por poseer una adherencia plástica, potencial de diferenciación a osteocitos, adipocitos y condrocitos y presentar un determinado panel de moléculas de superficie. Fueron descritas en médula ósea por primera vez por Friedenstein y colaboradores [75], aunque están distribuidas en diferentes tejidos (tejido adiposo, médula ósea, tejido mamario, sangre de cordón o sangre periférica, tejido amniótico, tendón o ligamento, membranas sinoviales, mucosa olfativa, pulmón, hígado fetal, bazo,…)[76].

Entre los marcadores de expresión característicos de las MSCs se encuentran, CD29, CD44, CD51, CD73, SCA1, CD105, CD166 y Stro-1, pero su mayor o menor expresión es muy dependiente del microambiente y tejido en el que se encuentren estas células. Como marcadores negativos se encuentran algunos hematopoyéticos y endoteliales como son, CD11b, CD14, CD31 y CD45[77].

Las MSCs son células multipotentes capaces de diferenciarse a cualquiera de los linajes del mesodermo como son, cartílago, hueso o tejido adiposo. Pero con el tiempo se ha visto que además son capaces de dar lugar a otros tipos de linajes celulares como músculo esquelético, tendón, ligamento, tejido nervioso, cardiomiocitos o epitelio[78-80].

Aunque las células MSCs humanas (hMSCs) son fáciles de aislar, el análisis de sus potenciales aplicaciones (actividad terapéutica) y características (migración, inmunomodulación, etc) requieren de modelos animales. Las células hMSCs tienen propiedades muy similares a las MSC de otras especies como ratón (mMSCs)[81, 82] o rata (rMSCs) [82] en lo que se refiere a la morfología, marcadores y funciones principales. Sin embargo existen algunas diferencias que hay que tener presentes cuando se trasladan los resultados obtenidos en modelos animales a lo que ocurriría en humanos. Meseil y colaboradores [83], han descrito que las células hMSCs, tras estimulación inflamatoria combinada con microbiana, activan la vía de degradación del triptófano (Trp), mediante la enzima IDO (indoleamina 2,3-dioxygenasa). Sin embargo, cuando sometían al mismo estímulo

células MSCs murinas, esta vía permanecía inalterada, mientras que se activaba iNOS (óxido nítrico sintasa inducible), la cual no se ve afectada en humanas.

3.2. Capacidad migratoria.

Las MSC son células que además de tener características de células madre adultas con capacidad de diferenciación, poseen otras propiedades que las hacen muy interesantes para su uso en terapia, como son la capacidad especifica de migrar hacia un tumor o a un sitio dañado y actuar como células inmunomoduladoras/secretoras una vez allí [84]. Tanto en los tumores como en un lugar inflamado se generan una serie de mediadores inflamatorios como citoquinas, quimoquinas y otras moléculas quimoatrayentes [85]. La existencia de un ambiente hipóxico (baja tensión de O2), activa determinados factores de transcripción, que dan lugar a la expresión de estos mediadores inflamatorios por células residentes produciéndose la infiltración de células del SI así como de MSCs en el sitio inflamado [86-88]. Esto se debe a la expresión de diferentes marcadores de superficie implicados en migración (como receptores de citoquinas y quimoquinas, así como moléculas de adhesión) que poseen las MSC en común con las células del S.I. Entre los receptores de citoquinas/quimoquinas que expresan las MSCs están CCR1-10, CXC1-6, CXCR1 y XCR1. También expresan moléculas de adhesión como VCAM-1 (VLA-4), ICAM-1/-3, ALCAM, Endoglina (CD105), TLR1. [89]

3.3. Capacidad inmunomoduladora.

Las MSCs son capaces de modular tanto la respuesta inmune adaptativa como la innata alterando el patrón de secreción de citoquiinas en células dendríticas (CDs), células T vírgenes y efectoras y células NK, induciendo un fenotipo anti-inflamatorio y/o tolerogénico [90]. En concreto las MSCs inducen la reducción de secreción TNFα en las CDs tipo 1 y el incremento de IL10 en CDs tipo 2. En la misma línea de acción inhiben la secreción de IFNγ en células Th1 y NKs e inducen la secreción de IL4 por células Th2. Por otro lado incrementan la proporción de células T supresoras, aunque este punto está menos claro.

El efecto de las MSCs sobre las células del sistema inmunológico puede involucrar interacción directa célula-célula o la secreción de factores solubles [91, 92]. En presencia de un ambiente pro-inflamatorio (IFNγ y TNFα), se inducen en las MSCs diversos mecanismos de inhibición de la respuesta inmunológica (figura 5):

- *Células T.* La inhibición de la respuesta T parece estar mediada principalmente por factores solubles [93, 94] como PGE2, IDO, NO, TGFß y HGF [83, 95, 96].
- *Células dendríticas.* La maduración de las CDs juega un papel fundamental en la activación de la respuesta T. Existen evidencias de que las MSCs inhiben las tres funciones principales que caracterizan el proceso de maduración de las CDs[97]: 1- La capacidad de presentación antigénica, 2- la expresión de moléculas co-estimuladoras y 3- la capacidad de migración a CCL19[90].
- *Células NKs.* Se ha demostrado que las MSCs inhiben la proliferación y la actividad lítica de las NKs mediante mecanismos que involucra IDO, PGE2 y TGFß [98]
- *Linfocitos B.* Se ha visto que las MSCs son capaces de inhibir su proliferación en presencia de IFNγ.

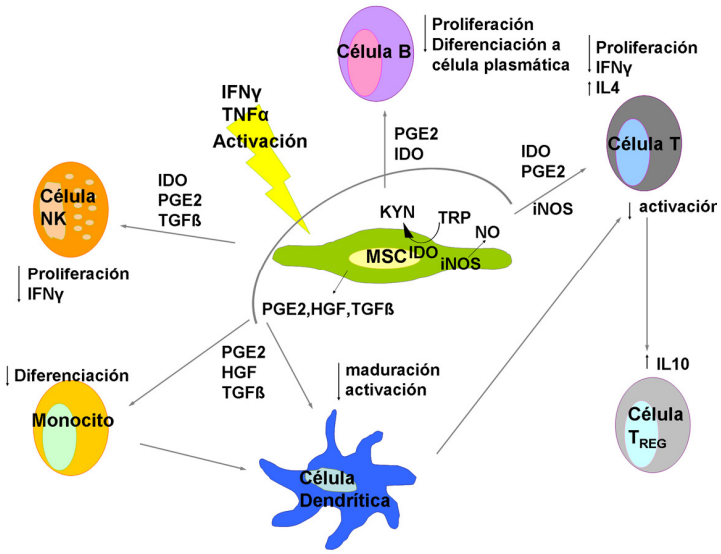

Figura 5: Mecanismos de inmunomodulación de las MSCs. Tras activación por un ambiente pro-inflamatorio, actúan inhibiendo las respuestas, NKs, B y T, mientras que favorecen la población Tregs.

3.4. MSCs y sus efectos en neuroprotección.

No están claros los mecanismos por los cuales las MSCs son capaces de mejorar la función neuronal [99]. Existen diversas teorías que incluyen la capacidad de las MSCs de transdiferenciarse a diferentes tipos celulares del SNC. Sin embargo es actualmente aceptado que la practica totalidad de los beneficios descritos se deben a la secreción de diferentes moléculas involucradas en reparación y protección neuronal [100].

Los estudios *in vitro* muestran que, en un ambiente pro-inflamatorio, las MSCs actúan sobre la microglía activada haciendo que ésta secrete factores neurotróficos como el brain derived neurotrophic factor (BDNF) y Nerve growth factor (NGF), que ayudarían a la remielinización de los axones por los oligodendrocitos. Además, la inoculación de MSCs en el hipocampo de ratones inmunodeficientes promueve la neurogénesis aumentando la secreción endógena de factores tróficos como vascular endotelial growth factor (VEGF), ciliary neurotrophic factor (CNTF), fibroblast growth factor 2 (FGF-2) y B lymphoma Mo-MLV insertion region 1 homolog (BMI-1) [101].

Además se ha visto la capacidad de dar lugar *in vitro* a células neuronales, ya sea bien por adición de cocktails químicos al medio[102-104] o por cocultivo con células neuronales [105, 106]. Sin embargo, son actualmente muy pocos los resultados que apoyen que las MSCs, tras su administración en animales o en pacientes, estén diferenciándose a componentes del SNC y ejerciendo un efecto positivo debido a este potencial.

3.5. Terapia celular de EAE con MSCs.

Dadas las características mencionadas anteriormente de las MSCs, es lógico pensar que pudiesen tener un efecto terapéutico en enfermedades como la EM, donde existe un componente inflamatorio y neurodegenerativo. Por ello se han realizado numerosos estudios en el modelo de EAE, estudiando la eficiencia y viabilidad de las MSCs como alternativa terapéutica para EM. Los diferentes trabajos han mostrado que las MSCs son capaces de prevenir el desarrollo de la enfermedad cuando se inoculan vía sistémica (intraperitoneal o intravenosa)

tanto en modelos de remitencia-recurrencia como en modelos crónicos[107] [108].

Otros autores demostraron que el efecto preventivo de las MSCs venía acompañado de secreción de PGE2[108] y que era necesaria la secreción de CCL2[93]. Además de su efecto preventivo, la administración de MSCs puede llegar a revertir el desarrollo de la enfermedad en modelo de RR tanto si se administran cuando comienzan los síntomas[108]como si se administran en fase crónica [109]. Sin embargo, en el modelo de EAE crónico, el efecto de las MSCs está menos claro y sólo tras 2 inyecciones consecutivas y en un modelo poco severo (máximo grado de enfermedad = 2.5), se logró efecto terapéutico claro[109].

Todos estos estudios han demostrado que las MSCs tienen un efecto terapéutico en EAE mediante la supresión del sistema inmunológico en las fases tempranas de la enfermedad e induciendo neurorregeneración local por pregenitores endógenos en fases tempranas y en modelos poco severos de la enfermedad [109].

3.6. Terapia celular génica con MSCs.

A pesar de su potencial, existen varias propiedades de las MSCs que podrían mejorarse con la finalidad de lograr mejores beneficios terapéuticos. Una opción es su modificación génica para incrementar sus efectos inmunomoduladores y neuroprotectores o su capacidad migratoria[110]. El desarrollo de estrategias de terapia génica usando como vehículo las MSCs, supone un método altamente eficaz para la distribución de la expresión del gen terapéutico.

Entre los diferentes ensayos en los que se han usado estas células como vehículo de un gen terapéutico se encuentran, MSC/IFNß, para tratamiento de melanoma, mama, y pulmón [111-113], MSC/IL10, para prevención de daño isquémico en pulmón [114], MSC/neurotrophin-3, MSC/BMP-9, MSC/BMP-2, para mejorar la reparación espinal [99, 115, 116], MSC/angiopoietin-1, MSC/P1GF, para mejorar la isquemia cerebral [117, 118], MSC/CXCR4, para la mejora de recuperación tras un infarto de miocardio [119], MSC/TGFß1 y MSC/BMP-2, para ayudar a la reparación de cartílago [120, 121], MSC/BDNF,

para promover la recuperación funcional y reducir la probabilidad de infarto [122]., MSC/CNTF, para promover la mielinización y reducir la inflamación en enfermedades neurodegenerativas [123].

3.7. Ensayos clínicos con MSCs en EM.

Dado los resultados preclínicos obtenidos en el tratamiento de EAE en diferentes modelos con MSCs, tanto en vía intravenosa [124, 125], intraventricular (intratecal) [125] e intraperitoneal[93], es razonable plantearse su uso clínico en humanos. Puesto que los procesos actuales no permiten el aislamiento de suficientes MSCs para su uso directo en clínica, es necesaria su expansión *in vitro*. En experimentación animal la dosis usada es de 40-80 x 10^6 células/kg, mientras que en ensayos humanos es de 2 x 10^6 células/kg. Para su uso en estudios clínicos el Comité del grupo Europeo de Transplantes de Sangre y Médula (EBMT) ha establecido una serie de criterios encaminados a estandarizar los protocolos de expansión de las MSCs [126].

En la mayoría de los ensayos, las células MSCs son obtenidas de médula ósea e inoculadas vía intravenosa (i.v.), recomendándose una expansión mínima para evitar transformaciones. En la actualidad existen diferentes ensayos clínicos con MSCs que se están llevando a cabo, pero en la mayoría se desconocen aún los resultados. En china, Yun Xu está al frente de un ensayo en el que utilizan MSCs de cordón umbilical para el estudio en fases I/II de enfermos de EM en fases progresivas y con neuromielitis óptica. En España se están realizando dos, uno de ellos en Barcelona (Albert Saiz) y otro en Sevilla y Málaga (Guillermo Izquierdo Ayuso). El primero es en fase II de las diferentes formas de EM (RR, SP y PP), con grados clínicos comprendidos entre 3 y 6,5 (con capacidad para caminar) inoculando 2x10^6células/kg. El ensayo de Sevilla/Málaga es en fase I/II en enfermos que cursan SP con grados entre 5,5 y 9 (con limitaciones para caminar o en sillas de ruedas) y utilizan dos dosis diferentes (1x10^6células/kg y 4x10^6células/kg) de MSCs de tejido adiposo. En EEUU (Cleveland), Jeff Cohen está llevando a cabo otro estudio para ver en fase I el efecto de la inoculación i.v. de 2x10^6células/kg, de enfermos que estén en las tres formas de EM en la fase de recaída, en grados entre 3 y 6,5. Otro estudio en Irán, comprende en fase I/II, el

estudio del efecto terapéutico de la inoculación i.v. de MSC a pacientes en fase RR (grados comprendidos entre 3 y 6,5) [127].

Aunque los estudios clínicos no están aun terminados y ni publicados, parece ser que el primer enfermo tratado en Cleveland ha recuperado parte de la movilidad de su pierna izquierda, pero hay que esperar aún los resultados del resto de pacientes tratados para confirmar que efectivamente es debido al tratamiento y no a una recuperación espontánea del al enfermedad.

4. Terapia génica.

La terapia génica consiste en la suplementación de un producto génico defectuoso, mediante la transferencia de una nueva copia funcional del gen dentro de la célula afectada, con el objetivo de corregir el error génico. Sin embargo, actualmente el concepto de terapia génica va más allá, incluyendo transferencias génicas para proveer a la célula de nuevas funciones (como la inserción de genes inmunoestimuladores, o inmunosupresores), transferencias de tipo preventivas y aquéllas que contribuyen a la investigación médica.

4.1. Vectores.

El vector es la herramienta necesaria para introducir el material genético en las células deseadas, denominadas células diana, que serán modificadas por el mismo. Las células diana pueden ser células afectadas por una patología concreta, células pluripotenciales, células del sistema inmunológico, células de tejidos normales que pueden actuar como "fábrica" de proteína/s necesaria/s, de la/s que se carece. Cuando hablamos de vectores hemos de tener en cuenta dos factores determinantes: bioseguridad y eficiencia[128, 129].

En este punto hemos de distinguir entre vectores no virales (Liposomas, Policationes, ADN desnudo y Conjugados moleculares) que nos aseguran la bioseguridad, y vectores virales (Retrovirus simples, Lentivirus, Adenovirus, AAV (Adeno-Asociated-Virus) y Herpes virus) que se caracterizan por su eficiencia.

De entre todos estos vectores, los únicos integrativos son los basados en retrovirus (gammaretrovirus, Lentivirus y Foamy virus). Cuando se busca una expresión estable del transgén se requiere una integración del vector, sobre todo si las células se dividen activamente. Además, si se pretende desarrollar líneas celulares expresando un gen terapéutico (tal es el caso de la presente tesis) es mucho más práctico y eficiente modificar genéticamente un número pequeño de células y después proceder a su expansión. Si en este caso se pretendiera utilizar vectores no integrativos deberíamos modificar genéticamente todas las células que vamos a inocular, haciendo el proceso mucho más tedioso y difícil de conseguir.

Las características principales de lo retrovirus son [130, 131]:

1-La captación de las células diana se produce por una interacción de alta afinidad entre una proteína de la cubierta del virus y un antígeno de superficie de la célula diana. Los retrovirus tienen la capacidad de integrar en su envuelta, proteínas de distinto origen, captadas de la membrana de la célula diana tras la liberación de las partículas virales (tropismo del virus). Este proceso denominado pseudotipaje, da gran versatilidad al virus y a su vez ha sido utilizado para generar vectores con proteínas alternativas capaces de reconocer receptores de distintos tipos celulares [130, 132, 133].

2-El genoma viral consta de dos cadenas simples de ARN, que ha de ser liberado en la célula diana, para que sea transformado en una doble molécula de ADN por reverso transcripción. Esta doble molécula de ADN se integra en el genoma celular para generar un ciclo infectivo activo o puede mantenerse latente hasta que se den los factores ambientales que desencadenen un nuevo ciclo infectivo. Por lo que los vectores retrovirales permitirían una expresión estable del transgén en la célula diana y en su progenie [131, 134].

3-Existen tres genes que son requeridos para replicación del virus: *gag* (codifica para las proteínas de la matriz, cápsida y nucleocápsida del virus), *pol* (codifica para la proteasa, reversotranscriptasa e integrasa) y *env* (codifica para las glucoproteínas de la envuelta necesarias par la unión a las células diana). Estos genes pueden ser aportados en *trans*, de modo que el genoma del vector retroviral solamente expresa el gen terapéutico, aunque contiene secuencias requeridas en *cis* necesarias para empaquetamiento, integración y transcripción en reverso del vector. Estas secuencias tienden a minimizarse para evitar el riesgo de

recombinación homóloga entre los elementos aportados en *trans* y el vector [131, 134].

De entre los vectores retrovirales los más eficientes y seguros actualmente son los lentivirales.

4.2. Vectores lentivirales.

Dentro de la familia *Retroviridae,* los lentivirus son interesantes en el contexto de que son capaces de infectar células que no están en división (arrestadas en el ciclo celular) [135], debido a que su complejo de preintegración les permite penetrar la membrana nuclear.

Las primeras generaciones de vectores lentivirales (LVs) contenían todas las proteínas virales excepto las de la envuelta. Más tarde se fueron seleccionando otros genes como Vpr, Vif, Vpu y Nef [136], viéndose que no afectaba a las propiedades del vector. El sistema utilizado en la actualidad aporta los genes necesarios para las proteínas virales en *trans* en otros plásmidos, como son, rev (proteína necesaria para exportar el mARN del núcleo), gag, pol, env y tat (proteína reguladora de la transcripción del ADN viral). Gracias a la aportación en *trans* evitamos la reconstitución del virus original por recombinación homóloga. . Para producir los vectores se requieren un mínimo de tres plásmidos de expresión que expresen los diferentes componentes de la partícula viral: la cápsida (genes *gag-pol*), la proteína de la envuelta (gen *env*) y el ARN genoma que va a ser empaquetado conteniendo el gen terapéutico (figura 6). Estos plásmidos son transfectados a una células empaquetadoras (293T) que hacen de fábrica de las partículas virales recombinantes (figura 6, células azules). Estas células empaquetadoras ensamblan todos los componentes del vector y forman partículas que salen al medio por envaginación de la membrana. Este medio conteniendo las células se puede usar para modificar las células diana (figura 6, célula verde).

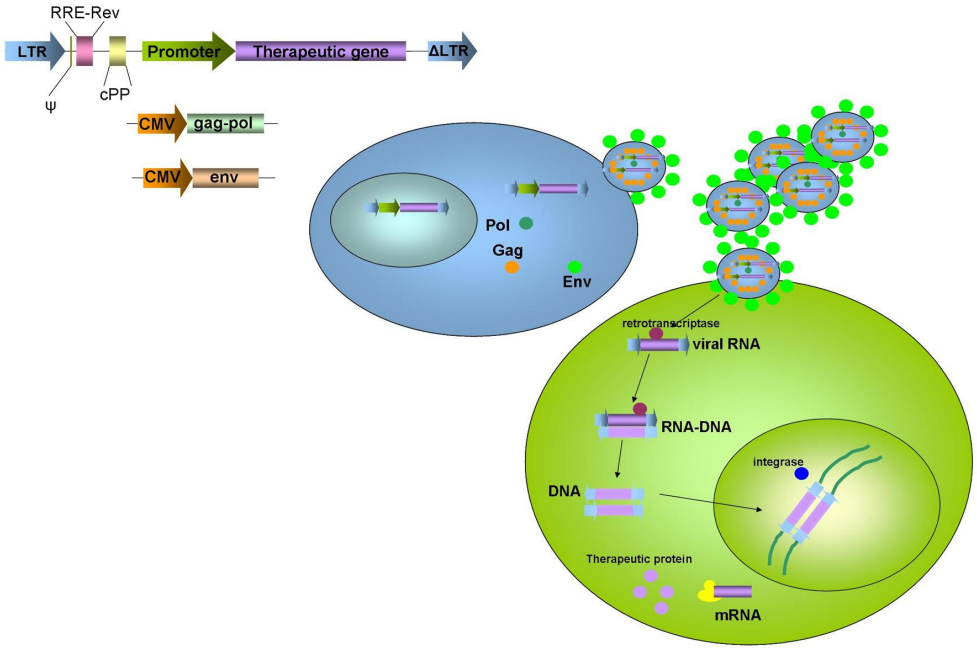

Figura 6: Producción de vectores lentivirales y transducción de la célula diana. Mediante una célula empaquetadora generamos las partículas por cotrasfección con diferentes plámidos. Los sobrenadantes contienen las partículas virales para translucir la célula diana.

4.3. Bioseguridad de los vectores lentivirales.

La inserción del material génico en el cromosoma de las células diana puede producir alteraciones en el patrón de expresión génica que causen trasnformación celular (genotoxicidad). Como todos los vectores retrovirales, los lentivirales tienen preferencia de inserción en zonas cercanas de cualquier gen activo, sin embargo se diferencian de los gammaretrovirales en que no favorecen integraciones cerca del sitio de inicio de transcripción, disminuyendo así su genotoxicidad.

4.3.1. Vectores autoinactivables.

Mediante modificaciones del genoma de los vectores lentivirales se han logrado mejoras en la bioseguridad de los mismos por escisión de diferentes genes virales, que simplemente se eliminan o son aportados en *trans*. Los genes *rev* y *tat* son genes reguladores fundamentales para la replicación del HIV, sin

embargo se ha visto que la presencia de un promotor constitutivo que sustituya a la región U3 del LTR en 5' hace prescindible a *tat*. [137].

Uno de los avances en bioseguridad más significativo fue el diseño de vectores autoinactivables (SIN). Esto se logra truncando el U3 del LTR en 3´, de modo que tras la reverso-transcripción e integración en el ADN celular, este U3 no podrá actuar como promotor. Este tipo de vectores, además de impedir que las células diana expresen de nuevo el ARN del vector completo (con la señal de empaquetamiento), permite el diseño de vectores de expresión tejido específico mediante la introducción de diferentes promotores río abajo del LTR 5'. [130, 134, 135, 138, 139].

4.3.2. Expresión regulable por drogas.

El sistema TetOn, es un ejemplo de cómo regular la expresión de un transgén mediante la adición de una droga[140]. La activación controlada por tetraciclina es un método de expresión inducible que permite encender o apagar la expresión de un gen por la presencia del antibiótico tetraciclina o su análogo no tóxico, doxiciclina. Para ello se introducen elementos en la región promotora que permiten este tipo de regulación. En nuestro grupo hemos estado trabajando con el sistema basado en el uso del represor original TetR [141].

1- Un promotor expresando un represor (TetR),

2- Una zona operadora (TetO).

El sistema TetOn desarrollado en nuestro laboratorio se basa en un sistema dual o único que contiene por un lado un promotor constitutivo expresando TetR de forma constitutiva y por otro lado un promotor conteniendo la zona operadora (TetO) a la que se une el represor, inhibiendo la expresión del promotor rió arriba (figura 7). Por tanto, la expresión constitutiva de TetR permite que nuestro gen esté silenciado en ausencia de activador (tetraciclina). La adición de tetraciclina libera el represor de las secuencias TetO y permite la expresión del promotor regulado.

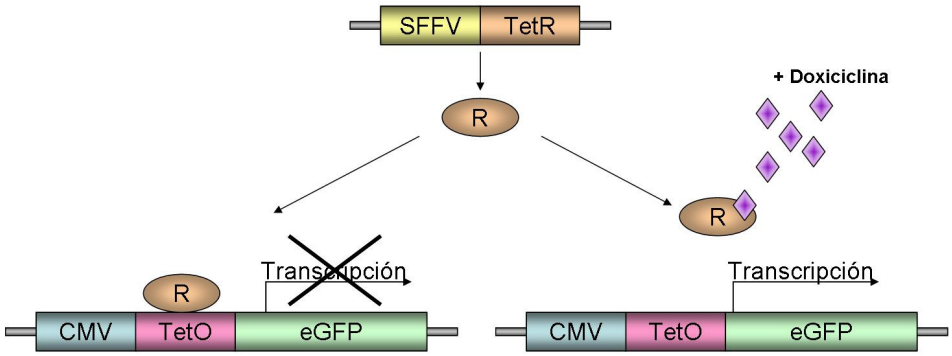

Figura 7: Sistema TetOn. Mediante la adición de doxiciclina, conseguimos que el represor no bloquee el operón, activándose la transcripción del transgén.

Recientemente, nuestro grupo ha desarrollado un sistema de expresión único, bicistrónico (CEST conteniendo un promotor regulable (CMVTetO) expresando eGFP seguido de un promotor fuerte (SFFV) expresando el represor (TetR) [142]. En este sistema, la expresión del transgénse consigue por adición de doxiciclina [142].

4.3.3. Inmunogenicidad.

Uno de los aspectos a tener en cuenta en la terapia génica es al inmunogenicidad, es decir, la posibilidad de que se desarrolle una respuesta inmunológica frente a los componentes del vector y/o del transgén. Además, en estrategias que conllevan un paso *ex vivo*, como cuando se implantan células del propio paciente modificadas, también puede existir una contaminación debida a proteínas de los medios de cultivo.

El transgén puede aportar ciertos problemas de inmunogenicidad, sobretodo relacionados con las moléculas del complejo principal de histocompatibilidad de tipo I y II[143]. En el caso de inmunodeficiencias primarias, sería probable que se desarrollara una respuesta frente al transgén, puesto que el SI no sería capaz de reconocerlo al no ser visto nunca antes por las células del receptor.

También se han observado respuestas inmunitarias frente a transgenes de tipo sintético, o provenientes de otras especies (xenogenes), como ocurre en el caso de GFP [144]. El nivel de expresión de estos transgenes también puede determinar que se produzca o no una respuesta por parte del sistema inmunológico [145].

El tipo de vector utilizado también determina la existencia o no de inmunogenicidad, ya que los vectores adenovirales, por ejemplo, poseen componentes estructurales inmunogénicos, [146, 147], y sin embargo los vectores retrovirales y lentivirales son muy poco inmunogénicos, sobre todo cuando son producidos en ausencia de suero. Esto es una característica importante cunado se busca analizar el efecto de la expresión de un gen terapéutico sin interferencias debido a respuestas inmunes frente al vector

4.3.4. Genotoxicidad.

Cuando se transduce una población celular pueden ocurrir mutaciones insercionales que producen un patrón de expresión alterado, pudiendo dar una ventaja clonal sobre estas células respecto a las otras existentes en la población total transducida. De ahí la importancia de un diseño más seguro y de la elección correcta del vector a usar en clínica.

En el caso de los vectores retrovirales hay que tener en cuenta una serie de problemas, como son la movilización del material genético del vector en el paciente, los posibles errores de la transcriptasa inversa durante la retro-transcripción, la expresión ectópica y desregulada del transgén y en el caso de onco-retrovirales, integración del vector en zonas activas de transcripción de proto-oncogenes [148].

Durante la infección viral se puede producir la activación de proto-oncogenes, por inserción del vector cercana a éstos. Ésta puede ser debida al aumento de expresión de promotores retrovirales o la disrupción de los genes supresores de tumores. El peligro de las inserciones en lugares preferentes, como las zonas cercanas al inicio de trascripción de ciertos genes tumorales, se puso de manifiesto por primera vez en un ensayo de terapia génica de una inmunodeficiencia severa ligada al cromosoma X (X-SCID), cuando 2[149] y posteriormente 3 [150] de los 16 enfermos tratados desarrollaron leucemias.

Los vectores MLV (murine leukenia virus), son vectores con tendencia a integrarse en zonas reguladoras mientras que los vectores basados en VIH-1 tienden a integrarse en zonas activas de expresión de genes[151]. Sin embargo, hasta ahora no se ha demostrado el desarrollo de tumores por integración del vector con vectores lentivirales derivados de virus de inmunodeficiencia humana

de tipo 1 (VIH-1). Habrá que seguir de cerca los futuros ensayos clínicos para determinar con precisión la capacidad trasnformante de estos vectores.

4.4. Aplicación de los vectores lentivirales en células primarias.

Los vectores lentivirales son unas herramientas muy prometedoras para su uso en terapia celular por su eficiencia para transducir tanto células quiescentes como en división. La capacidad de modificación genética de células quiescentes es una característica propia de los vectores lentivirales y viene dada por la capacidad del complejo de preintegración de penetrar la membrana nuclear[152]. Esto ha permitido el uso de los LVs para la modificación genética de células diana que habían resultado dianas difíciles para otros vectores. Entre estas células diana se encuentran las células dendríticas, los macrófagos/monocitos[153], las células primarias[129, 154] o las células madre hematopoyéticas (HSCs) [155].

El hecho de usar como célula diana una célula madre, nos permite la transmisión del transgén a las diferentes líneas progenitoras que darán lugar esa célula madre. Para ello son muy utilizadas hoy en día las células madre hematopoyéticas (HSCs). Estas células son una herramienta útil cuando se quieren tratar por ejemplo, enfermedades monogénicas del sistema sanguíneo para restaurar la expresión de algún gen. Las células madre mesenquimales, también están siendo muy usadas para terapia celular-génica.

Pero el uso de células madre para su modificación génica puede conllevar problemas genotóxicos. Estas células, al ser madre, expresan aún una serie de proto-oncogenes que las hace más susceptibles de ser transformadas por la integración del vector. Para estudiar el efecto genotóxico de los vectores retrovirales, Montini y colaboradores, desarrollaron un modelo de estudio utilizando células HSCs pretransformadas (Cdkn2a-/-)[156]. En este modelo, las células HSCcdkn2a-/- forman tumores espontáneos cuando son inoculadas en ratones singénicos. Cualquier alteración genotóxica que incremente el potencial tumorigénico de estas células será leída como un incremento en el número de tumores, un mayor tamaño de los mismos o una aparición más temprana.

B. JUSTIFICACIÓN Y OBJETIVOS

Las terapias actuales para el tratamiento de esclerosis múltiple son ineficaces y asociadas a diversos efectos secundarios. Nuestra hipótesis es que la falta de eficiencia se debe principalmente a que los medicamentos actuales; 1- no llegan a los tejidos afectados en las concentraciones necesarias y 2- actúan únicamente sobre el componente inmunológico de la enfermedad, siendo incapaces de frenar la neurodegeneración observada en las fases avanzadas de la enfermedad.

Las nuevas estrategias terapéuticas han de ser capaces de solventar estas carencias. Mediante estrategias de terapia génica y/o celular se pueden desarrollar potentes herramientas capaces de llegar a zonas de inflamación y de secretar de forma estable ó regulada el/los agente/s terapéutico/s.

Terapia génica. Los vectores lentivirales son una de las mejores herramientas para conseguir expresión estable de genes. Su alta eficiencia y su baja inmunogenicidad los hacen especialmente interesantes para tratamiento de enfermedades autoinmunes. Los potenciales beneficios de administración de vectores lentivirales frente a la administración sistémica de proteínas/péptidos son: 1- secreción del producto de forma constante en el tejido diana, 2- mayor actividad del producto terapéutico, al tratarse de una proteína nativa y no una sintética y 3- menor coste, ya que con una sola inoculación podría ser suficiente.

Terapia génica y celular. Las células madre mesenquimales (MSC) son especialmente atractivas para el tratamiento de esclerosis múltiple dado que, además de migrar selectivamente a los sitios de daño, inhiben el proceso inflamatorio y secretan factores neuroprotectores y pro-mielinizantes. La modificación génica de las MSC para expresión de genes terapéuticos es una potente alternativa a la inoculación directa de los vectores porque permite la secreción del agente terapéutico específicamente en los tejidos inflamados. Además, al efecto producido por la secreción local del agente terapéutico se sumaría el efecto propio de las células MSC.

El péptido intestinal vasoactivo (VIP) es un neuropéptido con actividad anti-inflamatoria, inmunomoduladora y neuroprotectora y con actividad terapéutica demostrada en el modelo murino de EAE.

El objetivo global de la presente tesis es desarrollar y comparar dos nuevas estrategias terapéuticas para las fases avanzadas de esclerosis múltiple basadas en terapia génica (administración directa de vectores expresando VIP) y terapia génica y celular (administración de células MSC modificadas genéticamente con vectores que expresan VIP).

Por ello nuestros objetivos son:

1. Estudiar el efecto terapéutico de los vectores lentivirales expresando VIP (LentiVIP) en un modelo crónico de encefalomielitis autoinmune experimental.

2. Desarrollar líneas MSCs secretoras de VIP. Para ello se procederá a:

   2.a) Determinar el mejor método de aislamiento y cultivo de las MSCs.

   2.b) Modificar genéticamente las MSC con LentiVIP.

   2.c) Caracterizar las líneas MSC/lentiVIP.

3. Estudiar el efecto terapéutico de las células MSC/LentiVIP en un modelo crónico de encefalomielitis autoinmune experimental.

4. Analizar los mecanismos implicados en los efectos encontrados por dicho tratamiento.

C. MATERIALES Y MÉTODOS

1. Líneas celulares y medios de cultivo.

Tanto para la producción de vectores como para su posterior titulación se utilizaron células 293T (HEKT) (células epiteliales de riñón), las cuales se crecieron en medio DMEM con glutamax, piruvato, 4,5 g/ml de glucosa y 10% de suero bovino fetal (PAA),. Se incubaron al 10% de CO_2.

Las células macrófagos de leucemia murinas, Raw 264, se cultivaron en medio DMEM con glutamax, piruvato, 4,5 g/ml de glucosa, penicilina/estreptomicina y 10% de suero bovino fetal (FBS) (PAA). Se incubaron al 5% de CO_2.

Las células madre mesenquimales (MSCs) se extrajeron o bien de médula ósea o de tejido adiposo abdominal de ratones machos Balb/c, y se cultivaron en condiciones de normoxia (20% O_2) o hipoxia (a 5% O_2) y al 5% CO_2.

Las células HeLa son epiteliales humanas procedentes de carcinoma, y se cultivan en medio DMEM con Glutamax, piruvato, 4,5 g/ml de glucosa, penicilina/estreptomicina y 10% de suero bovino fetal (PAA),. Se incubaron al 5% de CO_2.

Las células de la médula ósea (BM-MSC) se extrajeron mediante la inyección de DMEM con una jeringa tras cortar ambas extremidades del fémur y de la tibia de ambas patas traseras. Tras lavar dos veces y filtrar con filtro para células de 40 μm, se plaquearon utilizando una concentración de 20-40x10^3 células/cm^2. Las células se cultivaron en medio MesenCult (StemCell) conteniendo un 20% de suplementos de mesenquimales de ratón (StemCell) y 100 unidades de penicilina/estreptomicina (Gibco, Invitrogen).

La grasa fue extraída en esterilidad y llevada a medio HBSS (Invitrogen), en el que fue triturada, tras lavarla en pequeños trozos (=< 2 mm^3) y resuspendida en colagenasa tipo 1 (Sigma) a 2 mg/ml, usando 2.5 ml por gramo de grasa, e incubado a 37º C durante 30 min., agitando cada 5 min. La digestión se lavó 2 veces con HBSS y filtrada con filtro celular de 100μm primero y 40 μm después. Finalmente las células se resuspendieron en medio MesenCult (StemCell) conteniendo un 20% se suplementos de mesenquimales de ratón (StemCell) y 100 unidades de penicilina/estreptomicina (Gibco, Invitrogen). Se contaron y plaquearon en una densidad de 15-30000 células/cm^2. Las células no adheridas se eliminaron alas 24 h. En los pases siguientes se plaquearon a una

densidad de 5-10000 células/cm^2 en una parte de medio fresco MesenCult completo y otra parte de medio condicionado, obtenido por filtración por 0.22 μm de cultivos de ellas mismas confluentes.

Las células MSC/LentiVIP y MSC/LentiGFP fueron obtenidas por transducción de estas MSCs con los vectores LentiVIP y LentiGFP respectivamente, al ponerlas en contacto con los sobrenadantes virales durante 5h, con un MOI (multiplicidad de infección) de 5.

Las células mesenquimales de ratón con los genes escindidos p53 y p21 ($MSCp53^{-/-}p21^{-/-}$) del laboratorio de del Dr. García-Castro y el Dr. Menéndez, se transdujeron con ambos vectores (LentivIP y LentiGFP) y se cultivaron en Advanced DMEM, más glutamax, penicilina/estreptomicina (Gibco), y 10% de suero bovino fetal (PAA), al 5% de CO_2.

2. Plásmidos y construcciones lentivirales.

Los plásmidos usados para las proteínas de la envuelta y empaquetamiento fueron, pMD.G y pCMVΔR8.91, respectivamente, cedidos por el laboratorio del Dr. D. Trono. El plásmido de empaquetamiento codifica para las proteínas gag, pol, tat y rev, mientras que el de la envuelta para la glicoproteína VSVg.

El vector LentiGFP se obtuvo reemplazando el promotor SFFV de la construcción pHRSIN-CSEW (SEWP) del laboratorio de A.J. Thrasher, por el producto de PCR (reacción en cadena de al polimerasa) de un fragmento que contenía el promotor CMV, con los sitios EcoRI/Bam HI, obtenidos a su vez por PCR usando los cebadores:

EcoRI FW: 5'-CCG GAA TTC GTT GAC ATT GAT TAT TGA CTA

BamHI RV: 5' CGC GGA TCC CGG AAG ATG GAT CGG TCC,

usando como molde el pcDNA4/TO.

El producto se corrió en un gel de agarosa 1% con bromuro de etidio, se cortó y extrajo del gel (Perfectprep Clean up, Eppendorf). El LentiGFP se obtuvo ligando este fragmento en el esqueleto del SEWP digerido con EcoRI/Bam HI mediante el kit de ligación de roche.

El LentiVIP, se obtuvo sustituyendo en el LentiGFP, el gen de GFP, por el cDNA de VIP de 560pb (del locus humano NM-003381). El fragmento se

obtuvo por ampliación por PCR del ADNc de VIP del plásmido pCMV6-XL4-VIP (Trueclone) usando los cebadores:

BamHI-VIP FW: 5'CGG GAT CCA TGG ACA CCA GAA ATA AGG

PstI-VIP RV: 5'CAC TGC AGG GGA AGT TGT CAT CAG C.

Al igual que el anterior, el producto se corrió en un gel de agarosa, se cortó la banda y extrajo del gel, ligándose posteriormente en el esqueleto del LentiGFP, tras digerir con las enzimas, BamHI/PstI.

3. Producción viral.

Los vectores LVs se produjeron por cotransfección de los tres plásmidos pCMVΔR8.9, pMD.G y LentiGFP o LentiVIP, con Lipofectamina 2000 (Invitrogen), en células empaquetadoras 293T (HEKT), las cuales se cultivaron en placas de 10cm de diámetro. La lipofectamina se preparó en medio OPTIMEM frío según el protocolo. El resto del medio se puso a calentar para lavar las placas y realizar la transfección. Se incubaron previamente la lipofectamina con OPTIMEM por un lado (60μl de lipofectamina/1,5 ml de medio /placa), y el DNA por otro (24 μg de DNA/1,5 ml de medio /placa). De los 24 μg la relación de los plásmidos fue LentiVIP/LentiGFP: 8.9: VSVG=3:2.:1. Luego se juntaron las dos incubaciones y se volvieron a incubar 20 minutos a temperatura ambiente. Pasado este tiempo se añaden 3 ml de la mezcla a cada placa que contiene unos 5 ml de OPTIMEM y tras 7 h, se le realizó un cambio de medio para eliminar la lipofectamina sobrante, así como las partículas de VSVg que quedasen libres. La primera recogida de vectores es a las 48h y la segunda a las 52h y la tercera a las 72h. Los sobrenadantes se filtran por 0.22μm (Tras cada recogida se volvió a añadir OPTIMEM caliente para la siguiente).

4. Concentración de vectores.

Tras recoger los sobrenadantes virales se procedió a su concentración mediante filtros Amicon Ultra-15 de 100K (Millipore), previamente lavados con etanol 70% primero, para esterilizar y dos veces con PBS después. Se

centrifugaron a 1800g a 4ºC durante 15 min y se alicuotearon para ser usados o bien directamente o congelarlos a -80ºC. Los sobrenadantes se concentraron entre 25 y 45 veces.

5. Titulación de los vectores.

Para calcular el título de un vector (cantidad de unidades de transducción/ml) se procedió de dos maneras:

A) LentiGFP.

Se añadió una cantidad creciente de sobrenadante viral a un número definido de células y tras 5 días, se procedió a pasar éstas por el citómetro par ver la cantidad GFP por célula. Para calcular el título siempre se trabajó por debajo del 25% de transducción para evitar más de una inserción por célula.

B) LentiVIP.

Se añadió una cantidad creciente de sobrenadante viral a un número definido de células y tras 7 días, se extrajo el ADN genómico y la cuantificación del número de copias del gen VIP exógeno (ADNc de VIP), mediante q-PCR, usando como curva estándar cantidades conocidas del plásmido LentiVIP (10^6-10^2). A partir de esta curva se interpolaron los datos obtenidos, considerando 0.6 µg de ADN genómico el equivalente a 10^5 células. Los pares de cebadores usados fueron:

VIP: FW 5'-CCA CGC TGT TTT GAC CTC CAT,
RV 5'-GGG CCT TAT TTC TGG TGT CCA T,

usando el aparato de tiempo real de Stratagene MX3005Pro, con el kit de PCR de Qiagen, QuantiTect SYBRGreen**.**

6. Extracción de ADN genómico.

Para la extracción del ADN genómico, se precipitaron las células o trocearon los tejidos y se lisaron con el tampón SNET (SDS, NACl, EDTA y Tris), en presencia de proteinasa K (Roche)(100µg/ml), en agitación a 55ºC

durante 2-10 horas. Pasado este tiempo se inactivó la proteinasaK a 92ºC de 2-10 min. Se trató con RNasaA (sigma) (5 mg/ml,) 30' a 60ºC. Se extrajo con fenol (Sigma) la fase acuosa tras centrifugación a 14000 rpm 5min a 4ºC y se extrajo una vez más ésta con fenol: cloroformo: isoamílico (Sigma), 25:24:1(centrifugación a 14000 rpm 5min a 4ºC). El ADN de la fase acuosa se precipitó con etanol absoluto poniendo el doble del volumen de la muestra conteniendo acetato amónico 10M, 0.2 volúmenes de la muestra a -80ºC de 1 hora, y se precipitó a 14000 rpm 30min a 4ºC. El precipitado se lavó con etanol 70%, se secó y se resuspendió en tampón TE (Tris EDTA), diluido en agua 10 veces y previamente calentado a 90ºC.

7. Extracción de ARN y cuantificación de los transcritos.

El ARN de los diferentes tejidos de ratón se obtuvo utilizando Trizol (Invitrogen). Las muestras de ARN se pasaron a ADN complementario mediante reverso-transcripción usando el kit de Invitrogen, Superscript first-strand. Las q-PCRs se realizaron mediante el kit QuantiTect SYBRGreen en la real time de Stratagene anteriormente mencionada. Como calibrador se usó o bien actina o bien GAPDH. Pares de cebadores usados:

IL17: FW 5'-TTT AAC TCC CTT GGC GCA AAA
RV 5'-CTT TCC CTC CGC ATT GAC AC;
iNOS: FW 5'-GTT CTC AGC CCA ACA ATA CAA GA
RV 5'-GTG GAC GGG TCG ATG TC AC;
TNFα: FW 5'-GGC AGG TCT ACT TTG GAG TCA TTG C
RV 5'-ACA TTC GAG GCT CCA GTG AAT TCG G
IL10: FW 5'-CTG GAC AAC ATA CTG CTA ACC G
RV 5'-GGG CAT CAC TTC TAC CAG GTA A;
IL6: FW 5'-TAG TCC TTC CTA CCC CAA TTT CC
RV 5'-TTG GTC CTT AGC CAC TCC TTC;
FoxP3: FW 5'-CCC ATC CCC AGG AGT CTT G
RV 5'-ACC ATG ACT AGG GGC ACT GTA;
ADNP: FW 5'-AGA AAA GCC CGG AAA ACT GT,
RV 5'-AAG CAC TGC AGC AAA AAG GT;

BDNF: FW 5'-CCC TCC CCC TTT TAA CTG AA,
RV 5'-GCC TTC ATG CAA CCG AAG TA.
Actina: FW 5' GCCATCCAGGCTGTGCTGTC-3'
RV 5' -TGAGGTAGTCTGTCAGGTCC
GAPDH: FW 5'-CCT GCA CCA CCA ACT GCT TA
RV 5'-TCA TAC TTG GCA GGT TTC TCC A

8. Cálculo del número de copias de MSC/LentiVIP y MSC/LentiGFP.

Tras esto se determinó el número de copias por q-PCR para el caso de LentiVIP como se ha descrito anteriormente en el cálculo de título y para LentiGFP, utilizando los pares de cebadores:

eGFP: FW: 5' GCC CRAC AAC CAC TAC CT
RW: 5' CGT CCA TGC CGA GAG TGA

9. Determinación del VIP secretado.

Las células 293T, MSC/LentiVIP, MSC/LentiGFP y MSC se sembraron en placas de 6 pocillos, (4×10^5 células/pocillo en 2 ml) y tras 48h se recogieron los sobrenadantes. Los niveles de VIP se midieron por el kit de ELISA de Phoenix Pharmaceuticals.

10. Western Blot.

Las células precipitadas y los sobrenadantes liofilizados y concentrados en PBS 10X, se lisaron en tampón de lisis al 1% Nonidet P40 lysis conteniendo el cocktail de inhibición de proteasas (Sigma,St Louis, MO), y la muestra se pasó por un gel de electroforesis de poliacrilamida-SDS al 10% en condiciones reductoras. El gel se trasfirió a membrana de PVDF Hybond (Amersham Biosciences,Little Chalfont, UK). La membrana se bloqueó con leche desnatada al 5% durante 1 h. Tras esto se incubó con 2/µg/ml del anticuerpo monoclonal anti-VIP (clon H16; Santa Cruz Biotechnology, Santa Cruz, CA), y 0.05µg/m del

policlonal anti-ERK (Upstate, Chicago, IL). El análisis se llevó a acabo usando el kit ECL Advanced Western Blotting Detection Kit (Amersham Biosciences).

11. Diferenciación de MSCs.

A) Diferenciación Adipogénica:

Se sembraron las células en placas de 6 pocillos, 200.000 células/pocillo (95% de confluencia). Una vez adheridas, eliminamos el medio de cultivo y añadimos Adipogenic Induction Medium + SingleQuots Kit: 2ml/ pocillo de placa (Lonza) y alternamos con Adipogenic Manteniance Medium + SingleQuots Kit(Lonza), cambiando el medio cada 3-4 días. A las 2 semanas se tiñeron con Oil Red.

Tinción de adipocitos con Oil Red O:

Se eliminó el medio de cultivo, y se lavó 2 veces con PBS. Se fijaron las células con parafolmadehido 4% durante 20min. a temperatura ambiente, y se lavó de nuevo 2 veces con PBS. Luego se lavó una vez con Isopropanol al 60% y se añadieron 2 ml por pocillo de una solución preparada de Oil Red en isopropanol 60%. Se dejó actuar de 5-10 minutos y se lavó 2 veces con PBS, antes de realizar las fotografías.

B) Diferenciación Osteogénica:

Se sembraron las células en placas de 6 pocillos, 200.000 células/pocillo (95% de confluencia).Una vez adheridas, eliminamos el medio de cultivo y añadimos

Osteogenic-Differenciation Basal Medium + SingleQuots Kit: 2,5ml/ pocillo (Lonza), cambiando el medio cada 3-4 días.

Tinción de osteocitos.

Pasados unos 10 días, se lavó la placa 2 veces con PBS (sin calcio), se fijaron las células con parafolmadehido 4% durante 20min, se volvió a lavar 2 veces con PBS y se tiñó con una solución preparada del reactivo SIGMA FAST BCIP/NBT, que tiñe el sustrato de la fosfatasa alacalina, que se expresa por los

osteocitos. Tras 20 min. se lavaron las células 3 veces y se realizaron las fotografías.

C) Diferenciación Condrogénica:

Se centrifugaron $1x10^6$ células en tubos de 15 ml de poliestireno. El precipitado se lavó y se le añadió 500 µl Chondrogenic-Differenciation Basal Medium + SingleQuot Kit (Lonza). Se volvió a lavar y se le añadió nuevamente Chondrogenic-Differenciation Basal Medium + SingleQuot Kit + TGFß3 (sin TGFß3 en controles). El medio se le cambió cada 2-3 días. Tras 21 días se incluyeron los precipitados celulares con plasma y trombina (3:1), y se fijaron una vez coagulado en formol al 4%. Se realizaron cortes con el microtomo para teñirlos con posteriormente con un anticuerpo contra la proteína S100 expresada en condrocítos y Dapi para teñir los núcleos.

12. Medida de cAMP en macrófagos.

Para calcular el cAMP producido en macrófagos, 1ml de sobrenadantes de células 293T transducidas con 2 cantidades de LentiVIP y como controles, sobrenadantes de células transducidas con LentiGFP, se liofilizaron y se resuspendieron en 100µl de PBS. Luego se pusieron en contacto de células Raw, sembradas previamente en placa de 96 pocillos (10^6células/pocillo). Se añadió IBMX (3-isobutil-1-metil xantina), y tras 20min. de incubación, se lisaron las células con reactivos y según el protocolo de kit de Amersham, para determinar posteriormente por inmunoensayo enzimático, la cantidad de cAMP. Además, se añadió a otros pocillos que contenían sobrenadante de LentiVIP, anticuerpo anti-VIP (100µg/ml), para bloquear el efecto de éste.

13. Medida del TNFα producido por macrófagos.

De igual manera que en el experimento anterior, 1ml de sobrenadantes de células 293T transducidas con 2 cantidades de LentiVIP y como controles, sobrenadantes de células transducidas con LentiGFP, se liofilizaron y se resuspendieron en 100µl de PBS. Estos se añadieron sobre células Raw, las cuales se estimularon con LPS (500 ng/ml), durante 8h. Pasado este tiempo se

recogieron los sobrenadantes y se realizó una ELISA para determinar la cantidad secretada de TNFα.

14. Inducción de EAE.

Ratones hembras C57Bl/6 de 5 a 7 semanas, se inyectaron subcutáneamente (s.c) en tres puntos, con 100 μg de MOG_{35-55} (GeneScript) (diluido en PBS a una concentración de 2 mg/ml), emulsionado (1:1) en Adyuvante completo de Freund (CFA) conteniendo 0.55 mg de *M. tuberculosis*. Los ratones fueron inoculados intraperitonealmente (i.p.) con toxina pertussis (100 ng/ml) el mismo día de la inmunización y 48h más tarde.

Para las inyecciones s.c. se anestesiaron los ratones con 15-20ul/ratón intramuscular (i.m.) de 2/3 ketamina (imalgene) y 1/3 acepromacina (calmoneosan). Los síntomas comienzan a aparecer a las 2 semanas aproximadamente, administrándoseles agua gelificada una vez empiezan a aparecer los síntomas, y poniéndoles el pienso en el serrín de las cajas.

Los grados de EAE usados fueron:

0 Normal.

1 Pérdida completa de tonicidad cola.

2 Cola flácida y marcha anormal.

3 Parálisis de parcial de extremidades posteriores.

4 Parálisis parcial de extremidades anteriores y total de las posteriores.

5 Parálisis ambas extremidades anteriores además de las posteriores.

6 Muerte.

15. Tratamiento con vectores lentivirales.

El tratamiento consistió en una única inyección i.p. con $2x10^8$ copias/ratón (300 μl) de LentiVIP en el grupo tratado, en el control de tratamiento fue $2x10^8$ copias/ratón (300 μl) de LentiGFP y en el grupo control de enfermedad se inyectó el mismo volumen de PBS, en ratones con grado entre 3 y 3,5.

16. Tratamiento con MSCs y MSCs transducidas con los LVs.

El tratamiento consistió en una única inyección i.p. con 10^6 células /ratón (250 µl) tanto en el grupo tratado con MSC/LentiVIP, como en los tratados con MSCs o MSC/LentiGFP. Al grupo control de enfermedad se inyecto el mismo volumen de PBS. Las inyecciones se realizaron tanto a día 15 post-inmunización en grado crónico (grado EAE = 2.5-3.5).

17. Ensayo de supresión de proliferación por las MSCs

Para estudiar la capacidad de supresión de proliferación de linfocitos, de las MSCs, se irradiaron éstas a 42 Gy y plaquearon en triplicados en placas de 96 pocillos: 40000, 20000, 10000, 5000 y 0 células/pocillo. A cada pocillo se añadió 200.000 células aisladas de bazo (lisando previamente los eritrocitos, con tampón ACK, NH_4Cl, $KHCO_3$, $EDTA{\cdot}Na_2 2H_2O$, durante 5 min.), y sobre cada pocillo, excepto un triplicado de células de bazo solas, que sería el control no estimulado, se añadió concanavalina A (2.5 µg/ml) (Sigma) como estimulación. Tras 72 horas se añadió 0,5 µCi/pocillo de timidina-3H (Perkin Elmer) y pasadas 6 horas se recogieron en filtros de fibra de vidrio en LKB 96 well-harvester (Wallac Oy, Turku, Finland). La captación de timidina-3H se midió con un contador de centello líquido 1450 microbeta Trilux (Wallac).

18. Ensayo de proliferación.

Para el análisis *in vitro* de las células MOG-específicas, se obtuvieron suspensiones celulares de ganglios linfáticos de drenaje. Se plaquearon $4x10^5$ células/pocillo en placas de 96 pocillos por triplicado, y unos triplicados o no se estimularon, o se estimularon con anti-CD3 (1µg/ml) o con MOG_{35-55} (50µg/ml). Al igual que en experimento anterior, tras 72 horas se añadió 0,5 µCi/pocillo de timidina-3H (Perkin Elmer) y pasadas 6 horas se recogieron en filtros de fibra de vidrio en LKB 96 well-harvester (Wallac Oy, Turku, Finland). La captación de timidina-3H se midió con un contador de centello líquido 1450 microbeta Trilux (Wallac).

19. Distribución del vector (LentiVIP) o de las células (MSC/LentiVIP) en diferentes órganos.

En ambos casos se vió por la distribución del ADNc de VIP tanto a nivel genómico (para inyección directa del vector y de las células), como de mensajero (en la inyección de las células). Para ello se trataron los órganos como se ha mencionado anteriormente y se realizaron q-PCRs con el kit de Qiagen QuantiTect SYBRGreen en el sistema de detección de Stratagene. Los pares de cebadores usados fueron:

VIP: FW 5´-CAC CAC CTG TCA GCT CCT TT
RV 5'-AAG CAG CGT ATC CAC ATA GCG

20. Análisis inmunofenotípico y tinción de FoxP3

Las células MSC, MSC/LentiVIP y MSC/LentiGFP, se tiñeron con anticuerpos contra las moléculas CD45, CD44, SCA1, MHCII, FLK1 y CD29 en APC y CD105 en PE (eBioscience). Par ver FoxP3, células o bien de ganglios linfáticos de drenaje o de bazo, extraídas 5 días tras los tratamientos e incubadas con 7AAD (Sigma) y 24G2 (eBioscience), y teñidas con el kit de FoxP3 de eBioscence, según el protocolo del kit. Las células se adquirieron en el FACS Canto II de BD usando para su análisis el programa FACS Diva de BD.

21. Cuantificaciones y tinciones inmunohistoquímicas.

Los ratones se sacrificaron 7 días tras el tratamiento, se extrajeron los cerebros y las médulas espinales, se sumergieron en OCT, congelaron en 2-metilbutano, y se guardaron a -80ºC. Las secciones se cortaron a 4 µm y se tiñeron con los anticuerpos contra GFAP (Dako), CD11b (Millipore), beta-amyloide (Sigma), beta-tubulina (Millipore), MBP (Millipore) and DAPI (Vestashield, Vector). El examen histológico se realizó usando el microscopio de

fluorescencia Eclipse de Nikon. Se recogieron 10 imágenes por sección usando el controlador digital de Nikon con el programa NIS-element BR 3.10. Las condiciones de adquisición fueron siempre seleccionando los niveles de fondo relativos a los controles de isotipo. Cada imagen se analizó midiendo el número de puntos/célula. Para cada anticuerpo se usó su isotipo control contabilizado como cero. Las secciones de los ratones sanos se usaron para seleccionar las condiciones de medida, usándose cada área (px^2) con parámetros circulares de puntos restringidos por el programa NIS element, para focalizar la cuantificación a los puntos deseados. Una vez ajustadas las condiciones, todas las imágenes se procesaron de la misma manera para determinar el número de puntos.

22. Ensayo de tumorigenicidad.

Se inocularon ratones NOD/SCID IL2Ry$^{-/-}$, 7 ratones por grupo s.c. con $5x10^6$ células (MSCp53$^{-/-}$p21$^{-/-}$, MSCp53$^{-/-}$p21$^{-/-}$LentiVIP y MSCp53$^{-/-}$p21$^{-/-}$ LentiGFP) y se observaron semanalmente hasta la aparición de tumores, para ver la latencia que daba cada tipo celular. Una vez visibles, los animales eran sacrificados y los tumores escindidos, medidos y pesados.

23. Ensayo de transformación celular.

Las células MSCp53$^{-/-}$p21$^{-/-}$, MSCp53$^{-/-}$p21$^{-/-}$LentiVIP y MSCp53$^{-/-}$p21$^{-/-}$ LentiGFP, se plaquearon $7.5x10^5$ células/pocillo, por triplicados en pocillos de placa de 48, junto a aun control MSC normal y otro de células HeLa transformadas de la siguiente manera. Primero se puso una capa de agar base (DMEM+FBS, H_2O y CytoSelect Agar Matriz Solution) y se dejó enfriar. Mientras se prepararon las células a una concentración de $7.5x10^5$/ml y se mezclaron con agar y se plaquearon. Se dejaron enfriar a 4ºC 15 min., y luego a 37ºC otros 15 min. Se añadieron otros 100 µl de medio y se dejaron creciendo 12 días, antes de contar las colonias. A continuación se recuperaron las colonias para hacer ensayo WST-1 (sal de tetrazodio para estudiar viabilidad celular). Se lavaron las células y se dividieron en 2 placas una de 96 y otra de 46 pocillos para

hacer lectura en el mismo día y al siguiente, respectivamente. Se dejaron que se adhirieran, se añadieron 10µl de WST-1 en cada pocillo (sobre 0.5ml), se dejó actuar 3.5 h y se leyó a 450nm. Al día siguiente se pasaron las células a placa de 96 pocillos y se repitió el proceso anterior.

24. Análisis estadístico

Todos los resultados están expresados como la media ± DE/DEM. Para ver la significancia estadística se usó el examen Mann-Whitney, para compara los datos de manera no paramétrica.

D. RESULTADOS

Como se ha mencionado en la introducción, VIP es un neuropéptido con características inmunológicas y neuroprotectoras muy atractivas para su uso terapéutico en enfermedades autoinmunes e inflamatorias, pero es muy susceptible de ser degradado por proteasas. Por ello decidimos como terapia alternativa al péptido sintético, la elaboración de un vector lentiviral que portase como transgén el del VIP, y lo aplicamos en un modelo de artritis inducida por colágeno[72], consiguiéndose un beneficio considerable con respecto a la inyección diaria del péptido en el mismo modelo [71]. Con una sola inoculación de los vectores lentivirales i.p. vimos que tenía efecto preventivo y que revertían los síntomas, regenerando las articulaciones cuando era administrado en grados donde el péptido no poseía efecto terapéutico ninguno. Por ello decidimos estudiar su efecto en un modelo severo de esclerosis múltiple, como es el de encefalomielitis autoinmune experimental inducida por MOG.

1. Construcción y caracterización de los Vectores lentivirales.

a. Construcción de los vectores lentivirales.

Los vectores utilizados en este estudio (figuras 8 y 9), son vectores lentivirales autoinactivados SIN, basados en el virus del HIV de tipo 1, los cuales expresan o bien la proteína verde fluorescente (eGFP) en el caso de LentiGFP o el cDNA de VIP en el caso de LentiVIP. Poseen los LTR (Repetición Terminal Larga), con el LTR 3' truncado, el elemento de respuesta de la proteína Rev (RRE), el segmento de polipurina y el elemento regulador post-transcripcional woodchuck (WPRE)

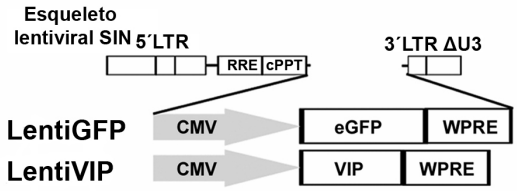

Figura 8: Construcciones lentivirales LentiVIP y LentiGFP. Se chequearon por enzimas de restricción. LentiVIP por PstI y XhoI, obteniéndose dos fragmentos de 0.769 kb y otro de 9.049kb, y LentiGFP con BamHI y XhoI, obteniéndose dos fragmentos de 1.5 kb y 8.5 kb. Los plásmidos se mandaron a secuenciar y la secuencia se llevó al programa Vector NTI (Invitrogen), donde se realizaron los mapas.

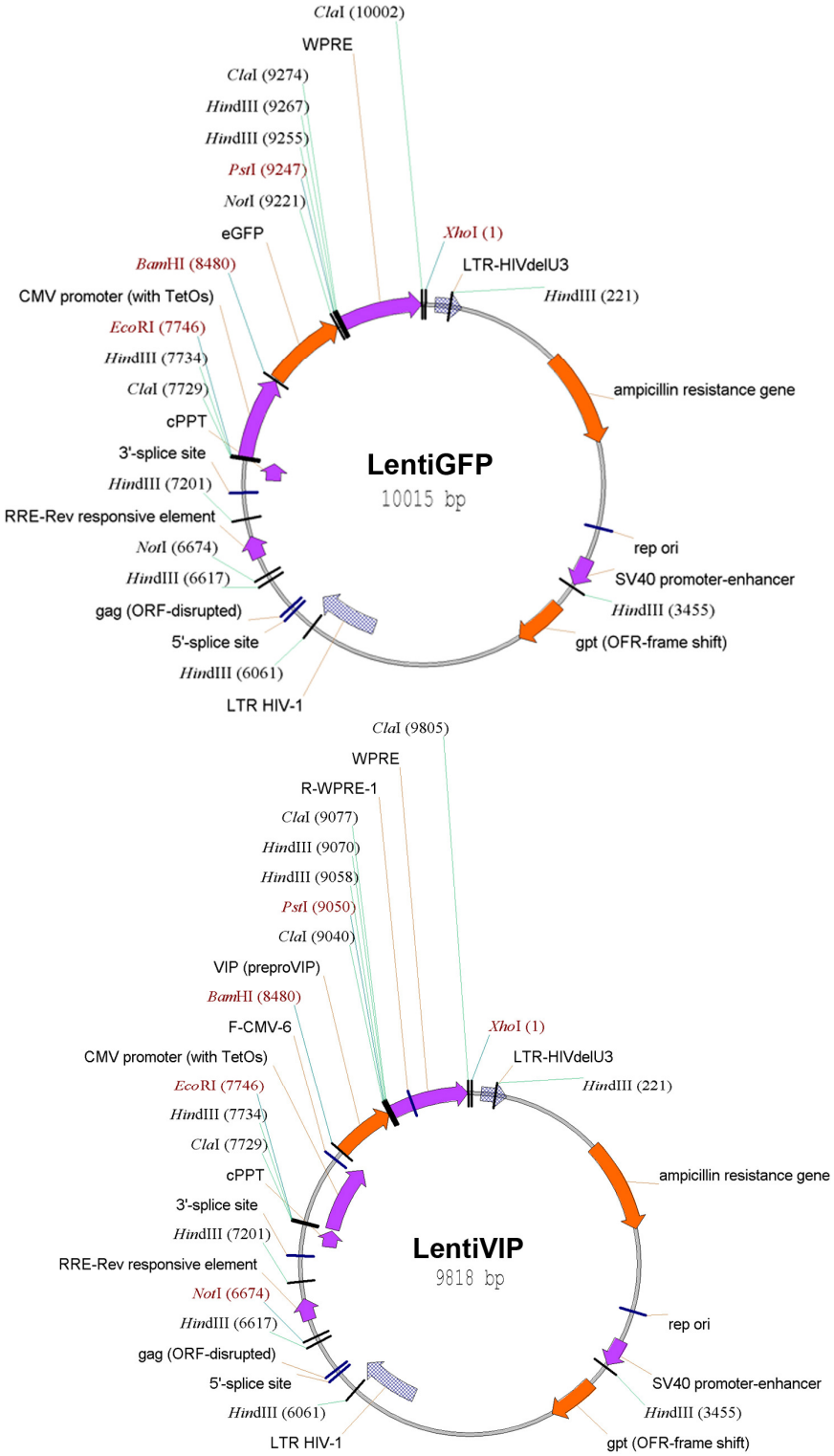

Figura 9: Mapas de las construcciones lentivirales LentiGFP y LentiVIP. Se realizaron, una vez obtenidas sus secuencias, con el programa Vector NTI de Invitogene.

b. Determinación de la expresión de VIP a través del vector lentiviral.

Una vez construido el vector LentiVIP, quisimos ver que efectivamente éste era capaz de expresar VIP. Para ello transdujimos células 293T con diferentes concentraciones de vector (MOIs: multiplicity of infection = número de vectores por célula) MOI= 0.1 y 1 y recogimos los sobrenadantes para su estudio por inmunoensayo enzimático (figura 10). Los controles utilizados fueron las células 293T transducidas con el vector LentiGFP a esos mismos MOIs.

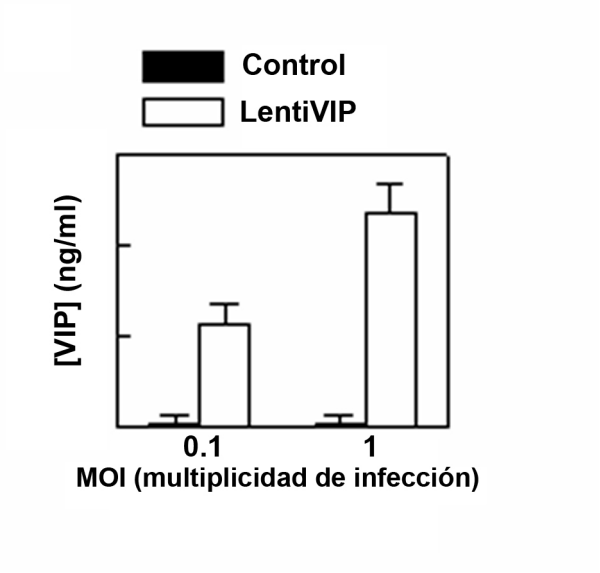

Figura 10: **ELISA de VIP.** Comprobamos así que las células transducidas con LentiVIP eran capaces de expresar VIP de una manera dosis dependiente, a través del vector.

Además de ver su expresión por ELISA quisimos ver también si éramos capaces de detectar las formas procesadas de VIP por Western Blot, tanto en lisados celulares como en sobrenadantes. La figura 11 muestra como solo fuimos capaces de detectar las formas no procesadas de VIP (preproVIP), tanto en lisados celulares como en sobrenadantes, indicando que esta es la forma mayoritaria en la que las células 293T están produciendo VIP.

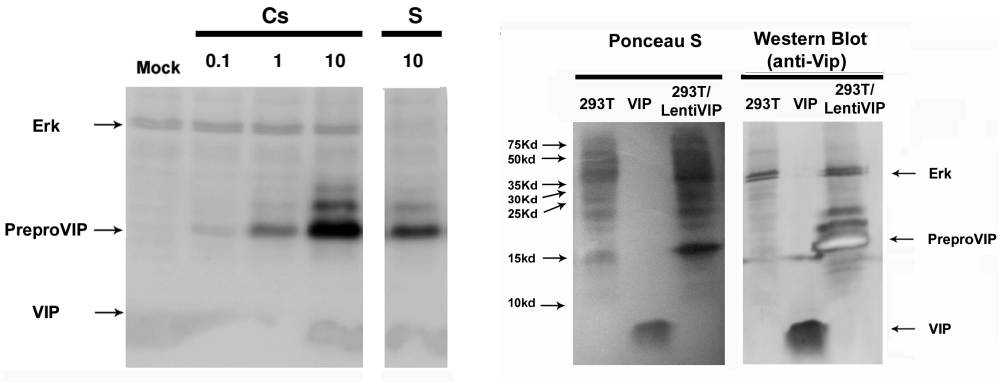

Figura 11: **Western Blot de VIP**. En el gel de la izquierda, tenemos de izquierda a derecha, un control de 293T no transducidas, y tres transducciones de MOIs, 0.1, 1 y 10, y por último el sobrenadante de las transducidas con MOI 10. En gel de la derecha, tenemos además un control de péptido VIP. Como control de carga se usó Erk.

c. Bioactividad del VIP producido por el vector.

Las células Raw (macrófagos de ratón) pre-estimuladas con LPS responden a la estimulación con VIP mediante la acumulación de cAMP y mediante una disminución en la secreción de TNFα. Para comprobar que el VIP producido por nuestras células transducidas era bioactivo, se realizaron dos ensayos con células Raw preactivadas a los que se les puso en contacto con los sobrenadantes de las células transducidas. En el primero se midió la acumulación de cAMP. En ambos experimentos se usaron como control los sobrenadantes de células transducidas con LentiGFP (figura 12). Los datos mostraron que el producto secretado por las células 293 transducidas con LentiVIP era bioactivo al ser capaz de inducir cAMP (figura 12, grafica izquierda, barras blancas) y de reducir la producción de TNFα (figura 12, gráfica derecha, barras blancas) de macrófagos activados. Como muestra de que el efecto observado era debido a VIP, se utilizó un anticuerpo bloqueante anti-VIP que efectivamente revertió el efecto de los sobrenandantes de las células transducidas con LentiVIP (figura 12, barras grises).

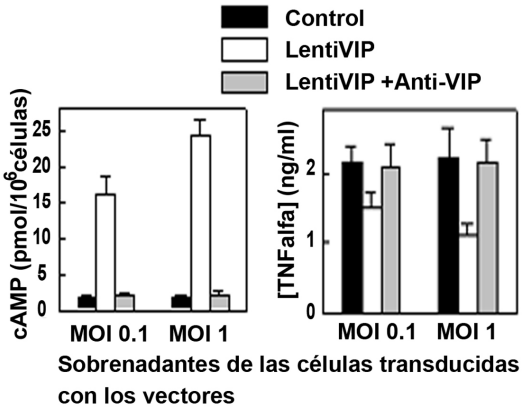

Figura 12: Bioactividad de VIP secretado. El VIP secretado por las células transducidas es capaz de disminuir la expresión de TNFα y aumentar la de cAMP en los macrófagos preactivados con LPS. La grafica de la izquierda muestra la acumulación de cAMP y la de la derecha la secreción de TNFα. En ambas gráficas se utilizaron dos MOI del vector (MOI=0.1 y MOI=1) con la finalidad de observar una correlación entre los niveles de expresión de VIP y el efecto en cAMP y TNFα (barras blancas). La adición de anticuerpo anti-VIP revierte el efecto de los sobrenadantes con LentiVIP (barras grises), obteniéndose lo mismo que en los macrófagos tratados con los sobrenadantes controles transducidas con LentiGFP (barras negras).

2. Terapia génica de EAE.

a. Inyección directa de los vectores lentivirales para terapia de EAE.

Para estudiar si existía un efecto terapéutico de la inoculación directa de los vectores, como se obtuvo en el modelo de artritis, se inyectaron, $2x10^8$ partículas virales por ratón, vía i.p., tanto de LentiVIP, como de LentiGFP y el mismo volumen (300µl) de PBS a un grupo control. Cada grupo fue de 9 ratones con un grado medio de EAE de 3,17. La inoculación se realizó a día 17 post-inmunización. El grado de enfermedad fue determinado cada dos días durante un periodo de 32 días. Como puede observarse en la figura 13 no se observaron diferencias significativas en la progresión de la enfermedad con ninguno de los tratamientos, incluido la administración de LentiVIP.

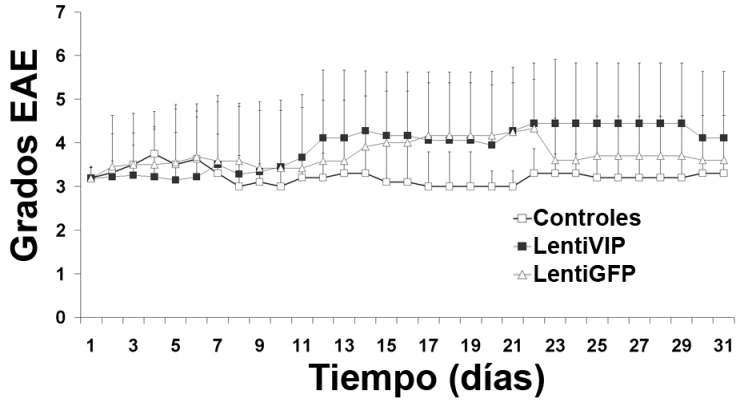

Figura 13: Seguimiento de los ratones tratados con LentiVIP y sus controles. La inoculación i.p. de los vectores no produce ningún beneficio terapéutico en grado crónico de EAE.

b. Distribución del vector.

Distribución del vector.

Uno de los puntos cruciales para conseguir beneficios terapéuticos tras inoculación directa de vectores virales es conseguir que estos se integren en los tejidos diana. Para estudiar la biodistribución del vector LentiVIP, se extrajo el ADN genómico de varios tejidos (Tabla 2) y se analizó por PCR su presencia en estos tejidos. De especial importancia para el tratamiento de EAE era que LentiVIP llegara a los órganos linfoides (ganglios linfáticos y bazo) y al sistema nervioso central (cerebro y medula espinal) Aunque los vectores LentiVIP lograron modificar tanto bazo como los ganglios linfáticos drenantes, no se detectó ningún vector en el SNC.

	Hígado	Bazo	Ganglios Linfáticos	Cerebro	Médula Espinal	Riñón
LentiVIP	+	+	+	-	-	-

Tabla 2: Distribución del cDNA del VIP. Proveniente de las inserciones del LentiVIP. El signo + significa presencia, y el – ausencia. Su análisis por q-PCR, mostró inserciones del vector sólo en hígado, bazo, ganglios linfáticos de drenaje, por lo que una posible explicación de no haber encontrado efecto terapéutico puede ser la no llegada del vector al SNC.

3. Obtención y caracterización de MSCs.

Nuestra hipótesis fue que la ineficacia de lentiVIP para el tratamiento de EAE era probablemente debido a que el vector no era capaz de llegar al SNC. Por tanto decidimos utilizar las MSC como vehículo capaz de hacer llegar la expresión de VIP a nuestro tejidos diana. Para ello procedimos en primer lugar analizar las MSCs obtenidas de diferentes procedencias y cultivadas en diferentes condiciones:

3.1. Comparación entre BM-MSCs y Ad-MSCs.

En primer lugar estudiamos los diferentes medios de crecimiento utilizados por diferentes grupos para el crecimiento de MSC: 1- DMEM con glutamax, piruvato, 4,5 g/ml de glucosa, penicilina/estreptomicina y 10% de suero bovino fetal, 2- OPTIMEM con glutamax, penicilina/estreptomicina y 10% de suero bovino fetal, o 3- con MesenCult (StemCell Technologies) más suplementos de ratón, Glutamax y penicilina/estreptomicina, observándose que este último daba mejores resultados en cuanto a morfología y crecimiento (datos no mostrados)

A continuación decidimos estudiar cual de las MSCs descritas en la literatura, procedentes de médula ósea o de tejido adiposo tenían mejores características para nuestro propósito. Pudimos observar que las MSC de grasa (Ad-MSC) eran más fáciles de aislar y crecían mejor que las derivadas de medula espinal (datos no mostrados). Además de comparar diferentes medios, comparamos crecimiento tanto en condiciones de normoxia como de hipoxia (5% de O_2), viendo que en hipoxia crecían mejor (datos no mostrados). Análisis fenotípicos de expresión de marcadores de superficie (figura 14) mostraron que las Ad-MSC tenían un perfil de expresión de marcadores más cercano a lo observado en MSC obtenidas mediante diferentes protocolos (negativas para CD45 y niveles mayores de SCA1 y FLK1)

A) Fenotipo:

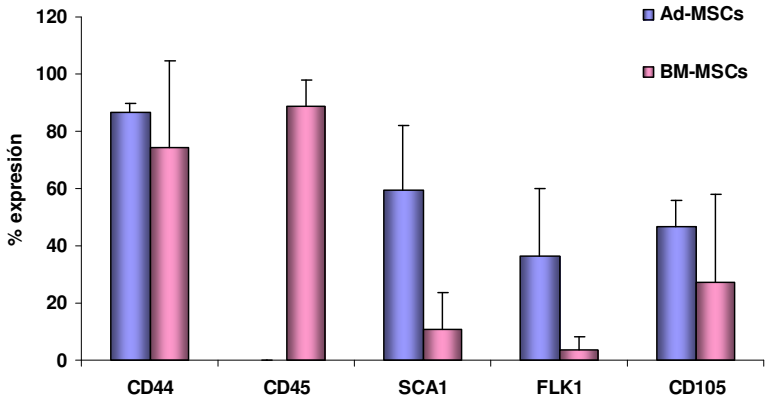

Figura 14: El análisis fenotípico de BM-MSC y Ad-MSC. El análisis es de al menos 3 líneas de cada una con pases entre 2 y 5, muestra que las Ad-MSC, presentan un perfil más acorde con el publicado para las MSCs (CD44, SCA1, CD105 y FLK1 positivas, y CD45 negativas).

B) Capacidad supresora de proliferación celular.

Además del fenotipo, las dos características más importantes que buscamos de las MSC son su capacidad inmunosupresora y su capacidad de migración. Por lo tanto analizamos las Ad-MSC y las BM-MSC crecidas en hipoxia y normoxia en cuanto a su capacidad de inhibir la respuesta T (figura 15). Los resultados mostraron que las células AdMSC crecidas en hipoxia mostraban el mayor efecto inmunosupresor, siendo las peores las BM-MSC crecidas en hipoxia. Por lo tanto se seleccionaron las Ad-MSC para posteriores estudios.

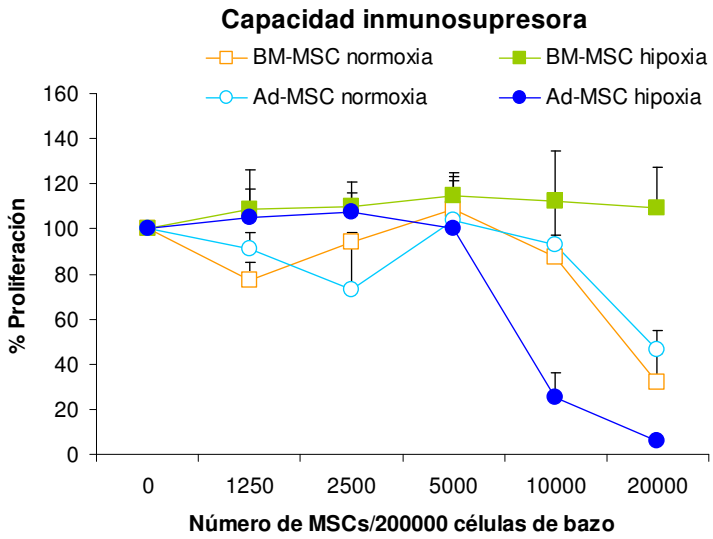

Figura 15: Capacidad inmunosupresora de las MSCs. Células MSCs derivadas de medula ósea (BM-MSC) o grasa (Ad-MSC) crecidas en normoxia o hipoxia se enfrentaron a células T activadas con PMA. En ausencia de inhibidores, las células T proliferan e incorporan timidina titriada (100% proliferación). Cuando existen factores que inhiben la proliferación de las células T, la incorporación de timidina disminuye. En la gráfica se observa como cuando se incrementa el número de MSCs (manteniendo fijo el número de células de bazo que contienen las células T) disminuye la proliferación.

3.2. Transducción y caracterización de las MSCs aisladas de tejido adiposo de ratón.

Se aislaron las MSCs de tejido adiposo abdominal de ratón, como se explica en materiales y métodos, y se procedió a translucirlas con diferentes MOIs de LentiGFP y LentiVIP. Por lo tanto de cada extracción se obtenían tres líneas: las MSCs, MSC/LentiVIP, MSC/LentiGFP. Cada una de las líneas obtenidas se caracterizó mediante determinación del número de copias del vector, de marcadores de superficie (figura 16), de expresión (figura 17) y secreción (figura 18) de VIP. Finalmente se analizó la estabilidad del VIP secretado (figura 19) así como la capacidad de diferenciación (figuras 20, 21 y 22) y de inmunosupresión (figura 23) de las células modificadas genéticamente:

A) Análisis fenotipico:

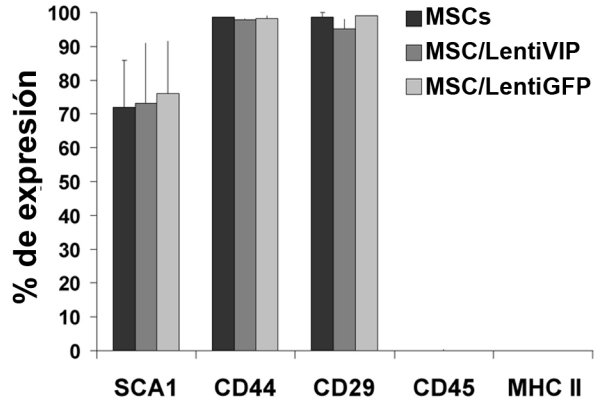

Figura 16: Fenotipo de las MSCs transducidas y sin .transducir. Los datos corresponden a al menos 3 líneas celulares de entre 4 y 8 pases. Comprobamos que las MSC transducidas mantenían el fenotipo de las MSC sin modificar.

B) Expresión de VIP por MSC/LentiVIP:

En primer lugar se determinó la estabilidad de expresión del vector. Se analizó los niveles de mensajero de VIP procedente del vector en MSC transducidas con dos MOIs diferentes y crecidas durante 5, 8 y 15 pases (figura 17). Los datos mostraron una reducción en los niveles de expresión de casi 10 veces desde pase 5 a pase 8, aunque estos niveles eran mantenidos constantes desde el pase 8 a pase 15, evidenciando un proceso de silenciamiento sólo en los primeros pases después de la transducción.

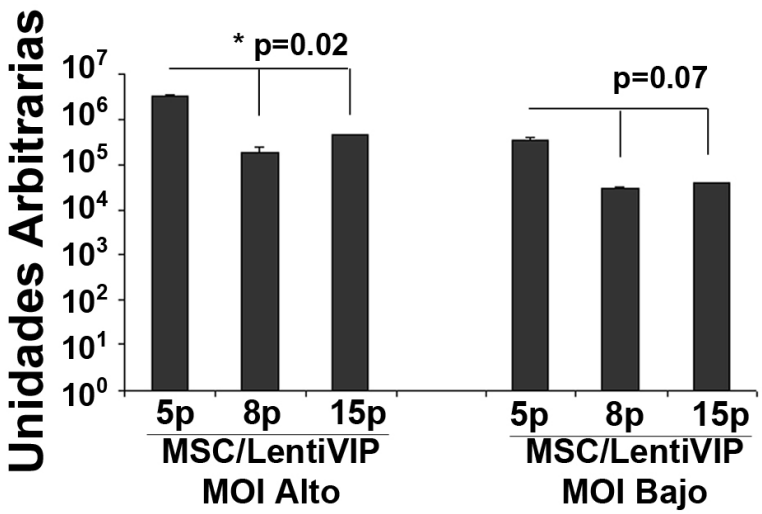

Figura 17: Expresión de VIP por las MSC/LentiVIP con los pases. El rARN se extrajo y se trato con DNasa, antes de hacer la reverso-transcripción. Una vez obtenido el cDNA se realizó la qPCR como se indica en materiales y métodos Se utilizó actina como normalizador y como calibrador, células MSC no transducidas. Se analizaron dos líneas con diferentes MOIs alto o bajo. La normalización se realizó frente a células MSCs no transducidas y se representa como unidades arbitrarias.

A continuación se analizó si las MSC transducidas con LentiVIP eran capaces de secretar VIP. La figura 18 muestra los resultados obtenidos mediante ELISA donde se observa secreción de VIP solo en las MSC transducidas por el vector.

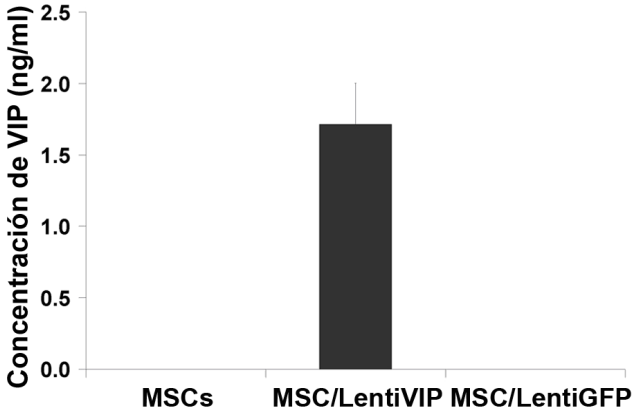

Figura 18: Expresión de VIP por las MSCs. La grafica muestra la concentración en ng/ml de VIP secretado por las MSCs, MSCs transducidas con LentiVIP (MSC/LentiVIP) y MSC transducidas con LentieGFP (MSC/lentiGFP).

C) Estudio de la estabilidad del VIP secretado por las MSC/LentiVIP.

Una particularidad de muchas proteínas/péptidos secretados (incluido VIP) es el encontrase en diferentes formas una vez secretados, resultado de la actuación de proteasas. Estas diferentes formas tienen diferente estabilidad y actividad. Una vez demostrada la bioactividad del producto expresado por LentiVIP (ver figura 12), quisimos comparar la estabilidad del producto secretado por las MSC/LentiVIP con la estabilidad de VIP sintético. Para ello se recogieron sobrenadantes de células MSC/LentiVIP. Como control de VIP sintético se utilizó sobrenadantes de MSC no transdudidas a las que se les añadió 5ng/ml de péptido VIP sintético. Ambos sobrenadantes fueron incubados a 37ºC durante 0, 6, 24 y 48 horas (figura 19), analizando por ELISA la presencia de VIP tras estas incubaciones. Los datos mostraron que el VIP secretado por las células mesenquimales (SN MSC/LentiVIP) era más estable que el VIP péptido sintético comercial.

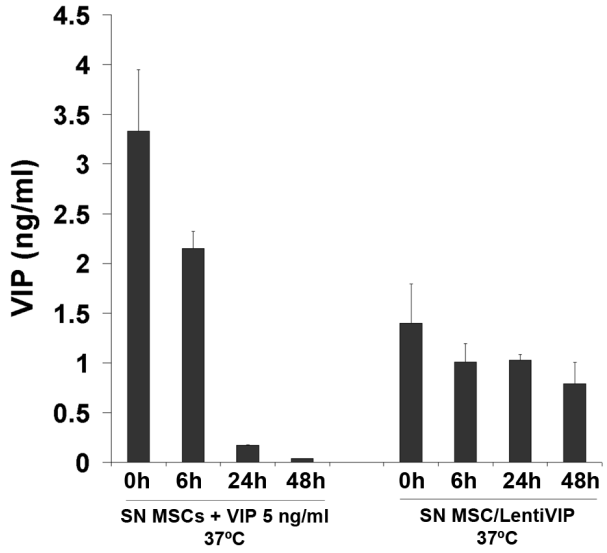

Figura 19: Estabilidad del VIP secretado a 37ºC. Sobrenadantes de células MSC/LentiVIP (SN MSC/LentiVIP) y 5ng/ml de VIP sintético resuspendido en sobrenadantes de MSC no transdudidas (SN MSC + VIP 5ng/ml) fueron incubados a 37 grados durante 0, 6, 24 y 48 horas. Las graficas muestran la concentración de VIP que permanecía sin degradarse en el sobrenadante en cada uno de los tiempos de incubación.

D) Capacidad de diferenciación de las células MSCs.

Una característica principal de las MSCS es su capacidad de diferenciación a adipositos, osteocitos y condrocitos. Por lo tanto decidimos estudiar si el proceso de modificación genética y/o la sobreexpresión de VIP alteraban esta capacidad de las MSC. Por lo tanto siguiendo el protocolo descrito en materiales y métodos, de cada línea de MSCs que se obtuvo con su correspondientes MSC/LentiVIP y MSC/LentiGFP se realizaron las diferenciaciones a adipocitos (figura 20), osteocitos (figura 21) y condrocitos (figura 22).

D1) Diferenciación a adipocitos.

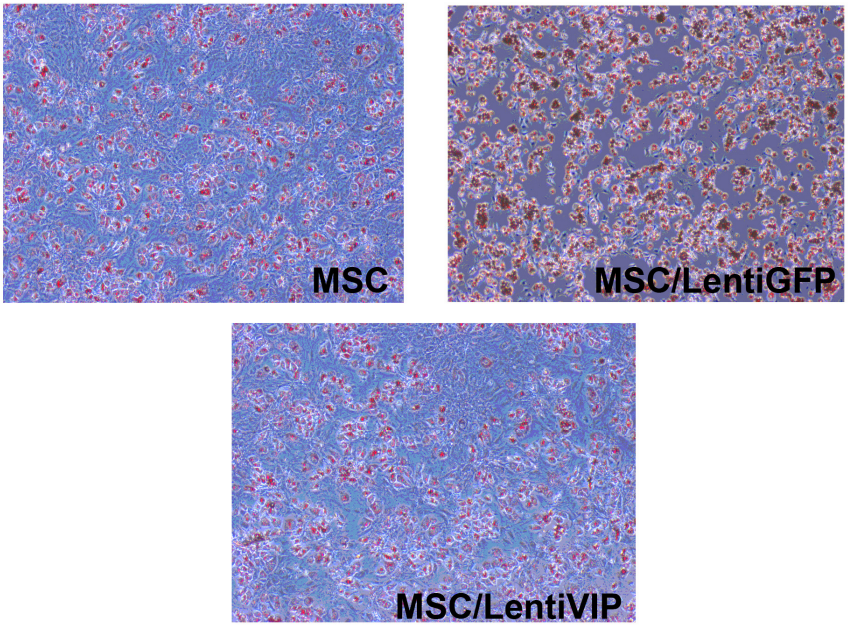

Figura 20: Diferenciación a adipocitos de las MSCs. MSC, MSC/LentiGFP y MSC/LentiVIP se incubaron en medio de diferenciación para adipogénesis (ver material y métodos). Tras 2 semanas se apreciaban al microscopio óptico las vesículas lipídicas típicas de células adipocíticas. Las fotografías muestran las diferentes MSC diferenciadas a adipositos tras su tinción con Oil Red.

D2) Diferenciación a osteocitos.

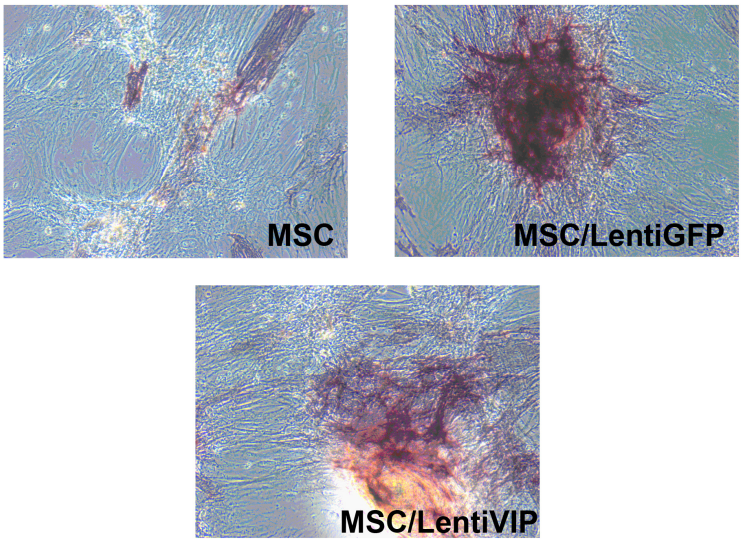

Figura 21: Diferenciación a osteocitos e las MSCs. MSC, MSC/GFP y MSC/LentiVIP se incubaron en medio de diferenciación para osteogénesis (ver material y métodos). Tras 10 días se apreciaba al microscopio óptico la típica matriz ramificada que acompaña a los osteocitos. Las fotografías muestran las diferentes MSC diferenciadas a osteocitos tras su tinción con SIGMA FAST BCIP/NBT.

D3) Diferenciación a condrocitos.

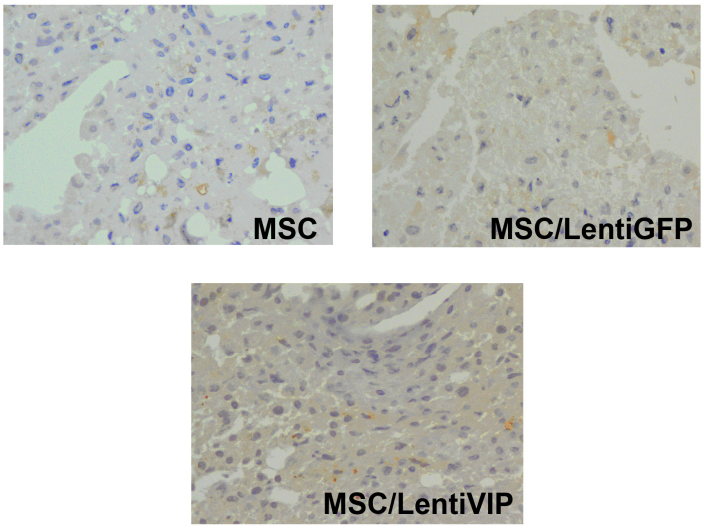

Figura 22: Diferenciación a condrocitos de las MCSs. MSC, MSC/GFP y MSC/LentiVIP se incubaron en medio de diferenciación para condrogénesis (ver material y métodos). Tras 21 días, el precipitado producido por las MSC diferenciadas se recogió para su fijación y tinción. Las fotografías muestran cortes histológicos de las diferentes MSC diferenciadas a condrocitos tras su tinción con el anticuerpo contra la proteína S100.

Es importante destacar que en ninguno de los caso se observaron diferencias significativas entre las células provenientes de una misma línea, aunque si se observaron entre líneas diferentes, debido quizás al número de pases.

E) Capacidad inmunosupresora de las MSCs.

Finalmente se procedió a analizar si la transducción de las MSCs afectaba a la capacidad inmunosupresora de las MSCs. Para ello se realizó el mismo experimento de proliferación de células de bazo utilizado en la Figura 15, solo que en este caso se realizó una comparativa de las diferentes líneas (MSC, MSC/LentiGFP y MSC/LentiVIP. La figura 23 muestra como todas las MSC, modificadas con los LVs o no, mantienen la misma capacidad inmunosupresora de proliferación de célula T. Interesantemente comprobamos que al transducir las MSCs con los vectores LentiVIP, no sólo no se veía disminuida su capacidad sino que siempre se veía un poco incrementada aunque no llegaba a ser significativo.

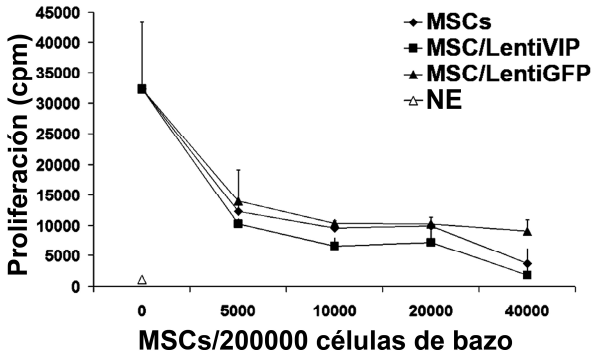

Figura 23: Capacidad inmunosupresora de las MSCs transducidas con vectores lentivirales. Células MSCs, MSC/LentiGFP y MSC/LentiVIP se enfrentaron a células T (procedentes de bazo) activadas con PMA. En ausencia de inhibidores, las células T proliferan e incorporan timidina tritriada (35000 cuentas por minuto=máxima proliferación). En la gráfica se observa como todas las MSC inhiben la proliferación de las células T de manera dosis dependiente, aunque la inhibición con las MSC/LentiVIP era un poco mejor, aunque no significativo.

4. Terapia celular-génica de EAE.

4.1. Experimento de terapéutica en EAE en el pico de la enfermedad. Seguimiento.

Una vez demostrada la capacidad de las células MSC/lentiVIP de producir VIP de forma estable y de mantener las características fenotípicas y de inmunosupresión, nos decidimos a evaluar su potencial terapéutico. Primero realizamos un ensayo para estudiar la migración de células MSC/LentiGFP por vía intravenosa y vía intraperitoneal, no encontrando diferencias significativas en los órganos donde hallamos las células, y decidiéndonos finalmente por la vía i.p., por su facilidad de administración (datos no mostrados).

Puesto que las MSCs han demostrado su eficiencia cuando se administran en las fases iniciales de la enfermedad, nosotros nos centramos en analizar el potencial terapéutico de las MSC/lentiVIP cuando se administran a animales con alto grado de EAE (>3; parálisis de las patas traseras y parcial de las delanteras). Se hicieron cuatro grupos de 10 animales (grado medio de 3.3 en todos los grupos), un grupo control (al que se le inyectó PBS), otro tratado con MSCs, otro con MSC/LentiGFP, y otro con MSC/LentiVIP (figura 24). Se inocularon $1x10^6$ células por vía intraperitoneal (i.p.) a cada ratón. Las células MSC/LentiVIP secretaban una media de 2 ng/ml de VIP.

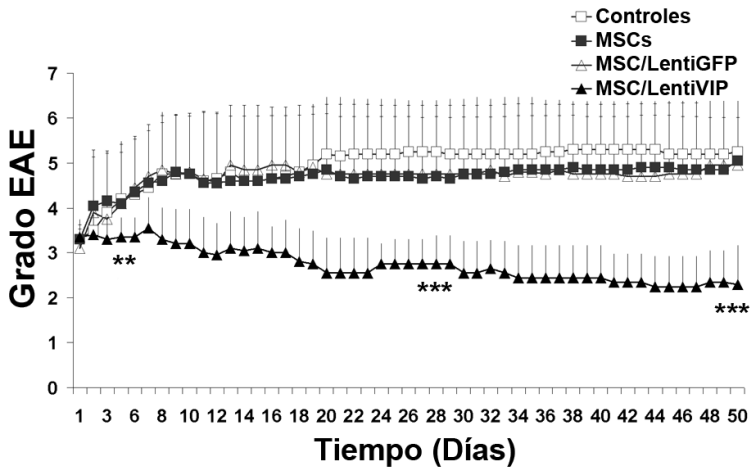

Figura 24: Actividad terapéutica de las MSC/LentiVIP en el modelo crónico de EAE. Ratones C57BL/6 inoculados con MOG (ver material y métodos) desarrollaron EAE severo. A los 15 días post-inoculación (día 1 en la grafica) se hicieron cuatro grupos de 10 animales con un grado medio de

3.3 en todos los grupos; un grupo control (cuadrados blancos), otro tratado con MSCs (cuadrados negros), otro con MSC/LentiGFP (triángulos blancos), y otro con MSC/LentiVIP (triángulos negros). El grado de enfermedad se determinó cada 2 días por un periodo de 50 dias. ** $p<0.01$, *** $p<0.001$

Sólo vimos un efecto terapéutico con el tratamiento de MSC/LentiVIP, el cual no solo evitó la progresión de la enfermedad, sino que recuperó la movilidad parcialmente de las patas traseras de los ratones tratados. Además al final del experimento obtuvimos una supervivencia del 100 % en los animales tratados con MSC/lentiVIP, mientras que solamente el 30% (grupo control), 50% (grupo MSC) y 40% (grupo MSC/LentiGFP) de los ratones sobrevivió en los otros grupos, ya que tuvieron que ser sacrificados por su mal estado. Estos datos se correlacionan con el índice de enfermedad acumulado (CDI), el cual es de 131±32 en los tratados con MSC/LentiVIP(p=0,001), comparado con los no tratados (245±60), tratados con MSC (226±65) y MSC/LentiGFP (227±74) (Tabla 3).

Día post-tratamiento	Día 0			Día 50			CDI (Indice de enfermedad acumulado)
Grado EAE	medio	moderado	severo	medio	moderado	severo	
No tratados	30%	50%	20%	0%	20%	80%	245.45±60.31
MSC	20%	70%	10%	0%	0%	100%	226.25±64.65
MSC/LentiGFP	40%	50%	10%	30%	0%	70%	227.25±73.95
MSC/LentiVIP	30%	60%	10%	70%	20%	10%	130.75±32.32

Tabla 3: Resumen de los grados de EAE en los diferentes grupos de tratamiento. Los grados se han clasificado en medio (1-2.5), moderado (3-3.5) y severo (4-6). El día 0 es el día del tratamiento donde los grupos se realizaron homogéneamente conteniendo ratones en grados desde 2,5 a 4. El índice de enfermedad acumulado (CDI) se calculó sumando los grados diariamente de cada ratón hasta el día 50 post-tratamiento. Los datos son la media ± DEM (n=10)

4.2. Distribución de VIP.

Para estudiar la distribución de las MSC/LentiVIP, se realizaron q-PCR tanto de expresión de VIP como de inserciones en genómico de diferentes órganos (tabla 2). Fue interesante comprobar que éramos capaces de detectar tanto integraciones del vector (tabla 4) como expresión del mismo (datos no mostrados) en el sistema linfoide (ganglios linfáticos y bazo) y en el SNC (cerebro y médula espinal)

	Hígado	Bazo	Ganglios Linfáticos	Cerebro	Médula Espinal	Riñón	Pulmón
MSC/LentiVIP	+	+	+	+	+	+	-

Tabla 4: Distribución del VIP proveniente de las MSC/LentiVIP. El signo + significa presencia, y el – ausencia. Gracias a la utilización de MSCs como vehículo del vector, además de cómo agente terapéutico, conseguimos llegar al SNC.

4.3. Estudio del efecto terapéutico a nivel periférico.

Dado el incremento en beneficio terapéutico observado con las MSC/LentiVIP (comparado con las MSCs), decidimos analizar los factores involucrados. En primer lugar analizamos el efecto a nivel periférico (regulación de la repuesta T en órganos linfoides periféricos) sobre las células T autorreactivas (especificas para MOG) y sobre las células T reguladoras. Para ello, en un nuevo experimento, se sacrificaron tres ratones de cada grupo (los grupos se hicieron siguiendo los mismos criterios que en el experimento de terapéutica) 7 días post-tratamiento para su análisis.

Efecto del tratamiento sobre las células T antígeno específicas.

EAE es una enfermedad mediada por linfocitos T autorreactivos. Puesto que VIP tiene la capacidad de inhibir la repuesta T autorreactiva, esto podría ser una posible explicación de las diferencias entre los tratamientos MSC/LentiVIP y MSC. Analizamos por tanto la respuesta específica a MOG (autorreactiva)

mediante ensayo de proliferación de células de ganglios linfáticos de drenaje (conteniendo las células T) (figura 25).

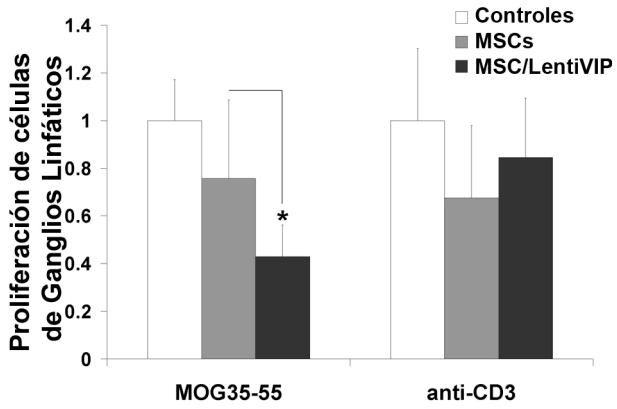

Figura 25: Estudio de la respuesta T MOG específica en los ganglios linfáticos de drenaje. Células de ganglios linfáticos provenientes de ratones con EAE tratados con MSC (barras grises), MSC/lentiVIP (barras negras) o sin tratamiento (barras claras) fueron extraídas 7 días post-inoculación. Los ratones tenían un grado EAE =3.2 en el momento de la inoculación de las células. La capacidad de las células T de proliferar en presencia de MOG fue determinada por incorporación de timidina tritiada (ver material y métodos). La gráfica representa datos relativos a la proliferación obtenida en ratones con EAE sin tratamiento (valor =1, barras blancas). * $p<0.05$. Como control se realizó el mismo experimento de proliferación utilizando anti-CD3 (parte derecha de la gráfica).**-**Los valores corresponden a la media de 9 ratones por grupo ± DEM

Los datos mostraron una disminución significativa ($p<0.05$) de la respuesta MOG específica sólo en los ratones tratados con MSC/LentiVIP, indicando que, al menos parte del efecto terapéutico de estas células se debe a una reducción del proceso autoinmune. Es interesante hacer notar que, en este estadío de la enfermedad, las MSC no lograron disminuir la respuesta MOG-específica de manera significativa, indicando que el efecto era debido en parte a la secreción de VIP por las células MSC/lentiVIP. El efecto conseguido tras estimular con anti-CD3 es similar en los 3 grupos, por lo que el número de linfocitos de los diferentes grupos es similar.

Efecto en la generación de Tregs.

Como esta descrito, tanto VIP como las MSCs son capaces de generar células Treg[157, 158]por lo que estudiamos a nivel de ganglios linfáticos de drenaje y de bazo las poblaciones TCD4+ FoxP3. Para ello se tiñeron con un anticuerpo anti-FoxP3-PE (phycoerythrin) y con anti-CD4 en FITC. (fluorescein isothiocyanate).

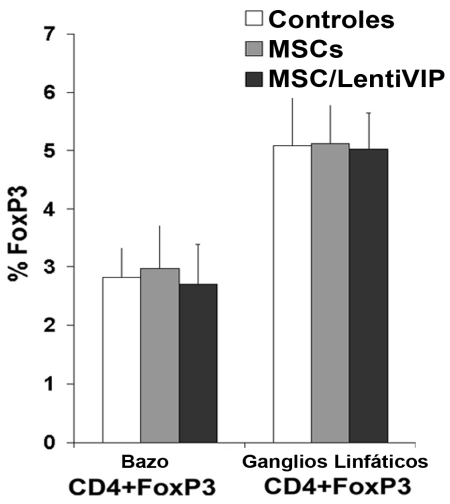

Figura 26: Porcentajes de TCD4$^+$FoxP3$^+$ en bazo y nódulos linfáticos de ratones tratados con MSCs. Células de bazo y ganglios linfáticos provenientes de ratones con EAE tratados con MSC (barras grises), MSC/lentiVIP (barras negras) o sin tratamiento (barras claras) fueron extraídas 7 días post-inoculación. Los ratones tenían un grado EAE =3.2 en el momento del tratamiento. Los porcentajes de células CD4$^+$Foxp3$^+$ fueron determinados por FACS (ver material y métodos). Los valores corresponden a la media de 8 ratones por grupo ± DEM

Aunque observamos una tendencia en el incremento del porcentaje de células totales expresando FoxP3 (datos no mostrados), no encontramos ningunas diferencias significativas en los porcentajes de células TCD4$^+$FoxP3$^+$.

4.4. Efecto del tratamiento a nivel del SNC

Además de un efecto periférico, a nivel de una reducción de la respuesta autoinmune, nuestra estrategia perseguía lograr efectos directos en el SNC, inhibiendo la neurodegeneración y/o promoviendo la neurorregeneración. Con esto en mente decidimos analizar el efecto de nuestro tratamiento en el SNC, tanto a nivel de cerebro como de medula espinal. Para ello ratones enfermos con EAE que habían sido tratados tal y como se describió anteriormente fueron sacrificados a día 7 (para histología y RT-q-PCR) o a día 50 (histología):

4.4.1. Análisis de expresión de ARNm en médula espinal a día 7 post-tratamiento.

Muestras de médula espinal de 3 ratones de cada grupo (MSC, MSC/lentiVIP, no tratados) se analizaron por RT-qPCR de diferentes marcadores para: 1- inflamación (IL17, IL6, iNOS, TNFα), 2- de regulación inmunológica (IL10, Foxp3) y 3- de neuroprotección (ADNP, Activity-Dependent-Neuroprotective-Protein), BDNF, Brain-Derived-Neurotrophic Factor).

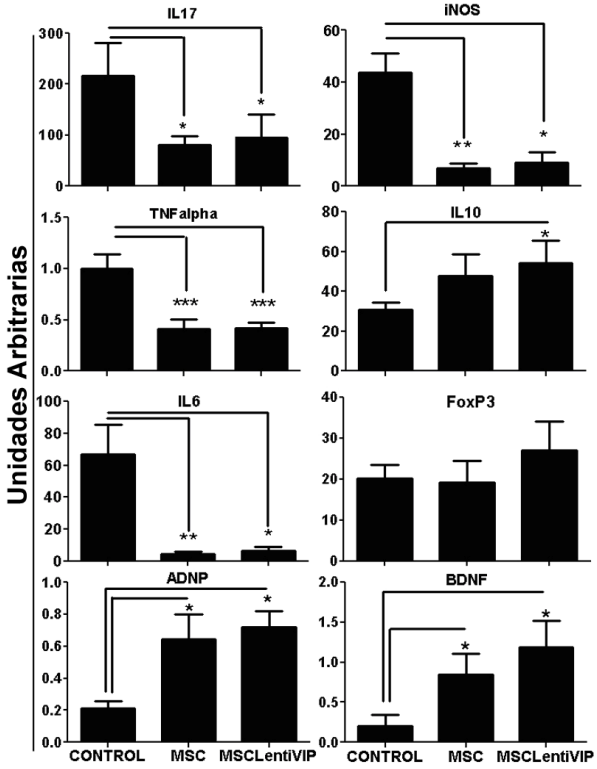

Figura 27: El tratamiento con MSC y MSC/LentiVIP reduce los niveles de citoquiinas pro-inflamatorias en incrementa los niveles de factores neuroprotectores. El ARNm fue extraído de médula espinal de ratones sin tratar (CONTROL), tratados con MSC (MSC) o tratados con MSC transducidos con LentiVIP (MSC/LentiVIP) sacrificados 7 días post-tratamiento. Los niveles de ARNm de citoquinas proinflamatorias (IL17, TNF-alpha, IL6), anti-inflamatorias (IL10), Tregs (FoxP3), estrés oxidativo (iNOS) y factores neuroprotectores (ADNP y BDNF) fueron determinados por RT-qPCR (ver material y métodos para detalles). Los datos mostrados son media ± DEM. (*$p<0.05$, ** $p<0.01$, ***$p<0.001$).

Aunque en todos los ratones tratados se ve una disminución en factores inflamatorios y un aumento en los reguladores y neuroprotectores, no pudimos detectar diferencias significativas entre los ratones tratados con MSCs y los tratados con MSC/LentiVIP. Sin embargo sí que pudimos observar una tendencia (no significativa tras el análisis estadístico) en el incremento de los niveles de IL10, FoxP3 y BDNF en ratones tratados con MSC/LentiVIP comparados con MSCs.

4.4.2. Análisis de inmunohistoquímico en cerebro

Los ratones tratados y controles se sacrificaron a día 7 y 50 post-tratamiento, y los cerebros se incluyeron en resina OCT. Secciones de estas inclusiones se tiñeron con distintos anticuerpos para estudiar astrogliosis (GFAP), infliltración de macrófagos o microglía (CD11b), degeneración neuronal (beta-amieloide), presencia de neuronas (beta-tubulinaIII). A 50 días post-tratamiento se analizó también la mielina.

Día 7 post-tratamiento

A)

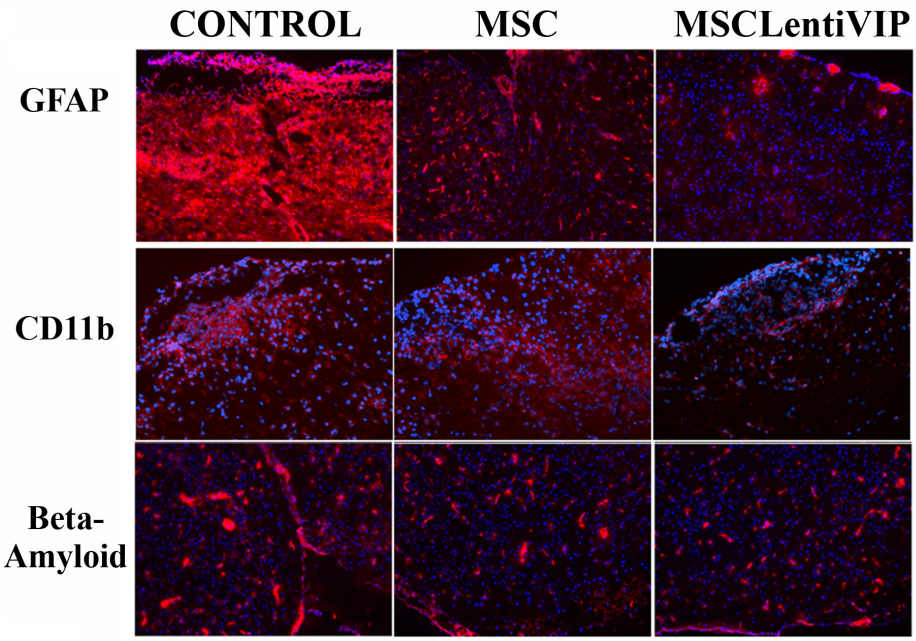

B)

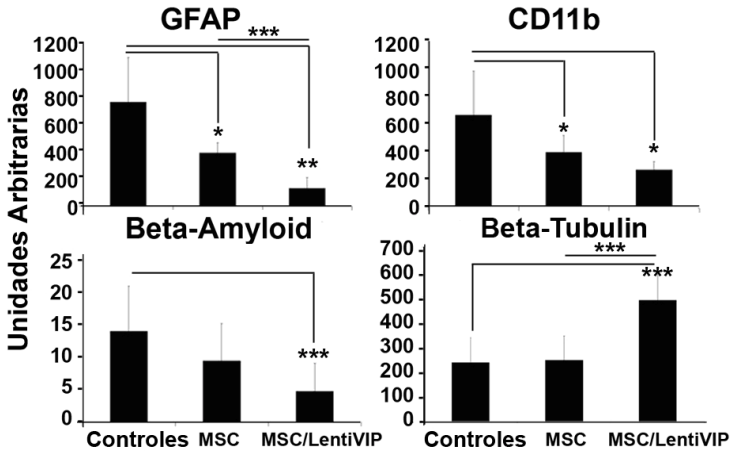

Figura 28: La administración de MSC/LentiVIP reduce astrogliosis y neurodegeneración en el SNC de ratones con EAE establecida Ratones con EAE con un grado de 3-3.5 fueron tratados con MSC, MSC/LentiVIP o dejados sin tratar (Control). Siete días después los ratones fueron sacrificados y los cerebros incluidos en resina OCT. Los cerebros fueron seccionados y teñidos para marcadores de astrogliosis (GFAP), macrofagos/glia (CD11b), degeneración neuronal (beta-amieloide) y marcadores neurales (beta-tubulina). Todos las muestras fueron teñidas con DAPI para visualizar los núcleos celulares A) Imágenes representativas de los cortes de cerebro en la zona del cortex de ratones sin tratar (paneles de la izquierda), tratados con MSC (paneles centrales) y tratados con

MSC/LentiVIP (paneles de la derecha) teñidos con los diferentes marcadores (indicados en la izquierda). B) Cuantificación de los diferentes marcadores tal y como se indica en material y métodos. (*p<0.05, ** p<0.01, ***p<0.001)

Estos análisis mostraron que, ya desde el día 7 de tratamiento, se puede observar una reducción significativa del daño neuronal (menos beta-amieloides y más beta-tubulina-III) y astrogliosis (menor GFAP) en los ratones tratados con MSC/LentiVIP en relación a los tratados con MSCs. Si bien es verdad que también se observa una reducción en los cuerpos beta-amieloides (indicativo de neurodegeneración) con las MSC, las diferencias con respecto al control no llegan a ser significativas.

Día 50 post-tratamiento.

Una vez terminado el experimento de seguimiento a los 50 días post-tratamiento, se sacrificaron los ratones y se obtuvieron los cerebros, que se incluyeron en resina de OCT para ver por inmunohistoquímica diferentes marcadores (figura 29).

A)

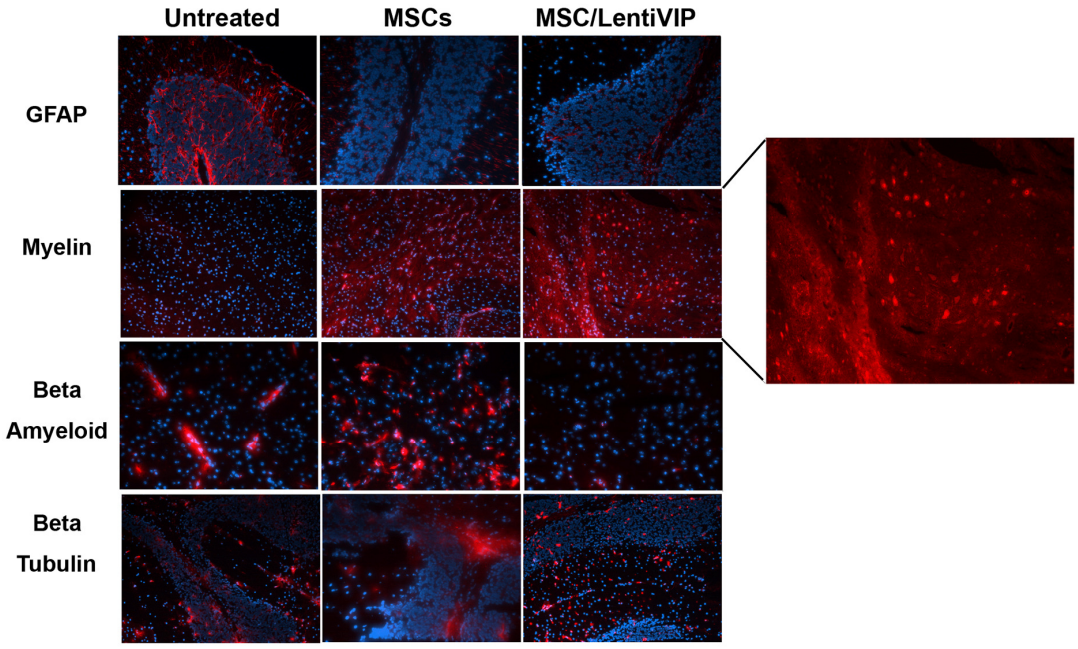

B)

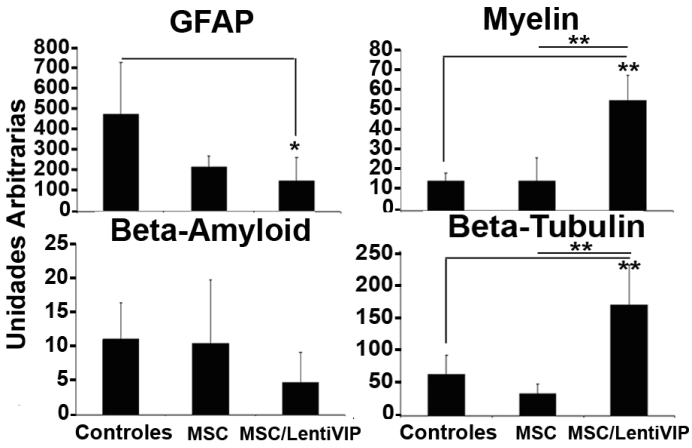

Figura 29: Análisis inmunohistoquímico del cerebro 50 días post-tratamiento. Los ratones del experimento de terapéutica fueron sacrificados a día 50 y sus cerebros incluidos en resina OCT. Los cerebros fueron seccionados y teñidos para marcadores de astrogliosis (GFAP), mielina (Mielina), degeneración neuronal (beta-amyloide) y marcadores neurales (beta-tubulina-III). Todas las muestras fueron teñidas con DAPI para visualizar los núcleos celulares A) Imágenes representativas de los cortes de cerebro en la zona del cortex de ratones sin tratar (paneles de la izquierda), tratados con MSC (paneles centrales) y tratados con MSC/LentiVIP (paneles de la derecha) teñidos con los diferentes marcadores (indicados a la izquierda). B) Cuantificación de los diferentes marcadores tal y como se indica en material y métodos. (*$p<0.05$, ** $p<0.01$, ***$p<0.001$)

Los resultados mostraron diferencias significativas en el tratamiento de MSC/LentiVIP con respecto MSCs, tanto en el aumento de mielina como en el número de neuronas. Estas diferencias muestran que las MSC/LentiVIP son mejores que las MSC, no solo reduciendo la actividad autoinmune en periferia sino que son capaces de inhibir el proceso de desmielinización y los procesos de neurodegeneración causantes de la invalidez de los ratones con EAE en las fases tardías.

5. Estudio de la genotoxicidad

La ausencia de formación de tumores en los ratones tratados con MSC/LentiVIP o MSC/lentiGFP indica que ni el proceso de transducción (con LentiGFP) ni la sobreexpresión de VIP tienen un efecto transformante fuerte en las MSC. Sin embargo, para transformar a las MSC se requieren múltiples pasos (activación de varios oncogenes). Esto implica que si nuestros vectores tienen una capacidad de transformación pequeña/mediana, seríamos incapaces de detectarlo. Con la finalidad de detectar de forma sensible los potenciales efectos genotóxicos (transformantes) de nuestros vectores LentiVIP en las MSC pensamos en desarrollar un modelo celular basado en células mesenquimales murinas pre-trasformadas (MSCp53$^{-/-}$p21$^{-/-}$). Estas células forman tumores unos 100 días después de su inoculación en ratones inmunodeficientes. Cualquier insulto que incremente la tumorigenicidad de estas células se reflejará en un incremento de la velocidad de aparición del tumor y/o del tamaño del mismo. Por otro lado ensayos *in Vitro* de crecimiento de colonias en agar, permiten también hacer una evaluación de los niveles de transformación de las diferentes líneas.

Con esto en mente, las MSCp53$^{-/-}$p21$^{-/-}$ fueron transducidas con LentiVIP y LentiGFP a altos MOIs (MOI >50), expandidas y analizadas mediante estos dos tipos de ensayo: 1- *In vivo*. Analizando la generación de tumores en ratones inmunodeficientes y 2- *in vitro*. Determinando la transformación celular por crecimiento en agar.

5.1. *In vivo.*

Para los análisis *In vivo* se utilizaron ratones inmunodeficientes de 1-2 semanas a los que administró las diferentes líneas celulares modificadas con altos MOIs de LentiVIP o LentiGFP. Tras la administración, los ratones fueron monitorizados cada 3-4 días durante un periodo de 5 meses. La Figura 30 muestra que el periodo de aparición medio de los tumores era de alrededor de 100 días y que no variaba en los diferentes grupos de manera significativa. Por lo tanto, ni la modificación genética (LentiGFP) ni la siobreexpresión de VIP producen alteraciones significativas en la tumorigenicidad de las células en nuestro modelo.

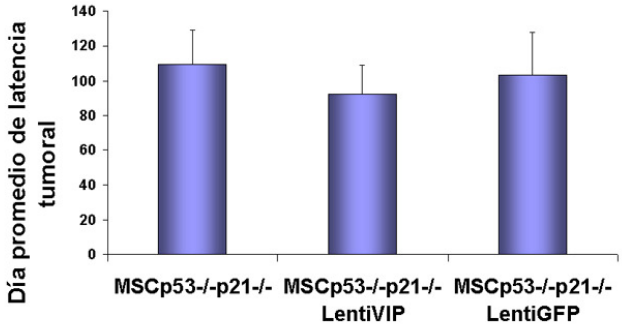

Figura 30: La modificación genética de las células MSCp53$^{-/-}$ p21$^{-/-}$ con LentiGFP y LentiVIP no incrementa la tumorigenicidad. Ratones NOD-SCID fueron inoculados vía s.c. con 5 millones de células MSCp53$^{-/-}$p21$^{-/-}$ controles (izquierda), MSCp53$^{-/-}$p21$^{-/-}$LentiVIP (centro) y MSCp53$^{-/-}$p21$^{-/-}$LentiGFP (derecha) en grupos de 7 ratones. En la gráfica se muestra el día medio de aparición tumoral de los 7 ratones inyectados.

5.2. *In vitro.*

Para estudiar la posibilidad de efectos en la transformación celular por nuestros LVs en estas células, procedimos a realizar un ensayo de trasformación celular mediante el estudio de formación de colonias en agar.

A)

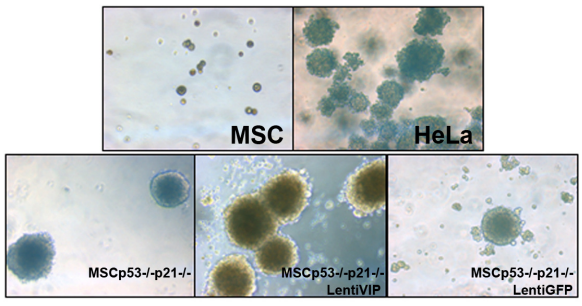

B)

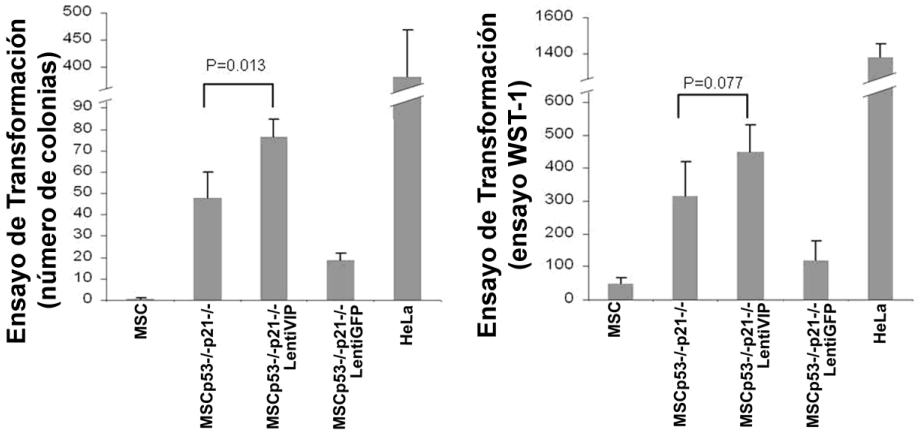

Figura 31: Estudio de trasformación celular en las MSCp53$^{-/-}$p21$^{-/-}$. A) Imágenes representativas de los clones formados en agar por los diferentes tipos celulares. B) Cuantificación de la transformación mediante dos métodos. La gráfica de la izquierda muestra el número de colonias formadas mediante contaje de cada una de éstas, mientras que la gráfica de la derecha muestra la cuantificación mediante WST-1 (sal de tetrazodio para estudiar viabilidad celular). En ambos casos se ha usado como control negativo una línea MSC (wild type), y como control positivo, HeLa (línea celular transformada).

En este modelo de transformación celular se observó un ligero incremento en el número de colonias de MSCp53$^{-/-}$p21$^{-/-}$LentiVIP respecto a las MSCp53$^{-/-}$p21$^{-/-}$ (figura 31A). Sin embargo, el ensayo de WST-1 (figura 31B) dio diferencias significativas. En el caso de MSCp53$^{-/-}$p21$^{-/-}$LentiGFP, se observa un inesperado retardo del crecimiento respecto a MSCp53$^{-/-}$p21$^{-/-}$. Estos datos podrían indicar una leve tendencia de los vectores LentiVIP a incrementar la formación de colonias en las células MSCp53$^{-/-}$p21$^{-/-}$. Sin embargo el hecho de que las células transducidas con LentiGFP no afecten a ninguno de los parámetros nos indica que, de haber efecto, este es debido a la expresión de VIP. Esto podría tener algún sentido dado que VIP puede inducir la expresión de metaloproteasas, favoreciendo la expansión de las células en agar.

E. DISCUSIÓN

La Esclerosis Múltiple, es una enfermedad crónica, cuya terapia actual sólo es capaz de aliviar los síntomas relacionados con el proceso inflamatorio, y además de ser parcialmente efectivos, conllevan efectos secundarios o toxicidad. Por ello, las estrategias terapéuticas deben buscar dos vías de actuación. Por un lado deben frenar el proceso inflamatorio/autoinmune, y por otro deben promover la neuroregeneración [22]

En la actualidad se están buscando nuevas estrategias terapéuticas que actúen sobre diferentes aspectos de la enfermedad, como a nivel de la barrera-hemato-encefálica[159], de bloqueo de la transcripción de citoquinas proinflamatorias [160], inhibiendo las respuestas Th1 y Th17[161], buscando factores neurotróficos[162], etc.

Sin embargo, la mayoría los ensayos clínicos que se están llevando a cabo en la actualidad, se basan en estrategias dirigidas a inmunomodular la respuesta linfocitaria únicamente y sólo son parcialmente eficaces en fases iniciales de la enfermedad, siendo ineficaces en las fases progresivas [163].

Por otro lado, la administración sistémica de un agente terapéutico sintético, además de resultar costosa, requiere la administración continuada de altas dosis para que llegue al sistema nervioso central (SNC) y/o a los órganos linfoides periféricos. Estas altas dosis suelen tener efectos secundarios muy graves a medio ó largo plazo.

La terapia génica, mediante el uso de vectores integrativos (retrovirales) podría ser de gran utilidad para solventar estos problemas, ya que permite una producción constante del agente terapéutico. Además, con la modificaciones pertinentes del vector, se podría lograr la expresión selectiva en los tejidos diana (órganos linfoides y SNC) [164].

Por ello en este trabajo, uno de los objetivos fue el de terapia génica de EAE, mediante un vector lentiviral capaz de expresar VIP (LentiVIP), para disminuir inflamación y proteger de la neurodegeneración característica de la fase crónica de la enfermedad. Nuestro laboratorio previamente publicó los beneficios terapéuticos de LentiVIP, en un modelo de artritis inducida por colágeno (CIA) [72], lo que nos llevó a pensar en su posible efecto terapéutico en un modelo más crónico de enfermedad autoinmune, como es el EM. Sin embargo, en el modelo crónico de EAE, no hemos visto efecto alguno.

Debemos tener en cuenta que se trata de dos modelos diferentes, y que en el caso de CIA, la inyección intraperitoneal de los vectores consiguió modificación genética de células presentes en las articulaciones (tejido diana del proceso autoinmune). Sin embargo en el modelo de EAE no fuimos capaces de llegar al SNC, lo cual podría explicar la ausencia de beneficio terapéutico. Además en CIA si conseguimos tener un efecto tanto a nivel anti-inflamatorio como inmunomodulador, generando un aumento en la población de células $TCD4^{+}FoxP3^{+}$, mientras que en EAE no vimos diferencias significativas en los diferentes grupos de tratamiento (datos no mostrados).

Una posible solución para la ausencia de expresión de VIP en el SNC dañado sería la inoculación de los vectores vía intratecal, combinada con otra que permita la actuación de VIP a nivel periférico (intraperitoneal). Sin embargo en nuestras manos los ratones en el pico de enfermedad, se encuentran tan delicados que no soportan una intervención de este tipo (datos no mostrados). Otros autores si han mostrado ciertos beneficios tras administración intratecal de vectores virales, aunque inoculados cuando la enfermedad no es tan severa. En el trabajo de Ruffini et al, expresan FGF-II (fibroblast growth factor) mediante virus derivados del herpes simples virus (HSV). El tratamiento se inicia en grado 1.7 (poca dificultad al andar y cola flácida) y consiguen una disminución de 0.5 grados. Sin embargo es un modelo poco severo, en el que los controles llegan a grado 2.5 al final del experimento[165]. Furlan y colaboradores, desarrollaron un HSV expresando IL4 para tratar le EAE-RR, encontrando una disminución en la duración de los ataques, el grado máximo alcanzado y un aumento en el periodo de remitencia[166]. Y por último Martino y colaboradores, desarrollan unos vectores HSV que expresan IL4, IL10 o IL1Ra, para tratamiento preventivo y al comienzo de la enfermedad encontrando mejoría en los ratones tratados [165-167]. Estos estudios demuestran la factibilidad de la administración intratecal como estrategia terapéutica para EAE. Por otro lado existen ensayos clínicos de EM usando esta vía para inocular diferentes drogas como gabapentina, baclofen[168] y rituximab, o células madre mesenquimales[127]. Esto sugiere que, utilizando los vectores y la ruta de administración adecuada se podría conseguir mejores resultados que los obtenidos mediante inoculación intraperitoneal utilizada en nuestro trabajo. En este sentido trabajos futuros encaminados a la administración directa de vectores deberían plantear el uso

combinado de administraciones intraperitoneales (modificación periférica de la respuesta inmune) con administraciones intratecales (modificación de los procesos inflamatorios y neurodegenerativos locales) de vectores altamente eficientes tales como los vectores lentivirales o los adenoasociados, más pequeños y que poseen tropismo natural hacia el SNC[169-171]

Como alternativa terapéutica para hacer llegar la expresión del transgén, podemos pensar en la utilización de vehículos celulares. Entre éstos podríamos pensar en células progenitoras de tipo neuronal (NSC), de oligodendrocitos (OPCs), mesenquimales (MSCs) o hematopoyéticos (HSCs). Todas estas células tienen una capacidad demostrada de migración hacia sitios de inflamación y/o daño tisular. Además, algunos de estos tipos celulares tienen la capacidad de remielinación y/o diferenciación a oligodendrocitos [172-176]. Sin embargo los datos clínicos y preclínicos muestran que el principal beneficio se obtiene mediante inhibición del proceso autoinmune[176-181]. Nosotros seleccionamos las células madre mesenquimales (MSC) por varias razones: 1- facilidad de obtención. Las MSCs se pueden obtener de diversas fuentes accesibles, como son la médula ósea, el tejido adiposo ó la sangre [182-184] , 2- facilidad de cultivo y expansión. Las células MSC crecen sin dificultad por más de 20 pases. 3- capacidad de inmunosupresión y neuroprotección[97, 107, 185-187]. En este sentido, se ha demostrado que la administración sistémica de MSCs tiene efectos terapéuticos claros en el modelo murino de EAE, sobre todo en las fases iniciales de la enfermedad[109, 188, 189].

En este trabajo hemos sido capaces de desarrollar un sistema sencillo para la producción de líneas MSC expresando VIP (MSC/LentiVIP) de manera constitutiva sin que se vean afectadas ninguna de sus propiedades básicas. La inoculación de MSC/LentiVIP en ratones con EAE severa mostró claros beneficios comparándolos con la administración de MSC o de MSC/LentiGFP. Efectivamente datos de otros grupos demuestran que para que las MSC tengan efecto terapéutico hay que administrarlas en las fase iniciales de la enfermedad o cuando no exista un grado muy severo (por debajo de 2). Efectivamente, cuando la enfermedad progresa a las fases más tardías (pico de enfermedad) la administración de MSC no tiene efecto a no ser que se administre en varias dosis [109, 189, 190].

Las principales diferencias que observamos entre la administración directa de los vectores lentivirales y la de las MSC/LentiVIP son, por un lado la presencia VIP (dirigida por el vector) en el SNC y por otro una menor respuesta Th1 antígeno específica contra MOG. Tanto VIP como las MSCs son capaces de producir anergia a través de la inducción de células dendríticas tolerogénicas [157, 191], pudiendo VIP arrestar el ciclo celular a diferentes niveles, por lo que podemos pensar que las MSC/LentiVIP, podrían inducir células T anérgicas, tanto al comienzo de la activación en los ganglios linfáticos como en la periferia o en el SNC. Sin embargo, nuestros datos experimentales no mostraron diferencias significativas en la generación de células $TCD4^{+}FoxP3^{+}$ (que podría inducirse por efecto de la expresión de VIP). Sin embargo si que encontramos un incremento leve de los niveles de ARNm de *foxp3* en médula espinal, aunque dicho incremento no alcanza significancia comparado con los tratados con MSC. VIP es capaz de inducir BDNF y ADNP, por lo que sería lógico pensar, que son estos factores los encargados de potenciar el efecto de las MSCs en esta fase de EAE, sin embargo, encontramos valores similares en ambos tratamientos.

Nuestros datos de expresión en médula espinal a día 7 post-tratamiento muestran que tanto los tratamientos con MSCs como con MSC/lentiVIP producen una disminución de factores inflamatorios y un aumento de factores neurotróficos, sin diferencias significativas entre ambos tratamientos. Sin embargo, los datos histológicos a día 7 y a día 50 post-tratamiento, muestran una menor infiltración de macrófagos/microglía (menor astrogliosis) así como un menor daño neuronal en los ratones tratados con MSC/LentiVIP. Un posible mecanismo del efecto diferencial entre los tratamientos de MSC y MSC/LentiVIP podría involucrar la actuación de VIP en microglía (a través de los receptores PAC1 y VPAC1) inhibiendo la secreción de citoquinas y quimoquinas pro-inflamatorias.[192] [60].

Existen otros estudios donde utilizan la terapia celular-génica para tratamiento de EAE. El realizado por T.K. Makar y colaboradores, se basa en una inoculación de HSCs obtenidas de médula ósea y transformadas con un vector retroviral que expresa IFNß. Aquí inoculan las células 6 semanas antes de inmunizar con PLP vía i.v en un modelo de EAE-RR. Los autores observaron una disminución media de casi un grado de los ratones tratados con respecto a los controles [193]. Lu Z. y colaboradores, inoculan células hMSC de médula

ósea 10 días post-inmunización sobreexpresando CNTF (ciliary neurothropic factor) mediante un adenovirus recombinate. Ven un retardo en la aparición y una disminución de los síntomas. Pero estos efectos no son significativamente diferentes con respecto a los controles[123]. Por lo que nuestro trabajo aporta un beneficio terapéutico mayor en un modelo más severo que los publicados hasta la fecha.

La introducción de varias copias de nuestros vectores en las MSCs no ha dado lugar en ninguno de los tratamientos animales a la formación de tumores. Sin embargo, para plantear una futura aplicación clínica de esta estrategia sería conveniente buscar un modelo que nos permita estudiar los posibles efectos genotóxicos de las transducciones en las MSCs. Para ello desarrollamos un modelo que nos permitiera detectar fenómenos genotóxicos con una alta sensibilidad. Para ello usamos células MSCs pretransformadas ($p53^{-/-}p21^{-/-}$) [156]. Estas células, al tener el ciclo celular alterado, son capaces de formar tumores tras su administración en ratones SCID con una latencia de entre 30-40 días y una incidencia del 50%. Cualquier alteración en la expresión génica de estas células que acelere la formación de tumores o que los haga más agresivos se verá reflejada en un incremento en la frecuencia o en la rapidez de aparición. Las células fueron transducidas con un MOI de 100 con la finalidad de forzar el sistema y detectar alteraciones como causa de la modificación genética a la que sometíamos las MSCs. Utilizando este sistema no fuimos capaces de encontrar incrementos significativos en la frecuencia y/o velocidad de aparición de los tumores cuando utilizamos vectores expresando eGFP, indicando que los vectores utilizados tienen un bajo potencial genotóxico. Sin embargo, cuando estas células se someten a un ensayo de transformación *in vitro*, encontramos diferencias significativas que indican un leve incremento de la transformación celularcuando las MSCs eran transducidas con los vectores expresando VIP, aunque no cuando las MSC eran transducidas con los vectores expresando eGFP. Este incremento en la capacidad de formación de colonias podría ser por tanto un efecto indirecto de la expresión de VIP en cuanto a su capacidad de formación de colonias que podría no ser representativo de procesos genotóxicos de la modificación génica

A pesar de haber conseguido un beneficio claro en esta fase de la enfermedad con respecto a los ensayos preclínicos publicados, existen varias maneras de mejorar el sistema desarrollado:

- Haciendo la expresión del vector regulable mediante la adición de doxiciclina, permitiéndonos una expresión del transgén controlada por la adición de la droga, sólo cuando la enfermedad lo requiera.

- Mejorando la migración de las MSCs hacia el lugar de daño, aumentando la expresión de los receptores de ciertas quimioquinas (CXCR4 y CXCR5), mediante la transducción con vectores lentivirales, que aumenten el efecto llamada al SNC dañado.

- Buscando otras células vehiculo como pueden ser las células madre hematopoyéticas (HSCs). Estas células migran muy activamente al SNC dañado donde son capaces de diferenciarse a microglía. Sin embargo, son más difíciles de expandir y aislar que las MSCs.

- Estudiando el efecto terapéutico de otros péptidos/genes con potencial inunoregulador y neuroprotector de características similares a VIP, como puede ser PACAP, o mediante la expresión conjunta de genes inmunomoduladores y neuroprotectores, mediante un sistema policistrónico.

F. CONCLUSIONES

1. Una única inyección intraperitoneal de vectores LentiVIP en el pico de la enfermedad en modelo crónico de EAE,no es suficiente para tener un efecto terapéutico, posiblemente por no llegar al SNC inflamado.

2. Las MSCs transducidas con LentiVIP, MSC/LentiVIP, son capaces de expresar y secretar VIP estable sin verse afectadas sus capacidades inmunomoduladoras y de diferenciación.

3. La administración intraperitoneal de MSC/LentiVIP en el pico de enfermedad en modelo crónico de EAE, no sóo evita la progresión de la enfermedad, sino que recupera la movilidad de las patas traseras de los animales tratados, efecto que se corrobora con una menor cantidad de respuesta Th1 autorreactiva en los ganglios linfáticos.

4. La administración intraperitoneal de MSC/LentiVIP en el pico de enfermedad en modelo crónico de EAE, reduce la inflamación, aumenta la expresión de factores neurotróficos y reduce la degeneración neuronal en el SNC inflamado.

G. REFERENCIAS

REFERENCIAS

1. Sospedra, M. and R. Martin, *Immunology of multiple sclerosis.* Annu Rev Immunol, 2005. **23**: p. 683-747.
2. Greenamyre, J.R.C.a.T., *The role of environmental exposures in neurodegeneration and neurodegenerative diseases.* Toxicological Sciences, 2011.
3. Kallaur, A.P., et al., *Genetic polymorphisms associated with the development and clinical course of multiple sclerosis (review).* Int J Mol Med. **28**(4): p. 467-79.
4. de Sa, J.C., et al., *Symptomatic therapy in multiple sclerosis: a review for a multimodal approach in clinical practice.* Ther Adv Neurol Disord. **4**(3): p. 139-68.
5. Compston, A. and A. Coles, *Multiple sclerosis.* The Lancet, 2008. **372**(9648): p. 1502-1517.
6. Burns, J., et al., *Isolation of myelin basic protein-reactive T-cell lines from normal human blood.* Cell Immunol, 1983. **81**(2): p. 435-40.
7. Tsuchida, T., et al., *Autoreactive CD8+ T-cell responses to human myelin protein-derived peptides.* Proc Natl Acad Sci U S A, 1994. **91**(23): p. 10859-63.
8. Sakaguchi, S., et al., *FOXP3+ regulatory T cells in the human immune system.* Nat Rev Immunol. **10**(7): p. 490-500.
9. Goverman, J., *Autoimmune T cell responses in the central nervous system.* Nat Rev Immunol, 2009. **9**(6): p. 393-407.
10. Zhu, J., H. Yamane, and W.E. Paul, *Differentiation of effector CD4 T cell populations (*).* Annu Rev Immunol. **28**: p. 445-89.
11. Iwakura, Y., et al., *The roles of IL-17A in inflammatory immune responses and host defense against pathogens.* Immunol Rev, 2008. **226**: p. 57-79.
12. Mosmann, T.R., et al., *Two types of murine helper T cell clone. I. Definition according to profiles of lymphokine activities and secreted proteins.* J Immunol, 1986. **136**(7): p. 2348-57.
13. Fujio, K., T. Okamura, and K. Yamamoto, *The Family of IL-10-secreting CD4+ T cells.* Adv Immunol. **105**: p. 99-130.

14. Kebir, H., et al., *Human TH17 lymphocytes promote blood-brain barrier disruption and central nervous system inflammation.* Nat Med, 2007. **13**(10): p. 1173-5.
15. Giovanni, F., et al., *Circulating CD8+CD56â¯perforin+ T cells are increased in multiple sclerosis patients.* Journal of Neuroimmunology, (0).
16. Haile, Y., et al., *Granule-Derived Granzyme B Mediates the Vulnerability of Human Neurons to T Cell-Induced Neurotoxicity.* The Journal of Immunology. **187**(9): p. 4861-4872.
17. Huang, W.X., et al., *Apoptosis mediators FasL and TRAIL are upregulated in peripheral blood mononuclear cells in MS.* Neurology, 2000. **55**(7): p. 928-934.
18. McFarland, H.F. and R. Martin, *Multiple sclerosis: a complicated picture of autoimmunity.* Nat Immunol, 2007. **8**(9): p. 913-9.
19. Elyaman, W., et al., *Potential application of tregitopes as immunomodulating agents in multiple sclerosis.* Neurol Res Int. **2011**: p. 256460.
20. Compston, A. and A. Coles, *Multiple sclerosis.* Lancet, 2008. **372**(9648): p. 1502-17.
21. John, G.R., et al., *Multiple sclerosis: re-expression of a developmental pathway that restricts oligodendrocyte maturation.* Nat Med, 2002. **8**(10): p. 1115-21.
22. Hohlfeld, R., *Myelin failure in multiple sclerosis: breaking the spell of Notch.* Nat Med, 2002. **8**(10): p. 1075-6.
23. Chari, D.M., A.J. Crang, and W.F. Blakemore, *Decline in rate of colonization of oligodendrocyte progenitor cell (OPC)-depleted tissue by adult OPCs with age.* J Neuropathol Exp Neurol, 2003. **62**(9): p. 908-16.
24. Niehaus, A., et al., *Patients with active relapsing-remitting multiple sclerosis synthesize antibodies recognizing oligodendrocyte progenitor cell surface protein: implications for remyelination.* Ann Neurol, 2000. **48**(3): p. 362-71.

25. Franklin, R.J., *Why does remyelination fail in multiple sclerosis?* Nat Rev Neurosci, 2002. **3**(9): p. 705-14.
26. Sherman, L.S. and S.A. Back, *A 'GAG' reflex prevents repair of the damaged CNS.* Trends Neurosci, 2008. **31**(1): p. 44-52.
27. Limmroth, V., N. Putzki, and N.J. Kachuck, *The interferon beta therapies for treatment of relapsingâ€“remitting multiple sclerosis: are they equally efficacious? A comparative review of open-label studies evaluating the efficacy, safety, or dosing of different interferon beta formulations alone or in combination.* Therapeutic Advances in Neurological Disorders. **4**(5): p. 281-296.
28. Pucci, E., et al., *Natalizumab for relapsing remitting multiple sclerosis.* Cochrane Database Syst Rev. **10**: p. CD007621.
29. Lalive, P.H., et al., *Glatiramer Acetate in the Treatment of Multiple Sclerosis: Emerging Concepts Regarding its Mechanism of Action.* CNS Drugs. **25**(5): p. 401-414 10.2165/11588120-000000000-00000.
30. Buck, D. and B. Hemmer, *Treatment of multiple sclerosis: current concepts and future perspectives.* Journal of Neurology: p. 1-16.
31. Barten, L.J., et al., *New approaches in the management of multiple sclerosis.* Drug Des Devel Ther. **4**: p. 343-66.
32. Rivers, T.M., D.H. Sprunt, and G.P. Berry, *Observations on Attempts to Produce Acute Disseminated Encephalomyelitis in Monkeys.* J Exp Med, 1933. **58**(1): p. 39-53.
33. Krishnamoorthy, G. and H. Wekerle, *EAE: an immunologist's magic eye.* Eur J Immunol, 2009. **39**(8): p. 2031-5.
34. Denic, A., et al., *The relevance of animal models in multiple sclerosis research.* Pathophysiology. **18**(1): p. 21-9.
35. Teitelbaum, D., et al., *Suppression of experimental allergic encephalomyelitis by a synthetic polypeptide.* European Journal of Immunology, 1971. **1**(4): p. 242-248.
36. Yednock, T.A., et al., *Prevention of experimental autoimmune encephalomyelitis by antibodies against [alpha]4[beta]1 integrin.* Nature, 1992. **356**(6364): p. 63-66.

37. t Hart, B.A., B. Gran, and R. Weissert, *EAE: imperfect but useful models of multiple sclerosis.* Trends Mol Med. **17**(3): p. 119-25.

38. Lassmann, H. and R.M. Ransohoff, *The CD4-Th1 model for multiple sclerosis: a critical [correction of crucial] re-appraisal.* Trends Immunol, 2004. **25**(3): p. 132-7.

39. Said, S.I. and V. Mutt, *Polypeptide with broad biological activity: isolation from small intestine.* Science, 1970. **169**(951): p. 1217-8.

40. Dejda, A., P. Sokolowska, and J.Z. Nowak, *Neuroprotective potential of three neuropeptides PACAP, VIP and PHI.* Pharmacol Rep, 2005. **57**(3): p. 307-20.

41. Delgado, M., D. Pozo, and D. Ganea, *The Significance of Vasoactive Intestinal Peptide in Immunomodulation.* Pharmacological Reviews, 2004. **56**(2): p. 249-290.

42. Itoh, N., et al., *Human preprovasoactive intestinal polypeptide contains a novel PHI-27-like peptide, PHM-27.* Nature, 1983. **304**(5926): p. 547-9.

43. Tan, Y.V., et al., *Peptide agonist docking in the N-terminal ectodomain of a class II G protein-coupled receptor, the VPAC1 receptor. Photoaffinity, NMR, and molecular modeling.* J Biol Chem, 2006. **281**(18): p. 12792-8.

44. Harmar, A.J., *Family-B G-protein-coupled receptors.* Genome Biol, 2001. **2**(12): p. REVIEWS3013.

45. Kolakowski, L.F., Jr., *GCRDb: a G-protein-coupled receptor database.* Receptors Channels, 1994. **2**(1): p. 1-7.

46. Chorny, A., et al., *Signaling mechanisms of vasoactive intestinal peptide in inflammatory conditions.* Regul Pept, 2006. **137**(1-2): p. 67-74.

47. Yadav, M. and E.J. Goetzl, *Vasoactive Intestinal Peptide–Mediated Th17 Differentiation.* Annals of the New York Academy of Sciences, 2008. **1144**(1): p. 83-89.

48. Bandyopadhyay, A., S. Chakder, and S. Rattan, *Regulation of inducible and neuronal nitric oxide synthase gene expression by*

interferon-gamma and VIP. Am J Physiol, 1997. **272**(6 Pt 1): p. C1790-7.

49. Delgado, M. and D. Ganea, *Inhibition of endotoxin-induced macrophage chemokine production by VIP and PACAP in vitro and in vivo.* Arch Physiol Biochem, 2001. **109**(4): p. 377-82.
50. Delgado, M., J. Leceta, and D. Ganea, *Vasoactive intestinal peptide and pituitary adenylate cyclase-activating polypeptide inhibit the production of inflammatory mediators by activated microglia.* J Leukoc Biol, 2003. **73**(1): p. 155-64.
51. Delgado, M., et al., *Vasoactive intestinal peptide and pituitary adenylate cyclase-activating polypeptide enhance IL-10 production by murine macrophages: in vitro and in vivo studies.* J Immunol, 1999. **162**(3): p. 1707-16.
52. Delgado, M., et al., *Vasoactive intestinal peptide and pituitary adenylate cyclase-activating polypeptide prevent inducible nitric oxide synthase transcription in macrophages by inhibiting NF-kappa B and IFN regulatory factor 1 activation.* J Immunol, 1999. **162**(8): p. 4685-96.
53. Delgado, M., J. Leceta, and D. Ganea, *Vasoactive intestinal peptide and pituitary adenylate cyclase-activating polypeptide promote in vivo generation of memory Th2 cells.* FASEB J, 2002. **16**(13): p. 1844-6.
54. Delgado, M., et al., *Vasoactive intestinal peptide and pituitary adenylate cyclase-activating polypeptide stimulate the induction of Th2 responses by up-regulating B7.2 expression.* J Immunol, 1999. **163**(7): p. 3629-35.
55. Gonzalez-Rey, E., P. Anderson, and M. Delgado, *Emerging roles of vasoactive intestinal peptide: a new approach for autoimmune therapy.* Annals of the Rheumatic Diseases, 2007. **66**(suppl_3): p. iii70-iii76.
56. Delgado, M., E. Gonzalez-Rey, and D. Ganea, *The neuropeptide vasoactive intestinal peptide generates tolerogenic dendritic cells.* J Immunol, 2005. **175**(11): p. 7311-24.

57. Ganea, D., R. Rodriguez, and M. Delgado, *Vasoactive intestinal peptide and pituitary adenylate cyclase-activating polypeptide: players in innate and adaptive immunity.* Cell Mol Biol (Noisy-le-grand), 2003. **49**(2): p. 127-42.

58. Gonzalez-Rey, E., et al., *Vasoactive intestinal peptide induces CD4+,CD25+ T regulatory cells with therapeutic effect in collagen-induced arthritis.* Arthritis Rheum, 2006. **54**(3): p. 864-76.

59. Kim, W.K., D. Ganea, and G.M. Jonakait, *Inhibition of microglial CD40 expression by pituitary adenylate cyclase-activating polypeptide is mediated by interleukin-10.* J Neuroimmunol, 2002. **126**(1-2): p. 16-24.

60. Delgado, M., N. Varela, and E. Gonzalez-Rey, *Vasoactive intestinal peptide protects against β-amyloid-induced neurodegeneration by inhibiting microglia activation at multiple levels.* Glia, 2008. **56**(10): p. 1091-1103.

61. Gozes, I., et al., *From vasoactive intestinal peptide (VIP) through activity-dependent neuroprotective protein (ADNP) to NAP: a view of neuroprotection and cell division.* J Mol Neurosci, 2003. **20**(3): p. 315-22.

62. Brenneman, D.E., *Neuroprotection: A comparative view of vasoactive intestinal peptide and pituitary adenylate cyclase-activating polypeptide.* Peptides, 2007. **28**(9): p. 1720-1726.

63. Korkmaz, O., et al., *Vasoactive Intestinal Peptide (VIP) Treatment of Parkinsonian Rats Increases Thalamic Gamma-Aminobutyric Acid (GABA) Levels and Alters the Release of Nerve Growth Factor (NGF) by Mast Cells.* Journal of Molecular Neuroscience. **41**(2): p. 278-287.

64. Keino, H., et al., *Prevention of experimental autoimmune uveoretinitis by vasoactive intestinal peptide.* Archives of ophthalmology, 2004. **122**(8): p. 1179-1184.

65. Fernandez-Martin, A., et al., *VIP prevents experimental multiple sclerosis by downregulating both inflammatory and autoimmune components of the disease.* Ann N Y Acad Sci, 2006. **1070**: p. 276-81.

66. Gonzalez-Rey, E., et al., *Therapeutic effect of vasoactive intestinal peptide on experimental autoimmune encephalomyelitis: down-regulation of inflammatory and autoimmune responses.* Am J Pathol, 2006. **168**(4): p. 1179-88.

67. Camelo, S., et al., *Protective effect of intravitreal injection of vasoactive intestinal peptide-loaded liposomes on experimental autoimmune uveoretinitis.* J Ocul Pharmacol Ther, 2009. **25**(1): p. 9-21.

68. Jimeno, R., et al., *New insights into the role of VIP on the ratio of T-cell subsets during the development of autoimmune diabetes.* Immunol Cell Biol. **88**(7): p. 734-45.

69. Abad, C., et al., *Therapeutic effects of vasoactive intestinal peptide in the trinitrobenzene sulfonic acid mice model of Crohn's disease.* Gastroenterology, 2003. **124**(4): p. 961-71.

70. Tuncel, N., et al., *Vasoactive intestinal peptide inhibits degranulation and changes granular content of mast cells: a potential therapeutic strategy in controlling septic shock.* Peptides, 2000. **21**(1): p. 81-9.

71. Delgado, M., et al., *Vasoactive intestinal peptide prevents experimental arthritis by downregulating both autoimmune and inflammatory components of the disease.* Nat Med, 2001. **7**(5): p. 563-8.

72. Delgado, M., et al., *In vivo delivery of lentiviral vectors expressing vasoactive intestinal peptide complementary DNA as gene therapy for collagen-induced arthritis.* Arthritis Rheum, 2008. **58**(4): p. 1026-37.

73. Li, H., et al., *Vasoactive Intestinal Polypeptide Suppressed Experimental Autoimmune Encephalomyelitis by Inhibiting T Helper 1 Responses.* Journal of Clinical Immunology, 2006. **26**(5): p. 430-437.

74. Fernandez-Martin, A., et al., *VIP Prevents Experimental Multiple Sclerosis by Downregulating Both Inflammatory and Autoimmune Components of the Disease.* Annals of the New York Academy of Sciences, 2006. **1070**(1): p. 276-281.

75. Friedenstein, A.J., J.F. Gorskaja, and N.N. Kulagina, *Fibroblast precursors in normal and irradiated mouse hematopoietic organs.* Exp Hematol, 1976. **4**(5): p. 267-74.

76. Chamberlain, G., et al., *Concise review: mesenchymal stem cells: their phenotype, differentiation capacity, immunological features, and potential for homing.* Stem Cells, 2007. **25**(11): p. 2739-49.

77. Pittenger, M.F., et al., *Multilineage potential of adult human mesenchymal stem cells.* Science, 1999. **284**(5411): p. 143-7.

78. Kumar, B.M., et al., *Neurogenic and cardiomyogenic differentiation of mesenchymal stem cells isolated from minipig bone marrow.* Research in Veterinary Science, (0).

79. Goncalves, M.A.F.V., et al., *Transcription Factor Rational Design Improves Directed Differentiation of Human Mesenchymal Stem Cells Into Skeletal Myocytes.* Mol Ther. **19**(7): p. 1331-1341.

80. Alberton, P., et al., *Conversion of Human Bone Marrow-Derived Mesenchymal Stem Cells into Tendon Progenitor Cells by Ectopic Expression of Scleraxis.* Stem Cells Dev.

81. Lien, C.Y., O.K. Lee, and Y. Su, *Cbfb enhances the osteogenic differentiation of both human and mouse mesenchymal stem cells induced by Cbfa-1 via reducing its ubiquitination-mediated degradation.* Stem Cells, 2007. **25**(6): p. 1462-8.

82. Chabannes, D., et al., *A role for heme oxygenase-1 in the immunosuppressive effect of adult rat and human mesenchymal stem cells.* Blood, 2007. **110**(10): p. 3691-4.

83. Meisel, R., et al., *Human but not murine multipotent mesenchymal stromal cells exhibit broad-spectrum antimicrobial effector function mediated by indoleamine 2,3-dioxygenase.* Leukemia. **25**(4): p. 648-54.

84. Lee, J.W., et al., *Concise Review: Mesenchymal Stem Cells for Acute Lung Injury: Role of Paracrine Soluble Factors.* Stem Cells. **29**(6): p. 913-919.

85. Bianchi, G., et al., *Immunosuppressive cells and tumour microenvironment: focus on mesenchymal stem cells and myeloid derived suppressor cells.* Histol Histopathol. **26**(7): p. 941-51.

86. Gregory, J.L., et al., *Macrophage migration inhibitory factor induces macrophage recruitment via CC chemokine ligand 2.* J Immunol, 2006. **177**(11): p. 8072-9.

87. Ubogu, E.E., et al., *Determinants of CCL5-driven mononuclear cell migration across the blood-brain barrier. Implications for therapeutically modulating neuroinflammation.* J Neuroimmunol, 2006. **179**(1-2): p. 132-44.

88. Montecucco, F., et al., *Insulin primes human neutrophils for CCL3-induced migration: crucial role for JNK 1/2.* Ann N Y Acad Sci, 2006. **1090**: p. 399-407.

89. Spaeth, E., et al., *Inflammation and tumor microenvironments: defining the migratory itinerary of mesenchymal stem cells.* Gene Ther, 2008. **15**(10): p. 730-8.

90. Yagi, H., et al., *Mesenchymal stem cells: Mechanisms of immunomodulation and homing.* Cell Transplant. **19**(6): p. 667-79.

91. Krampera, M., et al., *Bone marrow mesenchymal stem cells inhibit the response of naive and memory antigen-specific T cells to their cognate peptide.* Blood, 2003. **101**(9): p. 3722-9.

92. Zanjani, E.D., et al., *Homing of human cells in the fetal sheep model: modulation by antibodies activating or inhibiting very late activation antigen-4-dependent function.* Blood, 1999. **94**(7): p. 2515-22.

93. Rafei, M., et al., *Mesenchymal stromal cells ameliorate experimental autoimmune encephalomyelitis by inhibiting CD4 Th17 T cells in a CC chemokine ligand 2-dependent manner.* J Immunol, 2009. **182**(10): p. 5994-6002.

94. Gonzalez-Rey, E., et al., *Human adipose-derived mesenchymal stem cells reduce inflammatory and T cell responses and induce regulatory T cells in vitro in rheumatoid arthritis.* Ann Rheum Dis. **69**(1): p. 241-8.

95. Aggarwal, S. and M.F. Pittenger, *Human mesenchymal stem cells modulate allogeneic immune cell responses.* Blood, 2005. **105**(4): p. 1815-22.

96. Sato, K., et al., *Nitric oxide plays a critical role in suppression of T-cell proliferation by mesenchymal stem cells.* Blood, 2007. **109**(1): p. 228-34.

97. Chan, J., et al., *Transplantation of bone marrow transduced to express self-antigen establishes deletional tolerance and permanently remits autoimmune disease.* J Immunol, 2008. **181**(11): p. 7571-80.

98. Spaggiari, G.M., et al., *Mesenchymal stem cells inhibit natural killer-cell proliferation, cytotoxicity, and cytokine production: role of indoleamine 2,3-dioxygenase and prostaglandin E2.* Blood, 2008. **111**(3): p. 1327-33.

99. Zhang, W., et al., *Implantation of adult bone marrow-derived mesenchymal stem cells transfected with the neurotrophin-3 gene and pretreated with retinoic acid in completely transected spinal cord.* Brain Res. **1359**: p. 256-71.

100. Maltman, D.J., S.A. Hardy, and S.A. Przyborski, *Role of mesenchymal stem cells in neurogenesis and nervous system repair.* Neurochemistry International. **In Press, Uncorrected Proof**.

101. Munoz, J.R., et al., *Human stem/progenitor cells from bone marrow promote neurogenesis of endogenous neural stem cells in the hippocampus of mice.* Proceedings of the National Academy of Sciences of the United States of America, 2005. **102**(50): p. 18171-18176.

102. Deng, W., et al., *In vitro differentiation of human marrow stromal cells into early progenitors of neural cells by conditions that increase intracellular cyclic AMP.* Biochem Biophys Res Commun, 2001. **282**(1): p. 148-52.

103. Hermann, A., et al., *Efficient generation of neural stem cell-like cells from adult human bone marrow stromal cells.* J Cell Sci, 2004. **117**(Pt 19): p. 4411-22.

104. Hung, S.C., et al., *In vitro differentiation of size-sieved stem cells into electrically active neural cells.* Stem Cells, 2002. **20**(6): p. 522-9.

105. Choong, P.F., et al., *Generating neuron-like cells from BM-derived mesenchymal stromal cells in vitro.* Cytotherapy, 2007. **9**(2): p. 170-83.

106. Sanchez-Ramos, J., et al., *Adult bone marrow stromal cells differentiate into neural cells in vitro.* Exp Neurol, 2000. **164**(2): p. 247-56.

107. Kassis, I., et al., *Neuroprotection and Immunomodulation With Mesenchymal Stem Cells in Chronic Experimental Autoimmune Encephalomyelitis.* Arch Neurol, 2008. **65**(6): p. 753-761.

108. Matysiak, M., et al., *Immunoregulatory function of bone marrow mesenchymal stem cells in EAE depends on their differentiation state and secretion of PGE2.* J Neuroimmunol. **233**(1-2): p. 106-11.

109. Constantin, G., et al., *Adipose-derived mesenchymal stem cells ameliorate chronic experimental autoimmune encephalomyelitis.* Stem Cells, 2009. **27**(10): p. 2624-35.

110. Myers, T.J., et al., *Mesenchymal stem cells at the intersection of cell and gene therapy.* Expert Opin Biol Ther. **10**(12): p. 1663-79.

111. Kanehira, M., et al., *Targeted delivery of NK4 to multiple lung tumors by bone marrow-derived mesenchymal stem cells.* Cancer Gene Ther, 2007. **14**(11): p. 894-903.

112. Studeny, M., et al., *Mesenchymal stem cells: potential precursors for tumor stroma and targeted-delivery vehicles for anticancer agents.* J Natl Cancer Inst, 2004. **96**(21): p. 1593-603.

113. Hall, B., et al., *Mesenchymal stem cells in cancer: tumor-associated fibroblasts and cell-based delivery vehicles.* Int J Hematol, 2007. **86**(1): p. 8-16.

114. Manning, E., et al., *Interleukin-10 delivery via mesenchymal stem cells: a novel gene therapy approach to prevent lung ischemia-reperfusion injury.* Hum Gene Ther. **21**(6): p. 713-27.

115. Dumont, R.J., et al., *Ex vivo bone morphogenetic protein-9 gene therapy using human mesenchymal stem cells induces spinal fusion in rodents.* Neurosurgery, 2002. **51**(5): p. 1239-44; discussion 1244-5.

116. Miyazaki, M., et al., *Comparison of human mesenchymal stem cells derived from adipose tissue and bone marrow for ex vivo gene therapy in rat spinal fusion model.* Spine (Phila Pa 1976), 2008. **33**(8): p. 863-9.

117. Liu, H., et al., *Neuroprotection by PlGF gene-modified human mesenchymal stem cells after cerebral ischaemia.* Brain, 2006. **129**(Pt 10): p. 2734-45.

118. Toyama, K., et al., *Therapeutic benefits of angiogenetic gene-modified human mesenchymal stem cells after cerebral ischemia.* Exp Neurol, 2009. **216**(1): p. 47-55.

119. Cheng, Z., et al., *Targeted migration of mesenchymal stem cells modified with CXCR4 gene to infarcted myocardium improves cardiac performance.* Mol Ther, 2008. **16**(3): p. 571-9.

120. Palmer, G.D., et al., *Gene-induced chondrogenesis of primary mesenchymal stem cells in vitro.* Mol Ther, 2005. **12**(2): p. 219-28.

121. Pagnotto, M.R., et al., *Adeno-associated viral gene transfer of transforming growth factor-beta1 to human mesenchymal stem cells improves cartilage repair.* Gene Ther, 2007. **14**(10): p. 804-13.

122. Kurozumi, K., et al., *BDNF gene-modified mesenchymal stem cells promote functional recovery and reduce infarct size in the rat middle cerebral artery occlusion model.* Mol Ther, 2004. **9**(2): p. 189-97.

123. Lu, Z., et al., *Overexpression of CNTF in Mesenchymal Stem Cells reduces demyelination and induces clinical recovery in experimental autoimmune encephalomyelitis mice.* J Neuroimmunol, 2009. **206**(1-2): p. 58-69.

124. Bai, L., et al., *Human bone marrow-derived mesenchymal stem cells induce Th2-polarized immune response and promote endogenous repair in animal models of multiple sclerosis.* Glia, 2009. **57**(11): p. 1192-203.

125. Kassis, I., et al., *Neuroprotection and immunomodulation with mesenchymal stem cells in chronic experimental autoimmune encephalomyelitis.* Arch Neurol, 2008. **65**(6): p. 753-61.
126. Garcia-Gomez, I., et al., *Mesenchymal stem cells: biological properties and clinical applications.* Expert Opin Biol Ther. **10**(10): p. 1453-68.
127. ClinicalTrials.gov., *A service of U.S. National Institutes of Health.*
128. Romero, Z., et al., *A tissue-specific, activation-inducible, lentiviral vector regulated by human CD40L proximal promoter sequences.* Gene Ther. **18**(4): p. 364-71.
129. Toscano, M.G., et al., *Physiological and tissue-specific vectors for treatment of inherited diseases.* Gene Ther. **18**(2): p. 117-27.
130. Baum, C., et al., *Retrovirus vectors: toward the plentivirus?* Mol Ther, 2006. **13**(6): p. 1050-63.
131. Schambach, A., et al., *Overcoming promoter competition in packaging cells improves production of self-inactivating retroviral vectors.* Gene Ther, 2006. **13**(21): p. 1524-33.
132. Martin, F., et al., *Retroviral vector targeting to melanoma cells by single-chain antibody incorporation in envelope.* Hum Gene Ther, 1998. **9**(5): p. 737-46.
133. Martin, F., et al., *Retrovirus targeting by tropism restriction to melanoma cells.* J Virol, 1999. **73**(8): p. 6923-9.
134. Delenda, C., *Lentiviral vectors: optimization of packaging, transduction and gene expression.* J Gene Med, 2004. **6 Suppl 1**: p. S125-38.
135. Delenda, C., M. Audit, and O. Danos, *Biosafety issues in lentivector production.* Curr Top Microbiol Immunol, 2002. **261**: p. 123-41.
136. Zufferey, R., et al., *Multiply attenuated lentiviral vector achieves efficient gene delivery in vivo.* Nat Biotechnol, 1997. **15**(9): p. 871-5.
137. Dull, T., et al., *A third-generation lentivirus vector with a conditional packaging system.* J Virol, 1998. **72**(11): p. 8463-71.

138. Martin, F., et al., *Lentiviral vectors transcriptionally targeted to hematopoietic cells by WASP gene proximal promoter sequences.* Gene Ther, 2005. **12**(8): p. 715-23.

139. Frecha, C., et al., *Improved lentiviral vectors for Wiskott-Aldrich syndrome gene therapy mimic endogenous expression profiles throughout haematopoiesis.* Gene Ther, 2008. **15**(12): p. 930-41.

140. Gossen, M., et al., *Transcriptional activation by tetracyclines in mammalian cells.* Science, 1995. **268**(5218): p. 1766-9.

141. Ogueta, S.B., F. Yao, and W.A. Marasco, *Design and in vitro characterization of a single regulatory module for efficient control of gene expression in both plasmid DNA and a self-inactivating lentiviral vector.* Mol Med, 2001. **7**(8): p. 569-79.

142. Benabdellah, K., et al., *Development of an All-in-One Lentiviral Vector System Based on the Original <italic>TetR</italic> for the Easy Generation of Tet-ON Cell Lines.* PLoS ONE. **6**(8): p. e23734.

143. Dressel, R., et al., *Multipotent adult germ-line stem cells, like other pluripotent stem cells, can be killed by cytotoxic T lymphocytes despite low expression of major histocompatibility complex class I molecules.* Biol Direct, 2009. **4**: p. 31.

144. Rosenzweig, M., et al., *Induction of cytotoxic T lymphocyte and antibody responses to enhanced green fluorescent protein following transplantation of transduced CD34(+) hematopoietic cells.* Blood, 2001. **97**(7): p. 1951-9.

145. Eixarch, H., et al., *Transgene Expression Levels Determine the Immunogenicity of Transduced Hematopoietic Grafts in Partially Myeloablated Mice.* Mol Ther, 2009. **17**(11): p. 1904-1909.

146. Laredj, L.N. and P. Beard, *Adeno-associated virus activates an innate immune response in normal human cells but not osteosarcoma cells.* J. Virol.: p. JVI.05407-11.

147. Zaiss, A.K., et al., *Complement is an essential component of the immune response to adeno-associated virus vectors.* J Virol, 2008. **82**(6): p. 2727-40.

148. Baum, C., et al., *Side effects of retroviral gene transfer into hematopoietic stem cells.* Blood, 2003. **101**(6): p. 2099-114.

149. Hacein-Bey-Abina, S., et al., *LMO2-associated clonal T cell proliferation in two patients after gene therapy for SCID-X1.* Science, 2003. **302**(5644): p. 415-9.

150. Check, E., *Gene therapy put on hold as third child develops cancer.* Nature, 2005. **433**(7026): p. 561.

151. Taganov, K.D., et al., *Integrase-specific enhancement and suppression of retroviral DNA integration by compacted chromatin structure in vitro.* J Virol, 2004. **78**(11): p. 5848-55.

152. Naldini, L., et al., *In vivo gene delivery and stable transduction of nondividing cells by a lentiviral vector.* Science, 1996. **272**(5259): p. 263-7.

153. Neil, S., et al., *Postentry restriction to human immunodeficiency virus-based vector transduction in human monocytes.* J Virol, 2001. **75**(12): p. 5448-56.

154. Frecha, C., et al., *Stable transduction of quiescent T cells without induction of cycle progression by a novel lentiviral vector pseudotyped with measles virus glycoproteins.* Blood, 2008. **112**(13): p. 4843-52.

155. Frecha, C., et al., *In vivo gene delivery into hCD34+ cells in a humanized mouse model.* Methods Mol Biol. **737**: p. 367-90.

156. Montini, E., et al., *The genotoxic potential of retroviral vectors is strongly modulated by vector design and integration site selection in a mouse model of HSC gene therapy.* J Clin Invest, 2009. **119**(4): p. 964-75.

157. Pozo, D., P. Anderson, and E. Gonzalez-Rey, *Induction of alloantigen-specific human T regulatory cells by vasoactive intestinal peptide.* J Immunol, 2009. **183**(7): p. 4346-59.

158. English, K., et al., *Cell contact, prostaglandin E(2) and transforming growth factor beta 1 play non-redundant roles in human mesenchymal stem cell induction of CD4+CD25(High) forkhead box P3+ regulatory T cells.* Clin Exp Immunol, 2009. **156**(1): p. 149-60.

159. Huang, X.N., J. Fu, and W.Z. Wang, *The effects of fasudil on the permeability of the rat bloodâ€“brain barrier and bloodâ€“spinal cord barrier following experimental autoimmune encephalomyelitis.* Journal of Neuroimmunology, (0).

160. Srinivasan, M. and S. Janardhanam, *Novel p65 binding GILZ peptide suppresses experimental autoimmune encephalomyelitis.* Journal of Biological Chemistry.

161. Grigorian, A., et al., *N-acetylglucosamine inhibits T-helper 1 (Th1) / T-helper 17 (Th17) responses and treats experimental autoimmune encephalomyelitis.* Journal of Biological Chemistry.

162. Quintanar, J.L., E. Salinas, and A.s. Quintanar-Stephano, *Gonadotropin-releasing hormone reduces the severity of experimental autoimmune encephalomyelitis, a model of multiple sclerosis.* Neuropeptides. **45**(1): p. 43-48.

163. Linker, R.A., B.C. Kieseier, and R. Gold, *Identification and development of new therapeutics for multiple sclerosis.* Trends Pharmacol Sci, 2008. **29**(11): p. 558-65.

164. Nabel, G.J., *Genetic, cellular and immune approaches to disease therapy: past and future.* Nat Med, 2004. **10**(2): p. 135-41.

165. Ruffini, F., et al., *Fibroblast growth factor-II gene therapy reverts the clinical course and the pathological signs of chronic experimental autoimmune encephalomyelitis in C57BL/6 mice.* Gene Ther, 2001. **8**(16): p. 1207-13.

166. Furlan, R., et al., *Central nervous system gene therapy with interleukin-4 inhibits progression of ongoing relapsing-remitting autoimmune encephalomyelitis in Biozzi AB/H mice.* Gene Ther, 2001. **8**(1): p. 13-9.

167. Martino, G., et al., *Cytokine therapy in immune-mediated demyelinating diseases of the central nervous system: a novel gene therapy approach.* Journal of Neuroimmunology, 2000. **107**(2): p. 184-190.

168. Harned, M.E., S.S. Salles, and J.S. Grider, *An introduction to trialing intrathecal baclofen in patients with hemiparetic spasticity: a description of 3 cases.* Pain Physician. **14**(5): p. 483-9.

169. Han, D., et al., *Prevention and treatment of experimental autoimmune encephalomyelitis with recombinant adeno-associated virus-mediated [alpha]-melanocyte-stimulating hormone-transduced PLP139-151-specific T cells.* Gene Ther, 2006. **14**(5): p. 383-395.

170. Guy, J., X. Qi, and W.W. Hauswirth, *Adeno-associated viral-mediated catalase expression suppresses optic neuritis in experimental allergic encephalomyelitis.* Proceedings of the National Academy of Sciences, 1998. **95**(23): p. 13847-13852.

171. Douglas B. Howard, K.P., 1 Yun Wang,1 and Brandon K. Harvey1, *Tropism and toxicity of adeno-associated viral vector serotypes 1,2,5,6,7,8,9 in rat neurons and glia in vitro.*

172. Picard-Riera, N., et al., *Experimental autoimmune encephalomyelitis mobilizes neural progenitors from the subventricular zone to undergo oligodendrogenesis in adult mice.* Proc Natl Acad Sci U S A, 2002. **99**(20): p. 13211-6.

173. Sanchez-Ramos, J.R., *Neural cells derived from adult bone marrow and umbilical cord blood.* J Neurosci Res, 2002. **69**(6): p. 880-93.

174. Pluchino, S., et al., *Injection of adult neurospheres induces recovery in a chronic model of multiple sclerosis.* Nature, 2003. **422**(6933): p. 688-94.

175. Davoust, N., et al., *Bone marrow CD34+/B220+ progenitors target the inflamed brain and display in vitro differentiation potential toward microglia.* Faseb J, 2006. **20**(12): p. 2081-92.

176. Burt, R.K., et al., *Autologous non-myeloablative haemopoietic stem cell transplantation in relapsing-remitting multiple sclerosis: a phase I/II study.* Lancet Neurol, 2009.

177. Mancardi, G. and R. Saccardi, *Autologous haematopoietic stem-cell transplantation in multiple sclerosis.* Lancet Neurol, 2008. **7**(7): p. 626-36.

178. Karussis, D., et al., *Immunomodulation and neuroprotection with mesenchymal bone marrow stem cells (MSCs): a proposed treatment for multiple sclerosis and other neuroimmunological/neurodegenerative diseases.* J Neurol Sci, 2008. **265**(1-2): p. 131-5.

179. Uccelli, A., F. Frassoni, and G. Mancardi, *Stem cells for multiple sclerosis: promises and reality.* Regen Med, 2007. **2**(1): p. 7-9.

180. Pluchino, S. and G. Martino, *The therapeutic plasticity of neural stem/precursor cells in multiple sclerosis.* J Neurol Sci, 2008. **265**(1-2): p. 105-10.

181. Einstein, O., et al., *Neural precursors attenuate autoimmune encephalomyelitis by peripheral immunosuppression.* Ann Neurol, 2007. **61**(3): p. 209-18.

182. Jung, S., et al., *Human mesenchymal stem cell culture: rapid and efficient isolation and expansion in a defined serum-free medium.* Journal of Tissue Engineering and Regenerative Medicine: p. n/a-n/a.

183. Yang, X.F., et al., *High efficient isolation and systematic identification of human adipose-derived mesenchymal stem cells.* J Biomed Sci. **18**: p. 59.

184. Chong, P.-P., et al., *Human peripheral blood derived mesenchymal stem cells demonstrate similar characteristics and chondrogenic differentiation potential to bone marrow derived mesenchymal stem cells.* Journal of Orthopaedic Research: p. n/a-n/a.

185. Tarner, I.H., et al., *Treatment of autoimmune disease by adoptive cellular gene therapy.* Ann N Y Acad Sci, 2003. **998**: p. 512-9.

186. Kaji, E.H. and J.M. Leiden, *Gene and stem cell therapies.* Jama, 2001. **285**(5): p. 545-50.

187. Zhang, J., et al., *Human bone marrow stromal cell treatment improves neurological functional recovery in EAE mice.* Experimental Neurology, 2005. **195**(1): p. 16-26.

188. Gerdoni, E., et al., *Mesenchymal stem cells effectively modulate pathogenic immune response in experimental autoimmune encephalomyelitis.* Annals of Neurology, 2007. **61**(3): p. 219-227.

189. Gordon, D., et al., *Human mesenchymal stem cells infiltrate the spinal cord, reduce demyelination, and localize to white matter lesions in experimental autoimmune encephalomyelitis.* J Neuropathol Exp Neurol. **69**(11): p. 1087-95.

190. Rafei, M., et al., *Allogeneic Mesenchymal Stem Cells for Treatment of Experimental Autoimmune Encephalomyelitis.* Mol Ther, 2009. **17**(10): p. 1799-1803.

191. Anderson, P. and E. Gonzalez-Rey, *Vasoactive intestinal peptide induces cell cycle arrest and regulatory functions in human T cells at multiple levels.* Mol Cell Biol. **30**(10): p. 2537-51.

192. Mario, D., *Vasoactive intestinal peptide and pituitary adenylate cyclase-activating polypeptide inhibit CBPâ€“NF-Î°B interaction in activated microglia.* Biochemical and Biophysical Research Communications, 2002. **297**(5): p. 1181-1185.

193. Makar, T.K., et al., *Stem cell based delivery of IFN-beta reduces relapses in experimental autoimmune encephalomyelitis.* J Neuroimmunol, 2008. 196(1-2): p. 67-81.

H. ANEXO PUBLICACIONES

HUMAN GENE THERAPY 19:179–197 (February 2008)

DOI: 10.1089/hum.2007.098

Hematopoietic-Specific Lentiviral Vectors Circumvent Cellular Toxicity Due to Ectopic Expression of Wiskott-Aldrich Syndrome Protein

MIGUEL G. TOSCANO,[1,2] CECILIA FRECHA,[1] KARIM BENABDELLAH,[1] MARIEN COBO,[1] MIKE BLUNDELL,[3] ADRIAN J. THRASHER,[3] ENRIQUE GARCÍA-OLIVARES,[2] IGNACIO J. MOLINA,[2,*] and FRANCISCO MARTIN[1,*]

ABSTRACT

Efficient and safe gene modification of hematopoietic stem cells is a requirement for gene therapy of primary immunodeficiencies such as Wiskott-Aldrich syndrome. However, deregulated expression or ectopic expression in the progeny of transduced nonhematopoietic progenitor cells may lead to unwanted toxicity. We therefore analyzed the effect of ectopic expression of Wiskott-Aldrich syndrome protein (WASp) and the potential benefits of hematopoietic-specific lentiviral vectors (driven by the *WAS* proximal promoter). Overexpression of WASp by constitutive lentiviral vectors is highly toxic in nonhematopoietic cells because it causes dramatic changes in actin localization and polymerization that result in decreased cell viability, as evidenced by a significant growth disadvantage of WASp-overexpressing nonhematopoietic cells and increased cell death. These toxic effects do not affect cells of hematopoietic origin because, remarkably, we found that WASp cannot be readily overexpressed in T cells, even after multiple vector integrations per cell. The adverse cellular effects found after transduction of nonhematopoietic cells with constitutive lentiviral vectors are overcome by the use of transcriptionally targeted lentiviral vectors expressing WASp, which, at the same time, are efficient tools for gene therapy of WAS as demonstrated by their ability to reconstitute cellular defects from WASp-deficient mouse and human cells. We therefore postulate that transcriptionally regulated lentiviral vectors represent a safer and efficient alternative for the development of clinical protocols of WAS gene therapy.

INTRODUCTION

The Wiskott-Aldrich syndrome (WAS) is characterized by profound and progressive immunodeficiency, eczema, and decreased numbers of platelets of typically reduced size (Thrasher, 2002). Patients with classical WAS have heterogeneous mutations in the *WAS* gene, which usually result in the lack of expression of its encoded gene product (Wiskott-Aldrich syndrome protein [WASp]), or otherwise give rise to nonfunctional truncated proteins. *WAS* expression is restricted to cells of hematopoietic origin (Stewart *et al*., 1996) including progenitor cells (Parolini *et al*., 1997). WASp localizes in the cytoplasm, where it plays a fundamental role in integrating various extracellular signals with cytoskeletal reorganization (Kolluri *et al*., 1996; Symons *et al*., 1996). WASp belongs to a family of proteins that also includes the ubiquitous neural WASp (N-WASp) and at least four forms of WAVE (WASp verprolin-homologous protein). The conserved COOH terminus of these proteins stimulates the Arp2/3 complex to nucleate actin filaments, which then elongate at their free barbed ends (Machesky *et al*., 1999). WASp is a self-regulated protein with a COOH-terminal VCA (verprolin homology, cofilin homology, acidic) domain that is sufficient to activate nucleation (Machesky *et al*., 1999), a GTPase-binding domain (GBD) that regulates WASp activity through Cdc42 binding, a polyproline domain (PPP) (Kolluri *et al*., 1996) that binds profilin as well as

[1]Immunology and Cell Biology Department, Institute of Parasitology and Biomedicine López Neyra, CSIC, Parque Tecnológico Ciencias de la Salud, 18100 Granada, Spain.
[2]Immunology Unit, Institute of Biopathology and Regenerative Medicine, University of Granada School of Medicine, 18012 Granada, Spain.
[3]Molecular Immunology Unit, Institute of Child Health, University College London, London WC1N 1EH, United Kingdom.
*I.J.M. and F.M. share credit for senior authorship.

proteins containing SH3 domains stabilizing the active conformation (Finan *et al*., 1996), and a WH1 (WASp homology domain-1) responsible for the binding of WIP (WASp-interacting protein) stabilizing the inactive conformation of WASp (Ramesh *et al*., 1997) .

WAS-deficient T cells have a restricted defect in CD3-mediated proliferative responses and actin polymerization after engagement of the T cell receptor (TCR)–CD3 complex (Molina *et al*., 1993; Gallego *et al*., 1997). In addition, other immune functions requiring cytoskeletal reorganization of effector cells such as chemotaxis (Badolato *et al*., 1998), phagocytosis (Leverrier *et al*., 2001), or natural killer (NK) lytic activity (Gismondi *et al*., 2004) are also compromised. WASp is also essential for the adequate function of $CD4^+CD25^+Foxp3^+$ regulatory T cells (Humblet-Baron *et al*., 2007; Maillard *et al*., 2007; Marangoni *et al*., 2007).

HLA-identical bone marrow transplantation is an effective treatment for this disease. However, most children lack such donors and many patients undergo HLA-mismatched allogeneic hematopoietic stem cell transplantation with less successful results. The potential of gene therapy for the treatment of primary immunodeficiencies has been demonstrated (Cavazzana-Calvo *et al*., 2000; Aiuti *et al*., 2002; Gaspar *et al*., 2004; Ott *et al*., 2006), but at the same time, undesired side effects indicate the need for improving vector safety (Hacein-Bey-Abina *et al*., 2003). In this context, the latest generation of lentiviral (LV) vectors are self-inactivating (SIN) and drive the expression of the transgene only through the internal promoter, facilitating the development of transcriptionally regulated cassettes (Moreau-Gaudry *et al*., 2001; Cui *et al*., 2002). In addition, studies have demonstrated that human immunodeficiency virus (HIV)-1-based vectors are safer than conventional non-SIN murine leukemia virus (MLV)-based oncoretroviral vectors, at least in terms of genotoxicity (Montini *et al*., 2006).

Considering the importance of WASp in cytoskeletal organization (Thrasher, 2002) and the existence of homologous proteins that exert the same functions in nonhematopoietic cells (Takenawa and Miki, 2001), ectopic expression of WASp is a significant concern for gene therapy of WAS patients, and therefore it should be avoided. In fact, overexpression of WASp family proteins correlates with poor prognosis of several types of tumors (Yamazaki *et al*., 2005; Marx, 2006; Semba *et al*., 2006; Yamaguchi and Condeelis, 2006; Yang *et al*., 2006). In addition, hematopoietic stem cells (HSCs) purified by $CD34^+$ or Lin^- immune selection can contain progenitors for other somatic lineages, and may even differentiate into or fuse with nonhematopoietic cells (Lagasse *et al*., 2000; Vassilopoulos *et al*., 2003; Chan and Yoder, 2004). To improve the biosafety of gene therapy of WAS, we (Martin *et al*., 2005) and others (Dupre *et al*., 2004) have developed hematopoietic-specific LV vectors expressing the human *WAS* cDNA driven by various fragments of the *WAS* internal promoter. The use of tissue-specific promoters should reduce genotoxicity by eliminating the potent enhancer activity of the commonly used viral long terminal repeat (LTR) and, at the same time, should reduce potential problems of ectopic expression of the transgene in nontarget cells. However, a clear picture has not yet emerged of the possible deleterious effects due to overexpression of WASp. In addition, there is limited experimental evidence directly demonstrating that the use of transcriptionally targeted vectors represents a relevant improvement in biosafety.

In this paper we study the potential adverse effects of ectopic WASp expression and whether the transcriptionally targeted HIV-1-based vectors would avoid those undesired effects, maintaining at the same time a vigorous therapeutic activity. We show that overexpression of WASp in nonhematopoietic cells reduces cell viability by disturbing the cytoskeleton, which is overcome by transduction of cells with transcriptionally targeted LV vectors. Interestingly, the observed adverse effects do not affect the hematopoietic lineage because WASp cannot be overexpressed in these cells.

MATERIALS AND METHODS

Cell lines and culture media

The generation and characterization of herpesvirus saimiri-immortalized T cells derived from a WAS patient (HVS-WAS/1) and a normal individual (HVS-NORMAL) have been previously described (Gallego *et al*., 1997). A primary allospecific T cell line from a second WAS patient (ALLO-WAS/2) was generated in our laboratory by coculture of patient T cells at a 1:1 ratio with mitomycin C-treated Raji B cells followed by weekly restimulations as described (Molina *et al*., 1992). Culture medium was RPMI 1640 supplemented with fetal calf serum (FCS; GIBCO-BRL, Middlesex, UK) to 10%, or fresh human serum (kindly provided by the Granada Regional Transfusion Center, Granada, Spain), glutamine, penicillin–streptomycin, and recombinant human interleukin-2 (IL-2; 50 IU/ml) (Hoffman-LaRoche, Nutley, NJ; kindly supplied by the AIDS Research and Reference Reagent Program, National Institutes of Health, Rockville, MD); decidual stromal cells (DSCs) were obtained from human decidua as described previously (Garcia-Pacheco *et al*., 2001).

Preparation and transduction of murine WAS-deficient immature dendritic cells and human macrophages

Bone marrow from age-matched *WAS* knockout (KO) or 129/Sv control mice was harvested and cultured in RPMI buffered with 25 m*M* HEPES with 10% FCS, penicillin (100 IU/ml), streptomycin (100 μg/ml), and L-glutamine. Recombinant murine granulocyte-macrophage colony-stimulating factor (GM-CSF; Peprotech, London, UK) was added to a final concentration of 25 ng/ml and the cells were incubated for 48 hr. Thereafter, the medium was changed to remove nonadherent cells and fresh medium containing GM-CSF (25 ng/ml) and recombinant murine IL-4 (10 ng/ml) was added for a further 4 days. To assess the differentiation of murine dendritic cells (DCs), cells were harvested and stained with anti-CD11c monoclonal antibody (HL3; BD Biosciences, San Jose, CA) labeled with fluorescein isothiocyanate (FITC) as previously described (de Noronha *et al*., 2005). Dendritic cells (10^5) were then seeded onto coverslips and infected with lentivirus at a multiplicity of infection (MOI) of 100.

Human macrophages were obtained from the peripheral blood of WAS patients as previously described (Neil *et al*., 2001), according to approved research protocols after obtaining informed consent, following institutional and national eth-

ical guidelines and with prior approval of the Ethics Committee of the University of Granada (Granada, Spain). Briefly, the mononuclear layer from treated blood was plated in RPMI–10% FCS to allow adherence. Suspension cells were washed and adherent cells were incubated in medium plus macrophage colony-stimulating factor (MCSF, 10 ng/ml). On day 6 macrophages were scraped off and used for transduction or staining.

Vectors

The HIV packaging plasmid (pCMVDR8.91) and VSV-G plasmid (pMD.G) are described elsewhere (Naldini *et al*., 1996; Zufferey *et al*., 1998). The HIV packaging plasmid pCMVDR8.91 encodes *gag*, *pol*, *tat*, and *rev* genes. The pMD.G plasmid encodes the vesicular stomatitis virus glycoprotein (VSV-G). The LV plasmid HRSIN-CSGW (SE) (Demaison *et al*., 2000) encodes the enhanced green fluorescent protein (eGFP) under the control of the spleen focus-forming virus (SFFV) promoter and contains the woodchuck postregulatory element (WPRE). The LV vector SW expressing the *WAS* gene was generated by replacing the *eGFP* cDNA in the SE vector for a full-length *WAS* cDNA from the WW vector (Martin *et al*., 2005). The SEW vector was generated by replacing the *eGFP* cDNA in the SE vector with the *eGFP-WAS* coding sequence from the Moloney-based retroviral vector plasmid (Burns *et al*., 2001). The WEW vector was generated by replacing the SFFV promoter in the SEW vector with a 500-bp fragment of the *WAS* proximal promoter in the WW vector (Martin *et al*., 2005). Vector production was performed as described elsewhere (Toscano *et al*., 2004). Briefly, 293T cells (6×10^6) were plated the day before transfection, and the vector, packaging, and envelope plasmids (total DNA, 27 μg; plasmid proportions of 3:2:1, respectively) were resuspended in 1.5 ml of Opti-MEM (GIBCO) mixed with 60 μl of Lipofectamine 2000 (Invitrogen, Carlsbad, CA) and diluted in 1.5 ml of Opti-MEM. The mixture was added to the 293T cells, which were incubated for 6–8 hr, washed, and cultured for an additional 48 hr. Viral supernatants were collected and filtered through a 0.45-μm (pore size) filter (Nalgene, Rochester, NY), aliquoted, and immediately frozen at −80°C.

Cell transduction and vector titration

Exponentially growing target cells were washed in phosphate-buffered saline (PBS) and seeded onto 24-well plates at a concentration of 2×10^5 cells per well in 500 μl of the appropriate medium. Vector supernatants were added to the culture and incubated overnight. For expression analysis of eGFP or eGFP–WASp, cells were analyzed 72 hr later, or at other time points if indicated, in a BD FACScan flow cytometer (BD Biosciences). For analysis of WASp-expressing vectors, the procedure was identical but the transduction efficiency was calculated by determining the vector copy number per cell by real-time polymerase chain reaction (PCR) (see below). Viral titers (transduction units [TU] per milliliter) were calculated on the basis of transduction of 293T cells by the various vectors. Each cell line was transduced at a predetermined MOI that allowed equivalent vector copy numbers among the different cells used in the panel, because the 293T cells or DSCs were four to six times more permissive than T cells (primary or HVS immortalized).

Proliferation assays

CD3-mediated proliferation. Primary T cells were used 10 days after allospecific stimulation and considered resting. ALLO-NORMAL, untransduced ALLO-WAS/2, as well as WE-transduced and WW-transduced ALLO-WAS/2 cells (5×10^4 cells per well) were cultured in 96-well plates coated with anti-CD3 antibody as well as in control plates coated with an irrelevant antibody (BD BioCoat Cellware; BD Biosciences). Cells were allowed to proliferate for 3 days in complete medium without exogenous IL-2 and assayed by the 3-(4,5-dimethylthiazol-2-yl)-2,5-diphenyltetrazolium bromide (MTT; Sigma-Aldrich, St. Louis, MO) colorimetric method as previously described in detail (Mosmann, 1983). Proliferation results are expressed as the increment in optical density (OD) readings (570 nm) of CD3-stimulated versus unstimulated cells.

Proliferation of growing cells. Cells transduced with the various vectors were harvested 7 days posttransduction and analyzed by the MTT assay as described above.

Immunostaining for microscopy and flow cytometry

For detection of WASp, cells were collected, washed, and permeabilized with BD Cytofix/Cytoperm (BD Biosciences) according to the manufacturer's recommendations. Cells were subsequently washed and preincubated for 20 min at 4°C in a PBS blocking solution containing 2% normal goat serum and 0.05% saponin. After washes, intracellular staining of WASp was carried out by indirect immunofluorescence, using 2 μg of anti-WASp monoclonal antibody B-9 (Santa Cruz Biotechnology, Santa Cruz, CA) diluted in 200 μl of blocking solution and incubated at 4°C for 1 hr with continuous agitation in an orbital shaker. Cells were washed in PBS–0.02% saponin and incubated again with 2 μg of phycoerythrin (PE)-labeled goat anti-mouse IgG antiserum (Invitrogen Caltag, Burlingame, CA) (diluted in PBS–0.05% saponin) for 45 min at 4°C with continuous agitation. Cells were washed twice in PBS–0.02% saponin followed by a final wash in PBS alone. Cells were analyzed in a FACScan flow cytometer.

For F-actin and vinculin staining of podosomes, dendritic cells or macrophages were fixed in PBS containing 4% paraformaldehyde, permeabilized with 0.1% Triton X, and blocked in PBS–1% bovine serum albumin (BSA) for 30 min. Cells were incubated with rhodamine-labeled phalloidin (1:50 dilution) (Invitrogen Molecular Probes, Leiden, The Netherlands) for 20 min to visualize F-actin and then with anti-vinculin antibody (hVIN-1 mouse IgG1 monoclonal, ascitic fluid used at 1:100 dilution; Sigma-Aldrich). Antibody binding was detected with a goat anti-mouse IgG conjugated to cyanine (Cy)-5 (for eGFP- or eGFP–WASp-expressing cells) or FITC (for WW- and SW-transduced cells) (Jackson ImmunoResearch Laboratories, West Grove, PA). Images were recorded with a Leica confocal microscope (TCS SP2; Leica Microsystems, Wetzlar, Germany) to obtain projections of 8–12 z sections. Images were processed with Photoshop (Adobe, San Jose, CA). F-actin staining in other cell types was carried out as described above, followed by examination of cells under a fluorescence or confocal microscope.

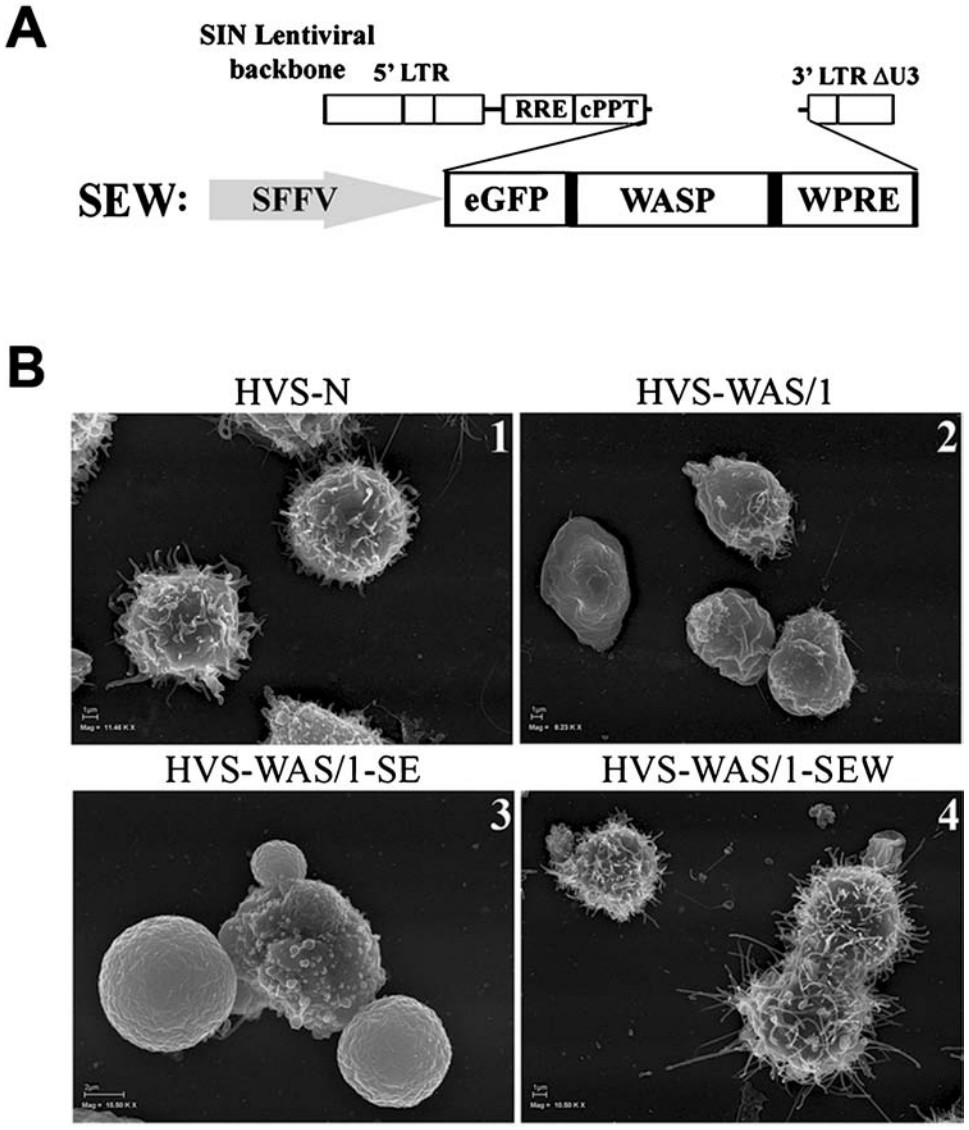

FIG. 1.

To discriminate live from dead cells, we incubated the various samples with 7-amino-actinomycin D (7-AAD; 5 μg/ml in PBS) for 20 min, washed them once with PBS, and analyzed them in a FACScan flow cytometer.

Scanning electron microscopy

Exponentially grown cells were harvested from culture and subjected to examination by scanning electron microscopy (SEM), as previously described (Gallego *et al*., 1997), at the Electron Microscopy Section of the Centro de Instrumentacion Científica (University of Granada). Briefly, normal and WAS HVS-T cells were washed in Ca^{2+}/Mg^{2+}-free PBS and allowed to bind to poly-L-lysine-coated slides simultaneously with the fixation process, which was achieved during an overnight incubation at 4°C in a glutaraldehyde vapor-saturated atmosphere. Cells were postfixed in 1% osmium tetroxide for 1 hr, dehydrated with graded ethanols, subjected to critical point drying from carbon dioxide, and finally coated with carbon. Cells were examined with a high-resolution field emission SEM microscope (LEO 1530 Gemini; LEO Electron Microscopy/Nano Technology Systems Division of Carl Zeiss NTS, Oberkochen, Germany). Percentages of reconstituted cells were determined by blind examination and counting of a minimum of 10 to 30 cells per field in randomly selected fields. Normal morphology requisites included rounded, homogeneous, and hairy cell surfaces and shapes shown by previously characterized HVS-NORMAL/1 cells (Gallego *et al*., 1997).

Quantitative Western blot

Cells were lysed with 1% Nonidet P-40 (NP-40) lysis buffer containing a protease inhibitor cocktail (Sigma-Aldrich), resolved by sodium dodecyl sulfate–polyacrylamide gel electrophoresis (SDS–PAGE; 10% polyacrylamide gels, reducing conditions), and electrotransferred to Hybond-P polyvinylidene

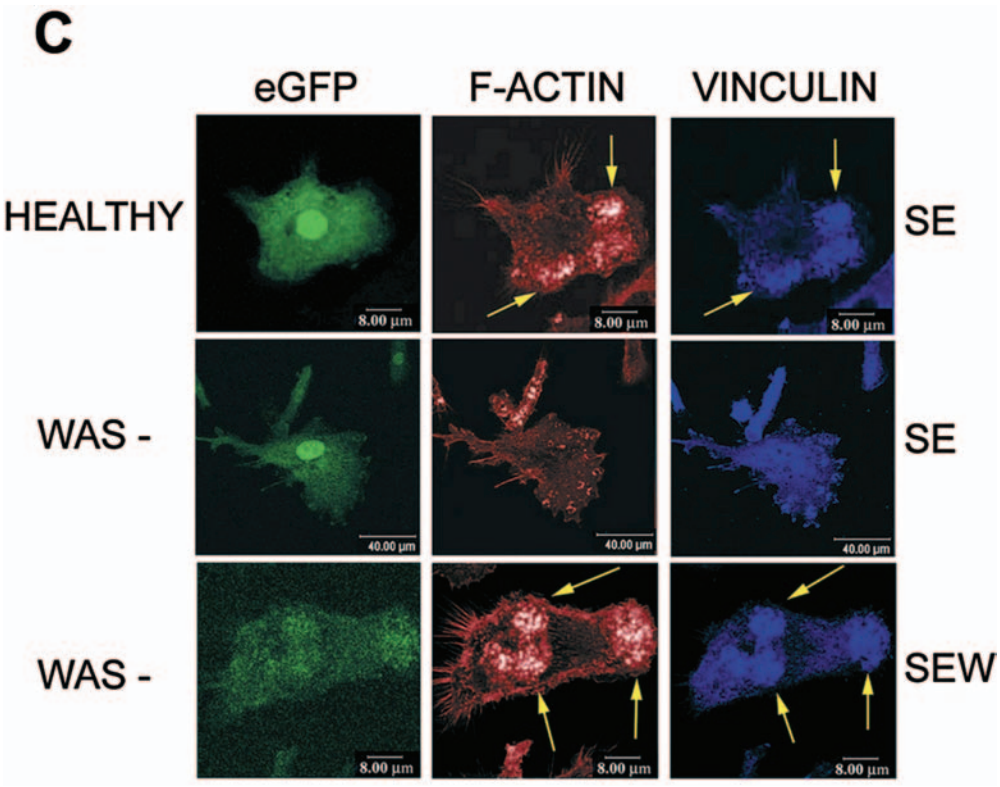

FIG. 1. Construction of a lentiviral vector containing an eGFP–WASp functional chimera. (**A**) Map of the SEW lentiviral vector expressing the eGFP–WASp chimera through the spleen focus-forming virus (SFFV) LTR constitutive promoter, with the presence of the woodchuck hepatitis virus posttranscriptional regulatory element (WPRE). (**B**) Morphological reconstitution of HVS-WAS T cells transduced with the SEW vector. Images are SEM microphotographs of (1) normal HVS-T lymphocytes (HVS-N), showing the characteristic round and hairy cell surface, (2) untransduced HVS-T cells derived from a WAS patient (HVS-WAS/1), (3) SE-transduced HVS-WAS/1 cells showing cell surfaces devoid of microvilli, and (4) SEW-transduced HVS-WAS/1 cells showing reconstitution of cell morphology and microvilli. (**C**) Podosome reconstitution of murine WASp-deficient dendritic cells (DCs) with the SEW lentiviral vector expressing the eGFP–WASp chimera. Podosomes (yellow arrows) were observed only in healthy DCs (*top*) and in SEW-transduced DCs from WAS-deficient mice (*bottom*). Transduction of cells with the control vector SE, expressing eGFP alone, has no effect in podosome formation (*middle*).

difluoride (PVDF) membranes (GE Healthcare Life Sciences, Buckinghamshire, UK). Membranes were blocked with 5% nonfat milk and probed for 1 hr at room temperature with anti-WASp monoclonal antibody D-1 (2 μg/ml; Santa Cruz Biotechnology) followed by incubation with horseradish peroxidase (HRP)-labeled goat anti-mouse antibody (1:10,000 dilution; Invitrogen Caltag). Quantitative analysis was performed with an ECL-Advance Western blotting detection system (GE Healthcare Life Sciences). Membranes were revealed after incubation for 1–5 min with ECL-Advance reagents. Quantification of light emission was done with a Molecular Imager ChemiDoc XRS system (Bio-Rad, Hercules, CA) and analyzed at 440 nm with Quantity One version 4.5.0 software (Bio-Rad). Contribution of each band was recorded and expressed as relative intensity per square millimeter.

To determine WASp expression in transduced cells, ERK (extracellular signal-regulated kinase) protein content was used as internal loading control. The ratio of WASp to ERK was calculated for each SW-transduced cell and for Jurkat cells (in the same blot). WASp expression levels of transduced cells were calculated relative to Jurkat cell levels (dividing the WASp:ERK ratio of the transduced cell by the ratio obtained in Jurkat cells). The eGFP:ERK ratio represents the relative expression level of eGFP.

DNA preparation and quantitative real-time PCR

Genomic DNA from cultured cells was isolated by adding 1 ml per 10^6 cells of SNET extraction buffer (20 m*M* Tris-HCl [pH 8], 5 m*M* EDTA [pH 8], 400 m*M* NaCl, 1% SDS; filtered and aliquoted) containing proteinase K (100 μg/ml; Sigma-Aldrich). DNA samples were incubated at 55°C for 2–18 hr, proteinase K was inactivated by a final heating at 95°C for 10 min, and RNase (1 μg/ml) was finally added for 30 min at 37°C. Proteins were extracted twice with phenol–chloroform and DNA was then precipitated and its concentration determined by spectrophotometry. Quantitative real-time PCRs were performed in an ABI PRISM 7000 sequence detection system (Applied Biosystems, Foster City, CA). Samples were mixed with iTaq Supermix with ROX (Bio-Rad) containing dNTPs, iTaq DNA polymerase (50 U/ml), 40 m*M* Tris-HCl (pH 8.4), 100 m*M* KCl, 10 m*M* $MgCl_2$, 1 μ*M* ROX internal reference dye,

and stabilizers. Specific primers were added at 400 n*M*. For SW- and WW-transduced cells, a pair of primers comprising *WAS* exons 9 and 10 (forward, 5′-AGG CTG TGC GGC AGG AGA T-3′; reverse, 5′-CAG TGG ACC GAA CGA CCC TTG-3′) and a specific TaqMan probe (5′-FAM-CGC CAG GAG CCA CTT CCG CCG-TAMRA-3′) were used. The parameters for the PCR were as follows: 1× (95°C for 2 min), 45× (95°C for 30 sec, 58°C for 30 sec, and 72°C for 30 sec) 1× (50°C for 2 min). For SE- WE-, SEW-, and WEW-transduced cells vector copy number determination was done with eGFP primers (forward, 5′-GCCCGACAACCACTACCT-3′; reverse, 5′-CGT-CCATGCCGAGAGTGA-3′) and the TaqMan probe (5′-FAM-CGGCGGCGGTCACGAACTCCA-TAMRA-3′). The parameters for the PCR were as follows: 1× (95°C for 2 min), 45× (95°C for 30 sec, 61.4°C for 30 sec, and 72°C for 30 sec), 1× (72°C 2 min). 293T cells (1×10^5) were mixed with 10-fold-increasing amounts of plasmid DNA (10^2 up to 1×10^7 copies) to determine the standard curve in each experiment.

RESULTS

Overexpression of functional eGFP–WASp chimera is toxic for nonhematopoietic cells

To study the possible adverse effects of WASp overexpression in gene-modified cells, we constructed the eGFP–WASp LV vector under the transcriptional control of the strong viral promoter SFFV (Fig. 1A). This chimeric construct (SEW) was needed to analyze the effects of various amounts of WASp (which correlates with green fluorescence intensity) at the individual cell level as well as to analyze the effect of WASp overexpression in cytoskeletal organization. To ascertain that the eGFP–WASp chimera was fully functional, WAS-deficient cells from both humans and mice were transduced with the SEW vector at an MOI of 10. Functional reconstitution of herpesvirus saimiri-immortalized T lymphocytes from a WAS patient (HVS-WAS/1) was achieved with the transgene as demonstrated by scanning electron microscopy (Fig. 1B). It can be observed that the typical cell surface devoid of microvilli of WAS-deficient cells (Fig. 1B, panel 2) is restored in SEW-transduced HVS-WAS T cells (Fig. 1B, panel 4), whereas transduction of these cells with the SE control vector, which contains eGFP alone, does not have any effect (Fig. 1B, panel 3). The eGFP–WASp chimera was also fully functional in WAS-deficient mouse dendritic cells (DCs), as determined by its ability to reconstitute the characteristic defect to form podosomes (Fig. 1C), a cell structure defined by the colocalization of actin and vinculin (Linder *et al*., 1999; Linder and Aepfelbacher, 2003).

Transduction of nonhematopoietic 293T cells with the SEW vector at an MOI of 10 results in dramatic alterations in cell morphology and viability. 293T cells overexpressing eGFP–WASp grow as clusters loosely attached to the culture dish (Fig. 2A, top right), whereas most cells transduced with eGFP alone (MOI of 10) retain their fibroblast-like morphology, with only a small percentage of loosely attached cells, probably due to the intrinsic toxicity of the VSV-G envelope protein (Fig. 2A, top left). Similar results were obtained with human microvascular endothelial cells (data not shown). In addition, analysis of cell size and complexity (Fig. 2C, left) as well as 7-AAD staining (Fig. 2C, right) revealed a 2- to 3-fold increase in cell death of the 293T-SEW-transduced population (Fig. 2C; bottom) compared with the SE-transduced population (Fig. 2C, top). However, transduction of human WAS T cells (ALLO-WAS/2) at an MOI of 40 with the SEW vector did not induce any morphological changes (Fig. 2A, bottom). This MOI was calculated to achieve equivalent vector copy numbers as with the 293T cells, because we previously demonstrated that allospecific and HVS-immortalized T cells are three to six times more resistant to lentiviral transduction than are 293T cells (Toscano *et al*., 2004). To determine whether the absence of deleterious effects in T cells is due to differences in transgene expression, we analyzed the expression patterns of SE and SEW vectors in 15–30% transduced 293T and ALLO-WAS/2 cells (Fig. 2B). The mean fluorescence intensity (MFI) of SEW-transduced hematopoietic cells (Fig. 2B, bottom right; MFI of 19) was consistently lower than that obtained with the same vector in nonhematopoietic cells (Fig. 2B, bottom left; MFI of 205) or in hematopoietic cells transduced with the SE vector expressing eGFP alone (Fig. 2B, top right; MFI of 136). The lower expression of the SEW vector achieved in T cells, together with the higher resistance of these cells to transduction, could explain, at least in part, the lack of toxicity of eGFP–WASp overexpression in T cells.

To elucidate the mechanism by which eGFP–WASp causes toxicity and morphological defects in nonhematopoietic cells, and because of the key role that WASp plays in actin reorganization, we analyzed by confocal microscopy individual cells expressing different amounts of eGFP–WASp. Nonhematopoietic decidual stromal cells (DSCs) were transduced with the SE and SEW vectors at an MOI of 5 and their F-actin organization was studied 7 days later by staining with tetrarhodamine isothiocyanate (TRITC)-labeled phalloidin. Figure 3A shows a general view of DSCs transduced with the SE vector (Fig. 3A, left) and the SEW vector (Fig. 3A, right). Aberrant morphologies were observed only within the SEW-transduced population (arrows in Fig. 3A, right). A significant proportion of cells overexpressing eGFP–WASp acquired a typical round–trapezoidal morphology clearly different from the mesenchymal-like morphology of cells expressing eGFP alone (Fig. 3A, left). A detailed analysis of individual cells expressing increasing amounts of the eGFP–WASp chimera (Fig. 3B) revealed two important findings. First, expression of low-to-moderate levels of eGFP–WASp does not interfere with the formation of F-actin bundle filaments (stress fibers) (Fig. 3B, panels 1 and 2) and the cells have the same morphology as the mock-transduced or SE-transduced DSCs. Furthermore, if the cells shown in Fig. 3B, panel 1, are reexamined after increasing the sensitivity of the confocal microscope (laser, from 20 to 100%; pinhole, from 0.2 to 1), a clear colocalization of F-actin and eGFP–WASp is observed (Fig. 3C, images and graphs). And second, we found that overexpression of eGFP–WASp clearly interferes with the formation of F-actin bundle filaments, therefore disrupting stress fibers (Fig. 3B; panels 3 and 4). Two different cellular patterns resulted from this disruption. In some cells, eGFP–WASp still colocalized with F-actin, but formed clusters instead of stress fibers (Fig. 3B, panel 3 and associated graph). In cells overexpressing even higher amounts of eGFP–WASp, no colocalization could be observed, because the F-actin is excluded from the eGFP–WASp clusters and confined to the periphery (Fig. 3B, panel 4 and associated graph).

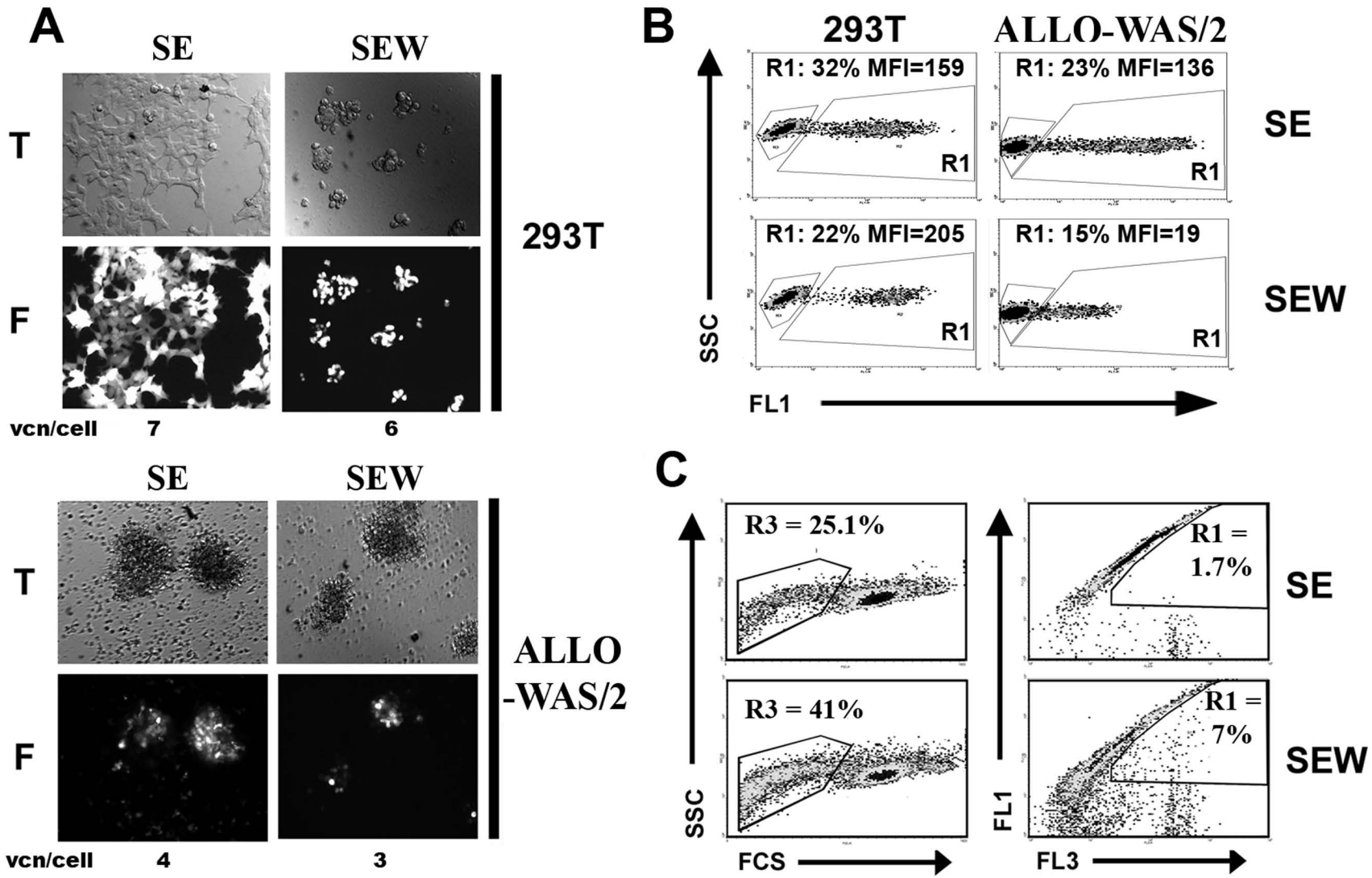

FIG. 2. Overexpression of the eGFP–WASp chimera induces morphologic alterations in nonhematopoietic cells. (**A**) Transmission (T) and fluorescence (F) microphotographs of 293T nonhematopoietic cells and ALLO/WAS/2 T cells transduced with the control SE vector expressing eGFP alone or the SEW vector expressing the eGFP–WASp chimera as indicated (MOI of 10 for 293T cells and MOI of 40 for ALLO/WAS/2 T cells to achieve comparable transduction efficiencies). Morphologic alterations were observed only in SEW-transduced 293T cells overexpressing eGFP–WASp (*top right*). Vector copy number per cell (VCN/cell) is shown at the bottom of each microphotograph. (**B**) Transgene expression achieved with the control SE vector and the SEW vector in 293T and ALLO-WAS/2 cells and analyzed by flow cytometry. Different MOIs were used for 293T cells (MOI of 0.3) and ALLO-WAS/2 cells (MOI of 2) to achieve transduction efficiencies ranging from 15 to 30% to ensure single integrants. (**C**) Cell viability assayed by 7-AAD staining of 293T cells transduced with the SE vector (*top*) or SEW vector (*bottom*) (MOI of 10). Forward versus side scatter (*left*) and FL1 (green) versus FL3 (7-AAD staining) (*right*) density plots are shown. The R3 region indicates a small and low-complexity population representing dead cells. The R1 region indicates the population of dead cells (positive for 7-AAD) inside the eGFP-expressing population.

Nonhematopoietic cells overexpressing WASp have a growth disadvantage

To study in more detail the possible adverse effects of ectopic expression of WASp in nonhematopoietic cells, we constructed an LV vector expressing WASp under the transcriptional control of the strong SFFV promoter (SW) based on the eGFP-expressing SE vector (Demaison *et al*., 2002) (Fig. 4A). Nonhematopoietic 293T cells and DSCs as well as human T cells from a WAS patient were transduced with the LV vector, using a wide range of MOIs (0.5–50) because of the various susceptibilities of the cells to lentiviral transduction. Cell viability and proliferation were assessed by the MTT colorimetric assay. We did not observe any differences in cell proliferation between cells transduced with the SW vector (Fig. 4B, solid columns) and cells transduced with the eGFP control (Fig. 4B, open columns). As expected (Konno *et al*., 2004; Martin *et al*., 2005), WAS-deficient cells transduced with the SW vector showed a slightly increased proliferation rate over SE-transduced cells. However, cell viability was significantly affected in nonhematopoietic cells transduced with both SW and SE vectors at an MOI of 50, whereas hematopoietic cells remained unaffected. The presence of the highly toxic VSV-G envelope accounts for the observed effect, thereby masking the possible adverse effect of WASp overexpression. We hypothesized that, if the expression of WASp is innocuous to nonhematopoietic cells, WASp levels should remain stable over time. Therefore, both cell types were transduced with the SW vector at an MOI of 2 and monitored over a period of 60 days in culture. Figure 4C shows that WASp levels (indicated as the WASp:ERK ratio) in SW-transduced DSCs decreased from 0.95 on day 7 to 0.34 on day 60 (a 2- to 3-fold drop). Similarly, the WASp:ERK ratio in SW-transduced 293T cells changed from 1.82 on day 7 to 0.88 on day 60 (a 2-fold drop). This fall in WASp expression correlates with a decrease in the vector copy number per cell. In DSCs, the average insertion of vectors per cell decreased from 1 copy per cell 7 days after transduction to 0.4 copy per cell 60 days after transduction; likewise, the number of vector integrations in 293T cells transduced under similar conditions fell from 0.7 on day 7 to 0.34 on day 60, as determined by quantitative PCR.

WASp cannot be efficiently overexpressed in hematopoietic cells

Because gene therapy protocols of WAS patients will target primarily hematopoietic cells, we addressed the effects of transgene overexpression in Jurkat T cells. We performed a similar time course experiment, transducing Jurkat cells with SW and SE vectors at an MOI of 5, followed by analysis of vector integrations and WASp or eGFP protein expression on days 7 and 60 after transduction. Surprisingly, we found that, as opposed to nonhematopoietic cells, the number of SW vector integrations as well as WASp protein levels in Jurkat cells remained unchanged over time (Fig. 5A, left). We also observed that expression of the inert protein eGFP driven by the SE vector remained steady over time in cultured Jurkat cells (Fig. 5A, right) and nonhematopoietic cells (data not shown).

To further study the potential toxicity of WASp overexpression in hematopoietic cells, we assessed in detail the WASp expression levels in Jurkat cells (as a model of highly permissive hematopoietic cells) after transduction at high MOIs with the SW LV, which expresses WASp through the viral SFFV promoter; the SFFV promoter is highly active in these cells (see Suppl. Fig. 1 at www.liebertonline.com/hum). Jurkat and 293T cells were transduced with the SW vector at increasing MOIs (2, 8, and 20) and analyzed for vector copy number and intracellular WASp content. Jurkat cells harboring up to 12 vectors per cell expressed only 3 times (0.12/0.04) the WASp levels of mock-transduced cells (Fig. 5B). In contrast, nonhematopoietic 293T cells with only 1.5 integrations per cell already expressed 8.5 times (0.34/0.04) the WASp amount of mock-transduced Jurkat cells (Fig. 5B). Interestingly, when comparing WASp:ERK ratios of Jurkat cells harboring 1.2 SW VCN/cell with those containing 11.6 copies, we observed only a 0.15-fold increase in intracellular WASp level (WASp:ERK ratios, 0.08 to 0.12). In contrast, the same increase in vector copy number per cell (from 1.5 to 15) in 293T cells rendered a 2.1-fold increase in WASp expression (WASp:ERK ratios from 0.34 to 0.72). These data suggest the presence of a hematopoietic-specific mechanism(s) that controls or silences WASp overexpression. Interestingly, a similar restriction can be observed when we try to overexpress the eGFP–WASp chimera in hematopoietic cells (see Suppl. Fig. 1), suggesting that similar mechanism(s) control overexpression of the chimeric construct.

Transcriptionally targeted LV vectors expressing WASp circumvent adverse cellular defects in nonhematopoietic cells and are efficient tools for gene therapy of WAS

We next addressed whether transcriptionally targeted LV vectors expressing eGFP–WASp could circumvent the adverse cellular effects found in nonhematopoietic cells transduced with the nonregulated SEW LV vector. We constructed the vector

FIG. 3. Overexpression of the eGFP–WASp chimera disrupts the cytoskeleton of nonhematopoietic cells. (**A**) Overview of DSCs transduced with the SE vector (*left*) or the SEW vector (*right*) at an MOI of 5. Colocalization of green (from eGFP or eGFP–WASp) and red (from stained F-actin) as well as aberrant shapes (arrows) was observed only in SEW-transduced cells. (**B**) Microphotographs show individual cells expressing increasing amounts of the eGFP–WASp chimera (panels 1 to 4). The parameters for green channel acquisitions were as follows: laser, 20%; pinhole, 0.2. The graphs below the photographs represent the red and green intensities detected with a confocal microscope along the lines drawn in each microphotograph. Green intensity represents the relative amount of eGFP–WASp chimera in that particular position; red represents the amount of F-actin. (**C**) Detail of cells shown in (**B**), panel 1 (expressing moderate levels of the eGFP–WASp chimera), after increasing the laser intensity to 100% and the pinhole to 1, in order to enhance detection of green fluorescence (*left and graph*). Amplification of the signal allows observation of a clear colocalization of stress fibers (stained red) and eGFP–WASp (stained green). Right microphotograph is a higher magnification of the indicated area, showing colocalization of eGFP–WASp and stress fibers. Red channel settings: laser power, 50%; pinhole, 0.3.

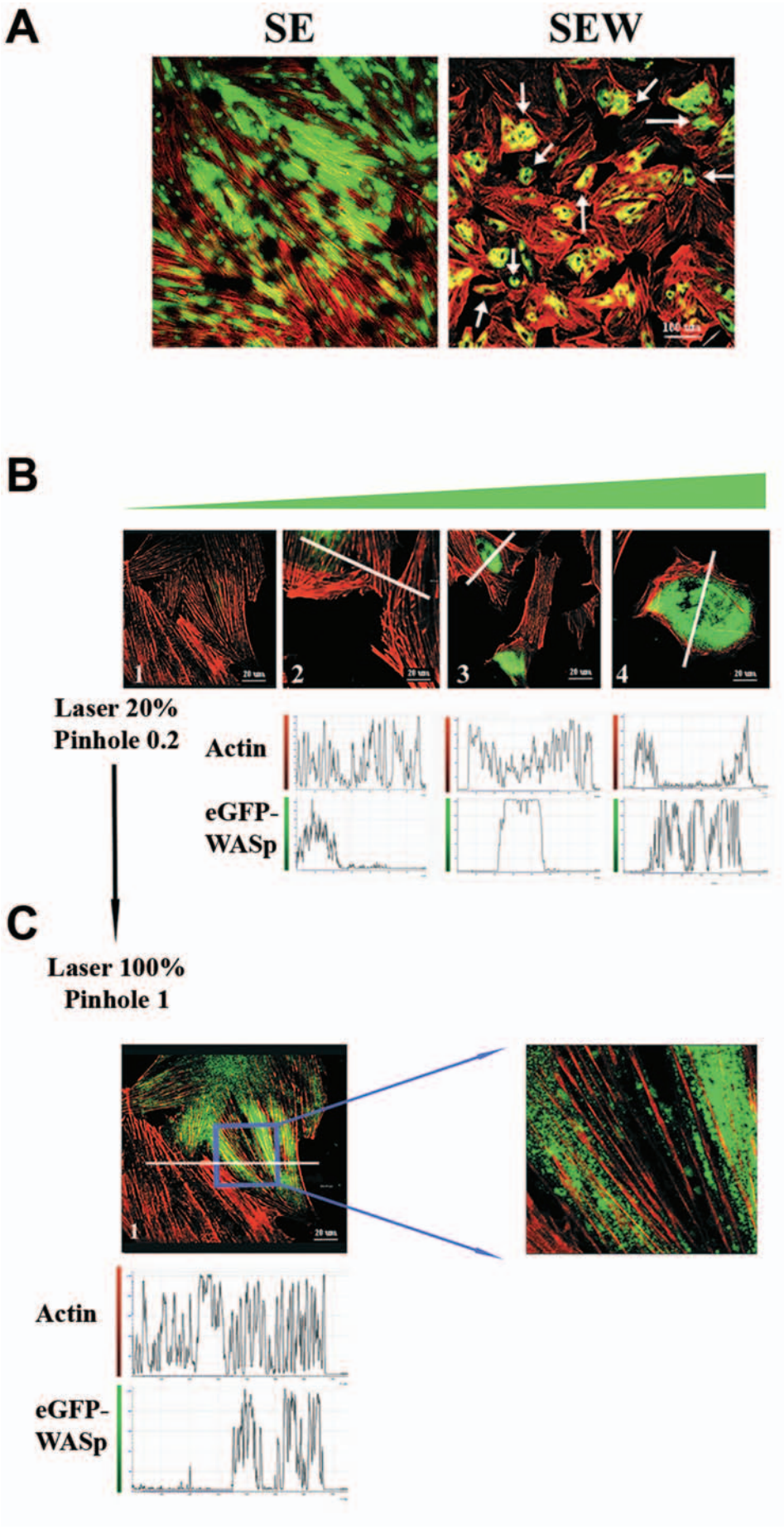
A
SE
SEW
B
1
2
3
4
Laser 20%
Pinhole 0.2
Actin
eGFP-
WASp
C
Laser 100%
Pinhole 1
Actin
eGFP-
WASp

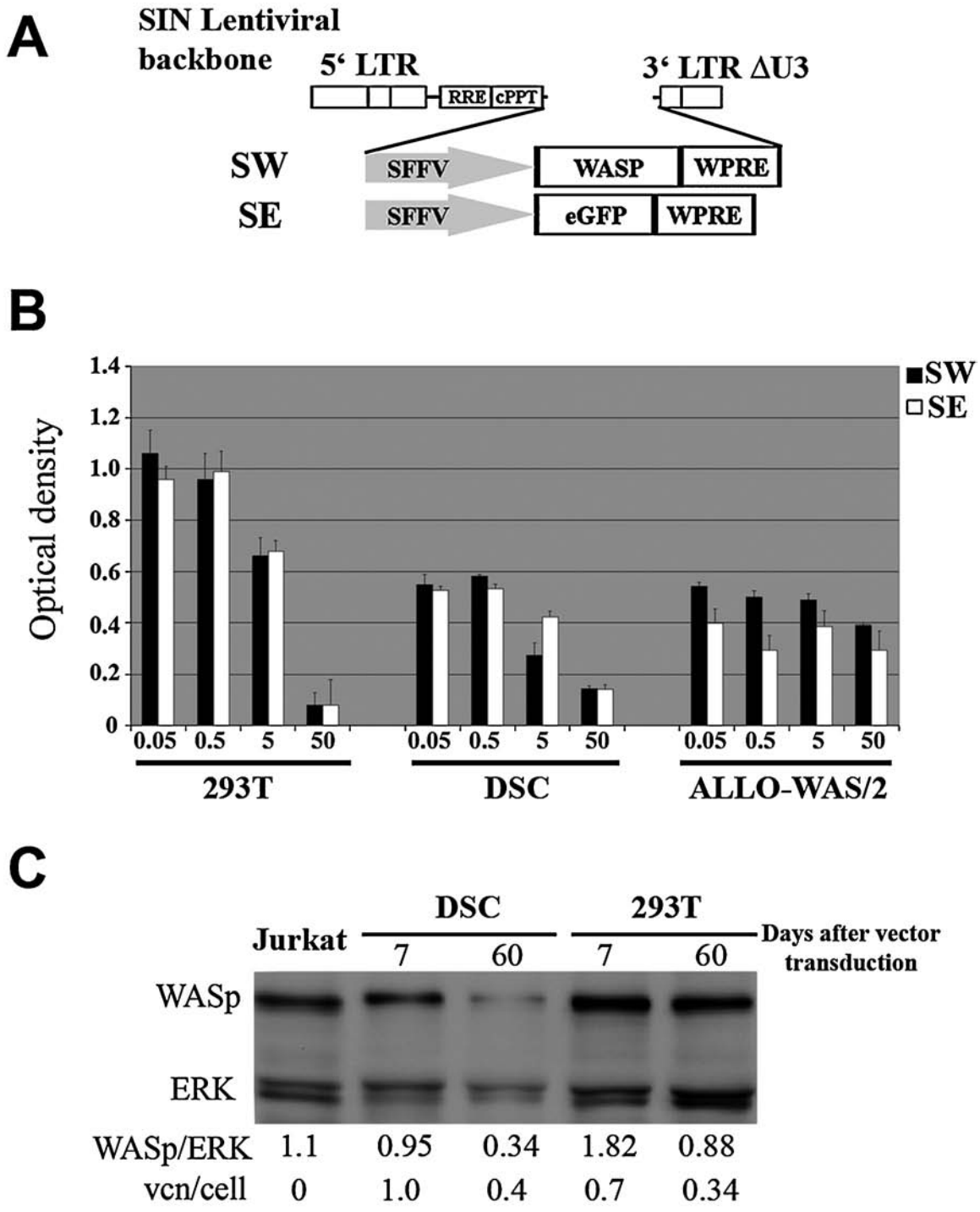

FIG. 4. WASp expression confers a negative growth advantage to nonhematopoietic cells. (**A**) Maps of the lentiviral vectors used for overexpression of WASp (SW) or eGFP (SE). Both vectors use the spleen focus-forming virus (SFFV) LTR promoter to express their transgenes. (**B**) Graph showing cell viability of nonhematopoietic cells (293T cells and DSCs) and hematopoietic cells (ALLO-WAS/2) 7 days after transduction with the SW or SE vector at MOIs of 0.05, 0.5, 5, and 50 as indicated at the base of the columns. Viability was determined by the MTT colorimetric assay. No differences were detected between SE- and SW-transduced cells. (**C**) Quantitative Western blot analysis showing WASp expression of SW-transduced DSCs and 293T cells (MOI of 2) on days 7 and 60 after treatment (as indicated at the top of each lane). ERK protein content was used as internal loading control. The WASp:ERK ratio and vector copy number per cell (VCN/cell) are indicated at the bottom of each lane. A clear downregulation of WASp expression that correlates with a drop in vector copy number per cell may be observed.

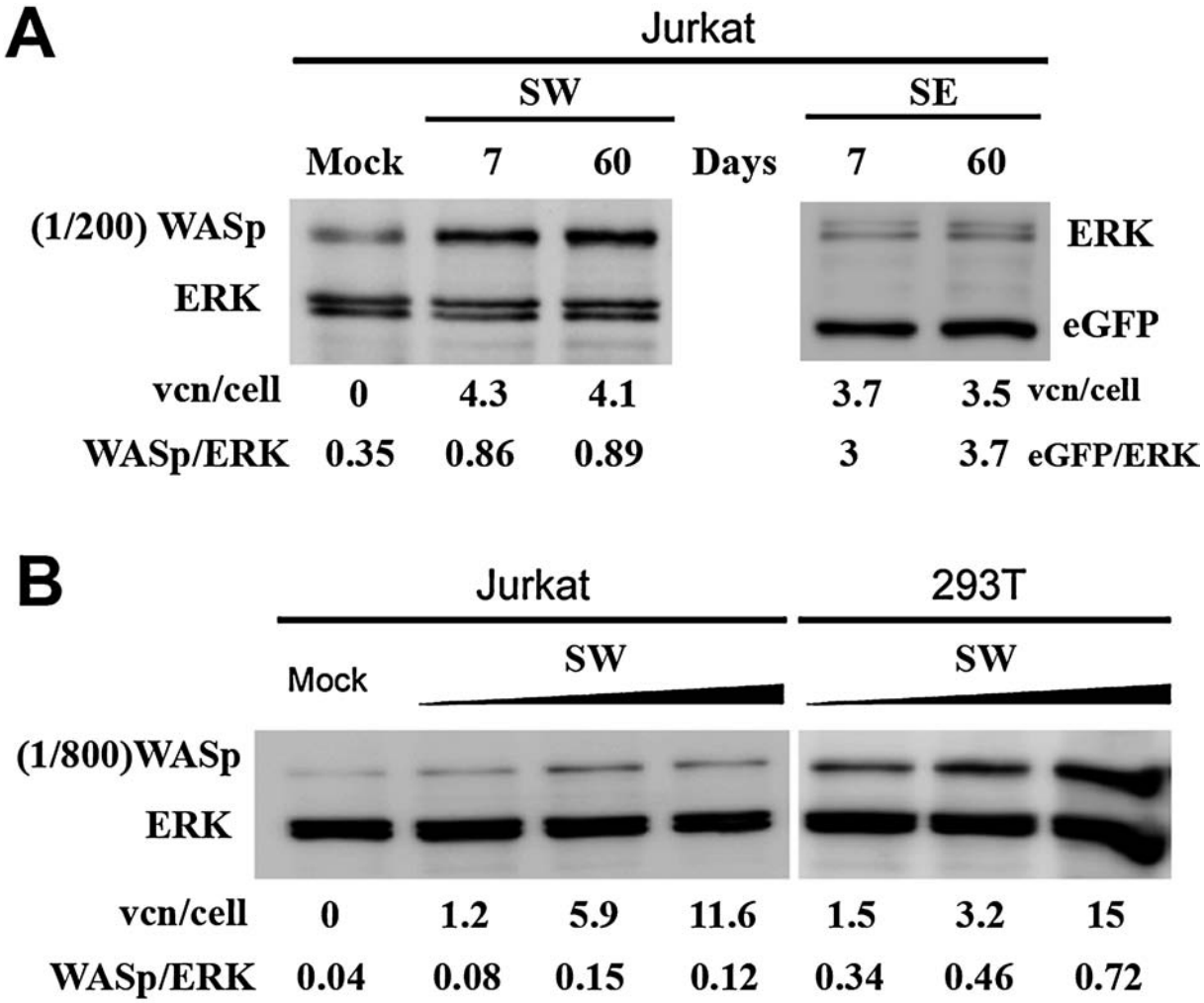

FIG. 5. Hematopoietic cells are resistant to WASp overexpression. (**A**) Stability of WASp expression in SW- and SE-transduced Jurkat cells. Quantitative Western blot analysis showing WASp (*left*) and eGFP (*right*) expression in SW- and SE-transduced (MOI of 5) Jurkat T cells on days 7 and 60 after transduction as indicated. Optimal dilutions of 1:200 of the anti-WASp antibody and 1:500 of the anti-eGFP antibody were used for detection. (**B**) Quantitative Western blot to detect expression of WASp in hematopoietic (Jurkat) and nonhematopoietic (293T) cells transduced with increasing amounts of SW vector (MOIs of 2, 8, and 20) and analyzed 7 days posttransduction. A 1:800 dilution of the anti-WASp antibody was used to avoid a saturating signal obtained in transduced nonhematopoietic cells that made precise quantification of the WASp:ERK ratio difficult. Mock-transduced Jurkat cells are shown as reference. ERK protein is used as internal loading control. The WASp:ERK ratio and vector copy number per cell (VCN/cell) are indicated at the bottom of each lane. A clear resistance to WASp overexpression was observed in Jurkat cells but not in 293T cells.

WEW (Fig. 6A), which drives eGFP–WASp expression from a 500-bp fragment of the WAS proximal promoter. Nonhematopoietic cells (293T) and hematopoietic cells (ALLO-WAS/2) were transduced with WEW and SEW vectors at various MOIs (0.1, 1, and 10). As can be seen in Fig. 6B, SEW and WEW vectors had a similar expression profile in ALLO-WAS/2 T cells (Fig. 6B, bottom), but expression of WEW vectors in 293T cells was weak (Fig. 6B, 293T, bottom; MFI of 13.7 at an MOI of 10) compared with the expression achieved with the SEW vector (Fig. 6B, 293T, top; MFI of 1055 at an MOI of 10). These data show that the WEW vector achieves tissue-specific expression of the transgene, in accordance with our previous results obtained with the WW vector expressing WASp (Martin *et al*., 2005). Microscopy analysis showed no morphological alterations in any cell type analyzed, consistent with the lack of eGFP–WASp expression in nonhematopoietic cells (Fig. 6C, right) even at 10 vector integrations per cell. We further analyzed cytoskeletal alterations of WEW-transduced DSCs by confocal microscopy after staining for F-actin (Fig. 6D). Again, no significant variation in F-actin patterns could be observed in WEW-transduced DSCs (2.3 vectors/cell: Fig. 6D, bottom right) compared with SE- or mock-transduced cells (Fig. 6C, top right and top left, respectively). However, clear abnormalities could be detected in SEW-transduced DSCs (0.9

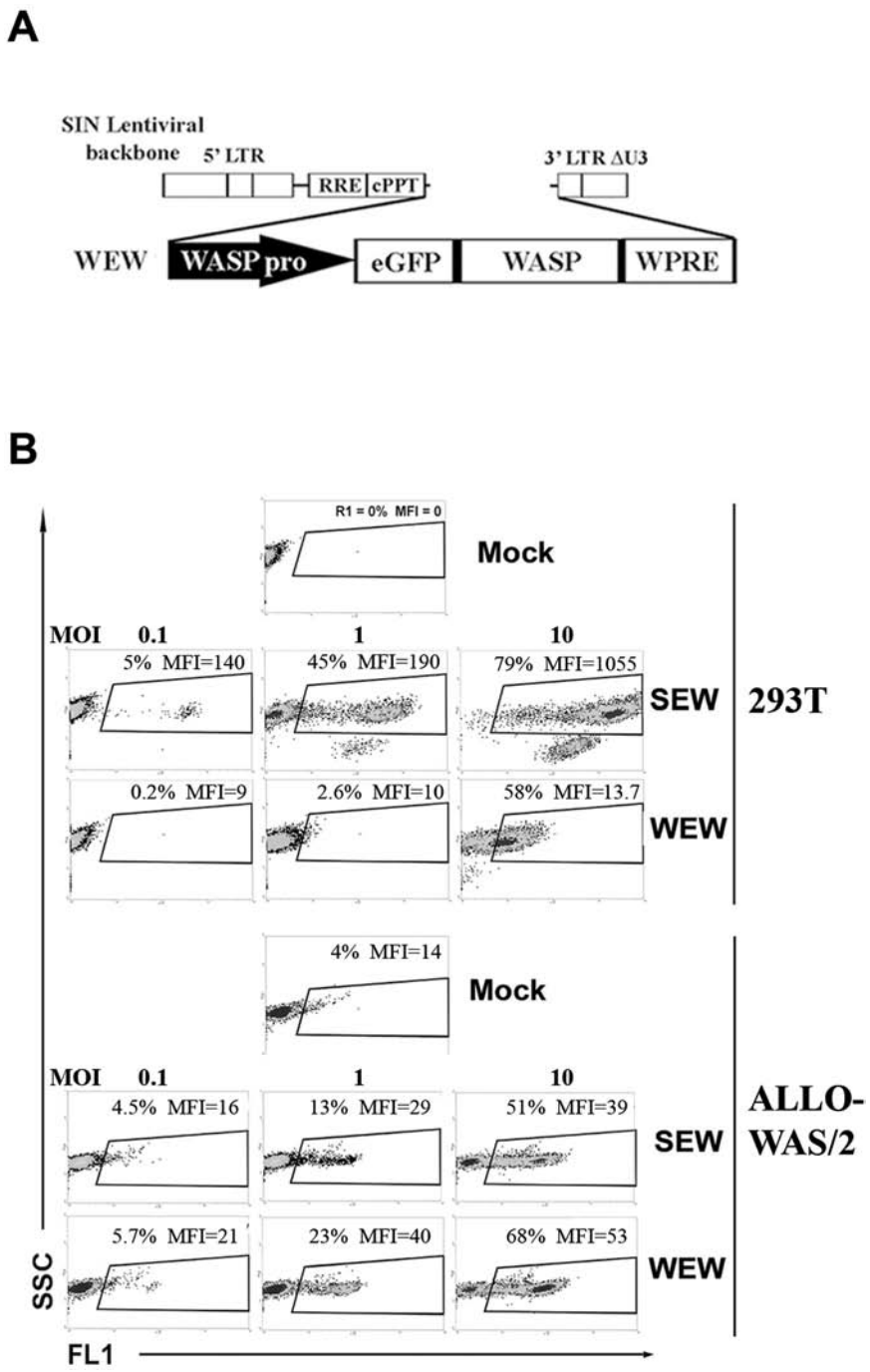

FIG. 6.

vector/cell: Fig. 6D, bottom left). 7-AAD staining of cells corroborated microscopy observations, indicating no increase in dead cells in the WEW-transduced population (data not shown).

Because we have proven in this experimental system that the use of hematopoietic-specific LV vectors represents a safer alternative to nonregulated vectors, we finally addressed whether our previously published regulated vector WW expressing WASp (Martin *et al*., 2005) is able to efficiently rescue WAS-deficient T cells from intrinsic functional and morphological defects. Mock-transduced WAS-deficient ALLO-WAS/2 T cells showed the impaired CD3-mediated proliferative response that is characteristic of WAS-deficient T cells (Fig. 7A). Transduction of ALLO-WAS/2 T cells with the WW LV vector achieved more than 80% WASp-positive cells (data not shown) and this population elicited a vigorous response after engagement of the TCR–CD3 receptor complex (Fig. 7A), comparable to that observed in ALLO-NORMAL cells (Fig. 7A). Examination of HVS-WAS/1 T cells under the scanning electron microscope revealed a cell surface that was typically devoid of microvilli (Fig. 7B, top right). Transduction of HVS-WAS/1 T

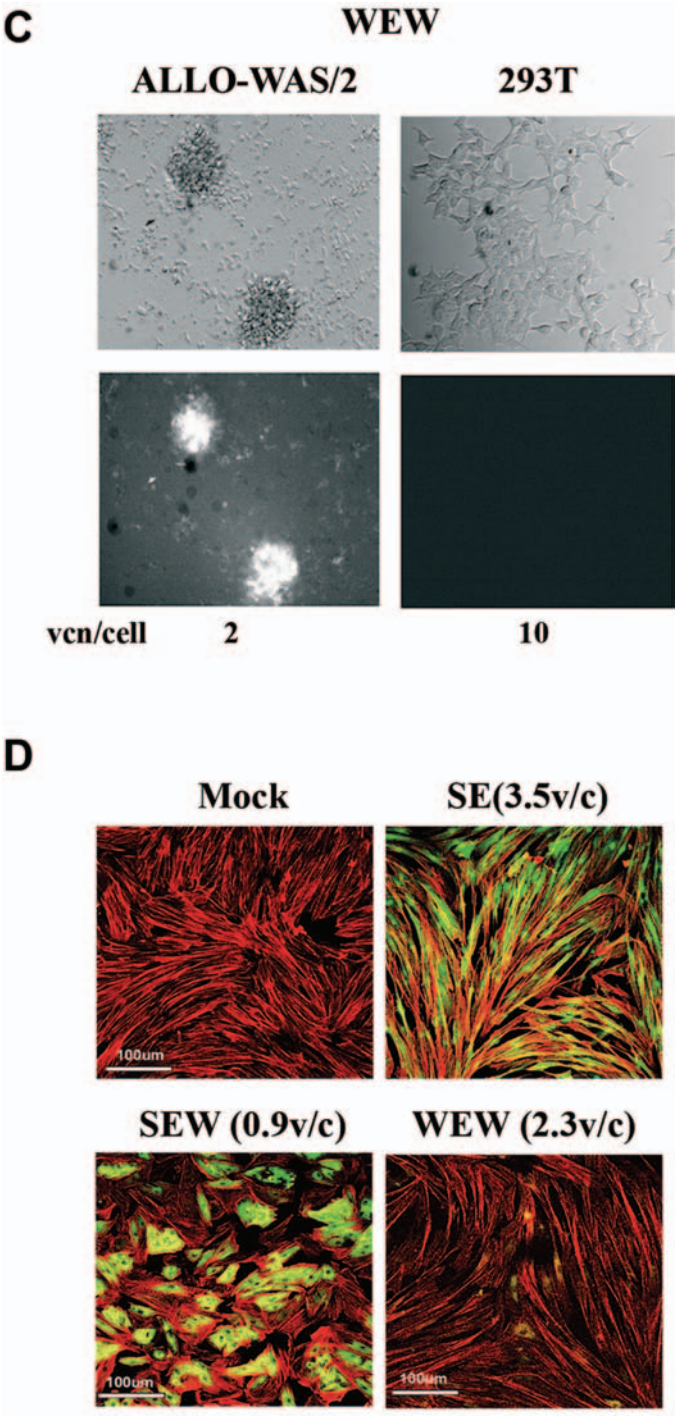

FIG. 6. Hematopoietic-specific lentiviral vectors avoid the toxic effect of the eGFP–WASp chimera. (**A**) Map showing the WEW transcriptionally targeted lentiviral vector expressing the eGFP–WASp chimera through a 500-bp fragment of the *WAS* proximal promoter. (**B**) 293T cells (*top*) and ALLO-WAS/2 cells (*bottom*) were transduced with SEW and WEW vectors at MOIs of 0.1 (*left*), 1 (*middle*), and 10 (*right*) as indicated and analyzed 7 days thereafter by flow cytometry. (**C**) Transmission (*top*) and fluorescence (*bottom*) microphotographs of nonhematopoietic cells (293T, *right*) and hematopoietic cells (ALLO-WAS/2, *left*) transduced with the WEW vector. 293T cells did not express detectable levels of eGFP (fluorescence image, *bottom right*) whereas ALLO-WAS/2 eGFP–WASp expression was easily detected (fluorescence image, *bottom left*). The transduction level is shown at the bottom of the photographs as vector copy number per cell, as determined by real-time PCR. (**D**) Confocal microscopy images of mock-, SE-, SEW-, and WEW-transduced DSCs. Cells were stained for F-actin, using TRITC-labeled phalloidin, and then analyzed by confocal microscopy. Red (for F-actin) (settings: laser power, 50%; pinhole, 0.3) and green (for eGFP–WASp) (settings: laser power, 20%; pinhole, 0.2) channels were acquired separately and then merged. No toxicity was observed in WEW-transduced DSCs. v/c, vectors per cell.

cells with the WW vector restored cell morphology (Fig. 7B, bottom right), presenting surface microvilli that were similar to those of HVS-immortalized T cells from a normal individual (HVS-N) (Fig. 7B, top left). As expected, transduction of WAS-deficient T cells with the WE vector (expressing eGFP driven by the WASp proximal promoter) did not modify either CD3-mediated proliferative responses (Fig. 7A) or cell surface morphology (Fig. 7B, bottom left). We also demonstrated that the WW vector efficiently transduced and reconstituted the ability of human WAS macrophages (Fig. 7C) and mouse WAS bone marrow-derived dendritic cells (Fig. 7D) to form normal podosome structures, which characteristically contain a central F-actin core and a peripheral ring of vinculin.

DISCUSSION

To minimize problems of genotoxicity and/or ectopic expression in WAS gene therapy protocols, and because the expression of WASp is restricted to hematopoietic cells, we

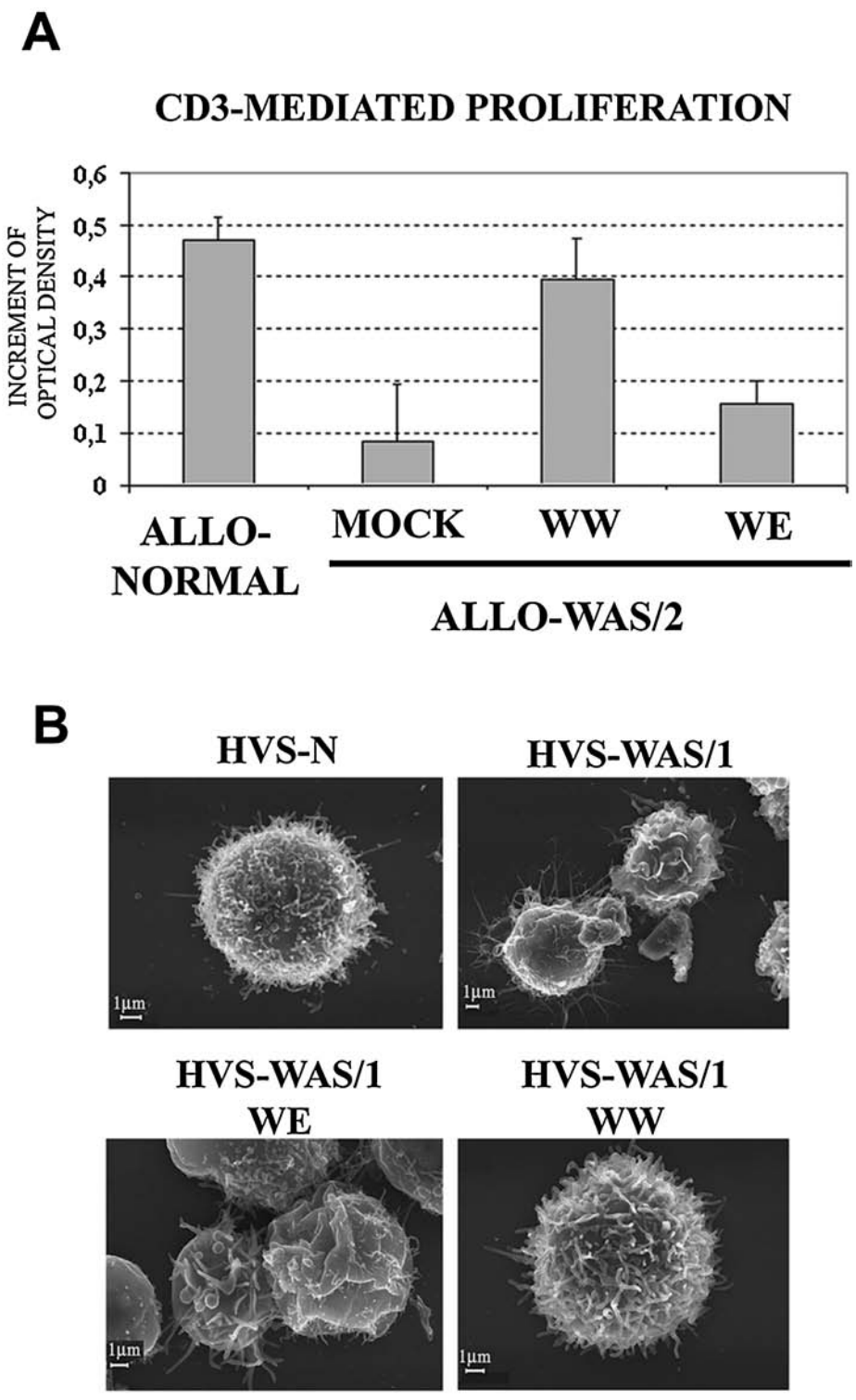

FIG. 7.

(Martin *et al*., 2005) and others (Dupre *et al*., 2004, 2006) have developed hematopoietic-specific HIV-1-based LV vectors expressing the *WAS* cDNA. The use of specific promoters should reduce genotoxicity by eliminating the potent enhancer activity of the commonly used viral promoters and, at the same time, should avoid ectopic expression of the transgene in nontarget cells. However, there is no general agreement concerning the deleterious effect of ectopic *WAS* expression in nonhematopoietic cells or to what extent the use of hematopoietic-specific vectors has any safety advantages over constitutive vectors.

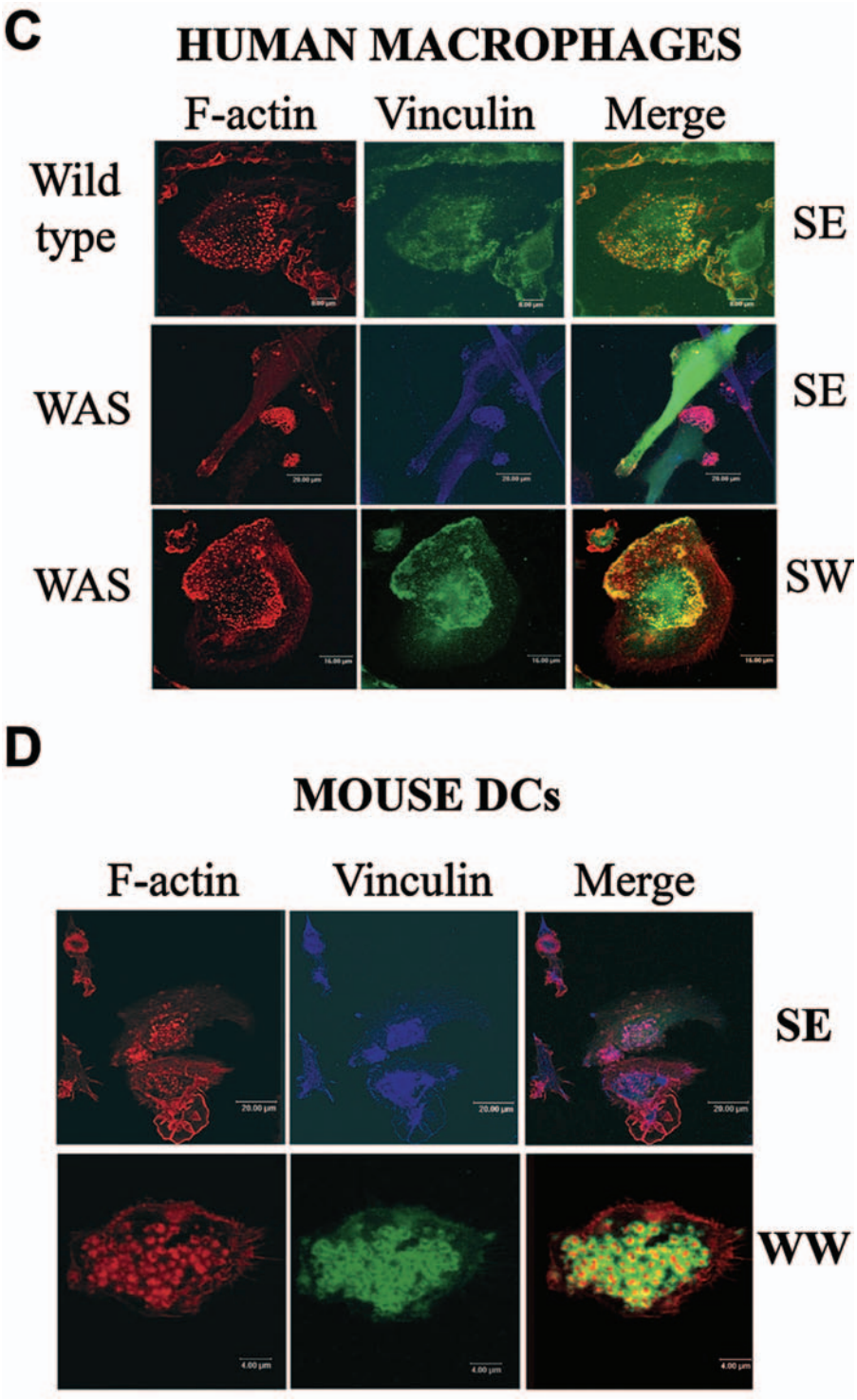

FIG. 7. Functional reconstitution of WAS cellular defects by hematopoietic-specific lentiviral vectors expressing WASp (WW). (**A**) Transduction of primary WAS allospecific T cells restored CD3-mediated proliferative responses. T cells from a WAS patient were mock transduced or transduced with WE or WW at an MOI of 5 and challenged with immobilized anti-CD3 monoclonal antibody, and cell proliferation was assayed by the MTT colorimetric method. Proliferation data are shown as increment in OD readings (570 nm) of CD3-stimulated versus unstimulated cells. Results represent means ± SD of four independent experiments. (**B**) Morphological reconstitution of HVS-WAS T cells transduced with the WW vector. Shown are SEM microphotographs of normal HVS-T cells (HVS-N, *top left*) and HVS-T cells derived from a patient with WAS (HVS-WAS/1) that were untransduced (*top right*), WE transduced (*bottom left*), or WW transduced (*bottom right*). Restoration of the characteristic round and hairy cell surface present in normal T cells was observed only in WW-transduced HVS-WAS/1 T cells. (**C**) Podosome reconstitution of human macrophages from a WAS patient with the WW hematopoietic-specific lentiviral vector expressing WASp. Normal podosomes, with a characteristic central F-actin core and a peripheral ring of vinculin, were observed in nontransduced (NT) wild-type macrophages (*top*) and in WW-transduced WASp-deficient macrophages (*bottom*), but were absent in SE-transduced WASp-deficient macrophages (*middle*). (**D**) Podosome reconstitution of murine WASp-deficient dendritic cells (DCs) with the WW hematopoietic-specific lentiviral vector expressing WASp. Podosomes were observed only in WW-transduced DCs (*bottom*), not in SE-transduced WASp-deficient DCs (*top*).

In this paper, we have shown that whereas moderate expression of WASp is not deleterious to nonhematopoietic cells (293T cells and DSCs), WASp overexpression is toxic (Figs. 2–4). To dissect this toxic effect of WASp, we used the eGFP–WASp chimera to correlate green fluorescence intensity with WASp function. This strategy allowed us to analyze individual cells expressing different levels of WASp. Although it had been previously shown that eGFP–WASp is functional after plasmid microinjection into DCs (Burns *et al*., 2001), we now further demonstrate that the lentivirus-encoded eGFP–WASp chimera is fully functional and able to reconstitute bulk WAS-deficient populations. The analysis of nonhematopoietic cells transduced with the SEW LV vector showed that expression of moderate levels of the eGFP–WASp chimera was well tolerated whereas its overexpression produced dramatic defects in cellular morphology and viability. We demonstrated that changes in morphology of eGFP–WASp-transduced nonhematopoietic cells were tightly associated with WASp protein levels and that its overexpression resulted in inhibition of polymerized actin. In agreement with the findings of Symons and coworkers (1996), we found that expression of high levels of WASp induced the formation of clusters in which F-actin and eGFP–WASp colocalize. We also showed that, when the chimera was expressed at low to moderate levels, stress fibers and eGFP–WASp strongly colocalized. This observation contrasts with those of Symons and coworkers (1996), who observed no colocalization of WASp with stress fibers. It is possible that this difference could be due to the sensitivity of detection, because the eGFP–WASp chimera combined with confocal microscopy yields a strong signal. We propose that the eGFP–WASp chimera undertakes similar functions in both hematopoietic and nonhematopoietic cells. In fact, it has been previously demonstrated that expression of WASp rescues some functional defects of N-WASp-deficient murine embryonic stem fibroblast-like cells (Snapper *et al*., 2001). Taking these data together, a possible explanation for the F-actin disruption caused by the overexpression of eGFP–WASp is the sequestering of WASp-interacting proteins (such as Cdc42, Rac, and WIP), which are required for F-actin polymerization, a phenomenon that is orchestrated by WASp-homologous proteins in nonhematopoietic cells.

We found it extremely difficult to overexpress WASp (Fig. 5B) or the eGFP–WASp chimeric protein (Fig. 2B, bottom) in hematopoietic cells after lentiviral transduction of transgenes driven by the strong SFFV viral promoter. This includes the highly permissive Jurkat T cell line, a target in which the SFFV promoter is particularly active, as can be observed in the expression levels of eGFP compared with eGFP–WASp (Fig. 2B). This could be due to SFFV promoter gene silencing caused by toxicity of WASp overexpression or to the existence in hematopoietic cells, but not in nonhematopoietic cells, of intracellular mechanisms responsible for maintaining adequate levels of WASp protein. Experiments are underway to investigate these possibilities. In this direction, data have demonstrated that WIP acts as a chaperone for WASp (de la Fuente *et al*., 2007) and that the expression of WIP is required for WASp expression (Konno *et al*., 2007). This ability of WIP to regulate WASp levels in hematopoietic cells could be a main player to avoid toxicity of the SEW vector by interfering with protein stability. Hence, when all available intracellular WIP depots are depleted to bind the excessive levels of WASp and protect it from proteasome degradation, all remaining free WASp proteins would be rapidly degraded. Taken together, our data suggest that overexpression of WASp in hematopoietic cells will not be a significant hurdle in gene therapy protocols of WAS patients even after stem cell transduction at high MOIs with constitutive vectors.

Nevertheless, we have clearly demonstrated throughout our study that transcriptionally targeted LV vectors, such as WEW, are a safer alternative for gene therapy protocols. In fact, the WEW vector circumvents alterations produced by the overexpression of eGFP–WASp in nonhematopoietic cells by the constitutive SEW LV vector. The WEW LV vector, which drives eGFP–WASp expression through a 500-bp *WAS* proximal promoter fragment, is not deleterious to nonhematopoietic cells, even at high MOI. This lack of toxicity is due to the fact that expression of the WEW vector is restricted to cells of the hematopoietic lineage. These experiments are among the first to provide direct evidence that the safety of transcriptionally targeted LV vectors may be increased by avoiding cytotoxicity caused by ectopic expression of the transgene. WASp-homologous proteins are overexpressed in cancer cells (Yamazaki *et al*., 2005; Semba *et al*., 2006) and are probably involved in invasion and metastasis (Marx, 2006). Because, in addition, WASp can undertake some of the functions of WASp-homologous proteins in nonhematopoietic cells (Snapper *et al*., 2001), we think it is an important advantage for safer WAS gene therapy protocols to avoid ectopic expression.

Transcriptionally targeted LV vectors are not only safer but also efficient tools for WAS gene therapy. We have previously demonstrated that the hematopoietic-specific WW vectors efficiently modify HSCs from WAS-deficient mice (Martin *et al*., 2005) and Dupre and coworkers (2006) have demonstrated that one copy of a similar LV vector expressing WASp through the 1.6-kb *WAS* proximal promoter was enough to achieve full T cell functional reconstitution in an *in vivo* study of WASp-deficient mice. In this paper we further demonstrate their ability to restore intrinsic WAS cellular defects of T cells and macrophages from WAS patients as well as dendritic cells from WAS-deficient mice. Charrier and coworkers (2006) have also demonstrated the ability of the WW vector to transduce human WAS HSCs and to reconstitute the functionality of its progeny. Taken together, these data demonstrate that the use of a tissue-specific promoter in an LV backbone, such as the WW vector, will avoid possible side effects derived from ectopic and/or unregulated expression of the transgene while maintaining its therapeutic potential.

ACKNOWLEDGMENTS

The authors are indebted to Ms. Concepción Hernández and Ms. Alicia González (Centro de Instrumentación Científica, University of Granada) for excellent sample preparation and SEM analysis. The authors are also grateful to Dr. Didier Trono (University of Geneva, Geneva, Switzerland) for providing the HIV packaging pCMV.R8.91 and envelope pMD.G plasmids. The authors acknowledge the continuous and generous supply

of rIL-2 (Hoffman-LaRoche, Nutley, NJ) provided by the National Institutes of Health AIDS Research and Reference Reagent Program (Rockville, MD). This work was supported by grant PI061035 (Fondo de Investigación Sanitaria, Instituto de Salud Carlos III) to F.M. and by grants SAF2006-06246 (Spanish Ministry of Education and Science) and P06-CTS-02112 (Consejería de Innovación y Ciencia, Junta de Andalucia, Regional Government of Andalusia) to I.J.M. The authors also thank the Wellcome Trust for financial support to A.J.T.

AUTHOR DISCLOSURE STATEMENT

For all authors, no competing financial interests exist.

REFERENCES

AIUTI, A., SLAVIN, S., AKER, M., FICARA, F., DEOLA, S., MORTELLARO, A., MORECKI, S., ANDOLFI, G., TABUCCHI, A., CARLUCCI, F., MARINELLO, E., CATTANEO, F., VAI, S., SERVIDA, P., MINIERO, R., RONCAROLO, M.G., and BORDIGNON, C. (2002). Correction of ADA-SCID by stem cell gene therapy combined with nonmyeloablative conditioning. Science **296,** 2410–2413.

BADOLATO, R., SOZZANI, S., MALACARNE, F., BRESCIANI, S., FIORINI, M., BORSATTI, A., ALBERTINI, A., MANTOVANI, A., UGAZIO, A.G., and NOTARANGELO, L.D. (1998). Monocytes from Wiskott-Aldrich patients display reduced chemotaxis and lack of cell polarization in response to monocyte chemoattractant protein-1 and formyl-methionyl-leucyl-phenylalanine. J. Immunol. **161,** 1026–1033.

BURNS, S., THRASHER, A.J., BLUNDELL, M.P., MACHESKY, L., and JONES, G.E. (2001). Configuration of human dendritic cell cytoskeleton by Rho GTPases, the WAS protein, and differentiation. Blood **98,** 1142–1149.

CAVAZZANA-CALVO, M., HACEIN-BEY, S., DE SAINT BASILE, G., GROSS, F., YVON, E., NUSBAUM, P., SELZ, F., HUE, C., CERTAIN, S., CASANOVA, J.L., BOUSSO, P., DEIST, F.L., and FISCHER, A. (2000). Gene therapy of human severe combined immunodeficiency (SCID)-X1 disease. Science **288,** 669–672.

CUI, Y., GOLOB, J., KELLEHER, E., YE, Z., PARDOLL, D., and CHENG, L. (2002). Targeting transgene expression to antigen-presenting cells derived from lentivirus-transduced engrafting human hematopoietic stem/progenitor cells. Blood **99,** 399–408.

CHAN, R.J., and YODER, M.C. (2004). The multiple facets of hematopoietic stem cells. Curr. Neurovasc. Res. **1,** 197–206.

CHARRIER, S., DUPRE, L., SCARAMUZZA, S., JEANSON-LEH, L., BLUNDELL, M.P., DANOS, O., CATTANEO, F., AIUTI, A., ECKENBERG, R., THRASHER, A.J., RONCAROLO, M.G., and GALY, A. (2006). Lentiviral vectors targeting WASp expression to hematopoietic cells, efficiently transduce and correct cells from WAS patients. Gene Ther. **14,** 415–428.

DE LA FUENTE, M.A., SASAHARA, Y., CALAMITO, M., ANTON, I.M., ELKHAL, A., GALLEGO, M.D., SURESH, K., SIMINOVITCH, K., OCHS, H.D., ANDERSON, K.C., ROSEN, F.S., GEHA, R.S., and RAMESH, N. (2007). WIP is a chaperone for Wiskott-Aldrich syndrome protein (WASP). Proc. Natl. Acad. Sci. U.S.A. **104,** 926–931.

DEMAISON, C., BROUNS, G., BLUNDELL, M.P., GOLDMAN, J.P., LEVINSKY, R.J., GREZ, M., KINNON, C., and THRASHER, A.J. (2000). A defined window for efficient gene marking of severe combined immunodeficient-repopulating cells using a gibbon ape leukemia virus-pseudotyped retroviral vector. Hum. Gene Ther. **11,** 91–100.

DEMAISON, C., PARSLEY, K., BROUNS, G., SCHERR, M., BATTMER, K., KINNON, C., GREZ, M., and THRASHER, A.J. (2002). High-level transduction and gene expression in hematopoietic repopulating cells using a human immunodeficiency [correction of imunodeficiency] virus type 1-based lentiviral vector containing an internal spleen focus forming virus promoter. Hum. Gene Ther. **13,** 803–813.

DE NORONHA, S., HARDY, S., SINCLAIR, J., BLUNDELL, M.P., STRID, J., SCHULZ, O., ZWIRNER, J., JONES, G.E., KATZ, D.R., KINNON, C., and THRASHER, A.J. (2005). Impaired dendritic-cell homing *in vivo* in the absence of Wiskott-Aldrich syndrome protein. Blood **105,** 1590–1597.

DUPRE, L., TRIFARI, S., FOLLENZI, A., MARANGONI, F., LAIN DE LERA, T., BERNAD, A., MARTINO, S., TSUCHIYA, S., BORDIGNON, C., NALDINI, L., AIUTI, A., and RONCAROLO, M.G. (2004). Lentiviral vector-mediated gene transfer in T cells from Wiskott-Aldrich syndrome patients leads to functional correction. Mol. Ther. **10,** 903–915.

DUPRE, L., MARANGONI, F., SCARAMUZZA, S., TRIFARI, S., HERNANDEZ, R.J., AIUTI, A., NALDINI, L., and RONCAROLO, M.G. (2006). Efficacy of gene therapy for Wiskott-Aldrich syndrome using a WAS promoter/cDNA-containing lentiviral vector and nonlethal irradiation. Hum. Gene Ther. **17,** 303–313.

FINAN, P.M., SOAMES, C.J., WILSON, L., NELSON, D.L., STEWART, D.M., TRUONG, O., HSUAN, J.J., and KELLIE, S. (1996). Identification of regions of the Wiskott-Aldrich syndrome protein responsible for association with selected Src homology 3 domains. J. Biol. Chem. **271,** 26291–26295.

GALLEGO, M.D., SANTAMARIA, M., PENA, J., and MOLINA, I.J. (1997). Defective actin reorganization and polymerization of Wiskott-Aldrich T cells in response to CD3-mediated stimulation. Blood **90,** 3089–3097.

GARCIA-PACHECO, J.M., OLIVER, C., KIMATRAI, M., BLANCO, F.J., and OLIVARES, E.G. (2001). Human decidual stromal cells express CD34 and STRO-1 and are related to bone marrow stromal precursors. Mol. Hum. Reprod. **7,** 1151–1157.

GASPAR, H.B., PARSLEY, K.L., HOWE, S., KING, D., GILMOUR, K.C., SINCLAIR, J., BROUNS, G., SCHMIDT, M., VON KALLE, C., BARINGTON, T., JAKOBSEN, M.A., CHRISTENSEN, H.O., AL GHONAIUM, A., WHITE, H.N., SMITH, J.L., LEVINSKY, R.J., ALI, R.R., KINNON, C., and THRASHER, A.J. (2004). Gene therapy of X-linked severe combined immunodeficiency by use of a pseudotyped gammaretroviral vector. Lancet **364,** 2181–2187.

GISMONDI, A., CIFALDI, L., MAZZA, C., GILIANI, S., PAROLINI, S., MORRONE, S., JACOBELLI, J., BANDIERA, E., NOTARANGELO, L., and SANTONI, A. (2004). Impaired natural and CD16-mediated NK cell cytotoxicity in patients with WAS and XLT: Ability of IL-2 to correct NK cell functional defect. Blood **104,** 436–443.

HACEIN-BEY-ABINA, S., VON KALLE, C., SCHMIDT, M., McCORMACK, M.P., WULFFRAAT, N., LEBOULCH, P., LIM, A., OSBORNE, C.S., PAWLIUK, R., MORILLON, E., SORENSEN, R., FORSTER, A., FRASER, P., COHEN, J.I., DE SAINT BASILE, G., ALEXANDER, I., WINTERGERST, U., FREBOURG, T., AURIAS, A., STOPPA-LYONNET, D., ROMANA, S., RADFORD-WEISS, I., GROSS, F., VALENSI, F., DELABESSE, E., MACINTYRE, E., SIGAUX, F., SOULIER, J., LEIVA, L.E., WISSLER, M., PRINZ, C., RABBITTS, T.H., LE DEIST, F., FISCHER, A., and CAVAZZANA-CALVO, M. (2003). *LMO2*-associated clonal T cell proliferation in two patients after gene therapy for SCID-X1. Science **302,** 415–419.

HUMBLET-BARON, S., SATHER, B., ANOVER, S., BECKER-HERMAN, S., KASPROWICZ, D.J., KHIM, S., NGUYEN, T., HUD-

KINS-LOYA, K., ALPERS, C.E., ZIEGLER, S.F., OCHS, H., TORGERSON, T., CAMPBELL, D.J., and RAWLINGS, D.J. (2007). Wiskott-Aldrich syndrome protein is required for regulatory T cell homeostasis. J. Clin. Invest. **117,** 407–418.

KOLLURI, R., TOLIAS, K.F., CARPENTER, C.L., ROSEN, F.S., and KIRCHHAUSEN, T. (1996). Direct interaction of the Wiskott-Aldrich syndrome protein with the GTPase Cdc42. Proc. Natl. Acad. Sci. U.S.A. **93,** 5615–5618.

KONNO, A., WADA, T., SCHURMAN, S.H., GARABEDIAN, E.K., KIRBY, M., ANDERSON, S.M., and CANDOTTI, F. (2004). Differential contribution of Wiskott-Aldrich syndrome protein to selective advantage in T- and B-cell lineages. Blood **103,** 676–678.

KONNO, A., KIRBY, M., ANDERSON, S.A., SCHWARTZBERG, P.L., and CANDOTTI, F. (2007). The expression of Wiskott-Aldrich syndrome protein (WASP) is dependent on WASP-interacting protein (WIP). Int. Immunol. **19,** 185–192.

LAGASSE, E., CONNORS, H., AL-DHALIMY, M., REITSMA, M., DOHSE, M., OSBORNE, L., WANG, X., FINEGOLD, M., WEISSMAN, I.L., and GROMPE, M. (2000). Purified hematopoietic stem cells can differentiate into hepatocytes *in vivo*. Nat. Med. **6,** 1229–1234.

LEVERRIER, Y., LORENZI, R., BLUNDELL, M.P., BRICKELL, P., KINNON, C., RIDLEY, A.J., and THRASHER, A.J. (2001). Cutting edge: The Wiskott-Aldrich syndrome protein is required for efficient phagocytosis of apoptotic cells. J. Immunol. **166,** 4831–4834.

LINDER, S., and AEPFELBACHER, M. (2003). Podosomes: Adhesion hot-spots of invasive cells. Trends Cell Biol. **13,** 376–385.

LINDER, S., NELSON, D., WEISS, M., and AEPFELBACHER, M. (1999). Wiskott-Aldrich syndrome protein regulates podosomes in primary human macrophages. Proc. Natl. Acad. Sci. U.S.A. **96,** 9648–9653.

MACHESKY, L.M., MULLINS, R.D., HIGGS, H.N., KAISER, D.A., BLANCHOIN, L., MAY, R.C., HALL, M.E., and POLLARD, T.D. (1999). Scar, a WASp-related protein, activates nucleation of actin filaments by the Arp2/3 complex. Proc. Natl. Acad. Sci. U.S.A. **96,** 3739–3744.

MAILLARD, M.H., COTTA-DE-ALMEIDA, V., TAKESHIMA, F., NGUYEN, D.D., MICHETTI, P., NAGLER, C., BHAN, A.K., and SNAPPER, S.B. (2007). The Wiskott-Aldrich syndrome protein is required for the function of $CD4^+CD25^+Foxp3^+$ regulatory T cells. J. Exp. Med. **204,** 381–391.

MARANGONI, F., TRIFARI, S., SCARAMUZZA, S., PANARONI, C., MARTINO, S., NOTARANGELO, L.D., BAZ, Z., METIN, A., CATTANEO, F., VILLA, A., AIUTI, A., BATTAGLIA, M., RONCAROLO, M.G., and DUPRE, L. (2007). WASP regulates suppressor activity of human and murine $CD4^+CD25^+FOXP3^+$ natural regulatory T cells. J. Exp. Med. **204,** 369–380.

MARTIN, F., TOSCANO, M.G., BLUNDELL, M., FRECHA, C., SRIVASTAVA, G.K., SANTAMARIA, M., THRASHER, A.J., and MOLINA, I.J. (2005). Lentiviral vectors transcriptionally targeted to hematopoietic cells by WASP gene proximal promoter sequences. Gene Ther. **12,** 715–723.

MARX, J. (2006). Cell biology: Podosomes and invadopodia help mobile cells step lively. Science **312,** 1868–1869.

MOLINA, I.J., KENNEY, D.M., ROSEN, F.S., and REMOLD-O'DONNELL, E. (1992). T cell lines characterize events in the pathogenesis of the Wiskott-Aldrich syndrome. J. Exp. Med. **176,** 867–874.

MOLINA, I.J., SANCHO, J., TERHORST, C., ROSEN, F.S., and REMOLD-O'DONNELL, E. (1993). T cells of patients with the Wiskott-Aldrich syndrome have a restricted defect in proliferative responses. J. Immunol. **151,** 4383–4390.

MONTINI, E., CESANA, D., SCHMIDT, M., SANVITO, F., PONZONI, M., BARTHOLOMAE, C., SERGI, L.S., BENEDICENTI, F., AMBROSI, A., DI SERIO, C., DOGLIONI, C., VON KALLE, C., and NALDINI, L. (2006). Hematopoietic stem cell gene transfer in a tumor-prone mouse model uncovers low genotoxicity of lentiviral vector integration. Nat. Biotechnol. **24,** 687–696.

MOREAU-GAUDRY, F., XIA, P., JIANG, G., PERELMAN, N.P., BAUER, G., ELLIS, J., SURINYA, K.H., MAVILIO, F., SHEN, C.K., and MALIK, P. (2001). High-level erythroid-specific gene expression in primary human and murine hematopoietic cells with self-inactivating lentiviral vectors. Blood **98,** 2664–2672.

MOSMANN, T. (1983). Rapid colorimetric assay for cellular growth and survival: Application to proliferation and cytotoxicity assays. J. Immunol. Methods **65,** 55–63.

NALDINI, L., BLOMER, U., GALLAY, P., ORY, D., MULLIGAN, R., GAGE, F.H., VERMA, I.M., and TRONO, D. (1996). *In vivo* gene delivery and stable transduction of nondividing cells by a lentiviral vector. Science **272,** 263–267.

NEIL, S., MARTIN, F., IKEDA, Y., and COLLINS, M. (2001). Post-entry restriction to human immunodeficiency virus-based vector transduction in human monocytes. J. Virol. **75,** 5448–5456.

OTT, M.G., SCHMIDT, M., SCHWARZWAELDER, K., STEIN, S., SILER, U., KOEHL, U., GLIMM, H., KUHLCKE, K., SCHILZ, A., KUNKEL, H., NAUNDORF, S., BRINKMANN, A., DEICHMANN, A., FISCHER, M., BALL, C., PILZ, I., DUNBAR, C., DU, Y., JENKINS, N.A., COPELAND, N.G., LUTHI, U., HASSAN, M., THRASHER, A.J., HOELZER, D., VON KALLE, C., SEGER, R., and GREZ, M. (2006). Correction of X-linked chronic granulomatous disease by gene therapy, augmented by insertional activation of MDS1-EVI1, PRDM16 or SETBP1. Nat. Med. **12,** 401–409.

PAROLINI, O., BERARDELLI, S., RIEDL, E., BELLO-FERNANDEZ, C., STROBL, H., MAJDIC, O., and KNAPP, W. (1997). Expression of Wiskott-Aldrich syndrome protein (WASP) gene during hematopoietic differentiation. Blood **90,** 70–75.

RAMESH, N., ANTON, I.M., HARTWIG, J.H., and GEHA, R.S. (1997). WIP, a protein associated with Wiskott-Aldrich syndrome protein, induces actin polymerization and redistribution in lymphoid cells. Proc. Natl. Acad. Sci. U.S.A. **94,** 14671–14676.

SEMBA, S., IWAYA, K., MATSUBAYASHI, J., SERIZAWA, H., KATABA, H., HIRANO, T., KATO, H., MATSUOKA, T., and MUKAI, K. (2006). Coexpression of actin-related protein 2 and Wiskott-Aldrich syndrome family verproline-homologous protein 2 in adenocarcinoma of the lung. Clin. Cancer Res. **12,** 2449–2454.

SNAPPER, S.B., TAKESHIMA, F., ANTON, I., LIU, C.H., THOMAS, S.M., NGUYEN, D., DUDLEY, D., FRASER, H., PURICH, D., LOPEZ-ILASACA, M., KLEIN, C., DAVIDSON, L., BRONSON, R., MULLIGAN, R.C., SOUTHWICK, F., GEHA, R., GOLDBERG, M.B., ROSEN, F.S., HARTWIG, J.H., and ALT, F.W. (2001). N-WASP deficiency reveals distinct pathways for cell surface projections and microbial actin-based motility. Nat. Cell Biol. **3,** 897–904.

STEWART, D.M., TREIBER-HELD, S., KURMAN, C.C., FACCHETTI, F., NOTARANGELO, L.D., and NELSON, D.L. (1996). Studies of the expression of the Wiskott-Aldrich syndrome protein. J. Clin. Invest. **97,** 2627–2634.

SYMONS, M., DERRY, J.M., KARLAK, B., JIANG, S., LEMAHIEU, V., McCORMICK, F., FRANCKE, U., and ABO, A. (1996). Wiskott-Aldrich syndrome protein, a novel effector for the GTPase CDC42Hs, is implicated in actin polymerization. Cell **84,** 723–734.

TAKENAWA, T., and MIKI, H. (2001). WASP and WAVE family proteins: Key molecules for rapid rearrangement of cortical actin filaments and cell movement. J. Cell Sci. **114,** 1801–1809.

THRASHER, A.J. (2002). WASp in immune-system organization and function. Nat. Rev. Immunol. **2,** 635–646.

TOSCANO, M.G., FRECHA, C., ORTEGA, C., SANTAMARIA, M., MARTIN, F., and MOLINA, I.J. (2004). Efficient lentiviral transduction of herpesvirus saimiri immortalized T cells as a model for gene therapy in primary immunodeficiencies. Gene Ther. **11,** 956–961.

VASSILOPOULOS, G., WANG, P.R., and RUSSELL, D.W. (2003). Transplanted bone marrow regenerates liver by cell fusion. Nature **422,** 901–904.

YAMAGUCHI, H., and CONDEELIS, J. (2006). Regulation of the actin cytoskeleton in cancer cell migration and invasion. Biochim. Biophys. Acta **1773,** 642–652.

YAMAZAKI, D., KURISU, S., and TAKENAWA, T. (2005). Regulation of cancer cell motility through actin reorganization. Cancer Sci. **96,** 379–386.

YANG, L.Y., TAO, Y.M., OU, D.P., WANG, W., CHANG, Z.G., and WU, F. (2006). Increased expression of Wiskott-Aldrich syndrome protein family verprolin-homologous protein 2 correlated with poor prognosis of hepatocellular carcinoma. Clin. Cancer Res. **12,** 5673–5679.

ZUFFEREY, R., DULL, T., MANDEL, R.J., BUKOVSKY, A., QUIROZ, D., NALDINI, L., and TRONO, D. (1998). Self-inactivating lentivirus vector for safe and efficient *in vivo* gene delivery. J. Virol. **72,** 9873–9880.

Address reprint requests to:
Dr. Francisco Martin
Parque Tecnológico Ciencias de la Salud
IPB Lopez Neyra (CSIC)
Avenida del Conocimiento s/n
18100 Armilla, Granada, Spain

E-mail: fmartin@ipb.csic.es

Received for publication August 23, 2007; accepted after revision November 22, 2007.

Published online: February 1, 2008.

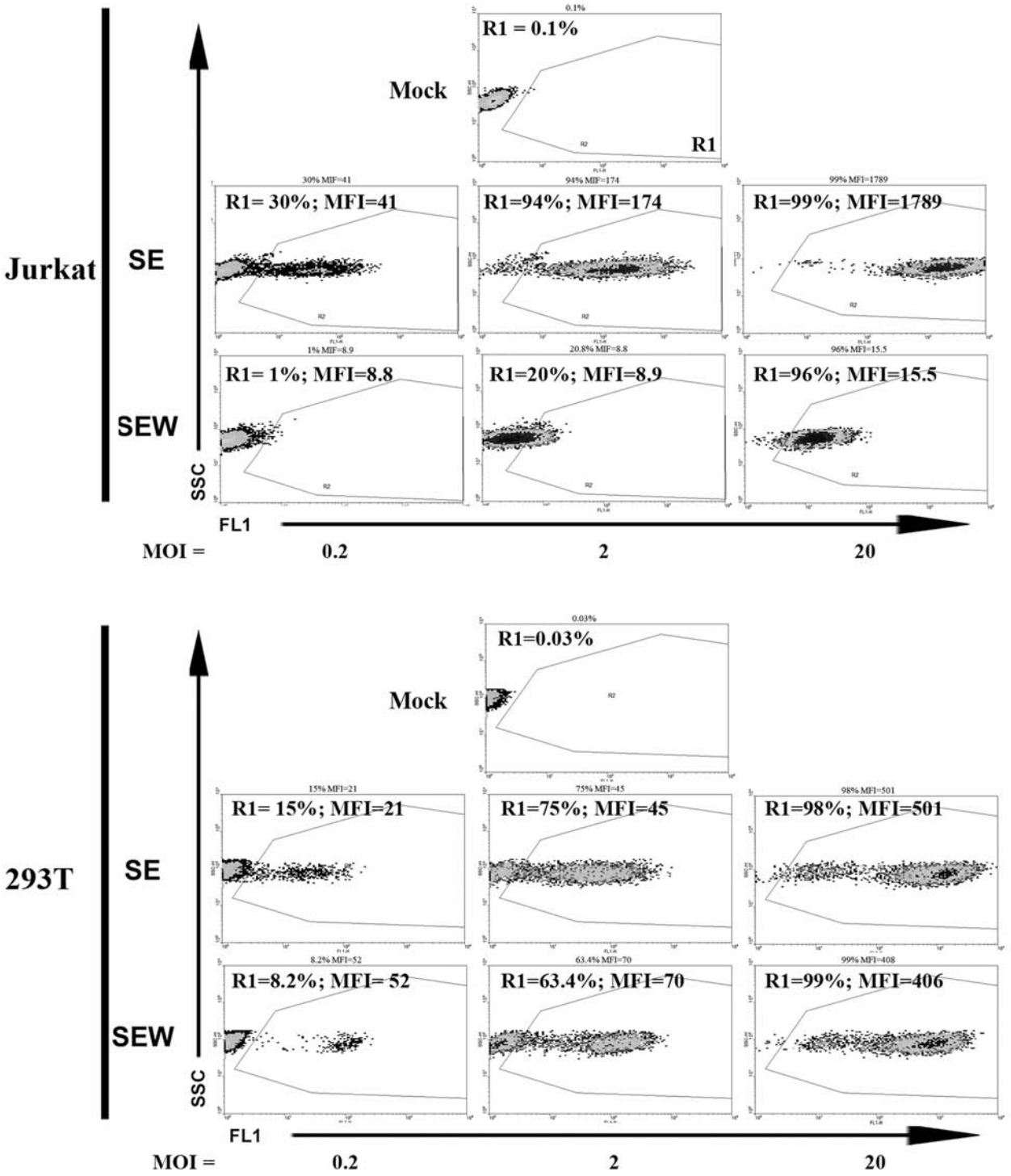

SUPPL. FIG. 1. Flow cytometric analysis of hematopoietic and nonhematopoietic cells transduced with SE and SEW lentiviral vectors expressing eGFP and eGFP–WASp, respectively. Jurkat cells (*top*) and 293T cells (*bottom*) were transduced at increasing MOIs (0.2, 2, and 20) with the indicated vectors and analyzed 7 days later. Both vectors expressed the transgene at similar levels in 293T cells, but a dramatic reduction of eGFP–WASp expression was observed in SEW-transduced Jurkat cells. On the other hand, the SE vector expressed eGFP efficiently in Jurkat cells, indicating that the SFFV promoter is active in this cell type. Therefore, restriction of the SEW vector (containing the SFFV promoter) to express eGFP–WASp in Jurkat cells is not due to promoter strength.

ARTHRITIS & RHEUMATISM
Vol. 58, No. 4, April 2008, pp 1026–1037
DOI 10.1002/art.23283

In Vivo Delivery of Lentiviral Vectors Expressing Vasoactive Intestinal Peptide Complementary DNA as Gene Therapy for Collagen-Induced Arthritis

Mario Delgado,[1] Miguel G. Toscano,[1] Karim Benabdellah,[1] Marien Cobo,[1] Francisco O'Valle,[2] Elena Gonzalez-Rey,[3] and Francisco Martín[1]

Objective. **Vasoactive intestinal peptide (VIP) has been shown to exert potent immunomodulatory activity, and the use of lentiviral vectors has been found to be an effective means of gene delivery. The present study was therefore undertaken to investigate the feasibility and efficiency of gene therapy using lentiviral vectors expressing VIP (LentiVIP) for the treatment of rheumatoid arthritis (RA).**

Methods. **We evaluated the therapeutic potential of the gene therapy strategy in the collagen-induced arthritis (CIA) mouse model, administrating the vectors at different phases of the disease. The inflammatory response was determined by measuring the levels of various inflammatory cytokines and chemokines in the joints and serum. The Th1-mediated response was evaluated by determining the proliferative response and cytokine profile of T cells stimulated with autoantigen.**

Results. **A single intraperitoneal injection of LentiVIP was highly effective in treating CIA. Mice with established, severe arthritis showed complete regression of the disease. The therapeutic effect of LentiVIP was associated with widespread biodistribution of the vector and increased VIP levels, especially in joints and lymphoid organs, and was mediated through a striking reduction of the 2 deleterious components of the disease, i.e., the autoimmune response (self-reactive Th1 cell activity and autoantibody production) and the inflammatory response. LentiVIP treatment also induced the generation and/or activation of CD4+,CD25+,FoxP3+ Treg cells in arthritic mice.**

Conclusion. **Our findings show that in vivo administration of lentiviral vector expressing VIP produces one of the most potent therapeutic effects described so far in any animal model of RA. We propose that VIP gene transfer should be further investigated as a potential novel, effective treatment of RA and other chronic autoimmune disorders.**

The main advantage of gene-based therapy strategies is that they enable continuous and/or regulated synthesis of therapeutic molecules inside the target tissue for long periods, increasing potency and reducing systemic toxicity. In addition, the therapeutic molecules are more active than their recombinant counterparts (1,2). A wide range of gene therapy strategies directed against the inflammatory response or damaged synovium has been assayed in animal models of rheumatoid arthritis (RA) (refs. 3–7; for review, see ref. 3) and in clinical trials (8,9). These studies have demonstrated feasibility and safety of the gene therapy strategies, but new protocols are still needed to demonstrate their potency as a viable alternative to current RA treatments. In theory, a single injection of therapeutic vectors, administered locally or systemically, could be enough to have potent benefits. However, clinical trials of gene therapy for RA, involving direct injection of naked DNA and/or retrovirus, have shown poor results (http://

Supported by the Junta de Andalucía (Proyectos de Excelencia), the Spanish Ministry of Education (Ramón y Cajal programme and grant SAF2003-00645), and the Fondo de Investigación Sanitaria (grant PI061035).

[1]Mario Delgado, PhD, Miguel G. Toscano, PhD (current address: Temple University, Philadelphia, Pennsylvania), Karim Benabdellah, PhD (current address Estación Experimental del Zaidin [CSIC], Granada, Spain), Marien Cobo, BS, Francisco Martín, PhD: Instituto de Parasitología y Biomedicina López Neyra, CSIC, Granada, Spain; [2]Francisco O'Valle, MD, PhD: University of Granada, Granada, Spain; [3]Elena Gonzalez-Rey, PhD: University of Seville, Seville, Spain.

Address correspondence and reprint requests to Francisco Martín, PhD, Immunology and Cell Biology Department, Instituto de Parasitología y Biomedicina CSIC, Avenida del Conocimiento s/n, PT Ciencias de la Salud, Armilla-18100, Granada, Spain. E-mail: fmartin@ipb.csic.es.

Submitted for publication August 28, 2007; accepted in revised form December 7, 2007.

www.wiley.co.uk/genmed/clinical/), due in part to poor transduction efficiency.

Plasmids as well as adenoviral and adeno-associated viral vectors have been used successfully for gene therapy of arthritis. They all prevented disease development (10–13) and also reduced severity when treatment was started shortly after disease onset (14–17). However, to date only partial therapeutic effect has been achieved when treatment is started in animals with established signs of severe arthritis (arthritis score >6) (for review, see ref. 3). Lentiviral vectors have been described as the most powerful of all integrative vector systems (18) and are one of the most efficient vectors for in vivo application (19,20). The latest generation of lentiviral vectors is one of the safest and most efficient tools for stable gene transfer (18,21), even eliminating the risk of vector mobilization, due to infection with a wild-type human immunodeficiency virus type 1 (HIV-1).

Vasoactive intestinal peptide (VIP) is a neuropeptide that elicits a broad spectrum of biologic functions (22), acting as a potent antiinflammatory factor, inhibiting Th1 responses, and promoting immune tolerance by inducing the generation of Treg cells (23). As a consequence, VIP has emerged as a promising tool for the treatment of autoimmune/inflammatory diseases (22,23), including RA, ulcerative colitis, multiple sclerosis, type 1 diabetes mellitus, and uveoretinitis (24–28). The therapeutic effect of VIP is associated with reduction of the 2 main phases of these immune disorders: autoimmunity to self tissue components and destructive inflammatory responses. Therefore, VIP shows therapeutic advantages versus agents directed against only 1 component of these diseases.

Despite these advantages, there are several obstacles to translating VIP-based treatment into viable clinical therapies. VIP is very unstable and extremely sensitive to the peptidases present in most tissues, requiring multiple injections of high doses of the peptide to achieve a sustained therapeutic effect. Therefore, in recent years, several groups have developed viral (29,30) and nonviral (27,31) vectors to deliver VIP for the treatment of autoimmune disorders, including experimental arthritis (31).

In this study we used lentiviral vectors to achieve steady expression of VIP for the treatment of experimental arthritis in a collagen-induced arthritis (CIA) model, in which Freund's complete adjuvant (CFA) was used instead of phosphate buffered saline (PBS) in the second immunization in order to simulate more aggressive disease. We showed that a single injection of lentiviral vectors expressing *VIP* complementary DNA (cDNA) provides highly effective treatment of CIA, with complete regression of established, severe arthritis correlating with a striking reduction of the autoimmune and inflammatory responses.

MATERIALS AND METHODS

Plasmids and lentiviral constructs. The HIV packaging (pCMVΔR8.91) and vesicular stomatitis virus G (pMD.G) plasmids (18) were kindly provided by Dr. D. Trono (University of Geneva, Geneva, Switzerland). The CEWP lentiviral vector expressing enhanced green fluorescent protein (EGFP) through the strong CMVTetO promoter was constructed by replacing the SFFV promoter in the pHRSIN-CSEW vector (SEWP) (32) as follows. A polymerase chain reaction (PCR) fragment containing the CMVTetO promoter and the *Eco* RI/*Bam* HI sites was obtained by PCR using the *Eco* RI forward (CCGGAATTCGTTGACATTGATTATTGACTA) and *Bam* HI reverse (CGCGGATCCCGGAAGATGGATCGGTCC) primers with pcDNA4/TO as template. The CE vector was obtained by inserting this fragment into the SEWP vector backbone by *Eco* RI/*Bam* HI direct ligation. The lentiviral vector expressing VIP (LentiVIP) was constructed by replacing *EGFP* in the CEWP plasmid with a 560-bp *VIP* cDNA fragment (nucleotides 173–724 from the human locus NM-003381). This fragment was obtained by PCR using the pCMV6-XL4-VIP plasmid containing the full-length *VIP* cDNA (Trueclone [catalog no. TC111704]; OriGene Technologies, Rockville, MD) using the *Bam* HI–VIP forward (5′-CGGGATCCATGGACACCAGAAATAAGG) and *Pst* I–VIP reverse (5′-CACTGCAGGGGAAGTTGTCATCAGC) primers. Direct cloning was performed after *Bam* HI/*Pst* I restriction of the PCR fragment and CEWP.

Vector production and titration. Lentiviral vectors were produced by cotransfection of 293T kidney cells (CRL11268; American Type Culture Collection; Rockville, MD) with 3 plasmids: 1) vector plasmid (CEWP or LentiVIP), 2) packaging plasmid (pCMVΔR8.91), and 3) envelope plasmid (pMD.G), as previously described (33), using Lipofectamine 2000 (Invitrogen, Carlsbad, CA). Vector titration was performed in 293T cells. CEWP vector titration was determined based on the percentage of EGFP-positive cells calculated by fluorescence-activated cell sorter analysis 7 days after transduction. For titration of LentiVIP vectors, transduced cells were lysed and DNA extracted after 7–10 days. Vector copy number per cell was determined using quantitative PCR as described below.

DNA preparation and quantitative real-time PCR. Genomic DNA from culture cells and tissue samples was isolated by adding 1 ml of SNET extraction buffer (34). Quantitative real-time PCR were performed with an ABI Prism 7000 sequence detection system (Applied Biosystems, Foster City, CA). Samples were mixed with 2× iQ SYBR Green Supermix (Bio-Rad, Richmond, CA). To quantitate LentiVIP integration, we used primers comprising vector (cytomegalovirus [CMV]) and *VIP* sequences (CMVVIP forward 5′-GAGCTCGTTTAGTGAACCGTCAGA-3′, reverse 5′-AAGGAGCTGGGCCTTATTTCTGGT-3′). For CEWP

quantification, EGFP forward primer (5′-GCCCGACAACC-ACTACCT-3′) and reverse primer (5′-CGTCCATGC-CGAGAGTGA-3′) were used.

Western blotting. Cells were lysed with 1% Nonidet P40 lysis buffer containing protease inhibitor cocktail (Sigma, St Louis, MO), resolved by sodium dodecyl sulfate–polyacrylamide gel electrophoresis (10% polyacrylamide gels under reducing conditions), and electrotransferred to Hybond P polyvinylidene difluoride membranes (Amersham Biosciences, Little Chalfont, UK). Membranes were blocked with 5% nonfat milk and probed for 1 hour at room temperature with 2 μg/ml of anti-VIP monoclonal antibody (mAb) (clone H16; Santa Cruz Biotechnology, Santa Cruz, CA), followed by incubation with horseradish peroxidase–labeled goat anti-mouse antibody (1:10,000 dilution, Caltag, Burlingame, CA). Analysis was performed using the ECL Advanced Western Blotting Detection Kit (Amersham Biosciences).

Determination of VIP levels and bioactivity. VIP levels in culture supernatants of LentiVIP-transduced cells and in sera and tissue from mice treated with LentiVIP were determined with an enzyme immunoassay kit (Phoenix Pharmaceuticals, Karlsruhe, Germany). To measure secretion of bioactive VIP by LentiVIP-transduced cells, 1 ml of culture supernatants was lyophilized, resuspended (100 μl) in PBS, and added to the murine macrophage cell line RAW 264.7 (10^6 cells/ml). Cells were cultured for 20 minutes in the presence of 3-isobutyl-1-methyl xanthine, lysed, and intracellular cAMP levels determined with an enzyme immunoassay kit (Amersham Biosciences). In addition, RAW 264.7 cells were stimulated with lipopolysaccharide (500 ng/ml) for 8 hours, and levels of tumor necrosis factor α (TNFα) in the culture supernatants were determined by enzyme-linked immunosorbent assay (ELISA).

Arthritis induction and treatment. Animal experimental protocols were reviewed and approved by the Ethics Committee of the Spanish Council of Scientific Research. To induce severe CIA, DBA/1J mice (7–10 weeks old; The Jackson Laboratory, Bar Harbor, ME) were injected subcutaneously with 200 μg of type II collagen (CII; Sigma) emulsified in CFA containing 200 μg *Mycobacterium tuberculosis* H37Ra (Difco, Detroit, MI). On day 21 after primary immunization, mice were boosted by subcutaneous injection of 100 μg of CII in CFA. LentiVIP treatment consisted of intraperitoneal administration of lentiviral vectors as indicated below. Mice with CIA were injected intraperitoneally with PBS or with CEWP vectors (expressing EGFP) as controls. Mice were assessed under blinded conditions every other day by 2 independent examiners, and scored for signs of arthritis as follows: grade 0 = no swelling; grade 1 = slight swelling and erythema; grade 2 = moderate swelling and edema; grade 3 = extreme swelling and pronounced edema; grade 4 = joint rigidity. Each limb was graded, for a maximum possible score of 16 per animal.

Histologic analysis. For histologic analysis, paws were collected at random by 2 independent investigators on day 70 after primary immunization, fixed in 4% buffered formaldehyde, decalcified, embedded in paraffin, sectioned, and stained with hematoxylin and eosin or Masson's-Goldner trichrome stain. Histopathologic changes were scored in a blinded manner based on cell infiltration, cartilage destruction, and bone erosion parameters as previously described (24). Neutrophil infiltration into the joints was monitored by measuring myeloperoxidase activity in joint extracts isolated on day 35 postimmunization as previously described (35).

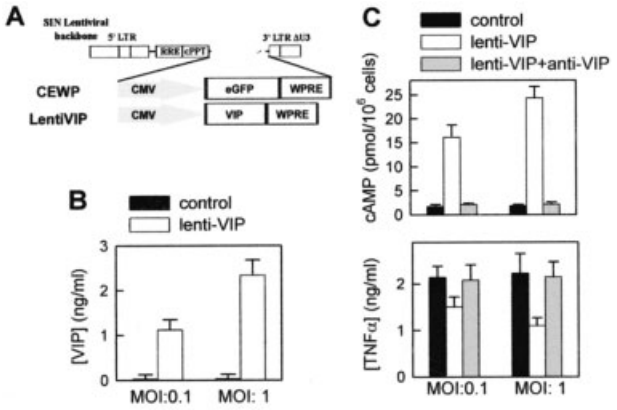

Figure 1. Evidence that lentiviral vectors driving the expression of vasoactive intestinal peptide (*VIP*) cDNA are efficient tools for expression of functional VIP. **A**, Maps of lentiviral vector used in the study. CEWP and LentiVIP are self-inactivated human immunodeficiency virus type 1–derived lentiviral vectors expressing enhanced green fluorescent protein (EGFP) and *VIP* cDNA, respectively, through the cytomegalovirus (CMV) minimal promoter. LTR = long terminal repeat; RRE = Rev-responsive element; cPPT = central polypurine tract; WPRE = woodchuck hepatitis posttranscriptional regulatory element. **B,** VIP levels in culture supernatants of cells transduced with LentiVIP at multiplicities of infection (MOI) of 0.1 and 1, determined by enzyme immunoassay. Controls were cells transduced with the same amount of CEWP vector. **C**, Production of bioactive VIP by LentiVIP-transduced cells. Culture supernatants of cells transduced with LentiVIP (MOI 0.1 and 1) were added to RAW 264.7 cells (10^6 cells/ml). In some samples, neutralizing concentrations of anti-VIP antibody (100 μg/ml) were added to cultures. Upper panel, Intracellular cAMP levels were determined by enzyme immunoassay after 20 minutes of culture. Lower panel, RAW 264.7 cells were stimulated with lipopolysaccharide (500 ng/ml) for 8 hours, and levels of tumor necrosis factor α (TNFα) in the culture supernatant were determined by enzyme-linked immunorsorbent assay. Controls were cells transduced with the same amount of CEWP vector. Values in **B** and **C** are the mean and SD from 3 experiments performed in duplicate.

Cytokine and autoantibody measurement. For determination of cytokine levels in the joints, protein extracts were isolated by homogenization of joints (50 mg tissue/ml) in 50 m*M* Tris HCl (pH 7.4) with 0.5 m*M* dithiothreitol and proteinase inhibitor cocktail (10 μg/ml; Sigma). Serum samples were collected at the peak of disease (day 35), and the levels of IgG, IgG1, and IgG2a anti-CII antibody were measured by ELISA as previously described (24). Cytokine and chemokine levels in the serum and joint protein extracts prepared on day 35 were determined with specific sandwich ELISAs using capture/biotinylated detection antibodies according to the recommendations of the manufacturer (BD PharMingen, San Diego, CA).

Assessment of T cell autoreactive response. Single-cell suspensions (10^6 cells/ml) pooled from spleen and draining lymph nodes or from knee joint synovial membrane were

obtained 35 days postimmunization. Cells were stimulated in complete medium (RPMI 1640 containing 10% fetal calf serum, 2 m*M* L-glutamine, 100 units/ml penicillin, and 100 μg/ml streptomycin) with various concentrations of heat-inactivated CII for 48 hours (for cytokine determination) or for 72 hours (for proliferative response assays). Cell proliferation was evaluated using a bromodeoxyuridine-based cell proliferation assay (Roche Diagnostics, Mannheim, Germany). Cytokine content in culture supernatants was determined by specific sandwich ELISA as described above. For intracellular analysis of cytokines, draining lymph node and synovial cells were stimulated with inactivated CII (10 μg/ml) for 8 hours in the presence of monensin, and then stained with peridin chlorophyll protein (PerCP)–conjugated anti-CD4 mAb at 4°C, washed, fixed, saponin permeabilized, stained with fluorescein (FITC)– and phycoerythrin (PE)–conjugated anticytokine-specific mAb (BD PharMingen), and analyzed on a FACSCalibur flow cytometer (Becton Dickinson, Mountain View, CA). To distinguish between monocyte/macrophage and T cell sources, intracellular cytokine analysis was performed exclusively on the PerCP-labeled CD4+ T cell population.

Flow cytometric analysis of Treg cells. Synovial and draining lymph node cells isolated on different days (as indicated below) were incubated with various mAb (FITC-conjugated anti-CD25, PE-conjugated anti-CD45RB, PerCP-conjugated anti-CD4 [2.5 μg/ml final concentration]) for 1 hour at 4°C. After extensive washing, cells were fixed, saponin permeabilized, incubated for 45 minutes at 4°C with PE-conjugated anti–forkhead box P3 (anti-FoxP3) mAb (0.5 μg/sample), diluted in 0.5% saponin, and analyzed on a FACSCalibur flow cytometer. Isotype-matched antibodies were used as controls, and IgG block (Sigma) was used to avoid nonspecific binding to Fc receptors.

Statistical analysis. Values were expressed as the mean ± SD, and the differences between groups were analyzed by Mann-Whitney U test and, if appropriate, by Kruskal-Wallis analysis of variance.

RESULTS

Efficient expression of functional VIP by the LentiVIP vector in vitro. The HIV-1–derived lentiviral vector LentiVIP was constructed by insertion of a 560-bp human *VIP* cDNA fragment (nucleotides 173–724 from the human locus NM-003381) into the CEWP vector backbone by direct cloning using *Eco* RI/*Bam* HI restriction enzymes (Figure 1A). We first investigated whether cells transduced with LentiVIP produce bioactive VIP. Western blot analysis of 293T embryonic cells transduced with increasing numbers of LentiVIP vectors showed high content of preproVIP in cell lysates and culture supernatants compared with cells transduced with the CEWP vector (expressing EGFP) (details available from the author upon request). A VIP-specific ELISA demonstrated that 293T cells transduced with LentiVIP produced VIP, in a dose-dependent manner (Figure 1B).

Because VIP inhibits TNFα production by activated macrophages by increasing production of the second messenger cAMP (22), we next investigated whether the secreted VIP is bioactive. Thus, we added the conditioned medium of LentiVIP-transduced 293T cells to macrophage cultures and measured the levels of cAMP and TNFα. Supernatants of 293T cells transduced with LentiVIP, but not with CEWP, increased the production of intracellular cAMP and inhibited the secretion of TNFα by endotoxin-activated macrophages (Figure 1C). Both effects were specific for the secreted VIP, because the addition of a neutralizing anti-VIP antibody to the cultures reversed them (Figure 1C). These results therefore indicate that transduction of cells with LentiVIP results in the secretion of bioactive VIP and/or preproVIP with significant antiinflammatory actions.

Reduction of the severity of CIA by LentiVIP. We next investigated the potential therapeutic application of lentiviral vectors containing VIP, using the experimental CIA mouse model. A single administration of LentiVIP at the onset of the disease or when arthritis was already established completely abrogated the clinical signs and reduced the percentage of mice with arthritis, as compared with untreated or CEWP-treated mice (Figure 2A). Interestingly, we observed no loss of the therapeutic effects 4 weeks after the initial LentiVIP treatment. Importantly with regard to therapy, injection of LentiVIP into animals with severe clinical signs of arthritis (clinical score >10) progressively attenuated the severity of CIA (Figure 2A). Histopathologic analysis of joints showed that delayed treatment with LentiVIP significantly reduced CIA-characteristic chronic inflammation of synovial tissue (infiltration of inflammatory cells [lymphocytes, plasma cells, macrophages, and neutrophils] into the joint cavity and periarticular soft tissue), pannus formation, cartilage destruction, and bone erosion (Figure 2B). The LentiVIP-mediated inhibition of neutrophil infiltration was confirmed by the finding of decreased joint myeloperoxidase activity (Figure 2B).

In order to investigate the association of the therapeutic effects of LentiVIP in arthritic mice with increased secretion of VIP in these animals, we determined the biodistribution of the inoculated vector and the levels of VIP in various tissues and organs. Quantitative real-time PCR of CMV and VIP sequences revealed a significant rate of transduction of the LentiVIP in spleen (>50%; 0.5 vectors/cell) (Figure 3A). Liver, adipose tissue, and lymph nodes were also transduced

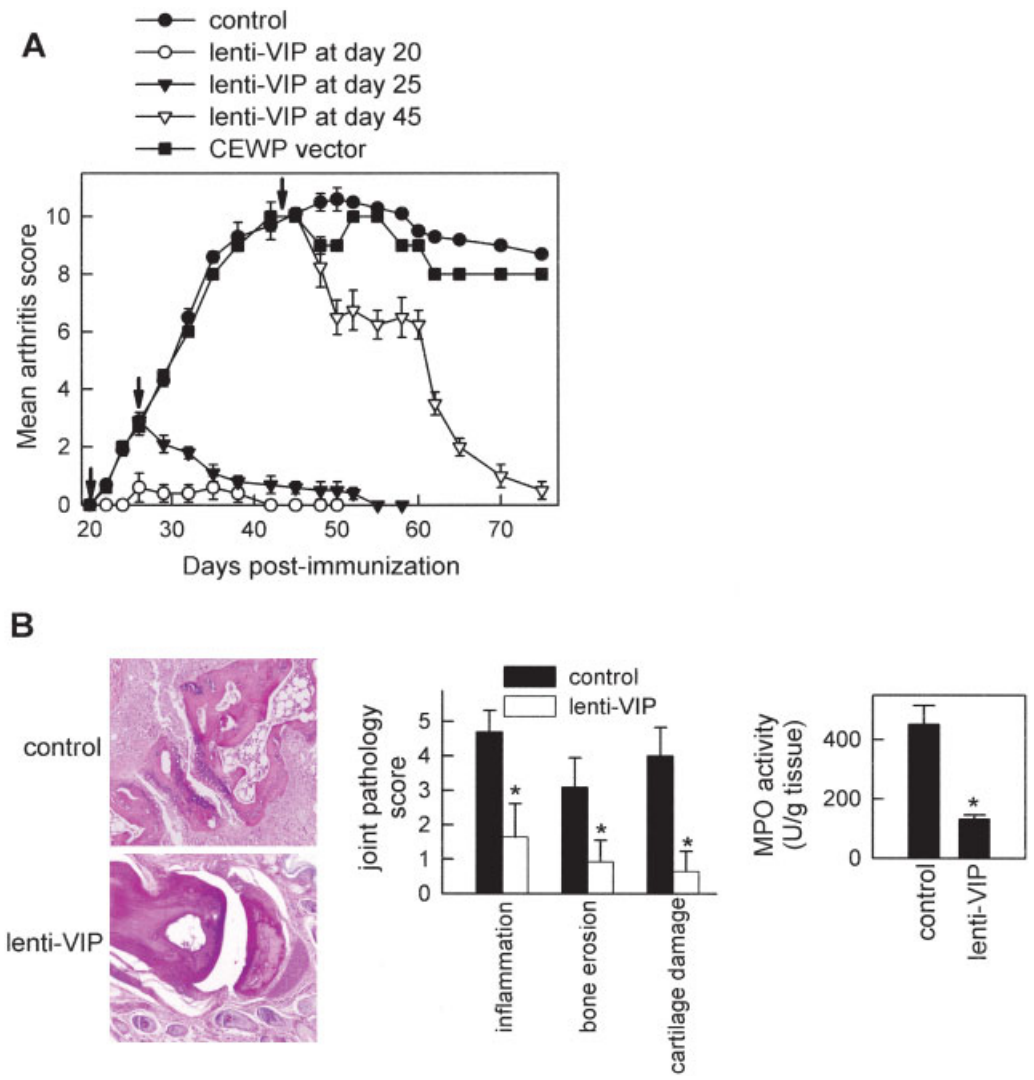

Figure 2. Evidence that lentiviral vector expressing vasoactive intestinal peptide (LentiVIP) reduces the severity of collagen-induced arthritis (CIA). **A**, DBA/1J mice with established CIA were injected intraperitoneally (arrows) either with phosphate buffered saline (PBS) (control) or with LentiVIP (10^8 copies of vector/mouse) on day 25 or day 45. In addition, prophylactic treatment with LentiVIP (10^7 copies of vector/mouse) was initiated on day 20. Clinical severity of arthritis was scored. Injection of the CEWP vector (10^7 copies of vector/mouse) into mice with CIA on day 20 did not affect disease progression. Values are the mean ± SD of 6–14 mice per group. **B**, Mice with severe CIA (mean arthritis score 10) were injected intraperitoneally either with PBS (control) or with LentiVIP (10^8 copies of vector/mouse) on day 45, and paw joints obtained on day 70 were assessed histologically (left panel) (original magnification × 200) and the results quantitated by scoring of inflammation, bone erosion, and cartilage damage (middle panel) and by measuring myeloperoxidase (MPO) activity in protein extracts isolated on day 70 to determine neutrophil infiltration into the joints (right panel). Values are the mean and SD of 6–14 mice per group. $* = P < 0.001$ versus controls.

with high efficiency (20%, 10%, and 3% respectively), whereas we did not observe detectable transduction of kidney cells (<0.1%) (Figure 3A). The wide spreading of the vector was paralleled by time-sustained increases in levels of VIP found in serum, spleen, and paws of animals treated with LentiVIP in comparison with arthritic mice injected with CEWP vector (Figure 3B).

Inhibition of the inflammatory response in CIA by LentiVIP. We next investigated the mechanisms underlying the decrease in severity of CIA following

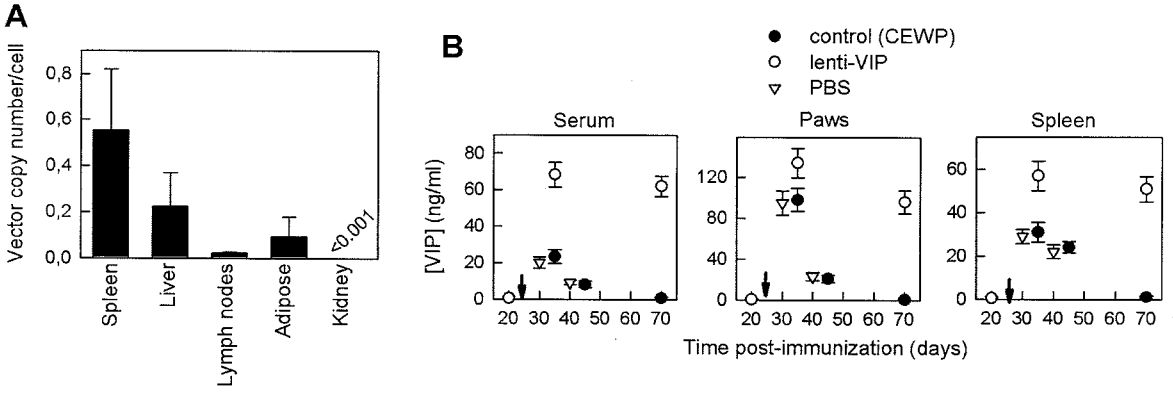

Figure 3. Vector distribution and VIP levels in LentiVIP-treated mice with CIA. DBA/1J mice with established CIA were injected intraperitoneally either with PBS, with CEWP vector (control), or with LentiVIP (10^8 copies of vector/mouse) on day 25. **A**, DNA from various tissues was obtained 15 days after LentiVIP inoculation, and the number of vector copies per cell was determined by quantitative polymerase chain reaction using cytomegalovirus and VIP cDNA sequences. Levels in the kidney were below the limit of detection (0.001 copy per cell = 0.1% of transduced cells). Values are the mean and SD of 3–5 mice per group. **B**, Serum and protein extracts of spleen and paws were obtained at different time points after LentiVIP injection (arrows), and VIP levels in serum and tissue were determined by enzyme immunoassay. Values are the mean ± SD of 3–5 mice per group. See Figure 2 for definitions.

LentiVIP treatment. We first evaluated the effect of LentiVIP on the production of inflammation mediators that are mechanistically linked to CIA severity. LentiVIP administration significantly reduced protein expression of inflammatory cytokines (TNFα, interferon-γ [IFNγ], interleukin-6 [IL-6], IL-1β, IL-12, and IL-17) and chemokines (RANTES and macrophage inhibitory protein 2) in the joints of arthritic mice (Figure 4A). In addition, joints of LentiVIP-treated mice showed increased levels of the regulatory cytokine IL-10 (Figure 4A). The broad antiinflammatory activity of LentiVIP in the inflamed joint was accompanied by down-regulation of the systemic inflammatory response, as demonstrated by the finding that LentiVIP decreased CIA-induced serum levels of the proinflammatory cytokines TNFα and IL-1β (Figure 4B).

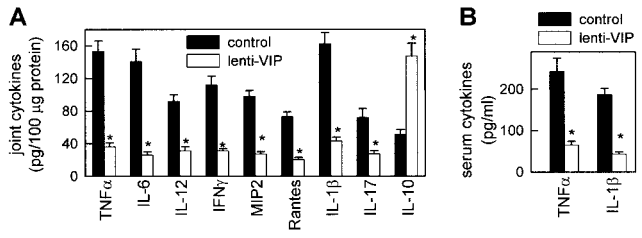

Figure 4. Evidence that vasoactive intestinal peptide (*VIP*) gene therapy inhibits the inflammatory response in collagen-induced arthritis (CIA). DBA/1J mice with established CIA (mean arthritis score >3) were injected intraperitoneally either with phosphate buffered saline (control) or with lentiviral vector expressing VIP (LentiVIP) (10^8 copies of vector/mouse) on day 25 postimmunization, and local and systemic expression of inflammation mediators in joint protein extracts (**A**) and sera (**B**) isolated on day 35 postimmunization was determined by enzyme-linked immunosorbent assay. Values are the mean and SD of 3–5 mice per group. $* = P < 0.001$ versus controls. TNFα = tumor necrosis factor α; IL-6 = interleukin-6; IFNγ = interferon-γ; MIP-2 = macrophage inhibitory protein 2.

Down-regulation of the Th1-mediated autoreactive response in CIA by LentiVIP. To determine whether LentiVIP could ameliorate CIA by reducing autoreactive T cell responses and/or their migration to the joints, we determined proliferation and cytokine profiles of pooled cells from spleen and draining lymph nodes isolated from control or LentiVIP-treated arthritic mice in response to antigen (CII) in vitro. Cells obtained from untreated mice with CIA showed marked CII-specific proliferation and effector T cell production of high levels of Th1-type cytokines (IFNγ, IL-2, and TNFα) and Th17-type cytokines (IL-17) and low levels of Th2-type cytokines (IL-4 and IL-10) (Figure 5A). In contrast, cells from LentiVIP-treated mice proliferated much less, and produced low levels of IL-17 and Th1-type cytokines and increased levels of suppressive cytokines (IL-10 and transforming growth factor β1 [TGFβ1]) and the Th2-type cytokine IL-4 (Figure 5A). This effect was antigen-specific, because LentiVIP treatment did not affect proliferation or cytokine production by anti-CD3–stimulated cells compared with findings in control mice with CIA (Figure 5A). This suggests that LentiVIP administration during CIA progression par-

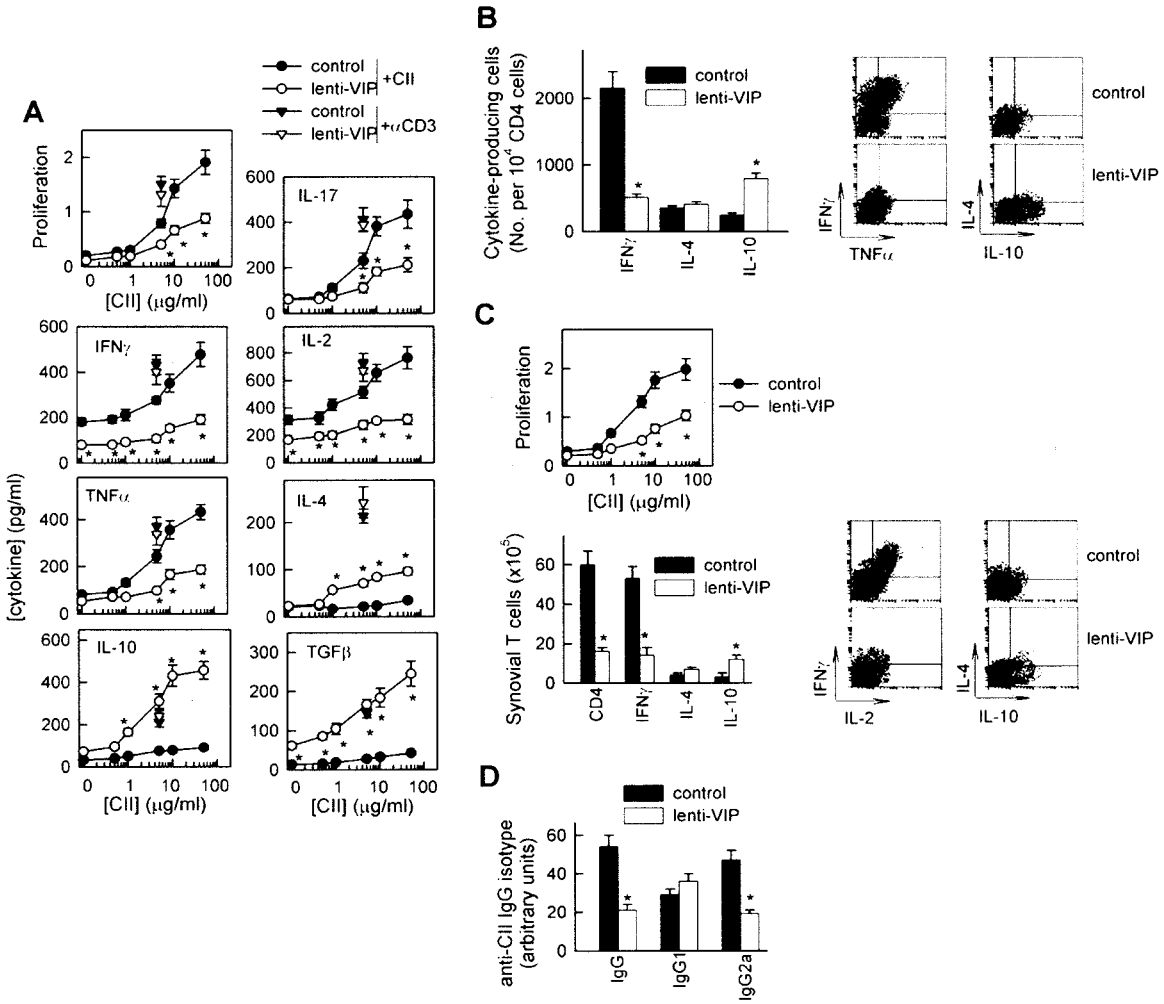

Figure 5. Evidence that LentiVIP down-regulates Th1-mediated responses in CIA. DBA/1J mice with established CIA (mean arthritis score >3) were injected intraperitoneally either with phosphate buffered saline (control) or with LentiVIP (10^8 copies of vector/mouse) on day 25 postimmunization. **A**, Proliferative response (absorbance at 405 nm) and cytokine production in pooled cells from spleen and draining lymph nodes isolated on day 30 from control or LentiVIP-treated mice with CIA after in vitro stimulation with type II collagen (CII) in various concentrations. Spleen cells were stimulated with anti-CD3 antibodies for assessment of nonspecific stimulation. A pool of 3 nonimmunized DBA/1J mouse cells was used for assessment of the basal response. No proliferation or cytokine production by T cells was detectable in the presence of an unrelated antigen (ovalbumin) (data not shown). Values are the mean ± SD of 3–5 mice per group. TGFβ = transforming growth factor β. **B,** Number of CII-specific cytokine-producing T cells. Cells from spleen and draining lymph nodes from control or LentiVIP-treated mice with CIA were restimulated in vitro with CII (10 μg/ml) and analyzed by flow cytometry for expression of CD4 and of intracellular cytokines in gated CD4+ T cells. Dot plots show representative double staining for IFNγ/TNFα or IL-4/IL-10 expression in gated CD4+ T cells. Mean and SD numbers of IFNγ-, IL-4–, and IL-10–expressing T cells are shown in the left panel. Data represent pooled values from 2 independent experiments. **C,** CII-specific proliferative response and number of cytokine-producing CD4+ T cells in synovial membrane cells isolated from control or LentiVIP-treated mice with CIA and stimulated in vitro with CII (10 μg/ml) for 48 hours. Dot plots show representative double staining for IFNγ/IL-2 or IL-4/IL-10 expression in gated CD4+ T cells. Mean ± SD levels of proliferation (absorbance at 405 nm) and numbers of CD4-, IFNγ-, IL-4–, and IL-10–expressing synovial membrane cells are shown in the left panels. Pooled synovial cells from 3 animals per group were used; data are from 2 independent experiments. **D,** Levels of CII-specific IgG, IgG1, and IgG2a antibodies in sera collected on day 35 from control or LentiVIP-treated mice with CIA, determined by enzyme-linked immunosorbent assay. Values are the mean and SD of 8–12 mice per group. $* = P < 0.001$ versus controls. See Figure 4 for other definitions.

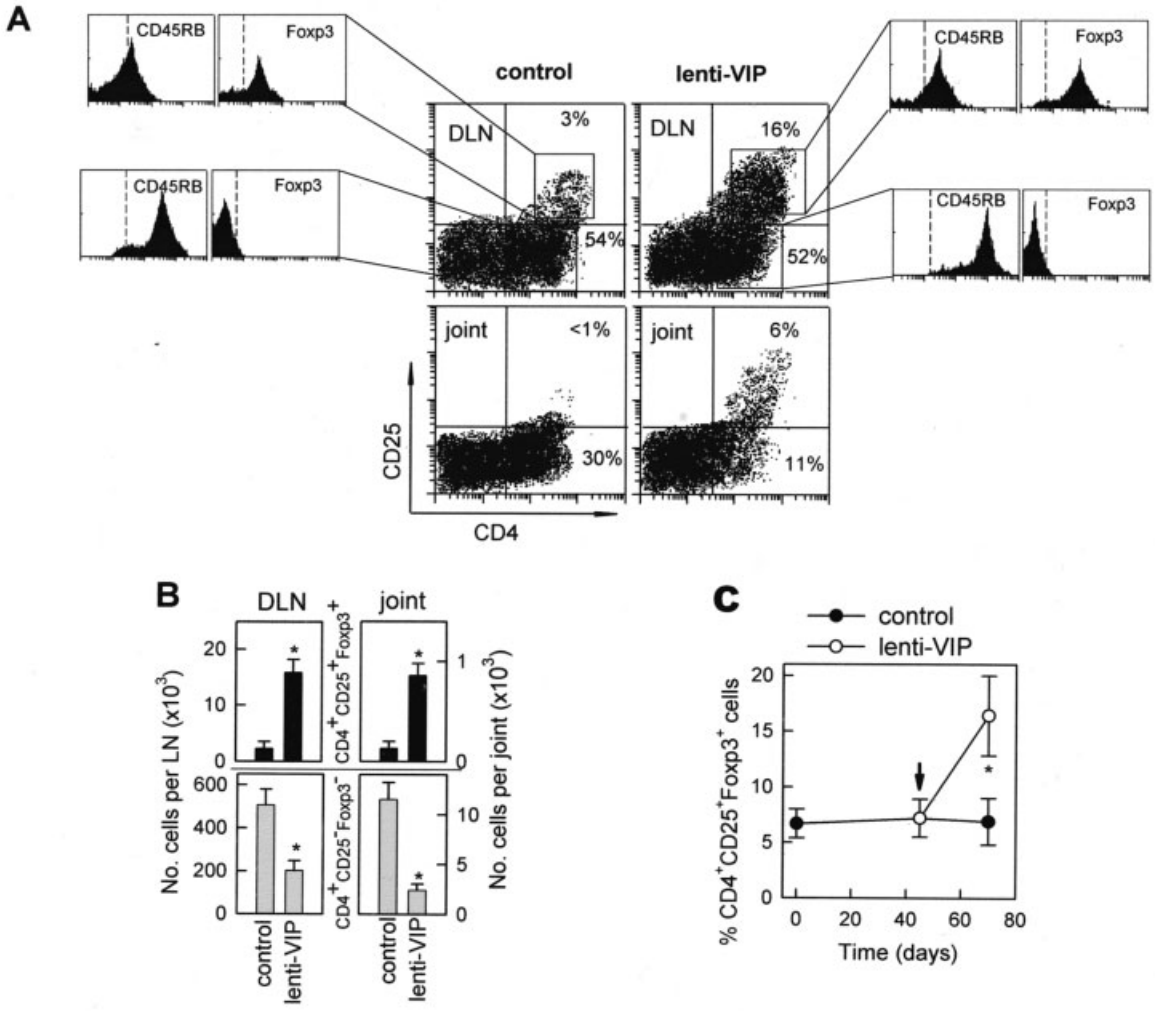

Figure 6. Evidence that LentiVIP induces the emergence of regulatory CD4+,CD25+,FoxP3+ T cells in CIA. **A,** DBA/1J mice with established CIA (mean arthritis score >3) were injected intraperitoneally either with PBS (control) or with LentiVIP (10^8 copies of vector/mouse) on day 25 postimmunization. Draining lymph node (DLN) and synovial (joint) cells isolated on day 35 were analyzed by flow cytometry for expression of CD4 and CD25. Numbers are the percentages of CD4+,CD25− and CD4+,CD25+ cells. Histograms show the expression of CD45RB and forkhead box P3 (FoxP3) in gated CD4+,CD25− and CD4+,CD25+ cells in draining lymph nodes. Similar histogram profiles were observed for synovial cells from LentiVIP-treated mice (data not shown). Dashed lines represent isotype antibody controls. **B**, Numbers of CD4+,CD25+,FoxP3+ cells and CD4+,CD25−,FoxP3− cells were determined in draining lymph nodes and synovial membrane (joint) isolated from control or LentiVIP-treated mice with CIA. Values are the mean and SD of 4 mice per group. $* = P < 0.001$ versus controls. **C,** DBA/1J mice with severe CIA (mean arthritis score >10) were injected intraperitoneally either with PBS (control) or with LentiVIP (10^8 copies of vector/mouse) on day 45 postimmunization (arrow). Draining lymph node cells were isolated at different time points, and the percentage of CD4+,CD25+,FoxP3+ cells was determined by flow cytometry. Values are the mean ± SD of 3 mice per group. $* = P < 0.001$ versus controls. See Figure 2 for other definitions.

tially inhibits CII-specific Th1 cell and, probably, Th17 cell clonal expansion.

In order to distinguish whether the decrease in Th1 cytokine production induced by LentiVIP treatment is a consequence of either down-regulation of cytokine release or inhibition of Th1 cell expansion, and to identify the source of IL-10 (macrophages or CD4+ T cells), we determined the intracellular expression of these cytokines by flow cytometry on sorted CD4+ T cells. LentiVIP treatment significantly reduced the number of IFNγ/TNFα-producing Th1 cells and increased the number of IL-10–producing CD4+ T cells from

draining lymph nodes and spleens (Figure 5B). We observed similar effects in synovial cells (Figure 5C). Thus, LentiVIP administration in mice with CIA regulates the expansion of autoreactive/inflammatory Th1 and Th17 cells and, presumably, IL-10–secreting T cells.

High levels of circulating antibodies directed against collagen-rich joint tissue invariably accompany the development of RA and CIA, and their production is a major factor in determining susceptibility to the disease. Administration of LentiVIP resulted in reduced serum levels of CII-specific IgG, particularly autoreactive IgG2a antibodies (Figure 5D), generally reflective of Th1 activity. These data provide further evidence that LentiVIP treatment during CIA reduces the autoreactive Th1 responses in both the joint and the periphery.

Emergence of regulatory CD4+,CD25+,FoxP3+ T cells induced by LentiVIP in CIA. Several studies have indicated that Treg cells confer significant protection against CIA by decreasing the activation and joint homing of autoreactive Th1 cells (36,37). Because delayed LentiVIP treatment also inhibits events during the inflammatory phase of CIA following activation of antigen-specific Th1 cells and induces the generation of IL-10/TGFβ1–producing T cells, we investigated whether LentiVIP induces Treg cells with suppressive activity during the progression of the disease. LentiVIP-treated mice with CIA were shown to have significantly higher percentages and numbers of CD4+,CD25+ cells in both draining lymph nodes and synovium compared with control mice with CIA (Figures 6A and B). Additionally, LentiVIP-induced CD4+,CD25+ cells from draining lymph nodes (Figure 6A) and synovium (data not shown) exhibited a Treg phenotype, i.e., $CD45RB^{low}$,FoxP3+. Interestingly, late administration of LentiVIP was still able to induce the emergence of CD4+,CD25+,FoxP3+ cells in mice with severe established arthritis (Figure 6C).

DISCUSSION

Although the etiology of RA is unknown, there is evidence that the recruitment and activation of neutrophils, macrophages, and lymphocytes into joint tissue and the formation of pannus are hallmarks of RA pathogenesis. Several studies of animal models indicate that Th1-derived cytokines play a pathogenic role by promoting macrophage and neutrophil infiltration and activation (38). Inflammation mediators, such as cytokines and free radicals, produced by infiltrating inflammatory cells have a key role in joint damage (38). Recent evidence has demonstrated the involvement of IL-17 produced by Th17 cells as an additional critical player in the pathogenesis of RA (39). Available therapies based on immunosuppressive agents inhibit the inflammatory component of RA and have the potential to slow the progression of disability by delaying erosion and deformity (40). However, they do not reduce the relapse rate, and because continued treatment is required in most cases to maintain a beneficial effect, they have multiple side effects. This illustrates the need for novel therapeutic approaches to prevent the inflammatory and autoimmune components of the disease and to promote restoration of immune tolerance.

Gene therapy has been considered as a potential strategy for RA treatment or cure since the early 1990s. In most animal models of RA, gene therapy has resulted in prevention of disease development and/or moderate inhibition of disease progression (12,41,42). However very few studies (using gene therapy or any other treatment strategy) have demonstrated regression of established arthritis (16,17,43,44), and to date, total regression of established severe disease has not been achieved with any RA treatment.

Our rationale in the present study was to use one of the most potent tools for in vivo gene delivery (lentiviral vectors) to express one of the most potent immunomodulatory molecules (VIP) to treat severe arthritis. We chose to work with the HIV-1–derived lentiviral vectors since they have one of the best safety and efficiency profiles for in vivo gene delivery of all vectors described to date. In addition, they can be easily modified to hold drug- or inflammation-regulated promoters that will allow tight regulation of the transgene. Other vectors, such as plasmid, adenoviral, or adeno-associated viral vectors, could be used for this approach and it would be interesting to test them in similar settings. However, their low efficiency (plasmid), high immunogenicity (adenoviral), or low cargo capacity (adeno-associated) could be a disadvantage to developing an efficient, nonimmunogenic therapeutic vector able to achieve conditional or regulated expression of VIP.

The CIA model has numerous immunologic and pathologic similarities to human RA. In fact, treatment studies using this experimental model have provided the basis for development of new treatments for RA (43,45). In this study we found that LentiVIP treatment decreased the presence of autoreactive Th1 cells in the periphery and the joint and strongly reduced the inflammatory response during CIA progression. Of relevance is the fact that administration of LentiVIP to arthritic mice also resulted in a decreased CII-specific Th17-

mediated response, which is critical for RA progression. As previously reported for VIP (46), administration of LentiVIP to mice with CIA also induced the appearance of CD4+,CD25+,FoxP3+ cells with a Treg phenotype in draining lymph nodes and joints. This parallels the fact that CD4+ T cells from LentiVIP-treated animals showed increased production of IL-10 and TGFβ, 2 key mediators of Treg cell function. These data partially explain the finding that delayed LentiVIP administration inhibits events during the inflammatory phase of CIA following activation/differentiation of antigen-specific effector Th1/Th17 cells. Therefore, this treatment based on *VIP* gene delivery is able to restore immune tolerance in arthritic mice by improving the balance between Treg cells and autoreactive Th1/Th17 cells.

Of note was the improvement in bone erosion and cartilage damage after LentiVIP administration on day 45 to mice with severe CIA (arthritis score 10–11) (Figure 2B). To our knowledge, this is the first time such improvement has been observed after treatment of established disease. This improvement can be explained by the effect of VIP on factors involved in bone remodeling, i.e., reduction of RANKL, RANK, inducible nitric oxide synthase, IL-1β, TNFα, IL-6, IL-11, IL-17, and cyclooxygenase 2 levels and augmentation of IL-4, IL-10, and osteoprotegerin levels (47). In addition, the self-regulation of the autoimmune process probably allows natural mechanisms of regeneration to take place.

Taken together, our findings demonstrate that in vivo LentiVIP administration reduces the frequency of severe arthritis, ameliorates symptoms, and prevents joint damage. With regard to treatment, it is important to take into account the ability of delayed administration of LentiVIP to completely regress ongoing disease, which fulfills an essential prerequisite for antiarthritic therapy. The fact that we did not observe a loss of its beneficial effect with time suggests that a single injection of LentiVIP could induce remission of the disease. Compared with other treatments (including other gene therapy strategies or direct injection of synthetic VIP), intraperitoneal injection of LentiVIP offers the most potent therapeutic activity described so far in any animal model of RA. The higher efficiency of LentiVIP is probably due to the steady expression of VIP in immune organs (spleen and draining lymph nodes) and joints. The continuous presence of active VIP in these tissues allows very potent reduction of inflammation and autoimmunity, the 2 main processes involved in the pathology of RA and CIA. This certainly was crucial in the advantage of this strategy compared with other treatments directed against a single mediator, such as the new biologic agents (anti-TNFα, IL-1 receptor antagonist).

Systemic treatments with TNFα inhibitors are associated with severe side effects linked to systemic immunosuppression. However, the treated animals in the present study did not exhibit any apparent adverse effects, such as hypotension or diarrhea, resulting from steady expression of VIP in many tissues, probably due to the low concentration of circulating VIP. In addition, serious side effects due to sustained immunosuppression are minimized because LentiVIP treatment affects only CII-specific responses and induces CII-specific Treg cells. In any case, these potential side effects could be minimized by controlling VIP expression with drugs (doxycycline) or inflammation-related promoters in the final therapeutic vectors. Such transcriptional/transductional targeting is mandatory before this strategy can be used in clinical trials.

As previously described (48), our study shows that systemic and joint levels of VIP are increased in arthritic mice throughout the progression of the disease. Therefore, it is attractive to speculate that the body responds to an exacerbated inflammatory/autoimmune response by increasing peripheral production of endogenous antiarthritic factors, such as VIP, in an attempt to restore the inflammatory homeostasis. Interestingly, although LentiVIP was administered intraperitoneally, we detected higher amounts of VIP locally in the joints than systemically in the serum. A potential explanation for this finding is that LentiVIP could more efficiently transduce immune cells present at the site of injection (peritoneal cavity) or in draining lymph nodes, and after their migration to the inflamed joint, the local production of transgenic VIP would significantly increase. We also found that, in addition to the processed VIP, LentiVIP-transduced cells are able to secrete the preproVIP precursor. To our knowledge, this is the first study to demonstrate secretion of the VIP precursor, although we still do not know whether it exerts any VIP-like immunomodulatory activity and contributes to the therapeutic effect of LentiVIP in CIA.

In summary, the results of this study suggest a novel strategy for the treatment of RA and other chronic autoimmune disorders, based on *VIP* gene transfer with lentiviral vectors. This strategy has been shown to be safe, inexpensive, and more effective than any other therapeutic approach in the CIA model. Therefore, although further modifications of LentiVIP vector would be necessary prior to translation to the clinical setting, the basic findings described here provide

grounds for optimism about the applications of antiinflammatory neuropeptide gene therapy to human autoimmune disorders.

ACKNOWLEDGMENTS

We are grateful to Dr. D. Trono (University of Geneva, Geneva, Switzerland) for providing the HIV packaging pCMV.R8.91 and envelope pMD.G plasmids and Dr. A. Thrasher (University College, London, UK) for providing the SEWP vector.

AUTHOR CONTRIBUTIONS

Dr. Martín had full access to all of the data in the study and takes responsibility for the integrity of the data and the accuracy of the data analysis.

Study design. Delgado, Martín.
Acquisition of data. Delgado, Toscano, Benabdellah, Cobo, O'Valle, Gonzalez-Rey, Martín.
Analysis and interpretation of data. Delgado, Toscano, Benabdellah, Martín.
Manuscript preparation. Delgado, Martín.
Statistical analysis. Delgado, Gonzalez-Rey, Martín.

REFERENCES

1. Gouze JN, Gouze E, Palmer GD, Liew VS, Pascher A, Betz OB, et al. A comparative study of the inhibitory effects of interleukin-1 receptor antagonist following administration as a recombinant protein or by gene transfer. Arthritis Res Ther 2003;5:R301–9.
2. Palmer GD, Steinert A, Pascher A, Gouze E, Gouze JN, Betz O, et al. Gene-induced chondrogenesis of primary mesenchymal stem cells in vitro. Mol Ther 2005;12:219–28.
3. Evans CH, Ghivizzani SC, Robbins PD. Gene therapy for arthritis: what next? [review]. Arthritis Rheum 2006;54:1714–29.
4. Van de Loo FA, Smeets RL, van den Berg WB. Gene therapy in animal models of rheumatoid arthritis: are we ready for the patients? Arthritis Res Ther 2004;6:183–96.
5. Fujio K, Okamoto A, Araki Y, Shoda H, Tahara H, Tsuno NH, et al. Gene therapy of arthritis with TCR isolated from the inflamed paw. J Immunol 2006;177:8140–7.
6. Morita Y, Yang J, Gupta R, Shimizu K, Shelden EA, Endres J, et al. Dendritic cells genetically engineered to express IL-4 inhibit murine collagen-induced arthritis. J Clin Invest 2001;107:1275–84.
7. Nakajima A, Seroogy CM, Sandora MR, Tarner IH, Costa GL, Taylor-Edwards C, et al. Antigen-specific T cell-mediated gene therapy in collagen-induced arthritis. J Clin Invest 2001;107: 1293–301.
8. Evans CH, Robbins PD, Ghivizzani SC, Wasko MC, Tomaino MM, Kang R, et al. Gene transfer to human joints: progress toward a gene therapy of arthritis. Proc Natl Acad Sci U S A 2005;102:8698–703.
9. Evans CH, Ghivizzani SC, Herndon JH, Wasko MC, Reinecke J, Wehling P, et al. Clinical trials in the gene therapy of arthritis. Clin Orthop Relat Res 2000;379 (Suppl):S300–7.
10. Zhang H, Yang Y, Horton JL, Samoilova EB, Judge TA, Turka LA, et al. Amelioration of collagen-induced arthritis by CD95 (Apo-1/Fas)-ligand gene transfer. J Clin Invest 1997;100:1951–7.
11. Miagkov AV, Varley AW, Munford RS, Makarov SS. Endogenous regulation of a therapeutic transgene restores homeostasis in arthritic joints. J Clin Invest 2002;109:1223–9.
12. Woods AM, Thompson SJ, Wooley PH, Panayi G, Klavinskis LS. Immune modulation of collagen-induced arthritis by intranasal cytokine gene delivery: a model for the therapy of rheumatoid arthritis. Arthritis Rheum 2005;52:3761–71.
13. Khoury M, Adriaansen J, Vervoordeldonk MJ, Gould D, Chernajovsky Y, Bigey P, et al. Inflammation-inducible anti-TNF gene expression mediated by intra-articular injection of serotype 5 adeno-associated virus reduces arthritis. J Gene Med 2007;9: 596–604.
14. Adriaansen J, Fallaux FJ, de Cortie CJ, Vervoordeldonk MJ, Tak PP. Local delivery of beta interferon using an adeno-associated virus type 5 effectively inhibits adjuvant arthritis in rats. J Gen Virol 2007;88:1717–21.
15. Adriaansen J, Khoury M, de Cortie CJ, Fallaux FJ, Bigey P, Scherman D, et al. Reduction of arthritis following intra-articular administration of an adeno-associated virus serotype 5 expressing a disease-inducible TNF-blocking agent. Ann Rheum Dis 2007;66: 1143–50.
16. Song XY, Gu M, Jin WW, Klinman DM, Wahl SM. Plasmid DNA encoding transforming growth factor-β1 suppresses chronic disease in a streptococcal cell wall-induced arthritis model. J Clin Invest 1998;101:2615–21.
17. Taniguchi K, Kohsaka H, Inoue N, Terada Y, Ito H, Hirokawa K, et al. Induction of the p16INK4a senescence gene as a new therapeutic strategy for the treatment of rheumatoid arthritis. Nat Med 1999;5:760–7.
18. Zufferey R, Dull T, Mandel RJ, Bukovsky A, Quiroz D, Naldini L, et al. Self-inactivating lentivirus vector for safe and efficient in vivo gene delivery. J Virol 1998;72:9873–80.
19. Naldini L. In vivo gene delivery by lentiviral vectors. Thromb Haemost 1999;82:552–4.
20. Evans CH, Gouze E, Gouze JN, Robbins PD, Ghivizzani SC. Gene therapeutic approaches—transfer in vivo. Adv Drug Deliv Rev 2006;58:243–58.
21. Montini E, Cesana D, Schmidt M, Sanvito F, Ponzoni M, Bartholomae C, et al. Hematopoietic stem cell gene transfer in a tumor-prone mouse model uncovers low genotoxicity of lentiviral vector integration. Nat Biotechnol 2006;24:687–96.
22. Delgado M, Pozo D, Ganea D. The significance of vasoactive intestinal peptide in immunomodulation. Pharmacol Rev 2004;56: 249–90.
23. Gonzalez-Rey E, Chorny A, Delgado M. Regulation of immune tolerance by anti-inflammatory neuropeptides. Nat Rev Immunol 2007;7:52–63.
24. Delgado M, Abad C, Martinez C, Leceta J, Gomariz RP. Vasoactive intestinal peptide prevents experimental arthritis by downregulating both autoimmune and inflammatory components of the disease. Nat Med 2001;7:563–8.
25. Abad C, Martinez C, Juarranz MG, Arranz A, Leceta J, Delgado M, et al. Therapeutic effects of vasoactive intestinal peptide in the trinitrobenzene sulfonic acid mice model of Crohn's disease. Gastroenterology 2003;124:961–71.
26. Gonzalez-Rey E, Fernandez-Martin A, Chorny A, Martin J, Pozo D, Ganea D, et al. Therapeutic effect of vasoactive intestinal peptide on experimental autoimmune encephalomyelitis: downregulation of inflammatory and autoimmune responses. Am J Pathol 2006;168:1179–88.
27. Herrera JL, Fernandez-Montesinos R, Gonzalez-Rey E, Delgado M, Pozo D. Protective role for plasmid DNA-mediated VIP gene transfer in non-obese diabetic mice. Ann N Y Acad Sci 2006;1070: 337–41.
28. Keino H, Kezuka T, Takeuchi M, Yamakawa N, Hattori T, Usui M. Prevention of experimental autoimmune uveoretinitis by vasoactive intestinal peptide. Arch Ophthalmol 2004;122:1179–84.
29. Lodde BM, Delporte C, Goldsmith CM, Tak PP, Baum BJ. A recombinant adenoviral vector encoding functional vasoactive intestinal peptide. Biochem Biophys Res Commun 2004;319: 189–92.
30. Lodde BM, Mineshiba F, Wang J, Cotrim AP, Afione S, Tak PP,

et al. Effect of human vasoactive intestinal peptide gene transfer in a murine model of Sjögren's syndrome. Ann Rheum Dis 2006;65: 195–200.
31. Zhang LQ, Shen JG. Experimental treatment of collagen-induced arthritis in rats with recombinant plasmid containing vasoactive intestinal peptide gene. Zhejiang Da Xue Xue Bao Yi Xue Ban 2006;35:403–10. In Chinese.
32. Demaison C, Parsley K, Brouns G, Scherr M, Battmer K, Kinnon C, et al. High-level transduction and gene expression in hematopoietic repopulating cells using a human immunodeficiency [correction of imunodeficiency] virus type 1-based lentiviral vector containing an internal spleen focus forming virus promoter. Hum Gene Ther 2002;13:803–13.
33. Toscano MG, Frecha C, Ortega C, Santamaria M, Martin F, Molina IJ. Efficient lentiviral transduction of Herpesvirus saimiri immortalized T cells as a model for gene therapy in primary immunodeficiencies. Gene Ther 2004;11:956–61.
34. Sambrook J, Russell DW. Molecular cloning: a laboratory manual. 3rd ed. Cold Spring Harbor (NY): Cold Spring Harbor Laboratory Press; 2001.
35. Kasama T, Strieter RM, Lukacs NW, Lincoln PM, Burdick MD, Kunkel SL. Interferon γ modulates the expression of neutrophil-derived chemokines. J Investig Med 1995;43:58–67.
36. Morgan ME, Flierman R, van Duivenvoorde LM, Witteveen HJ, van Ewijk W, van Laar JM, et al. Effective treatment of collagen-induced arthritis by adoptive transfer of CD25+ regulatory T cells. Arthritis Rheum 2005;52:2212–21.
37. Van Amelsfort JM, Jacobs KM, Bijlsma JW, Lafeber FP, Taams LS. CD4+CD25+ regulatory T cells in rheumatoid arthritis: differences in the presence, phenotype, and function between peripheral blood and synovial fluid. Arthritis Rheum 2004;50: 2775–85.
38. Feldmann M, Brennan FM, Maini RN. Role of cytokines in rheumatoid arthritis. Annu Rev Immunol 1996;14:397–440.
39. Lubberts E, Koenders MI, van den Berg WB. The role of T-cell interleukin-17 in conducting destructive arthritis: lessons from animal models. Arthritis Res Ther 2005;7:29–37.
40. Feldmann M, Maini RN. Anti-TNFα therapy of rheumatoid arthritis: what have we learned? Annu Rev Immunol 2001;19: 163–96.
41. Kim SH, Lechman ER, Bianco N, Menon R, Keravala A, Nash J, et al. Exosomes derived from IL-10-treated dendritic cells can suppress inflammation and collagen-induced arthritis. J Immunol 2005;174:6440–8.
42. Schopf L, Savinainen A, Anderson K, Kujawa J, DuPont M, Silva M, et al. IKKβ inhibition protects against bone and cartilage destruction in a rat model of rheumatoid arthritis. Arthritis Rheum 2006;54:3163–73.
43. Williams RO, Feldmann M, Maini RN. Anti-tumor necrosis factor ameliorates joint disease in murine collagen-induced arthritis. Proc Natl Acad Sci U S A 1992;89:9784–8.
44. Funk JL, Frye JB, Oyarzo JN, Kuscuoglu N, Wilson J, McCaffrey G, et al. Efficacy and mechanism of action of turmeric supplements in the treatment of experimental arthritis. Arthritis Rheum 2006;54:3452–64.
45. Feldmann M, Elliott MJ, Woody JN, Maini RN. Anti-tumor necrosis factor-α therapy of rheumatoid arthritis. Adv Immunol 1997;64:283–350.
46. Gonzalez-Rey E, Fernandez-Martin A, Chorny A, Delgado M. Vasoactive intestinal peptide induces CD4+,CD25+ T regulatory cells with therapeutic effect in collagen-induced arthritis. Arthritis Rheum 2006;54:864–76.
47. Juarranz Y, Abad C, Martinez C, Arranz A, Gutierrez-Canas I, Rosignoli F, et al. Protective effect of vasoactive intestinal peptide on bone destruction in the collagen-induced arthritis model of rheumatoid arthritis. Arthritis Res Ther 2005;7:R1034–45.
48. Delgado M, Abad C, Martinez C, Juarranz MG, Arranz A, Gomariz RP, et al. Vasoactive intestinal peptide in the immune system: potential therapeutic role in inflammatory and autoimmune diseases. J Mol Med 2002;80:16–24.

HUMAN GENE THERAPY 20:1279–1290 (November 2009)

DOI: 10.1089/hum.2009.118

Scientific Article

Was cDNA Sequences Modulate Transgene Expression of *Was* Promoter-Driven Lentiviral Vectors

Miguel G. Toscano,[1,2] Karim Benabdellah,[1,3] Pilar Muñoz,[4] Cecilia Frecha,[1,5] Marién Cobo,[4] and Francisco Martín[1,4]

Abstract

The development of vectors that express a therapeutic transgene efficiently and specifically in hematopoietic cells (HCs) is an important goal for gene therapy of hematological disorders. We have previously shown that a 500-bp fragment from the proximal *Was* gene promoter in a lentiviral vector (LV) was sufficient to achieve more than 100-fold higher levels of Wiskott-Aldrich syndrome protein in HCs than in nonhematopoietic cells (non-HCs). We show now that this differential was reduced up to 10 times when the enhanced green fluorescent protein gene (*eGFP*) was expressed instead of *Was* in the same LV backbone. Insertion of *Was* cDNA sequences downstream of *eGFP* in these LVs had a negative effect on transgene expression. This effect varied in different cell types but, overall, *Was* cDNA sequences increased the hematopoietic specificity of *Was* promoter-driven LV. We have characterized the minimal fragment required to increase hematopoietic specificity and have demonstrated that the mechanism involves *Was* promoter regulation and RNA processing. In addition, we have shown that *Was* cDNA sequences interfere with the enhancer activity of the woodchuck posttranscriptional regulatory element. These results represent the first data showing the role of *Was* intragenic sequences in gene regulation.

Introduction

The development of efficient, stable, and regulated gene transfer vectors is a major goal for both basic science and gene therapy approaches. At present lentiviral vectors (LVs) are the most powerful of all integrative vector systems (Wiznerowicz and Trono, 2005). They not only transduce efficiently most cell types, including quiescent cells, but also express the transgene stably (Case *et al.*, 1999). The development of self-inactivated LVs (Zufferey *et al.*, 1998) improved their biosafety and regulatory properties because the expression of the transgene is directed only through internal promoters and not through the 5′ long terminal repeat (LTR). This property allows the use of various promoters (tissue-specific, drug-regulated, etc.) to achieve regulated expression and to reduce genotoxicity (Modlich *et al.*, 2006; Zychlinski *et al.*, 2008). The latest lentiviral generations allow drug-regulated and tissue-specific delivery of transgenes both *in vitro* and *in vivo* (Barde *et al.*, 2006; Szulc *et al.*, 2006; Chang and Sadelain, 2007; Frecha *et al.*, 2008).

In most approaches, transcriptionally targeted LVs contain minimal promoter regions defined as accountable for transcriptional regulation of their genes. Using this strategy, several groups have obtained LVs that are finely regulated in liver (Oertel *et al.*, 2003), hematopoietic cells (Martin *et al.*, 2005), antigen-presenting cells (Cui *et al.*, 2002), B cells (Lutzko *et al.*, 2003; Moreau *et al.*, 2004), $CD4^+$ T cells (Marodon *et al.*, 2003), erythroid cells (Moreau-Gaudry *et al.*, 2001; Lotti *et al.*, 2002; Han *et al.*, 2007), and endothelial cells (Jager *et al.*, 1999; revised in Goverdhana *et al.*, 2005). However, the level of regulation of the transgene rarely mimics exactly the regulation of the gene in nature (Frecha *et al.*, 2008). This can be easily understood because the final activity of a promoter is dependent on multiple factors (position of the promoter in the chromatin, long distant enhancers or silencers, epigenetic modifications, etc.) (Osborne *et al.*, 2004) that are missing in

[1]Immunology and Cell Biology Department, Institute of Parasitology and Biomedicine López Neyra-CSIC, Parque Tecnológico Ciencias de la Salud, 18100 Granada, Spain.
[2]Present address: Department of Microbiology and Immunology, Temple University School of Medicine, Philadelphia, PA 19140.
[3]Present address: Estación Experimental del Zaidín-CSIC, 18008 Granada, Spain.
[4]Andalusian Stem Cell Bank, Center for Biomedical Research, Granada University, Parque Tecnológico Ciencias de la Salud, 18100 Armilla, 18100 Granada, Spain.
[5]Present address: Université de Lyon, F-69000 Lyon, France; INSERM, U758, Human Virology Department, F-69007 Lyon, France; Ecole Normale Supérieure de Lyon, F-69007 Lyon, France.

the integrated vector. Several approaches can be used to attain improved regulated expression by integrative vectors such as the use of insulators (Hawley, 2001; Robert-Richard *et al.*, 2007), or the combination of several elements that modulate promoter activity (Frecha *et al.*, 2008).

The woodchuck posttranscriptional regulatory element (WPRE) is an enhancer element that affects gene expression at the posttranscriptional level (Gaszner and Felsenfeld, 2006), and its effect over retroviral vectors depends both on the inserted promoter and the target cell (Donello *et al.*, 1998; Zufferey *et al.*, 1999; Werner *et al.*, 2004; Hlavaty *et al.*, 2005; Mastroyiannopoulos *et al.*, 2005). Moreau-Gaudry and co-workers demonstrated that inclusion of the WPRE in erythroid-specific LVs increased expression in erythroid cells without affecting expression in nontargeted cells (Moreau-Gaudry *et al.*, 2001).

Although most of the studies concerning transcriptional regulation focus on regions upstream of the promoter, there are solid data demonstrating that downstream regions can also play important roles in regulating promoter activity (Levine and Tjian, 2003). In fact, elements that modulate transcriptional activity can be found inside introns and exons of genes (Sakonju *et al.*, 1980; Sternberg *et al.*, 1988; Xu *et al.*, 1993; Cui *et al.*, 1998; Seshasayee *et al.*, 2000; Kobayashi *et al.*, 2001; Lin and Tam, 2001; Saur *et al.*, 2002; Wong *et al.*, 2004; Abbasi *et al.*, 2007). Therefore, in a retroviral backbone, if a gene contains regulatory elements inside exons, its expression will be modulated not only by the promoter used but also by these elements present in the cDNA.

The development of pan-hematopoietic specific LVs is of interest for both gene therapy approaches and basic research. We have developed a pan-hematopoietic specific *Was* promoter-driven LV that expresses the *Wiskott-Aldrich syndrome* (*Was*) gene more than 100 times more efficiently in hematopoietic cells than in nonhematopoietic cells (Martin *et al.*, 2005).

In this paper we show that the hematopoietic specificity of *Was* promoter-driven LVs drops up to 10 times when *eGFP* is expressed instead of the *Was* gene. We demonstrate that *Was* cDNA sequences play an important role in the highly specific hematopoietic expression of *Was* promoter-driven LVs. We show that the effect of *Was* cDNA on hematopoietic specific expression is due to both transcriptional and posttranscriptional activity and that this effect is governed by a 5′ 900-bp region. We also show that the *Was* cDNA interferes with the enhancer activity of the WPRE element, reducing its activity.

Material and Methods

Cell lines and culture media

HVS-WAS/1, herpesvirus saimiri-immortalized T cells derived from a patient with WAS, and ALLO-WAS/1, a primary allospecific T cell line from a second patient with WAS (Gallego *et al.*, 1997), were kindly provided by I. Molina (Granada University, Granada, Spain). ALLO-N/1 is a T cell line generated in our laboratory from a healthy donor (Martin *et al.*, 2005). U937 (monocytic), HEL (erythroblastic), and K562 (erythroleukemic) cells lines were used as hematopoietic cells (HCs) of myeloid origin. All hematopoietic cells were cultured in RPMI 1640 supplemented with fetal calf serum (FCS; GIBCO-BRL, Middlesex, UK) to 10%, or fresh human serum (kindly provided by the Granada Regional Transfusion Center, Granada, Spain), glutamine, penicillin–streptomycin, and recombinant human interleukin-2 (rIL-2, 50 IU/ml) (Hoffman-LaRoche, Nutley, NJ; kindly supplied by the AIDS Research and Reference Reagent Program, National Institutes of Health, Rockville, MD); primary decidual stromal cells (DSCs) were kindly provided by E. Garcia-Olivares (Granada University) and obtained from human decidua as described previously (Garcia-Pacheco *et al.*, 2001). Jurkat T cells were cultured in RPMI 1640 supplemented as described previously, without the addition of rIL-2. RKO (colon adenocarcinoma cells) and 293T (fetus kidney) cells were grown in Dulbecco's modified Eagle's medium, supplemented with 10% FCS, glutamine, and antibiotics as described previously. Human microvascular endothelial cells (HMECs) (ATCC, Molsheim, France) were grown in endothelial cell growth medium (PromoCell, Heidelberg, Germany).

Construction of vectors expressing Was, eGFP, *and* eGFP–Was

LVs were renamed according to the following letter code: W, *Was* gene endogenous promoter; WA, *Was* cDNA; S, spleen focus-forming virus LTR promoter; E, enhanced GFP cDNA; WP, woodchuck postregulatory element; EWA, eGFP–WASP (Wiskott-Aldrich syndrome protein) chimera. For simplicity, LVs previously described were renamed as indicated in Fig. 1A, Fig. 2A, and Fig. 5A. SEWP is the SE or HRSINCSGW vector in Demaison and colleagues (2002), SWA is the SW vector in Martin and colleagues (2005), WWA is the WW vector in Martin and colleagues (2005), and SEWAWP is the SEW vector in Toscano and colleagues (2008). All these plasmids share the self-inactivated (SIN) lentiviral backbone described by Zufferey and colleagues (1998). WEWAWP was obtained by replacing the SFFV-LTR promoter in the SEWAWP vector by the *Was* promoter, obtained by *Bam*HI/*Not*I digestion of WWA. SEWA and WEWA vectors were obtained by excision of WPRE by *Cla*I digestion from SEWAWP and WEWAWP, respectively. The same strategy was used to obtain SE and WE from SEWP and WEWP vectors, respectively.

Was cDNA fragments were obtained by digestions with *Bam*HI/*Cla*I (BC fragment, 1613 bp), *Bam*HI/*Xho*I (BX fragment, 960 bp), *Bam*HI/*Apa*L1 (BA fragment, 719 bp), *Apa*L1/*Cla*I (AC fragment, 894 bp) and *Xho*I/*Xho*I (XX fragment, 680 bp) and cloned by blunt ends into the unique *Pst*I site in the WE vector (right after the stop codon of *eGFP* cDNA). Of all the clones screened, only those inserted in the 5′ to 3′ orientation were selected. The resultant vectors were named WE-BC, WE-BX, WE-BA, WE-AC, and WE-XX (see Fig. 2A). The BC fragment was also cloned 5′ to 3′ into the SE and WEWP vectors, to obtain the SE-BC and WE-BC-WP vectors, using the *Pst*I site that is located after the stop codon in both vectors.

Vector production

LVs were produced by cotransfection of 293T cells with three plasmids: (1) vector plasmid, (2) packaging plasmid pCMVΔR8.9, and (3) envelope plasmid pMD.G, as previously described (Neil *et al.*, 2001). Briefly, 293T cells (6×10^6) were plated over a 10-cm tissue culture-grade Petri dish (Sarstedt, Newton, NC) the day before transfection to ensure exponential growth and more than 80% confluence. Vector plasmids, together with the packaging and envelope plasmids (total DNA, 27 μg; plasmid proportions of 3:2:1, respectively), were

resuspended in 1.5 ml of Opti-MEM (GIBCO-BRL), mixed at room temperature for 20 min with 60 μl of Lipofectamine 2000 (Invitrogen, Carlsbad, CA), and then diluted in 1.5 ml of Opti-MEM. The plasmid–Lipofectamine mixture was added to prewashed cells and then incubated for 6–8 hr. The producer cells were then washed and cultured for an additional 48 hr in 10 ml of Opti-MEM. Viral supernatants were collected and filtered through a 0.45-μm pore size filter (Nalgene, Rochester, NY), aliquoted, and immediately frozen at -80°C.

Cell transduction and vector titration

Exponentially growing target cells were washed in phosphate-buffered saline (PBS) and seeded onto 24-well plates at a concentration of 2×10^5 cells per well in 500 μl of the appropriate medium. Vector supernatants were added to the culture and incubated overnight. For expression analysis of eGFP or eGFP–WASP, cells were analyzed 72 hr later, or at other time points if indicated, in a BD FACScan flow cytometer (BD Biosciences, San Jose, CA). For analysis of *Was*-expressing vectors, the procedure was identical but the transduction efficiency was calculated by determining the vector copy number per cell by real-time polymerase chain reaction (PCR) (see later). Viral titers (transduction units [TU] per milliliter) were calculated on the basis of transduction of 293T cells by the various vectors. Each cell line was transduced at a predetermined multiplicity of infection (MOI) that allowed equivalent vector copy numbers among the different cells used in the panel, because the 293T cells or DSCs were four to six times more permissive than T cells (primary or HVS immortalized).

Quantitative Western blot

Cells were lysed with 1% Nonidet P-40 (NP-40) lysis buffer containing a protease inhibitor cocktail (Sigma-Aldrich, St. Louis, MO), resolved by sodium dodecyl sulfate–polyacrylamide gel electrophoresis (SDS–PAGE; 10% polyacrylamide gels, reducing conditions), and electrotransferred to Hybond-P polyvinylidene difluoride (PVDF) membranes (GE Healthcare Life Sciences, Buckinghamshire, UK). Membranes were blocked with 5% nonfat milk and probed for 1 hr at room temperature with anti-WASP monoclonal antibody D-1 (2 μg/ml; Santa Cruz Biotechnology, Santa Cruz, CA) or anti-GFP monoclonal antibody (Millipore, Billerica, MA) followed by incubation with horseradish peroxidase (HRP)-labeled goat anti-mouse antibody (1:10,000 dilution; Invitrogen Caltag). Quantitative analysis was performed with an ECL-Advance Western blotting detection system (GE Healthcare Life Sciences). Membranes were revealed after incubation for 1–5 min with ECL-Advance reagents. Quantification of light emission was done with a Molecular Imager ChemiDoc XRS system (Bio-Rad, Hercules, CA) and analyzed at 440 nm with Quantity One version 4.5.0 software (Bio-Rad). Contribution of each band was recorded and expressed as relative intensity per square millimeter. To determine WASP/eGFP expression in transduced cells, ERK (extracellular signal-regulated kinase) protein content was used as internal loading control. The ratio of WASP to ERK was calculated for each transduced cell and then normalized for vector copy number per cell.

The hematopoietic specificity of each vector was measured as follows: We first normalized transgene expression to protein loading (dividing by the ERK signal) and by the vector copy number (dividing this value again by the vector copy number) for each sample. The value obtained provided a relative measure of transgene expression per integrated vector (TEIV). To obtain the hematopoietic specific index of each vector we divided the TEIV obtained in HCs by the one obtained in non-HCs

Nucleic acid preparations and quantitative PCR and RT-PCR

Genomic DNA from cultured cells was isolated by adding 1 ml per 10^6 cells of SNET extraction buffer (20 m*M* Tris-HCl [pH 8], 5 m*M* EDTA [pH 8], 400 m*M* NaCl, 1% SDS; filtered and aliquoted) containing proteinase K (100 μg/ml; Sigma-Aldrich). DNA samples were incubated at 55°C for 2–18 hr, proteinase K was inactivated by a final heating at 95°C for 10 min, and RNase (1 μg/ml) was finally added for 30 min at 37°C.

Proteins were extracted twice with phenol–chloroform, and DNA was then precipitated and its concentration determined by spectrophotometry. Quantitative PCRs were performed in an ABI PRISM 7000 sequence detection system (Applied Biosystems, Foster City, CA). Samples were mixed with iTaq Supermix with ROX (Bio-Rad) containing dNTPs, iTaq DNA polymerase (50 U/ml), 40 m*M* Tris-HCl (pH 8.4), 100 m*M* KCl, 10 m*M* $MgCl_2$, 1 μ*M* ROX internal reference dye, and stabilizers. Specific primers were added at 400 n*M*. For SWA-, WWA-, SEWA-, and WEWA-transduced cells, a pair of primers comprising *WAS* exons 9 and 10 (forward, 5′-AGG CTG TGC GGC AGG AGA T-3′; reverse, 5′-CAG TGG ACC GAA CGA CCC TTG-3′) and a specific TaqMan probe (5′-FAM-CGC CAG GAG CCA CTT CCG CCG-TAMRA-3′) were used. The parameters for the PCR were as follows: 1×(95°C for 2 min), 45×(95°C for 30 sec, 58°C for 30 sec, and 72°C for 30 sec), 1×(50°C for 2 min). For WE-, WE (B-C)-, and WE (B-X)-transduced cells, vector copy number determination was done with *eGFP* primers (forward, 5′-GCCCGACAACCA CTACCT-3′; reverse, 5′-CGTCCATGCCGAGAGTGA-3′) and the TaqMan probe (5′-FAM-CGGCGGCGGTCACGAACTC CA-TAMRA-3′). The parameters for the PCR were as follows: 1×(95°C for 2 min), 45×(95°C for 30 sec, 61.4°C for 30 sec, and 72°C for 30 sec), 1×(72°C 2 min). 293T cells (1×10^5) were mixed with 10-fold increasing amounts of plasmid DNA (from 10^2 to 1×10^7 copies) to determine the standard curve in each experiment.

For comparative quantitative RT-PCR, total RNA was extracted with an RNeasy Plus minikit (Qiagen, Hilden, Germany) and 1 μg was reverse transcribed into cDNA with a high-capacity cDNA reverse transcription kit (Applied Biosystems). One microliter of the final reaction was used to amplify GFP by PCR, using a QuantiTect SYBR green PCR kit (Qiagen) and GFP-specific primers (forward, 5′-GCCCGACAACCACTACCT-3′; and reverse, 5′-CGTCC ATGCCGAGAGTGA-3′). The results were normalized by glyceraldehyde-3-phosphate dehydrogenase (GADPH) amplification of the same samples, using GADPH-specific primers (forward, 5′-GAAGGTGAAGGTCGGAGTC-3′; and reverse, 5′-GAAGATGGTGATGGGATTTC-3′). The PCR was done with a Stratagene Mx3005 P sequence detector (Stratagene, La Jolla, CA) and consisted of 40 cycles at 94°C (15 sec), then 60°C (30 sec) and 72°C (30 sec), and the results were analyzed with MxPro software (Stratagene).

Statistical analysis

Data are expressed as means ± SDEVP. Experiments were repeated two or three times with similar results. The analysis of significance was done using the Student *t* test (Microsoft Office Excel 2007; Microsoft, Redmond, WAS). $p < 0.05$ was consider significant.

Results

Hematopoietic specificity of Was *promoter-driven LVs is influenced by* Was *cDNA*

We have previously shown that the lentiviral vector (LV) WWA (Martin *et al.*, 2005) expressing the Wiskott-Aldrich syndrome protein (WASP) is more than 100 times more efficient in hematopoietic cells (HCs) than in non-HCs. We explore here whether the same backbone, a *Was* promoter-driven self-inactivated LV, could express other genes such as *eGFP* in a similar hematopoietic cell-specific manner as the *Was* gene. We constructed the WE and WEWA vectors with the same backbone as the WWA vector but expressing *eGFP* or *eGFP–Was*, respectively (Fig. 1A). Figure 1B shows eGFP (from WE vectors) or eGFP–WASP chimera (from WEWA) expression levels in ALLO-WAS/1 (WASP-deficient T cell line) and 293T (epithelial cell line). Contrary to previous data for the expression of WASP, the *Was* promoter-driven LV expressed eGFP efficiently in 293T cells, although still performing better in T cells than in 293T cells (Fig. 1B). Interestingly, the *Was* promoter-driven LVs expressing the eGFP–WASP chimera (WEWA vectors) were efficient only in T cells (Fig. 1B) as we observed previously for the WWA vectors (Martin *et al.*, 2005). Indeed, although WEWA-transduced 293T cells contained similar vector copy numbers per cell (vcn/c) as WE-transduced 293T cells (vcn/c = 0.4; data not shown), we could not detect any expression of the transgene (Fig. 1B, top right).

To quantify this effect in detail we performed quantitative Western blot analysis comparing transgene expression levels of WWA-, WE-, and WEWA-transduced T cells (ALLO-WAS/1 and HVS-WAS/1) and non-HCs (293T cells and DSCs) (Fig. 1C). We calculated the relative transgene expression per integrated vector (TEIV) for each cell line and vector (see Materials and Methods for detail). The TEIV values were used to estimate the hematopoietic specificity of each vector by dividing the TEIV of each HC line by the TEIV of each non-HC line. Figure 1D shows that the hematopoietic specificity of the WE vector is 5–10 times lower than the WWA vector ($p < 0.001$). This reduction in hematopoietic specificity is partially restored by the WEWA vectors ($p < 0.02$).

Was *cDNA influences transgene expression at various levels in various cell types*

The increased hematopoietic specificity of WASP-expressing LVs compared with eGFP-expressing LVs could be due to the presence of *Was* cDNA sequences in the vector (affecting RNA processing or *Was* promoter activity) or to the differences in WASP protein processing in HCs versus non-HCs. To determine the mechanism by which *Was* cDNA affects LV transgene expression, we first constructed the SE and SEWA vectors (Fig. 2A) expressing eGFP and eGFP–WASP proteins through the constitutive spleen focus-forming virus (SFFV) promoter. With these vectors we can determine whether the effect of *Was* cDNA implies RNA processing and/or protein stability. If that is the case, eGFP–WASP-expressing LVs will have reduced expression levels compared with eGFP-expressing LVs (as observed with WEWA vectors), independently of the promoter used to express the mRNA. Also, SEWA vectors should have improved hematopoietic specificity compared with SE vectors, as occurs for *Was* promoter-driven LVs. We therefore analyzed the expression pattern of SE and SEWA vectors in the 293T and ALLO-WAS/1 cell lines (Fig. 2B). Insertion of the *Was* cDNA into the SFFV-driven LV (SEWA vectors) did not downregulate transgene expression in 293T cells (see transgene expression of SE vs. SEWA vectors in Fig. 2B), indicating that the presence of *Was* cDNA sequence does not affect RNA processing or protein stability in this cell type. On the other hand, in ALLO-WAS/1 T cells we observed a substantial decrease in transgene expression of the SEWA vectors compared with SE vectors. These data indicate that, contrary to 293T cells, mRNA processing and/or protein stability (of eGFP vs. eGFP–WASP chimera) are important players in the reduced expression of *Was*-containing vectors (WEWA and SEWA) in T cells.

We further quantified the effect of *Was* cDNA sequences on SFFV-driven LVs by quantitative Western blot analysis, comparing transgene expression levels of SE- versus SEWA-transduced T cells (ALLO-WAS/1 and HVS-WAS/1) and non-HCs (293T and DSCs) (Fig. 2C). As in Fig. 1C, detail quantification was performed to compare transgene expression levels of the SE and SEWA vectors in the various cell lines. Interestingly, the hematopoietic specificity of SFFV-driven LVs harboring *Was* cDNA sequences was reduced (instead of increased as observed for *Was*-driven LVs) (Fig. 2D, SEWA vs. SE vector).

Part of the effect observed in WEWA and SEWA vectors compared with WE and SE vectors could be due in part to differences in protein processing (eGFP–WASP chimera vs. eGFP). To further investigate the mechanisms by which *Was* cDNA influences transgene expression we constructed a *Was* promoter-driven LV expressing *eGFP* harboring a full-length *Was* cDNA inserted downstream of the stop codon of the *eGFP* gene (Fig. 3A, WE-BC). Therefore, the WE-BC vector is identical to the WEWA vector but expresses eGFP instead of eGFP–WASP protein. We also constructed the SE-BC LV (same backbone as the WE-BC vector but driving expression through the SFFV promoter) to discriminate any effect due only to RNA processing (Fig. 3A, SE-BC). Six HC lines (HSV-WAS/1, ALLO-N/1 and ALLO-WAS/1, U937, HEL, and K562) and three non-HC lines (293T, RKO, and HMEC) were transduced with the SE, SE-BC, WE, and WE-BC vectors and analyzed by flow cytometry (Fig. 3B). As occurred with the WEWA vectors, the WE-BC vector expresses the transgene (*eGFP*) better in HCs (Fig. 3B, right: HCs, dark columns; non-HCs, light columns) and has a marked reduction in transgene expression in all cell lines compared with WE vectors. Interestingly, as also observed for WEWA vectors, this reduction is stronger in non-HCs than in HCs. On the other hand, the SE-BC vector (also harboring the *Was* cDNA sequence) maintains similar expression levels in non-HCs and in myeloid cells (U937 and K562) and therefore RNA processing is not affected by the presence of *Was* cDNA sequences in these cells. However, a strong reduction can be observed in T cells (as observed with the SEWA vectors),

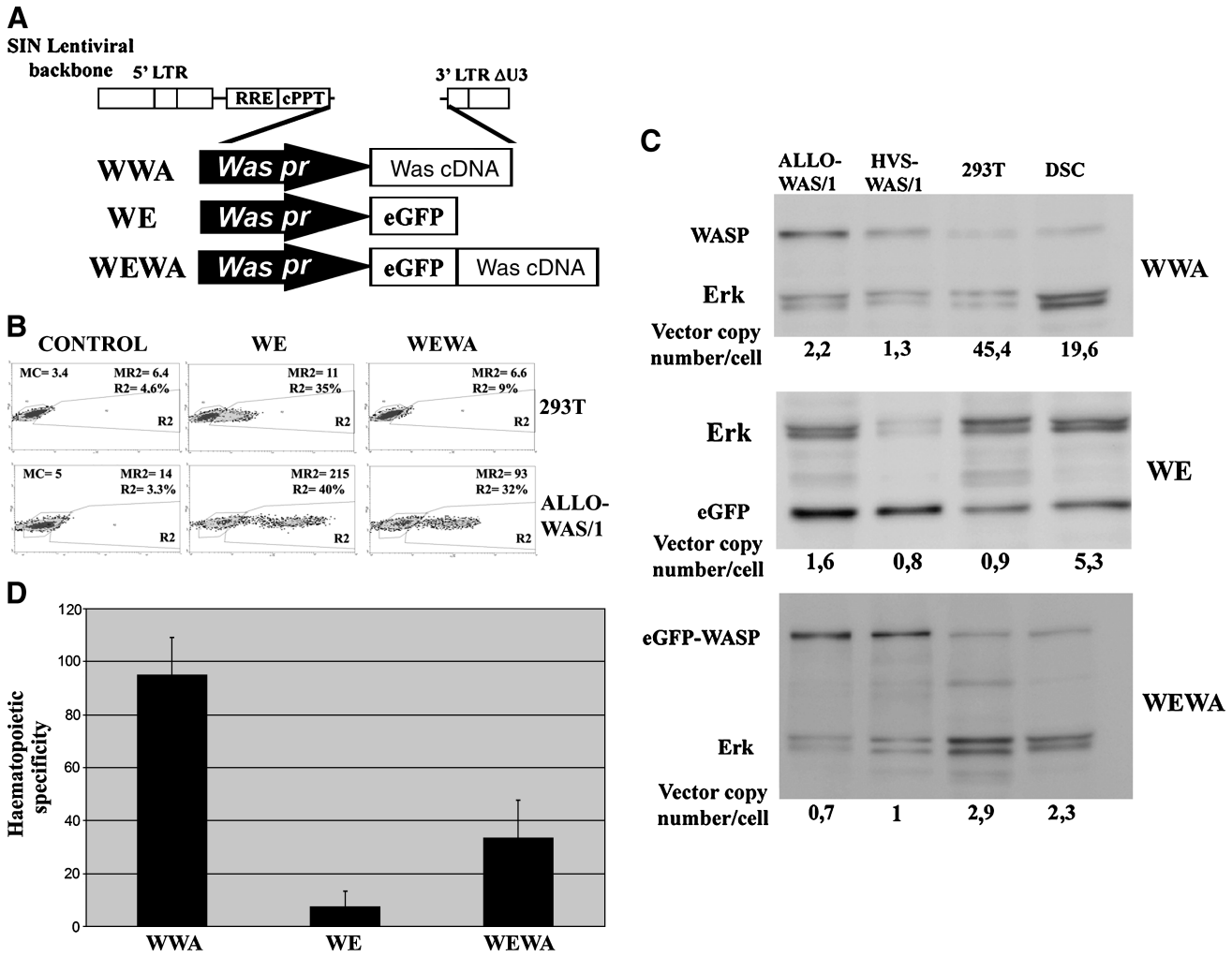

FIG. 1. Hematopoietic specificity of *Was* promoter-driven lentiviral vectors (LVs) is enhanced by *Was* cDNA. (**A**) Scheme of LVs expressing *Was*, *eGFP*, and *eGFP–Was* driven by the *Was* proximal promoter (*Was pr*). (**B**) Representative experiment showing eGFP (WE vectors) or eGFP–WASP (WEWA) expression levels in ALLO-WAS/1 T cells and 293T cells as analyzed by flow cytometry. Because of differences in cell permissiveness to LV transduction, 293T cells were incubated at a multiplicity of infection (MOI) of 0.4 and ALLO-WAS/1 cells at an MOI of 3 to achieve similar levels of transduced cells. MC, mean intensity of fluorescence of nonexpressing cells; MR2, mean intensity of fluorescence of expressing cells. (**C**) Western blot analysis to measure transgene expression levels of HCs (ALLO-WAS/1 and HVS-WAS/1) and non-HCs (293T and DSCs) transduced with *Was* promoter-driven LVs expressing WASP (*top:* WWA), eGFP (*middle:* WE) and eGFP–WASP chimera (*bottom:* WEWA). Expression levels were determined by Western blot using anti-WASP monoclonal antibody (for WWA- and WEWA-transduced cells) or anti-eGFP monoclonal antibody (for WE-transduced cells). Anti-ERK polyclonal antibody was used as reference. Cells were analyzed 1–2 weeks after transduction. Vectors copy numbers per cell are shown at the bottom of each lane. (**D**) Graph showing hematopoietic specificity of the various *Was* promoter-driven LVs. Relative transgene expression per integrated vector (TEIV) was calculated for each vector and cell line. The hematopoietic specificity index of each vector was calculated by dividing the TEIV of each HC line by the TEIV of each non-HC line. The graph shows the average ± SDEVP of the various HC/non-HC ratios (see Materials and Methods for details). cPPT, central polypurine tract; DSCs, decidual stromal cells; eGFP, enhanced green fluorescent protein; ERK, extracellular signal-regulated kinase; LTR, long terminal repeat; RRE, Rev responsive element; SIN, self-inactivating.

indicating that in T cells, the mRNAs containing *Was* cDNA sequences are either more instable or less well translated than the same RNA without this sequence.

Last, we quantified the effect of *Was* cDNA sequences on the transcriptional activity of LVs. We transduced 293T cells with *Was*- and *SFFV* promoter-driven LVs with or without the *Was* cDNA sequence and expressing eGFP (WE, WE-BC, SE, and SE-BC) and quantified relative *eGFP* mRNA levels by RT-PCR of transduced cells with identical vector copy numbers per cell. Figure 3C show the result of the comparative RT-PCR, using the BC-containing vector as reference. *Was* cDNA sequences dramatically reduced mRNA levels of *Was* promoter-driven LVs in 293T cells (WE-BC vectors expressed up to 60 times less RNA than WE vectors; Fig. 3C, left) but slightly increased mRNA levels of SFFV-driven LVs (Fig. 3C, right).

All these data together indicate that *Was* cDNA sequences have at least two different effects on LV transgene expression

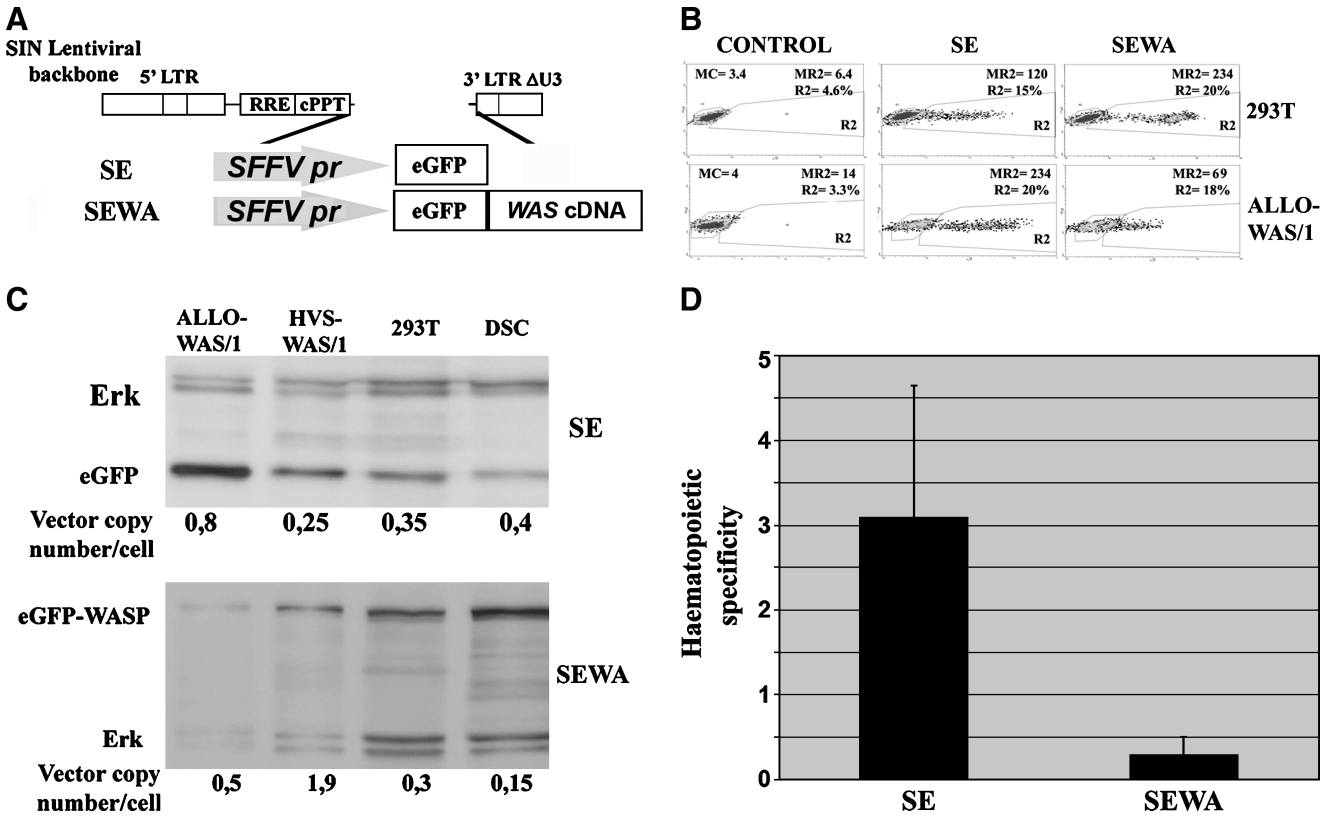

FIG. 2. Hematopoietic cell-specificity improvement of LVs by *Was* cDNA sequences requires a *Was* promoter. (**A**) Scheme of LVs expressing eGFP and eGFP–WASP chimera driven by the spleen focus-forming virus LTR promoter (SFFV). (**B**) Representative experiment showing the eGFP expression level (from SE vectors) or eGFP–WASP expression level (from SEWA vectors) in ALLO-WAS/1 and 293T cell lines. Because of differences in cell permissiveness to LV transduction, 293T cells were incubated at an MOI of 0.4 and ALLO-WAS/1 cells at an MOI of 3 to achieve similar levels of transduced cells. MC, mean intensity of fluorescence of nonexpressing cells; MR2, mean intensity of fluorescence of expressing cells. (**C**) Comparison of transgene expression levels in T cells (ALLO-WAS/1 and HVS-WAS/1) and non-HCs (293T cells and DSCs) transduced with *Was*-driven LVs expressing eGFP (SE) and eGFP–WASP chimera (SEWA). Expression levels were determined by Western blot, using anti-WASP monoclonal antibody (for SEWA-transduced cells) or anti-eGFP monoclonal antibody (for SE-transduced cells). Anti-ERK polyclonal antibody was used as reference. Cells were analyzed 1–2 weeks after transduction. Vector copy numbers per cell are shown at the bottom of each lane. (**D**) Graph showing hematopoietic specificity of SE and SEWA vectors. The relative transgene expression per integrated vector (TEIV) was calculated for each vector and cell line. The hematopoietic specificity index of each vector was calculated by dividing the TEIV of each HC line by the TEIV of each non-HC line. The graph shows the average ± SDEVP of the various HC/non-HC ratios (see Materials and Methods for details).

depending on the cell type. In T cells these sequences have a marked posttranscriptional effect, reducing either RNA stability and/or mRNA translation. In non-HCs such as 293T cells and HMECs, *Was* cDNA downregulates *Was* promoter activity but does not have any effect on the SFFV promoter or in posttranscriptional regulation.

A 900-bp fragment 5′ of the Was *cDNA contains regulatory sequences that influence transcription and increase hematopoietic specificity*

To further study the influence of the *Was* cDNA in *Was* promoter activity, we constructed a panel of LVs expressing *eGFP* and harboring different fragments of the *Was* cDNA downstream of the *eGFP* stop codon. We dissected the *Was* cDNA (BC, 1640 bp) into 5′ fragments (BA, 719 bp; and BX, 960 bp) and 3′ fragments (AC and XX) that included (BX and AC) or did not include (BA and XX) the 330-bp center of the *Was* cDNA (Fig. 4A). To study the minimal *Was* cDNA sequences that influence *Was* promoter activity we focused our studies on cells in which these sequences do not affect mRNA processing (non-HCs; 293T cells and HMECs). 293T cells and HMECs were transduced by the various vectors at high MOI (MOI of 5) to obtain detectable levels of eGFP expression with all vectors. Transduced cells were analyzed by fluorescence-activated cell sorting (FACS) 7 days posttransduction. The increments in fluorescence intensity of WE-, WE-BC-, WE-BA-, WE-AC-, WE-BX-, and WE-XX-transduced cells are plotted in Fig. 4B. All *Was* cDNA fragments but the 680-bp XX decreased significantly the eGFP expression of the *Was* promoter-driven LVs (Fig. 4B) in both cell lines. For instance, WE-transduced 293T cells expressed 10 times more eGFP than did WE-BC-transduced 293T cells ($p < 0.01$) and WE-transduced HMECs expressed 4 times more eGFP than did WE-BA-transduced HMECs ($p < 0.05$).

We next analyzed whether the presence of *Was* cDNA fragments resulted in improved hematopoietic specificity of eGFP-expressing vectors. We first performed an experiment

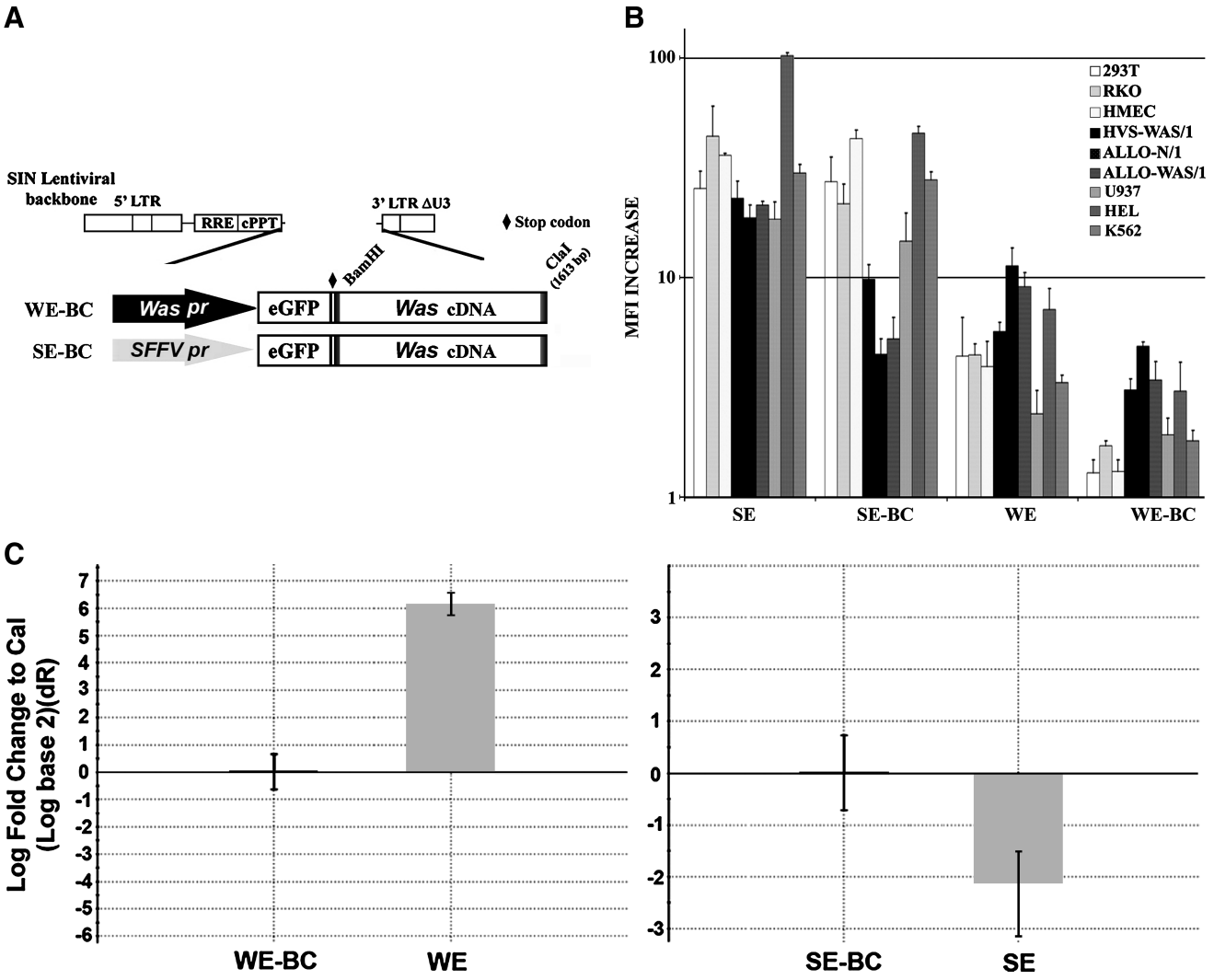

FIG. 3. The effect of *Was* cDNA sequences on LV expression depends on the promoter and the cell type. (**A**) Scheme of LVs incorporating the *Was* cDNA downstream of the *eGFP* stop codon in the WE and SE backbones. (**B**) Comparison of eGFP expression levels (increase in mean fluorescence intensity [MFI]) of SE, SE-BC, WE, and WE-BC vectors in non-HCs (293T, RKO, and HMEC; lighter columns) and HCs (HVS-WAS/1, ALLO-N/1, ALLO-WAS/1, U937, HEL, and K562; darker columns). The graph shows the average increment in mean fluorescence intensity (MFI) of transduced cells (relative to untransduced cells) obtained from at least three separate experiments. Only cells containing 0.2–0.4 vector copy numbers per cell (vcn/c) were used for the study. (**C**) *Was* sequences downregulate *Was* promoter activity in non-HCs. Shown are the relative mRNA levels in 293T cells transduced with WE versus WE-BC and with SE versus SE-BC (0.4 vcn/c). Data are shown relative to *Was* cDNA-containing vectors (WE-BC and SE-BC). A totally different effect of *Was* cDNA sequences on mRNA levels can be observed depending on the promoter driving its expression.

similar to that described previously but comparing the effect of *Was* cDNA sequences in HCs. HVS-WAS/1 and ALLO-WAS/1 T cells were transduced with the various vectors at an MOI of 1–2 and analyzed for eGFP expression. The increments in fluorescence intensity of the various vectors are plotted in Fig. 4C. As for non-HCs, all vectors containing *Was* cDNA fragments, except for the 680-bp XX, showed a reduction in eGFP expression in both cell lines compared with WE vectors. However, this effect was less marked than for HCs. For instance, WE-transduced HVS-WAS/1 cells expressed 1.6 times more eGFP than did WE-BC-transduced HVS-WAS/1 cells ($p < 0.01$) and WE-transduced ALLO-WAS/1 cells expressed 2.6 times more eGFP than did WE-BC-transduced ALLO-WAS/1 cells ($p < 0.05$). To further study this observation we performed quantitative Western blot analysis comparing eGFP expression levels of WE-, WE-BC-, and WE-BX-transduced HCs (ALLO-WAS/1) and non-HCs (293T) (Fig. 4D). A detailed quantification of band intensities (relative to ERK protein levels and vector copy number per cell) and of vector copy numbers per cell allowed us to measure the relative transgene expression per integrated vector (TEIV) (see Materials and Methods) and to determine the hematopoietic specificity of the WE, WE-BC, and WE-BX LVs by comparing the TEIV of each vector in 293T cells versus ALLO-WAS/1 T cells. Figure 4E shows that WE-BC and WE-BX vectors have improved hematopoietic specificity (four to six times better; $p < 0.05$) than the WE vector (Fig. 4D). These results corroborate the involvement of *Was* cDNA in

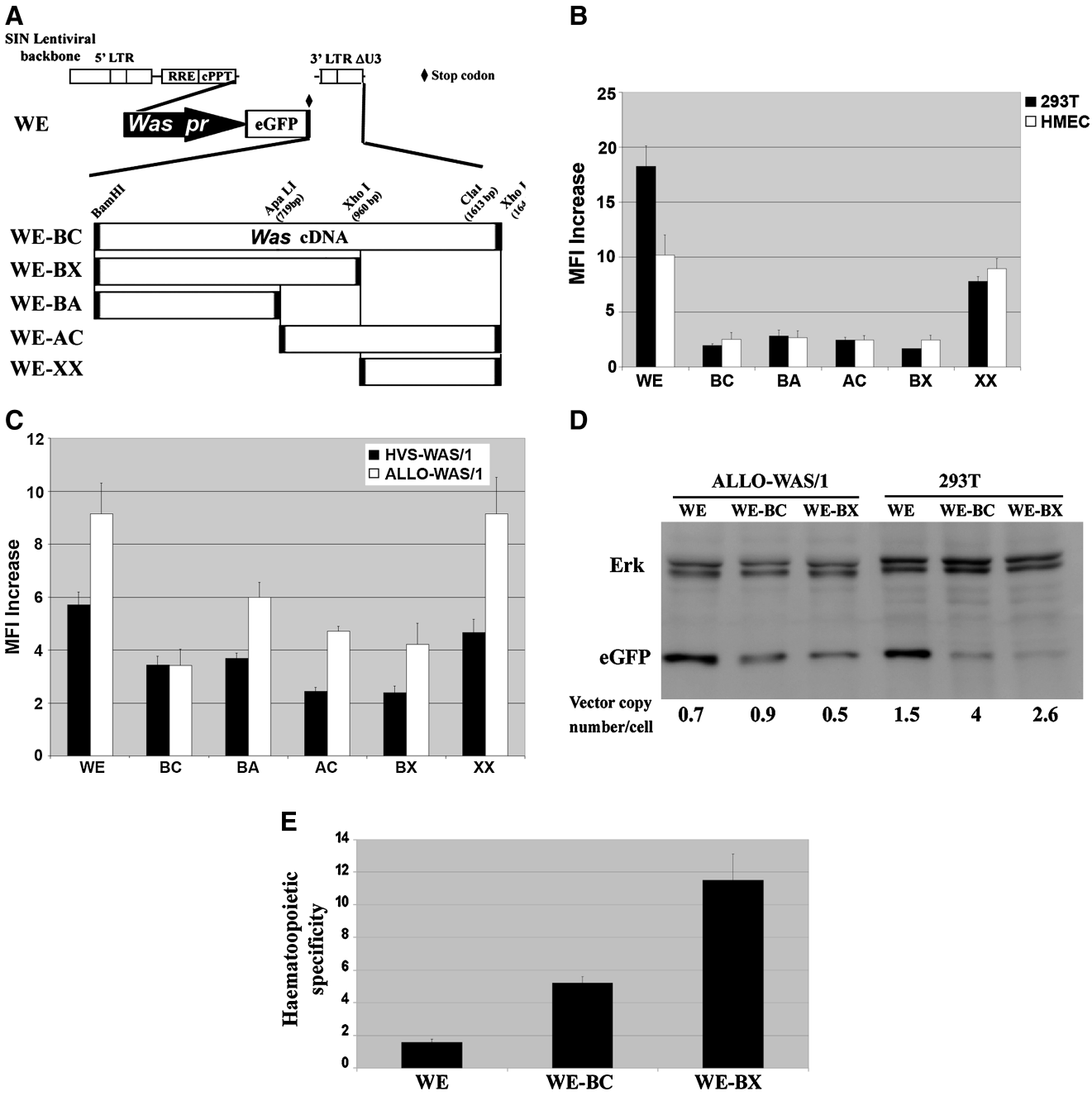

FIG. 4. The first half of the *Was* cDNA is enough to downregulate promoter activity in non-HCs and to increase hematopoietic cell-specific expression of eGFP. (**A**) Scheme of LVs incorporating various fragments of the *Was* cDNA downstream of the *eGFP* stop codon. (**B**) eGFP expression levels (MFI increase) of WE, WE-BC, WE-BA, WE-AC, WE-BX, and WE-XX vectors in non-HCs (293T cells and HMECs). The graph shows the average increment in mean fluorescence intensity (MFI) of transduced cells (relative to untransduced cells) obtained from at least three separate experiments. Because some vectors do not express detectable levels of eGFP at low MOI, only transduced cells containing two or three vectors per cell were used for the study. (**C**) eGFP expression levels (MFI increase) of WE, WE-BC, WE-BA, WE-AC, WE-BX, and WE-XX vectors in HCs (HVS-WAS/1 and ALLO-WAS/1). The graph shows the average increment in mean fluorescence intensity (MFI) of transduced cells (relative to untransduced cells) obtained from at least three separate experiments. Only cells containing 0.2–0.4 vector copy numbers per cell were used for the study. (**D**) Comparison of transgene expression levels of WE, WE-BC, and WE-BX vectors on 293T and ALLO-WAS/1 cell lines by Western blot, using an eGFP monoclonal antibody. Anti-ERK polyclonal antibody was used as reference. In each case, eGFP expression levels are normalized to ERK expression. Cells were analyzed 1–2 weeks after transduction. Vector copy numbers per cell are shown at the bottom of each lane. (**E**) Influence of BC and BX *Was* cDNA fragments on the hematopoietic specificity of the WE vector. The graph shows hematopoietic specificity estimated from two different experiments, as in (**C**). The hematopoietic specificity index of the WE, WE-BC, and WE-BX vectors was calculated as the ratio of the relative transgene expression per integrated vector (TEIV) of each vector in ALLO-WAS/1 T cells versus 293T cells. The graph shows the average ± SDEVP of the values obtained in two different experiments.

hematopoietic cell-specific expression and localize the area involved to the first 900 bp of the 5′ sequence.

Was *cDNA partially neutralizes the enhancer effect of WPRE in most cell types*

Moreau-Gaudry and colleagues have demonstrated the positive effect of the WPRE in erythroid-specific transgene expression (Moreau-Gaudry *et al.*, 2001). On the basis of these results we decided to study whether the WPRE could also increase transgene expression of *Was* promoter-driven LVs harboring *Was* cDNA fragments. We transduced ALLO-WAS/1 and 293T cells with SE, WE, SE-BC, and WE-BC LVs and with their WPRE-containing counterparts (Fig. 5A; SEWP, WEWP, SE-BCWP, and WE-BCWP). Figure 5B shows the increment in eGFP expression levels (measured as the MFI increase with the $WPRE^+$ vector divided by the MFI increase with its $WPRE^-$ counterpart) achieved by introduction of the WPRE into each vector analyzed. In general, the effect of the WPRE in transgene expression was higher in SFFV-driven than in *Was*-driven LVs. For instance, eGFP expression was 10 times higher with SEWP than with SE in 293T cells, and 4 times higher in ALLO-WAS/1 cells (Fig. 5B, solid columns). On the other hand, the presence of the WPRE in the WE backbone vector increased eGFP expression only four times in 293T cells and two times in ALLO-WAS/1 cells (Fig. 5B, open columns). Interestingly, the presence of *Was* cDNA in the SE and WE backbones reduced the effect of the WPRE in most cells, with a drastic effect in 293T cells. Indeed, in 293T cells, the WPRE increased the eGFP expression of SE vectors 10 times but only 2 times if incorporated into the SE-BC vector (Fig. 5B, solid columns vs. dashed columns; $p < 0.03$). A significant reduction was also observed in ALLO-WAS/1 cells (3-fold enhancement vs. no enhancement; $p < 0.01$). Similarly, the effect of the WPRE in the WE vector was lower when incorporated into *Was* cDNA-containing vectors (WE-BC): whereas the WPRE enhanced the eGFP expression of WE vectors four times in 293T cells and two times in ALLO-WAS/1 cells, the presence of *Was* sequences in the WE-BC vectors had almost no effect (Fig. 5B, open columns vs. gray columns; $p < 0.05$).

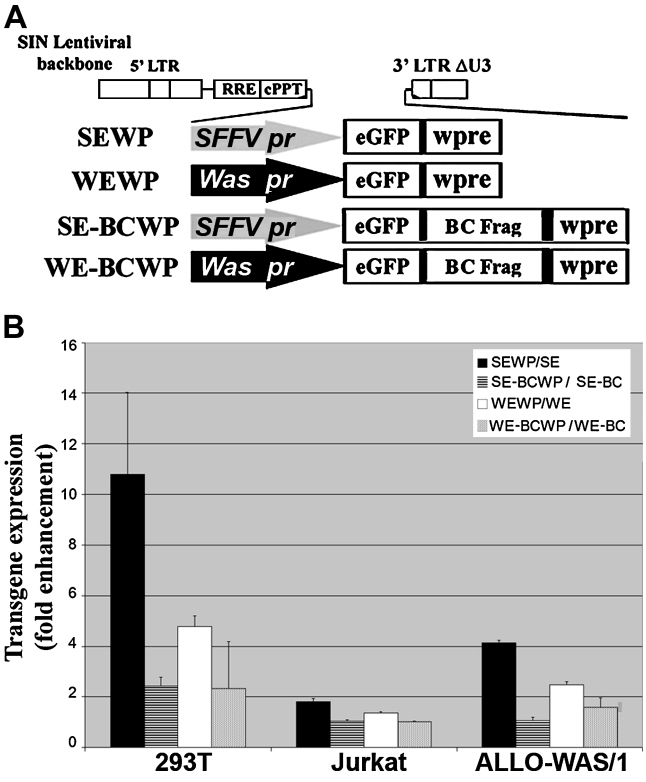

FIG. 5. Inclusion of the woodchuck posttranscriptional regulatory element (WPRE) in *Was* promoter-driven and *Was* cDNA-containing LVs does not improve expression. (**A**) Scheme of the various LVs incorporating the WPRE. (**B**) Graph representing the fold increment in transgene expression due to insertion of the WPRE. Values were obtained by dividing the MFI increase with WPRE-containing vectors by the MFI increase with their WPRE-deficient counterparts. Averages of two or three separate experiments are plotted.

Discussion

The development of vectors expressing a therapeutic transgene efficiently and specifically in hematopoietic cells (HCs) is an important goal for gene therapy of hematological disorders. We have previously shown that the WWA LV expressing the *Was* cDNA through a 500-bp fragment of the *Was* proximal promoter is more than 100 times more efficient in HCs than in non-HCs (Martin *et al.*, 2005). In this paper we have shown that the same LV expressing *eGFP* (WE) partially loses hematopoietic cell-specific expression. We demonstrated that the enhanced hematopoietic cell specificity of *Was*-expressing vectors is due to a combined effect of both transcriptional and posttranscriptional effects of *Was* cDNA.

To study the mechanism by which the *Was* cDNA influences the hematopoietic specificity of *Was* promoter-driven LVs, we first investigated whether mRNA and/or protein stability was a major player. If posttranscriptional regulation was involved, SFFV-driven LVs (SW, SEWA, and SE-BC) should also have increased hematopoietic expression compared with SE LVs. However, we found no effect in this sense. In fact, the transgene expression of SFFV-driven vectors carrying *Was* cDNA sequences was drastically reduced in T cells, with no effect in myeloid cells and non-HCs compared with SE vectors. We further showed that *Was* cDNA sequences reduced mRNA levels of *Was* promoter-driven LVs in 293T cells up to 64 times compared with *Was* promoter-driven LVs carrying this sequence, an effect possible only by having a direct effect in blocking *Was* promoter activity, because SFFV-driven LVs expressing the same RNA were not affected or even had increased mRNA levels (Fig. 3C). These data indicate that the effect of *Was* cDNA sequences on LV transgene expression is variable depending on the cell type. In non-HCs, we assume that transcriptional modulation is the only process acting to regulate transgene expression of *Was* promoter-driven LVs. However, in T cells we have a more complicated scenario and we propose that probably both mRNA processing and promoter regulation play a role.

We further characterized the region of the *Was* cDNA involved in transgene regulation by incorporating various *Was* cDNAs fragments downstream of *eGFP* in the WE vector and studying eGFP expression in HCs and non-HCs, both by FACS and quantitative Western blotting. The results obtained corroborate the involvement of *Was* cDNA in hematopoietic cell-specific expression and localize the area involved to the first 900 bp of the 5′ sequence of the cDNA.

All constructs but WE-XX decreased expression (compared with WE vectors) in all cell lines, with a stronger effect in non-HCs. The effect was independent of insert size because the WE-BA vector (719-bp insert size) was as efficient as the WE-BC vector (1640 bp) (Fig. 3B). In addition, the WE-XX vector (680-bp insert size) has an expression pattern similar to that of the WE vector. Transfac software analysis found potential inhibitory transcription factor (TF)-binding sites (CBF, WT1, GATA1, and C/EBPα) and potential activators (Sp1, Egr1, and Ap1) through the *Was* cDNA sequence; from *Bam*HI to *Apa*LI we have Sp1, Egr1, C/EBPα, Ap1, and GATA1 TF-binding sites. From *Apa*LI to *Xho*I, we found GATA1, WT1, and Ap1 TF-binding sites; and from *Xho*I to the 3′ end we found Sp1, Egr1, H4TF1, CBF-1, and C/EBPα TF-binding sites. Taking together expression profiles of the various constructs and TF-binding sites, one could hypothesize that WT1 and GATA1 could play a role in transcriptional repression and that Sp1, Ap1, and Egr1 could play a role in increasing hematopoietic specificity. Our laboratory is actively working to determine whether any of these TFs is actually involved in active regulation of *Was* promoter-driven LVs and whether this mechanism is also involved in physiological expression of the *Was* gene.

The mechanism involved in the improved hematopoietic specificity is complex because *Was* sequences negatively affect mRNA stability and/or translation only in T cells and not in 293T cells or HMECs, where these sequences strongly decreased eGFP expression because of promoter downregulation. Therefore the improved hematopoietic specificity must be the result of transcriptional and posttranscriptional modulation in the different cell types. The combined effects result in a general downregulation of transgene expression but a gain in hematopoietic specificity.

The *Was* promoter-driven and *Was* cDNA-containing LVs express low protein levels, and this could be a good characteristic for some purposes by minimizing vector genotoxicity. However, it would also be of interest to have hematopoietic cell-specific vectors expressing higher transgene levels. On the basis of the work of Moreau-Gaudry and colleagues, in which they demonstrated that inclusion of the WPRE in erythroid cell-specific LVs increased expression in erythroid cells (Moreau-Gaudry *et al.*, 2001), we decided to study whether the WPRE could improve the titer and transgene expression of our LVs. However, although we noticed an increase in vector titer (data not shown), the effect of WPRE in transgene expression was variable. In general, the effect of the WPRE in transgene expression was higher in SFFV-driven than in *Was*-driven LVs. Interestingly, the presence of *Was* cDNA in the LV backbone (SEWAWP, WEWAWP, and WE-BC vectors) blocks the enhancing effect of the WPRE in all cell lines and therefore partially inhibits its beneficial effect in our lentiviral backbone. Because *Was* sequences negatively modulate mRNA stability and/or translation, it is plausible that these sequences interfere with WPRE activity, partially neutralizing their effect on RNA stability.

In summary, this work demonstrated the effect of *Was* cDNA on LV transgene expression, showing an effect on *Was* promoter regulation and/or on mRNA processing, depending on the cell type. The global effect of these sequences on *Was* promoter-driven LVs is improved hematopoietic specificity, partially explaining the better performance when these vectors express WASP versus eGFP. We have characterized the minimal *Was* cDNA fragment required to increase hematopoietic specificity to the first 900 bp. Last, we have shown that inclusion of the WPRE in *Was* promoter-driven and *Was* cDNA-containing LVs does not improve expression of these vectors.

Acknowledgments

We are grateful to Dr. Didier Trono (University of Geneva, Geneva, Switzerland) for providing the HIV packaging pCMV.R8.91 and envelope pMD.G plasmids, Dr. A. Thrasher for providing the WEWP and SEWP vectors, and Dr. Ignacio Molina and Enrique Garcia Olivares (Granada University) for providing primary HVS-transformed T cell lines and DSCs, respectively. This work was supported by grant PI061035 to F.M.

Author Disclosure Statement

For all authors, no competing financial interests exist.

References

Abbasi, A.A., Paparidis, Z., Malik, S., Goode, D.K., Callaway, H., Elgar, G., and Grzeschik, K.H. (2007). Human GLI3 intragenic conserved non-coding sequences are tissue-specific enhancers. PLoS One 2, e366.

Barde, I., Zanta-Boussif, M.A., Paisant, S., Leboeuf, M., Rameau, P., Delenda, C., and Danos, O. (2006). Efficient control of gene expression in the hematopoietic system using a single Tet-on inducible lentiviral vector. Mol. Ther. 13, 382–390.

Case, S.S., Price, M.A., Jordan, C.T., Yu, X.J., Wang, L., Bauer, G., Haas, D.L., Xu, D., Stripecke, R., Naldini, L., Kohn, D.B., and Crooks, G.M. (1999). Stable transduction of quiescent $CD34^+$ $CD38^-$ human hematopoietic cells by HIV-1-based lentiviral vectors. Proc. Natl. Acad. Sci. U.S.A. 96, 2988–2993.

Cui, Y., Narayanan, C.S., Zhou, J., and Kumar, A. (1998). Exon-I is involved in positive as well as negative regulation of human angiotensinogen gene expression. Gene 224, 97–107.

Cui, Y., Golob, J., Kelleher, E., YE, Z., Pardoll, D., and Cheng, L. (2002). Targeting transgene expression to antigen-presenting cells derived from lentivirus-transduced engrafting human hematopoietic stem/progenitor cells. Blood 99, 399–408.

Chang, A.H., and Sadelain, M. (2007). The genetic engineering of hematopoietic stem cells: The rise of lentiviral vectors, the conundrum of the LTR, and the promise of lineage-restricted vectors. Mol. Ther. 15, 445–456.

Demaison, C., Parsley, K., Brouns, G., Scherr, M., Battmer, K., Kinnon, C., Grez, M., and Thrasher, A.J. (2002). High-level transduction and gene expression in hematopoietic repopulating cells using a human immunodeficiency [correction of imunodeficiency] virus type 1-based lentiviral vector containing an internal spleen focus forming virus promoter. Hum. Gene Ther. 13, 803–813.

Donello, J.E., Loeb, J.E., and Hope, T.J. (1998). Woodchuck hepatitis virus contains a tripartite posttranscriptional regulatory element. J. Virol. 72, 5085–5092.

Frecha, C., Toscano, M.G., Costa, C., Saez-Lara, M.J., Cosset, F.L., Verhoeyen, E., and Martin, F. (2008). Improved lentiviral vectors for Wiskott-Aldrich syndrome gene therapy mimic endogenous expression profiles throughout haematopoiesis. Gene Ther. 15, 930–941.

Gallego, M.D., Santamaria, M., Pena, J., and Molina, I.J. (1997). Defective actin reorganization and polymerization of Wiskott-

Aldrich T cells in response to CD3-mediated stimulation. Blood 90, 3089–3097.

Garcia-Pacheco, J.M., Oliver, C., Kimatrai, M., Blanco, F.J., and Olivares, E.G. (2001). Human decidual stromal cells express CD34 and STRO-1 and are related to bone marrow stromal precursors. Mol. Hum. Reprod. 7, 1151–1157.

Gaszner, M., and Felsenfeld, G. (2006). Insulators: Exploiting transcriptional and epigenetic mechanisms. Nat. Rev. 7, 703–713.

Goverdhana, S., Puntel, M., Xiong, W., ZIRGER, J.M., Barcia, C., Curtin, J.F., Soffer, E.B., Mondkar, S., King, G.D., Hu, J., Sciascia, S.A., Candolfi, M., Greengold, D.S., Lowenstein, P.R., and Castro, M.G. (2005). Regulatable gene expression systems for gene therapy applications: Progress and future challenges. Mol. Ther. 12, 189–211.

Han, X.D., Lin, C., Chang, J., Sadelain, M., and Kan, Y.W. (2007). Fetal gene therapy of α-thalassemia in a mouse model. Proc. Natl. Acad. Sci. U.S.A. 104, 9007–9011.

Hawley, R.G. (2001). Progress toward vector design for hematopoietic stem cell gene therapy. Curr, Gene Ther. 1, 1–17.

Hlavaty, J., Schittmayer, M., Stracke, A., Jandl, G., Knapp, E., Felber, B.K., Salmons, B., Gunzburg, W.H., and Renner, M. (2005). Effect of posttranscriptional regulatory elements on transgene expression and virus production in the context of retrovirus vectors. Virology 341, 1–11.

Jager, U., Zhao, Y., and Porter, C.D. (1999). Endothelial cell-specific transcriptional targeting from a hybrid long terminal repeat retrovirus vector containing human prepro-endothelin-1 promoter sequences. J. Virol. 73, 9702–9709.

Kobayashi, M., Nishikawa, K., and Yamamoto, M. (2001). Hematopoietic regulatory domain of *gata1* gene is positively regulated by GATA1 protein in zebrafish embryos. Development 128, 2341–2350.

Levine, M., and Tjian, R. (2003). Transcription regulation and animal diversity. Nature 424, 147–151.

Lin, C.J., and Tam, R.C. (2001). Transcriptional regulation of CD28 expression by CD28GR, a novel promoter element located in exon 1 of the CD28 gene. J. Immunol 166, 6134–6143.

Lotti, F., Menguzzato, E., Rossi, C., Naldini, L., Ailles, L., Mavilio, F., and Ferrari, G. (2002). Transcriptional targeting of lentiviral vectors by long terminal repeat enhancer replacement. J. Virol. 76, 3996–4007.

Lutzko, C., Senadheera, D., Skelton, D., Petersen, D., and Kohn, D.B. (2003). Lentivirus vectors incorporating the immunoglobulin heavy chain enhancer and matrix attachment regions provide position-independent expression in B lymphocytes. J. Virol. 77, 7341–7351.

Marodon, G., Mouly, E., Blair, E.J., Frisen, C., Lemoine, F.M., and Klatzmann, D. (2003). Specific transgene expression in human and mouse $CD4^+$ cells using lentiviral vectors with regulatory sequences from the CD4 gene. Blood 101, 3416–3423.

Martin, F., Toscano, M.G., Blundell, M., Frecha, C., Srivastava, G.K., Santamaria, M., Thrasher, A.J., and Molina, I.J. (2005). Lentiviral vectors transcriptionally targeted to hematopoietic cells by WASP gene proximal promoter sequences. Gene Ther. 12, 715–723.

Mastroyiannopoulos, N.P., Feldman, M.L., Uney, J.B., Mahadevan, M.S., and Phylactou, L.A. (2005). Woodchuck post-transcriptional element induces nuclear export of myotonic dystrophy 3′ untranslated region transcripts. EMBO Rep 6, 458–463.

Modlich, U., Bohne, J., Schmidt, M., Von Kalle, C., Knoss, S., Schambach, A., and Baum, C. (2006). Cell-culture assays reveal the importance of retroviral vector design for insertional genotoxicity. Blood 108, 2545–2553.

Moreau, T., Bardin, F., Imbert, J., Chabannon, C., and Tonnelle, C. (2004). Restriction of transgene expression to the B-lymphoid progeny of human lentivirally transduced $CD34^+$ cells. Mol. Ther. 10, 45–56.

Moreau-Gaudry, F., Xia, P., Jiang, G., Perelman, N.P., Bauer, G., Ellis, J., Surinya, K.H., Mavilio, F., Shen, C.K., and Malik, P. (2001). High-level erythroid-specific gene expression in primary human and murine hematopoietic cells with self-inactivating lentiviral vectors. Blood 98, 2664–2672.

Neil, S., Martin, F., Ikeda, Y., and Collins, M. (2001). Postentry restriction to human immunodeficiency virus-based vector transduction in human monocytes. J. Virol. 75, 5448–5456.

Oertel, M., Rosencrantz, R., Chen, Y.Q., Thota, P.N., Sandhu, J.S., Dabeva, M.D., Pacchia, A.L., Adelson, M.E., Dougherty, J.P., and Shafritz, D.A. (2003). Repopulation of rat liver by fetal hepatoblasts and adult hepatocytes transduced *ex vivo* with lentiviral vectors. Hepatology 37, 994–1005.

Osborne, C.S., Chakalova, L., Brown, K.E., Carter, D., Horton, A., Debrand, E., Goyenechea, B., Mitchell, J.A., Lopes, S., Reik, W., and Fraser, P. (2004). Active genes dynamically colocalize to shared sites of ongoing transcription. Nat. Genet. 36, 1065–1071.

Robert-Richard, E., Richard, E., Malik, P., Ged, C., De Verneuil, H., and Moreau-Gaudry, F. (2007). Murine retroviral but not human cellular promoters induce *in vivo* erythroid-specific deregulation that can be partially prevented by insulators. Mol. Ther. 15, 173–182.

Sakonju, S., Bogenhagen, D.F., and Brown, D.D. (1980). A control region in the center of the 5S RNA gene directs specific initiation of transcription. I. The 5′ border of the region. Cell 19, 13–25.

Saur, D., Seidler, B., Paehge, H., Schusdziarra, V., and Allescher, H.D. (2002). Complex regulation of human neuronal nitric-oxide synthase exon 1c gene transcription: Essential role of Sp and ZNF family members of transcription factors. J. Biol. Chem. 277, 25798–25814.

Seshasayee, D., Geiger, J.N., Gaines, P., and Wojchowski, D.M. (2000). Intron 1 elements promote erythroid-specific GATA-1 gene expression. J. Biol. Chem. 275, 22969–22977.

Sternberg, E.A., Spizz, G., Perry, W.M., Vizard, D., Weil, T., and Olson, E.N. (1988). Identification of upstream and intragenic regulatory elements that confer cell-type-restricted and differentiation-specific expression on the muscle creatine kinase gene. Mol. Cell. Biol. 8, 2896–2909.

Szulc, J., Wiznerowicz, M., Sauvain, M.O., Trono, D., and Aebischer, P. (2006). A versatile tool for conditional gene expression and knockdown. Nat. Methods 3, 109–116.

Toscano, M.G., Frecha, C., Benabdellah, K., Cobo, M., Blundell, M., Thrasher, A.J., Garcia-Olivares, E., Molina, I.J., and Martin, F. (2008). Hematopoietic-specific lentiviral vectors circumvent cellular toxicity due to ectopic expression of Wiskott-Aldrich syndrome protein. Hum. Gene Ther. 19, 179–197.

Werner, M., Kraunus, J., Baum, C., and Brocker, T. (2004). B-cell-specific transgene expression using a self-inactivating retroviral vector with human CD19 promoter and viral post-transcriptional regulatory element. Gene Ther. 11, 992–1000.

Wiznerowicz, M., and Trono, D. (2005). Harnessing HIV for therapy, basic research and biotechnology. Trends Biotechnol. 23, 42–47.

Wong, E.Y., Lin, J., Forget, B.G., Bodine, D.M., and Gallagher, P.G. (2004). Sequences downstream of the erythroid promoter are required for high level expression of the human α-spectrin gene. J. Biol. Chem. 279, 55024–55033.

Xu, L., Wallen, R., Patel, V., and Depinho, R.A. (1993). Role of first exon/intron sequences in the regulation of *myc* family oncogenic potency. Oncogene 8, 2547–2553.

Zufferey, R., Dull, T., Mandel, R.J., Bukovsky, A., Quiroz, D., Naldini, L., and Trono, D. (1998). Self-inactivating lentivirus vector for safe and efficient *in vivo* gene delivery. J. Virol. 72, 9873–9880.

Zufferey, R., Donello, J.E., Trono, D., and Hope, T.J. (1999). Woodchuck hepatitis virus posttranscriptional regulatory element enhances expression of transgenes delivered by retroviral vectors. J. Virol. 73, 2886–2892.

Zychlinski, D., Schambach, A., Modlich, U., Maetzig, T., Meyer, J., Grassman, E., Mishra, A., and Baum, C. (2008). Physiological promoters reduce the genotoxic risk of integrating gene vectors. Mol. Ther. 16, 718–725.

Address correspondence to:
Dr. Francisco Martin
Andalusian Stem Cell Bank, CIBM
Universidad de Granada
Parque Tecnológico Ciencias de la Salud
18100 Armilla, Granada, Spain

E-mail: francisco.martin.molina@juntadeandalucia.es

Received for publication July 12, 2009;
accepted after revision July 24, 2009.

Published online: September 21, 2009.

Gene Therapy (2011) 18, 364–371

www.nature.com/gt

ORIGINAL ARTICLE

A tissue-specific, activation-inducible, lentiviral vector regulated by human CD40L proximal promoter sequences

Z Romero[1], S Torres[1], M Cobo[2], P Muñoz[2], JD Unciti[1], F Martín[2,3] and IJ Molina[1,3]

The application of new protocols for gene therapy against monogenic diseases requires the development of safer therapeutic vectors, particularly in the case of diseases in which expression of the mutated gene is subject to fine regulation, as it is with CD40L (CD154). *CD40L*, the gene mutated in the X-linked hyper-immunoglobulin M syndrome (HIGM1), is tightly regulated to allow surface expression of its product only on T cells stimulated by antigen encounter. Previous studies in an HIGM1 animal model showed that transduction of progenitor cells corrected the syndrome but caused a thymic lymphoproliferative disease because of the unregulated expression of the transgene by constitutive vectors. To develop a tissue-specific, activation-inducible, lentiviral vector (LV) for gene therapy to counter HIGM1, we have constructed two self-inactivating LVs, pCD40L-eGFP and pCD40L-CD40L, regulated by a 1.3 kb fragment of the human CD40L proximal promoter. The expression of pCD40L-eGFP LV is restricted to cells in which mRNA transcripts of the endogenous *CD40L* gene can be detected. Moreover, the expression of the reporter gene in primary T lymphocytes depends on the activation state of the cells. Remarkably, primary HIGM1 lymphocytes transduced with pCD40L-CD40L LV expressed CD40L only after T-cell stimulation. Therefore, the CD40L-promoter-driven vectors are able to achieve a near-physiological expression pattern that follows very closely that of the endogenous CD40L gene.
Gene Therapy (2011) **18,** 364–371; doi:10.1038/gt.2010.144; published online 25 November 2010

Keywords: lentiviral vectors; hyper-IgM syndrome; CD40L promoter; activation-inducible vectors; tissue-specific vectors; transcriptional targeting

INTRODUCTION

Gene therapy to counter hematopoietic diseases has met with great success in recent years. Patients suffering from X-linked severe combined immunodeficiency, adenosin-deaminase deficiency, X-linked chronic granulomatous disease and Wiskott–Aldrich syndrome have benefited from the reconstitution of their immune systems by gene therapy (reviewed in the study by Thrasher[1] and Aiuti *et al.*[2]). Nevertheless, some patients have experienced undesired side effects in the form of lymphoproliferation because of integration of the transgene in the vicinity of transcriptionally active areas.[3,4] This severe setback has pointed to the need for improvement in the biosafety of gene therapy and the vectors used.

Several strategies have been devised to achieve this objective. Some authors, for instance, have inserted insulators based on β-globin gene sequences into the vector's backbone to protect promoters from the influence of regulatory elements found in the proximity of the genomic areas where the vectors are inserted.[5,6] Another strategy for improving biosafety has been to encourage tissue-specific expression of the transgene at physiological levels. In fact, the transcriptionally targeted expression of therapeutic genes in the hematopoietic lineage has been achieved by including tissue-specific promoters such as CD19,[7] CD4[8] or WASP[9,10] in the vector. This strategy ultimately aims to overcome the risk of ectopic expression of the transgene if transduced hematopoietic precursors differentiate into non-hematopoietic tissues. Although this issue remains controversial, clear-cut data do exist to indicate that hematopoietic stem cells may differentiate into or fuse with several non-hematopoietic cell types, such as hepatocytes, endothelial, epithelial, neuron or muscle cells.[11–13] Therefore, the expression of transduced hematopoietic genes in non-hematopoietic tissues may result in severe adverse effects. For instance, we have recently shown that the transduction of non-hematopoietic cells with unregulated lentiviral vectors (LV) expressing the protein encoded by the defective gene in the Wiskott–Aldrich syndrome (*WAS*) disrupts the cytoarchitecture and causes significant cytoskeletal abnormalities.[14] We also showed that the transduction of non-hematopoietic cells with a *WAS* complementary (c)DNA in the context of a transcriptionally regulated vector overcomes cytoskeletal defects by preventing the ectopic expression of the protein.[14]

The hurdles faced by gene therapy are even greater in diseases in which the expression of the defective gene is finely regulated. This is true for X-linked hyper-immunoglobulin (Ig) M syndrome (HIGM1), a primary immunodeficiency caused by mutations in the *CD40L* gene.[15,16] CD40L (CD154) is transiently expressed on the surface of activated T cells after antigen engagement of the T-cell receptor complex.[17,18] The molecule has a critical role in the mechanisms of the Ig isotype switch by providing appropriate signals to B cells after interaction with its ligand, the CD40 molecule expressed on B cells.[19] Patients with hyper-IgM also have defects in T-cell functions linked

[1]Institute of Biopathology and Regenerative Medicine, Center for Biomedical Research, University of Granada, Health-Science Technology Park, Armilla, Granada, Spain and [2]Andalucian Stem Cell Bank, Center for Biomedical Research, University of Granada and Andalucian Department of Health, Health-Science Technology Park, Armilla, Granada, Spain
Correspondence: Dr IJ Molina and Dr F Martín, Institute of Biopathology and Regenerative Medicine, Center for Biomedical Research, University of Granada, Health-Science Technology Park, Avda. del Conocimiento s/n, Armilla, Granada, Spain.
E-mail: imolina@ugr.es or francisco.martin.molina@juntadeandalucia.es
[3]These authors share senior authorship.
Received 30 May 2010; revised 4 September 2010; accepted 6 September 2010; published online 25 November 2010

to abnormalities in the maturation of antigen-presenting cells and in the antigen priming of lymphocytes.[20]

As with other immunodeficiencies, hyper-IgM patients show a high mortality rate, commonly due to opportunistic infections.[16] As the overall outcome of patients who undergo bone marrow transplantation is unsatisfactory,[16] we need to explore new therapeutic approaches to cure the disease, and gene therapy appears to be a viable alternative. In fact, attempts to correct the disease by transduction of hematopoietic precursors with unregulated vectors expressing CD40L led to the correction of humoral and cell immune responses.[21] Nevertheless, the majority of reconstituted mice developed a T-lymphoproliferative disorder as a consequence of the unregulated expression of the therapeutic gene in thymic cells.[21] Further complexity was added to CD40–CD40L interactions by the fact that CD40L transgenic mice generated by a construct controlled by a ubiquitous promoter showed severe lymphoid abnormalities.[22] This evidence has hindered further attempts to counter HIGM1 with gene therapy because of the potential risk of the procedure in humans in the absence of a tightly regulated therapeutic approach.

To explore new gene therapy alternatives in the fight against HIGM1 and other diseases that require stringent gene regulation mechanisms, we have constructed two LVs in which transgene expression is controlled by a 1.3 kb fragment of the human CD40L gene promoter. Our results demonstrate that both vectors express the transgene following a pattern that mimics that of the endogenous *CD40L* gene. Furthermore, both vectors obtained transgene expression depending on the activation state of the transduced cells. To our knowledge, this is the first LV capable of achieving tissue-specific, activation-dependent expression. This may be a key development in the treatment of diseases in which fine regulation of the transgene is essential.

RESULTS

A self-inactivating (SIN) LV controlled by a 1.3 kb fragment of the human CD40L promoter follows the expression pattern of the endogenous *CD40L* gene

CD40L is subject to tight regulatory mechanisms that are of critical functional importance,[19] and in fact the adverse effects described in animal models of hyper-IgM gene therapy have been linked to the constitutive expression of the constructs.[21,22] Because of this precedent, we reasoned that a critical requirement for hyper-IgM gene therapy must be the ready availability of tissue-specific, activation-inducible, stringent vectors. We hypothesized that these requirements might be fulfilled by constructing a vector that regulates the expression of the transgene by a fragment of the human CD40L promoter. Figure 1 shows a schematic map of the two SIN LVs controlled by a 1.3 kb fragment of the human CD40L promoter[23]. The resulting plasmid, pCD40L-eGFP, expresses the reporter *eGFP* gene, whereas pCD40L-CD40L is a SIN LV in which the expression of the human *CD40L* gene is controlled by its endogenous promoter.

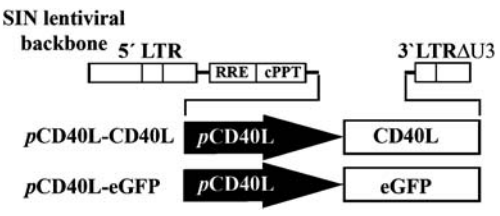

Figure 1 Maps of SIN LV under the control of a CD40L promoter fragment. A 1.3 kb human CD40L proximal promoter sequence was subcloned into a SIN lentiviral backbone to control the expression of either the human CD40L cDNA or the *eGFP* reporter gene.

First, we addressed the ability of the 1.3 kb fragment of the human CD40L promoter to drive a tissue-specific expression of the transgene when incorporated into a SIN LV backbone. Three hematopoietic cell lines (Jurkat, K562 and U937) and two non-hematopoietic lines (293T and Ecv-304) were transduced with the pCD40L-eGFP LV and expression of the reporter transgene was assessed by flow cytometry. The results of a representative experiment are shown in Figure 2a, wherein eGFP expression was observed in Jurkat cells but not in 293T, in spite of an efficient transduction of this cell line, yielding 1.64 vector integrations per cell. A quantitative analysis of pCD40L-eGFP expression levels related to the endogenous expression levels of CD40L mRNA in each cell line is shown in Figure 2b. A correlation between the expression of eGFP (regulated by the pCD40L-eGFP vector) and CD40L (regulated by the endogenous CD40L promoter) can be seen. Thus, the pCD40L-eGFP vector was expressed in cell lines that showed

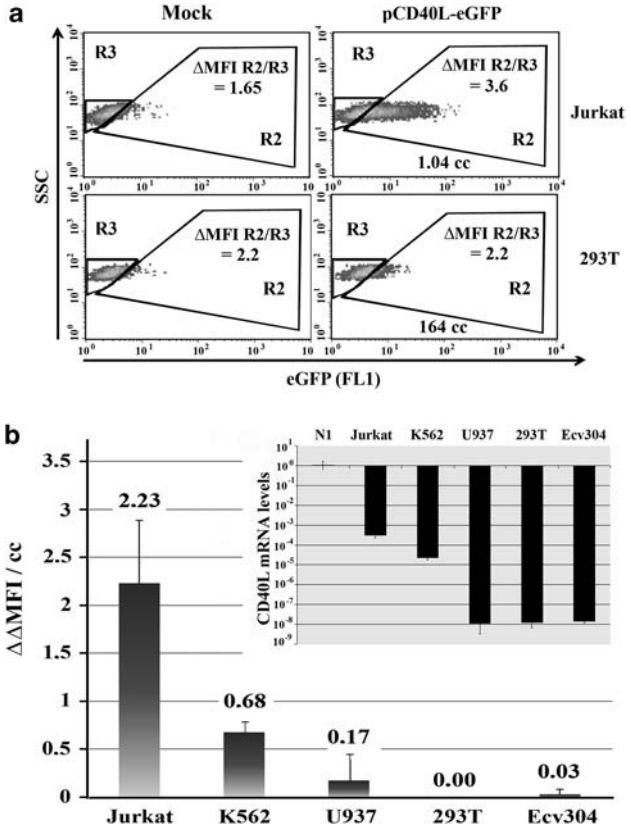

Figure 2 Expression of the pCD40L-eGFP lentiviral vector is restricted to CD40L-expressing cells. A panel of cell lines was transduced with the pCD40L-eGFP lentiviral vector at high multiplicity of infections. Expression of the *eGFP* reporter gene was assessed by flow cytometry and the vector copy number per cell (cc) was estimated by real-time PCR. (**a**) An example of the results obtained for all transduced cells is represented by Jurkat (hematopoietic) and 293T (non-hematopoietic) cell lines. Lentiviral vector expression levels were calculated in terms of the increase in mean fluorescence intensity (MFI) of the expressing cells (R2) over the non-expressing cells (R3) (MFI R2/MFI R3) compared with the vector copy number per cell obtained for each transduced cell line. (**b**) Summary of the pCD40L-eGFP expression levels for the different cell lines analyzed. The expression of endogenous CD40L-mRNA is shown for direct comparison of endogenous CD40L and LV-transgene expression. CD40L expression was detected by quantitative PCR and the values obtained were normalized against the expression levels of N1 cells as follows: Jurkat 10^{-3}; K562 $10^{-4.5}$; U937, 293T and Ecv304 10^{-8} (background levels) and represented in the inset graph. cc: vector copy number per cells.

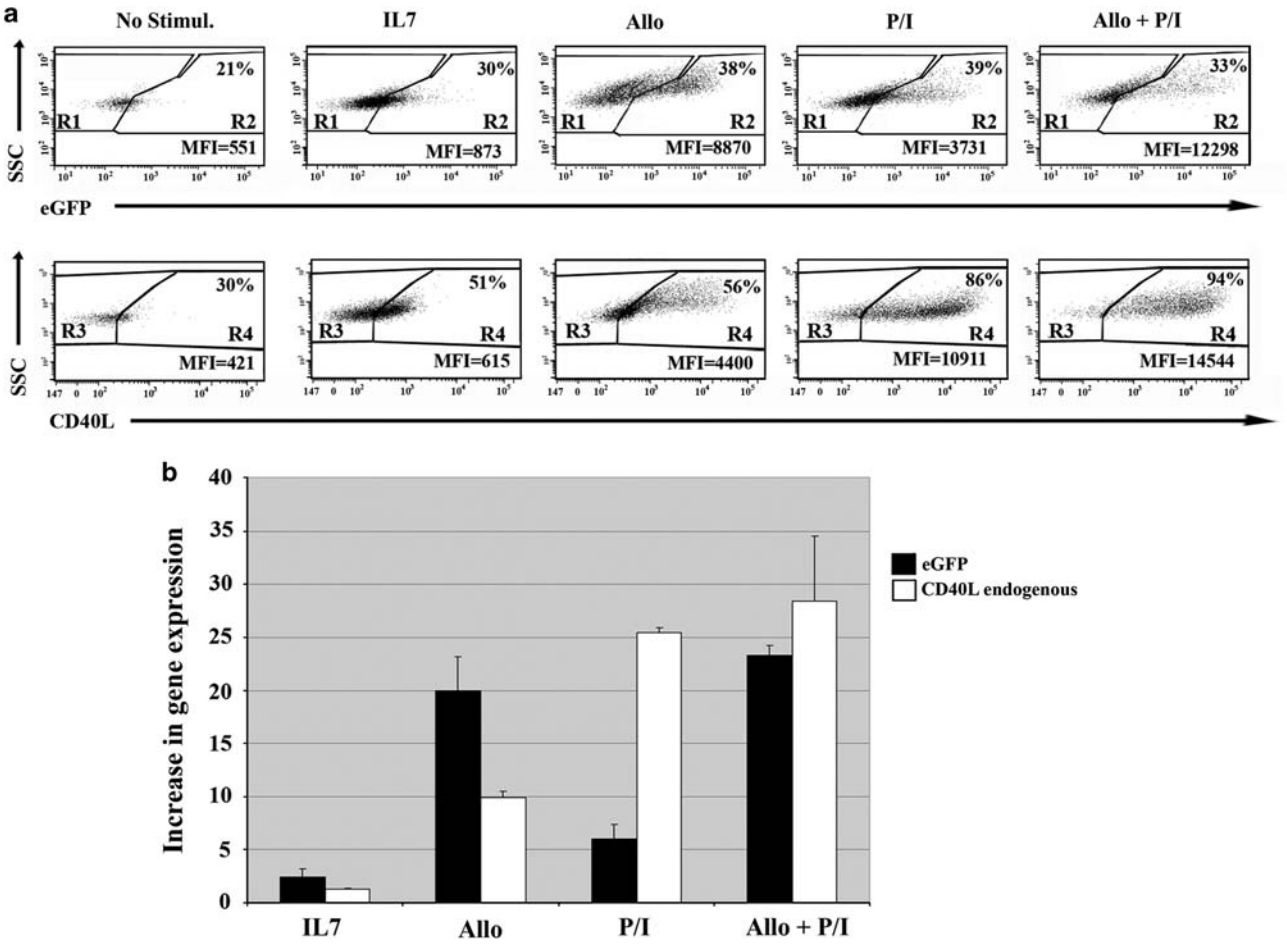

Figure 3 Expression of the pCD40L-eGFP lentiviral vector in primary human lymphocytes is activation dependent. Fresh peripheral lymphocytes from a healthy individual were transduced with the pCD40L-eGFP vector (multiplicity of infection=1) and the following day exposed to different conditions, as described in the Materials and methods section. (**a**) Results of a representative experiment showing eGFP expression levels (top panels) and endogenous CD40L (bottom panels) of transduced cells under different activation conditions: unstimulated cells (No Stimul.); IL-7 (IL7); allostimulation (Allo); PMA+ionomycin (P/I); and a combination of allostimulation and P/I (Allo+P/I). Mean fluorescence intensity (MFI) values and percentage of positive cells are indicated within the relevant gated regions. (**b**) Graph showing the relative expression levels of eGFP (solid bars) and endogenous CD40L (open bars) in pCD40L-eGFP-transduced lymphocytes under the different activation conditions. The relative expression values of eGFP and endogenous CD40L were obtained by dividing the MFI value obtained for each group of cells by the MFI value of unstimulated cells.

CD40L mRNA by quantitative PCR. The expression levels of endogenous CD40L in Jurkat cells compared with those of N1 cells were 10^{-3} and $10^{-4.5}$ for K562, as detected by a quantitative PCR (Figure 2b, inset). No expression of the construct was to be found in CD40L-negative non-hematopoietic cells 293T and Ecv-304, even after phorbol 12-myristate 13-acetate (PMA) stimulation (data not shown). Although the hematopoietic cell line U937 showed no detectable amounts of endogenous CD40L, with or without stimulation with PMA, a minimal expression of the transgene was obtained (Figure 2b).

The expression of LVs controlled by the CD40L promoter is activation dependent

The characteristics of the CD40L promoter fragment that governs the pCD40L-eGFP vector were further investigated in fresh peripheral lymphocytes. It was of interest to determine whether pCD40L was able to drive the expression of the transgene following the same expression pattern as the endogenous *CD40L* gene on different types of stimulation. We found that neither unstimulated nor interleukin (IL) 7-treated primary cells expressed significant levels of CD40L or the eGFP reporter gene (Figure 3a, left-hand panels). Interestingly, a highly fluorescent population was detected after allostimulation of eGFP-transduced cells (Figure 3a, upper-row panels; Allo), which mimicked the increase in surface CD40L observed in the same population (Figure 3a, lower-row panels; Allo). Although stimulation of transduced lymphocytes with PMA+ionomycin yielded a similar percentage of eGFP-positive cells as that obtained by allostimulation (Figure 3a, upper row; P/I), the level of transgene expression, as detected by the increase in fluorescence intensity, was significantly lower (Figure 3b, solid bars). The highest endogenous expression of CD40L was achieved, however, when cells were treated with PMA+ionomycin but not by allostimulation (Figure 3a, lower-row panels and Figure 3b). Therefore, it would appear that the pCD40L-eGFP vector functions as the endogenous CD40L promoter in the absence of stimuli, in the presence of IL7 and on allostimulation, whereas response to stronger signals such as PMA+ionomycin diminishes.

Characterization of an activation-dependent therapeutic vector for HIGM1

The ability of the pCD40L promoter contained in the pCD40L-eGFP vector to drive a tissue-specific, inducible expression of the reporter

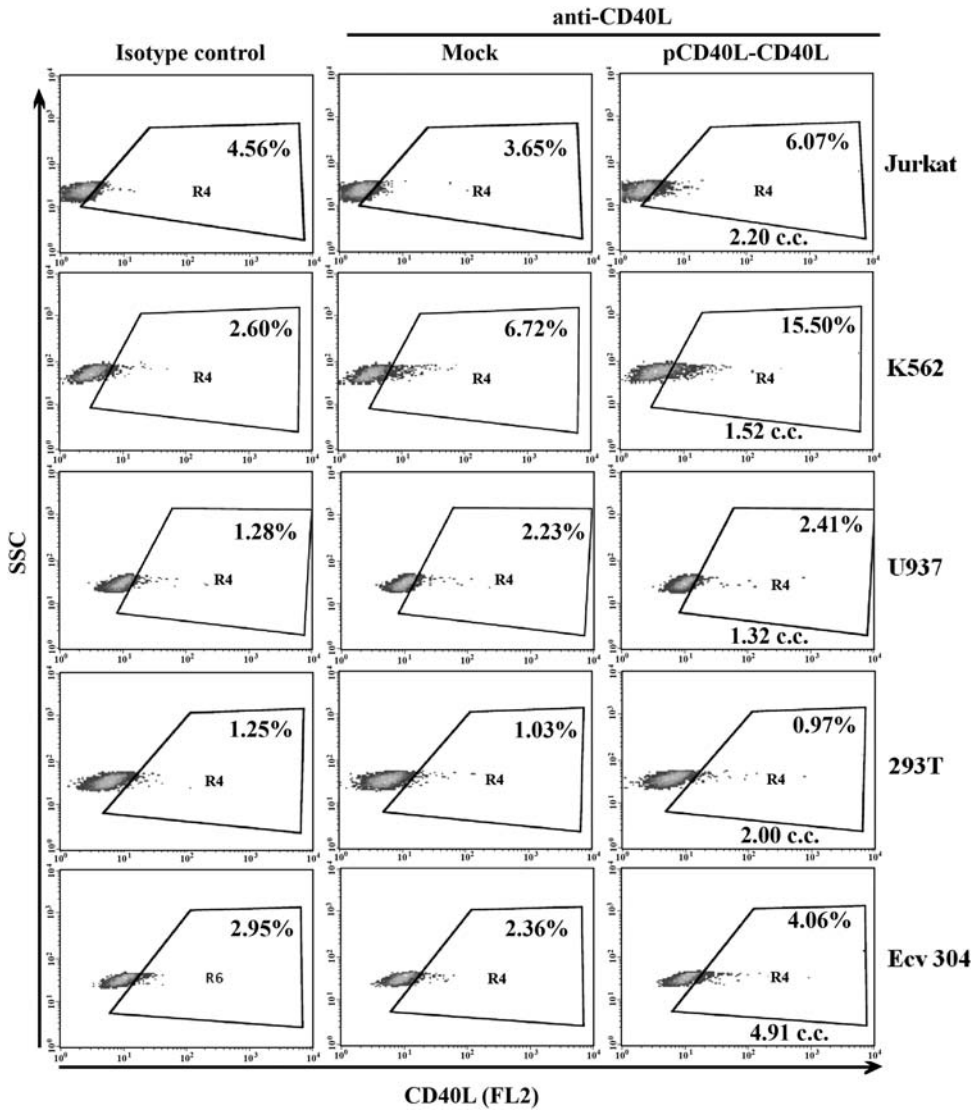

Figure 4 pCD40L-CD40L LV is weakly expressed or undetectable in unstimulated hematopoietic and non-hematopoietic cell lines. The pCD40L-CD40L lentiviral vector was used to transduce three hematopoietic (Jurkat, K562 and U937) and two non-hematopoietic (293T and Ecv304) cell lines. Mock-transduced cells (central panels) and pCD40L-CD40L-transduced cells (right-hand panels) were stained with the 24–31 anti-CD40L monoclonal antibody and analyzed by flow cytometry. Cells stained with an isotype-matched irrelevant monoclonal antibody are shown in the left-hand panels. cc: vector copy number per cell.

gene prompted us to develop a potentially therapeutic vector for HIGM1. The resulting SIN LV controls the expression of CD40L by a 1.3 kb fragment of the human promoter. The CD40L-negative Jurkat T cells were transduced with the pCD40L-CD40L LV in parallel to K562, U937, 293T and Ecv304 cells. We found no significant expression of the transgene in any of the cell lines tested, despite the efficient integration of the vector as determined by real-time PCR, with the exception of a small percentage of Jurkat and K562 cells (Figure 4, right-hand panels).

As untreated Jurkat cells transduced with the pCD40L-CD40L vector showed a minimal expression of CD40L, we investigated whether PMA+ionomycin stimulation of transduced cells led to the surface expression of the CD40L transgene. Stimulation of CD40L-negative Jurkat variant cells led to only a small net increase of 4.45% in CD40L surface expression (Figure 5, top panels). Interestingly, stimulation of pCD40L-CD40L-transduced Jurkat cells resulted in a higher increase (8.8%) in the percentage of cells expressing CD40L after stimulation, (Figure 5, bottom panels) as a result of CD40L transgene expression. We determined by quantitative PCR that the stimulation of transduced Jurkat cells with PMA resulted in a twofold increase in endogenous CD40L mRNA levels (data not shown).

To confirm these results and to address the physiological expression pattern of the construct in primary cells, we generated primary long-term allospecific $CD4^+$ T-cell lines from two HIGM1 patients harboring different mutations in the *CD40L* gene. The cells were transduced with pCD40L-CD40L LV and the expression of CD40L was determined under different conditions. Untransduced cells from a normal individual expressed CD40L on activation (Figure 6, top panels), whereas a cell line derived from an HIGM1 patient, PH3, failed to express surface CD40L after treatment with PMA+ionomycin (Figure 6, central-row panels). Interestingly, we were able to rescue activation-dependent CD40L expression in PH3 cells transduced with

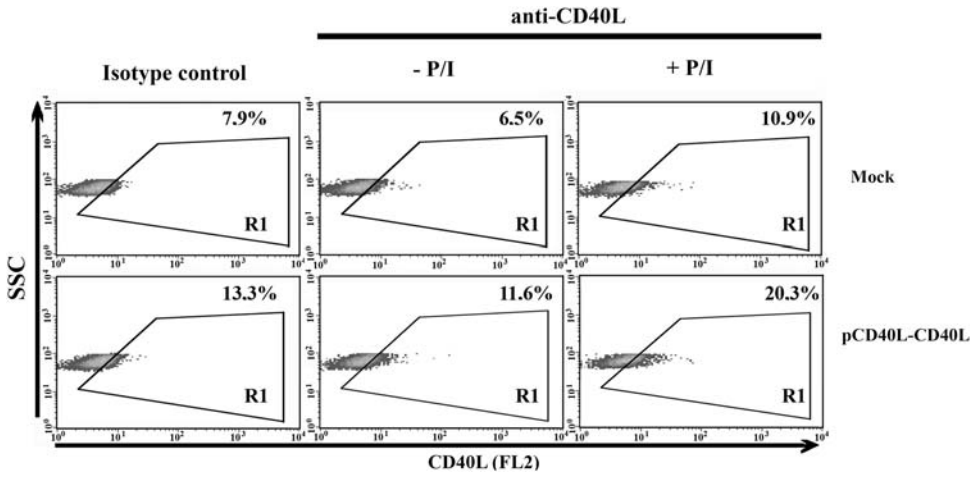

Figure 5 Jurkat cells transduced with pCD40L-CD40L LV express the CD40L molecule at their surface after stimulation. The CD40L-negative variant Jurkat cells were transduced with the pCD40L-CD40L vector and expression of the molecule was analyzed 7 days after transduction. Unstimulated cells (central panels) and cells stimulated overnight with PMA+ionomycin (right-hand panels) were stained with the anti-CD40L monoclonal antibody and analyzed by flow cytometry. Cells stained with an isotype-matched irrelevant antibody are shown in the left-hand panels. The percentage of cells contained within the R1 region is indicated in each panel. A significant increase in CD40L expression is detected in pCD40L-CD40L-transduced Jurkat cells after stimulation.

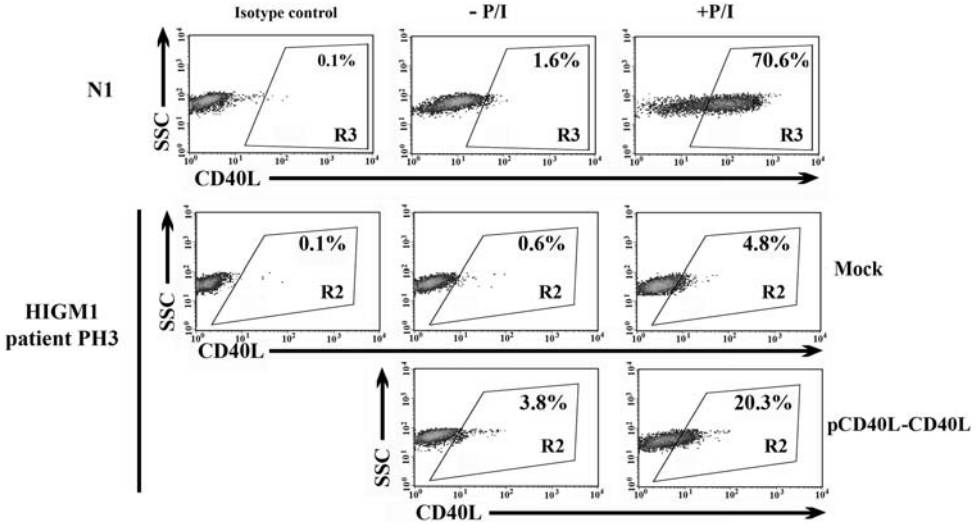

Figure 6 Primary T cells from a patient with HIGM1 transduced with the pCD40L-CD40L vector express the transgene only after stimulation. Long-term allospecific cells obtained from HIGM1 patient PH3 (harboring a Q174R mutation in the *CD40L* gene) were mock-transduced (middle-row panels) or transduced with the pCD40L-CD40L lentiviral vector (bottom-row panels). Surface expression of CD40L was studied 14 days after allostimulation (−P/I) and after 18 h of PMA+ionomycin treatment (+P/I). The surface expression of CD40L on allospecific cells from a normal individual (N1) is shown in the top-row panels. Results from staining cells with an isotype-matched irrelevant antibody are shown in the left-hand panels. The percentage of cells contained within the gated regions is indicated in each of the panels.

pCD40L-CD40L LV (Figure 6, bottom panels). Similar results were obtained with transduced cells obtained from HIGM1 patient PH2, who has an IVS3+5g/a mutation (data not shown).

To further characterize the expression pattern of CD40L on PH3 cells transduced with the pCD40L-CD40L therapeutic vector, transduced cells that had been allostimulated 14 days earlier, and thus were at near-resting state, were cocultured with Raji cells. The surface expression of CD40L was assessed at days 1, 3 and 5 after allostimulation. N1 cells revealed a vigorous expression of surface CD40L, which peaked at day 3 and fell significantly by day 5 (Figure 7, top panels). Untransduced cells from patient PH3 showed a leaky expression of CD40L, which reached a maximum on day 3 and subsequently decreased by day 5 (Figure 7, middle-row panels). Remarkably, PH3 cells transduced with the pCD40L-CD40L vector showed a similar expression pattern to that of normal cells. Thus, the surface expression of CD40L was not only higher on transduced cells compared with their untransduced counterparts (Figure 7, bottom panels) but also the maximum level of expression reached on day 3 after allospecific stimulation fell rapidly by day 5 to the levels obtained in unstimulated cells. Similar results were obtained on stimulation of cells with anti-CD3/CD28-coated immunobeads (data not shown).

DISCUSSION

The need to develop safer approaches for gene therapy became evident after the severe adverse effects observed in two human clinical trials of a primary immunodeficiency.[3,4] Other results obtained in animal

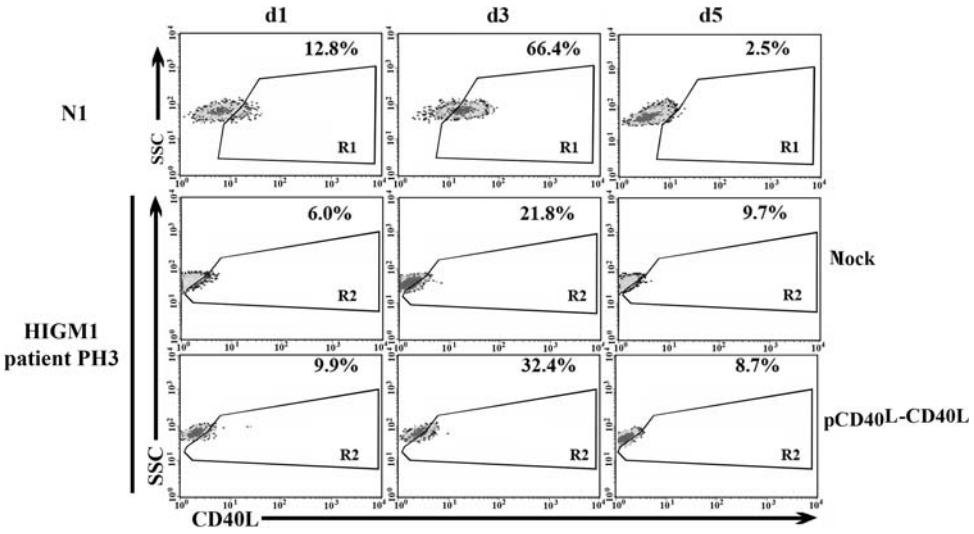

Figure 7 The activation-dependent CD40L expression of HIGM1 cells transduced with the pCD40L-CD40L vector reverts in resting cells. Resting long-term allospecific cells (14 days post stimulation) from a normal individual (N1; top panels) and from HIGM1 patient PH3 untransduced (middle panels) or transduced with pCD40L-CD40L (bottom panels) were cocultured with Raji cells and the expression of CD40L was assessed 1 day (left-hand panels), 3 days (central panels) and 5 days (right-hand panels) from the day of stimulation. Gate regions R1 (N1) and R2 (PH3) were drawn over the results obtained with cells stained with an isotype-matched control.

models are consistent with the dangers associated with the unregulated expression of therapeutic transgenes, as has been demonstrated in mouse models of hyper-IgM syndrome.[21,22]

We have designed an LV that regulates the transcription of the transgene by a 1.3 kb fragment of the human CD40 L promoter, which includes all transcriptionally active sequences present in this DNA fragment. In particular, we have included the four NF-AT binding motifs that appear to be critically important for optimum mRNA production.[23,24] This fragment also contains potential sites for binding Egr, Stat, AKNA, nuclear factor-κB and a CD28 response element.[24] Studies previous to ours had also demonstrated that the 1.3 kb proximal promoter was transcriptionally active in primary $CD4^+$ T cells, as demonstrated by the luciferase assay.[25]

We therefore assumed that this 1.3 kb proximal promoter sequence would retain the ability to drive gene transcription in a lentiviral setting, and this led us to construct the pCD40L-eGFP LV. Our results show that this vector achieves efficient expression of the reporter gene, with two important features: first, that the eGFP expression regulated by the pCD40L promoter fragment is restricted to cells in which constitutive transcripts of the endogenous CD40L mRNA are detected, thereby fulfilling the tissue-specificity requirement; second, that the expression of the reporter gene in transduced primary lymphocytes depends on cell stimulation, the other significant hurdle in the path toward safer gene therapy protocols.

The response of the promoter element of the pCD40L-eGFP vector is, however, slightly different from that of the endogenous CD40L promoter. In particular, we found that the increase in gene expression when transduced cells were treated with PMA+ionomycin was significantly lower with the vector than it was with endogenous CD40L (Figure 3b). When interpreting these results, we have to take several facts into consideration. For example, the presence of a T-cell-specific transcriptional enhancer rich in GATA and NFAT proteins has recently been discovered. This enhancer functions as a CD4-specific hypersensitivity site located upstream of the promoter sequences included in our promoter fragment[26] and is therefore not present in our construct. A second T-cell-specific nuclear factor-κB/Rel enhancer has been located in a 1284 bp region 3′ flanking the CD40L gene,[25] a region that was not included in our vector either. This enhancer element is particularly sensitive to PMA+ionomycin stimulation.[25] Finally, it has also been found that the CD40L 3′ region is important for the regulation of CD40L expression, as it controls mRNA stability during T-cell activation.[27] It remains to be determined whether the presence of any of the above-mentioned elements would have had a significant impact on the behavior of the promoter fragment or on the stability of the transgene mRNA.

As the 1.3 CD40L promoter fragment fulfilled our two biosafety requirements (tissue specificity and activation-dependent expression), we went on to study the ability of this promoter to regulate the expression of a potential therapeutic vector for HIGM1. The pCD40L-CD40L vector efficiently transduced a number of hematopoietic and non-hematopoietic cells, as determined by assessing the number of vector integrations by real-time PCR. Once more, the expression of the CD40L transgene remained restricted to stimulated cells in which endogenous CD40L mRNA transcripts were detected, such as our $CD40L^-$ Jurkat variant cells. These results were further confirmed in an *in vitro* model of HIGM1, that is, long-term allospecific T-cell lines from patients with HIGM1. The patients' cells were efficiently transduced by the pCD40L-CD40L vector, which achieved significant expression of the therapeutic gene. Most importantly, transgene expression was strictly dependent on cell activation, as transduced resting cells from two HIGM1 patients did not express any detectable surface CD40L, a molecule that was readily detected on cells from both patients after stimulation. It is noteworthy that the expression pattern of transduced cells stimulated with alloantigen or anti-CD3/CD28-coated immunobeads followed that of their normal counterparts. One critical feature of the pCD40L-CD40L vector is that not only does its triggering of the expression of CD40L depend strictly on stimulation but this expression also diminishes as the cells return to their resting state.

As mentioned in the Introduction section, attempts to develop gene therapy protocols for HIGM1 using constitutive vectors have in the past caused lymphoproliferative disease in thymic cells.[21,22] These adverse effects are, however, related to the unregulated expression of

the therapeutic protein and are not due to insertional mutagenesis. An elegant study in CD40L-deficient mice showed that a trans-splicing repair strategy was able to correct the mutant gene and allowed expression of the protein under the control of endogenous regulatory mechanisms.[28] Under these conditions, none of the treated mice developed lymphoproliferation, whereas they all showed an improvement in the hallmark symptoms of the immunodeficiency. Unfortunately, the implementation of gene therapy in humans based on trans-splicing approaches is not feasible because of their technical complexity and low efficiency.

Gene therapy for HIGM1 is therefore a sound therapeutic alternative, provided that the therapeutic transgene is delivered efficiently in a tightly regulated setting. Our pCD40L-CD40L vector has proved that it can fulfill the requirements for tissue specificity and activation-dependent expression. Furthermore, we have found that the expression of the therapeutic protein in transduced cells is abolished as the cells progress toward a resting state, a fact that is of critical importance in the avoidance of adverse thymic effects,[21] as it is known that overexpression of CD40L disrupts normal thymic organization.[29] To our knowledge, the vectors described in this work are the first tissue-specific, activation-inducible LVs and we believe that they represent a significant step forward in the application of gene therapy to diseases with stringent regulatory requirements, such as HIGM1. Nevertheless, it remains to be determined whether the pCD40L-CD40L vector is able to rescue the functional defects of HIGM1 cells and, in particular, whether CD40L-deficient mice reconstituted with this vector suffer from the lymphoproliferative syndrome observed after reconstitution with constitutive vectors. We are currently conducting experiments to ascertain the true therapeutic potential of this vector.

MATERIALS AND METHODS

Cell lines and culture media

Primary allospecific T-cell lines from healthy individuals and from two patients with HIMG1 were generated and maintained, as described elsewhere,[30] in Panserin medium (PAN Biotech, Aidenbach, Germany) supplemented with 5% human serum, glutamax, penicillin/streptomycin and 50 UI ml^{-1} of recombinant human IL-2 (kindly supplied by the National Institute of Health's AIDS reagent program, Rockville, MD, USA). Patient PH2 has a confirmed IVS3+5 g/a mutation, whereas patient PH3 has a Q174R mutation. The following cell lines, Jurkat (T-cell acute leukemia), K562 (chronic myelogenous leukemia), U937 (promyelocytic leukemia) and Ecv 304 (bladder carcinoma), were cultured in RPMI 1640 (Bio-Whittaker, Verviers, Belgium) supplemented with 10% fetal calf serum (FCS), glutamine and antibiotics as described above, and 293T (human embryonic kidney) was cultured in Dulbecco's modied Eagle's medium (Gibco-Invitrogen, Carlsbad, CA, USA). The Jurkat cell line used throughout this study is a serendipitous variant that is CD40L negative at surface level but expresses CD40L mRNA, as detected by reverse transcriptase-PCR.

Construction of plasmids and lentiviral vectors

The human immunodeficiency virus packaging (pCMVDR8.91), which encodes *gag*, *pol*, *tat* and *rev* genes, and the vesicular stomatitis virus-G envelope (pMD.G) plasmids were kindly provided by Dr D Trono (University of Geneva, Switzerland). The full-length *CD40L* cDNA was amplified by reverse transcriptase-PCR from stimulated T lymphocytes from a healthy individual using high-fidelity Pfu DNA polymerase (Promega, Madison, WI, USA) with the primers forward-CD40L (5′-CATTTCAACTTTAACACAGC-3′) and reverse-CD40L (5′-AGCTCCACCACAGCCTGC-3′), which yield an 837 bp cDNA. PCR conditions were 1×(95 °C, 2 min); 35×(94 °C, 30 s/50 °C, 1 min/72 °C, 3 min); 1×(72 °C 10 min). The cDNA obtained was subcloned into the plasmid pCRII-Blunt-TOPO (Invitrogen) and sequenced to confirm DNA amplification.

To construct the pCD40L-CD40L LV, we first generated the S-CD40L plasmid as an intermediate construct by excising the eGFP and WPRE elements present in the pHR' SIN cppt–SEW lentiviral plasmid[31] by BmaHI-XhoI digestion and then subcloning the CD40L cDNA. The resulting plasmid was further digested with BamHI-ClaI to eliminate the SFFV constitutive promoter, which was replaced by a fragment of the human CD40L promoter, spanning 1.3 kb upstream of the initiation codon[32] (GENEART, Regensburg, Germany).

The CD40L-eGFP plasmid was constructed by replacing the BamHI-XhoI fragment of the pCD40L-CD40L vector containing CD40L cDNA with the BamHI-XhoI fragment of the pHR' SIN cppt–SE containing eGFP cDNA.

Vector production

LVs were produced by co-transfecting exponentially growing 293T cells with vector plasmid, either *pCD40L*-CD40L or *pCD40L*-GFP, the packaging plasmid pCMVDR8.91 and the envelope plasmid pMD.G, as described elsewhere (27 μg total DNA; plasmid proportions of 3:2:1, respectively).[9] Briefly, 80% confluent cells were resuspended in 1.5 ml of OPTI-MEM media (Gibco) and mixed at room temperature for 20 min with 60 μl of Lipofectamine 2000 (Invitrogen) and then diluted in 1.5 ml of OPTI-MEM. The plasmid–Lipofectamine mixture was added to prewashed cells and incubated for 6–8 h at 37 °C and 10% CO_2. The producer cells were then washed and cultured for a further 48 h in 8 ml of OPTI-MEM medium. Viral supernatants were collected and filtered through a 0.45 μm filter (Nalgene, Rochester, NY, USA), aliquoted and immediately frozen at −80 °C.

Cell transduction and stimulation

Before the lentiviral transduction of cell lines, 10^5 cells per well were seeded in 24-well plates in 300 μl of medium and the viral supernatants were then added in serial dilution for 8 h. The medium was replaced and the cells were cultured for a further 5 days before being collected and analyzed for CD40L or eGFP expression by flow cytometry in a FACScan flow cytometer (Becton-Dickinson, San Jose, CA, USA). Fresh peripheral lymphocytes from a normal individual were isolated by Ficoll–Hypaque gradient centrifugation and maintained overnight in RPMI complete medium in the presence of 10 ng ml^{-1} of rIL-7. The cells were pooled in one well of a six-well plate and transduced overnight in the presence of rIL-7. The next day they were washed to remove rIL-7 and divided into the following groups: unstimulated cells kept in complete medium (which includes IL-2); cells kept in complete medium plus 10 ng ml^{-1} of IL-7; and cells allostimulated as indicated above. On day 6, aliquots of the unstimulated cells were cultured overnight with 5 ng ml^{-1} of PMA (Sigma, St Louis, MO, USA) and 0.5 μg ml^{-1} of ionomycin. Another aliquot of allostimulated cells was treated in a similar way with PMA+ionomycin. On day 7, after transduction the expression of the *eGFP* reporter gene or CD40L was determined by flow cytometry as indicated below.

DNA extraction and calculation of vector copy numbers by quantitative PCR

For genomic DNA extraction, cells were resuspended in Tris HCl 20 mM (pH 8), EDTA 5 mM (pH 8), NaCl 400 mM, 1% sodium dodecyl sulfate and proteinase K (100 μg ml^{-1}) and then incubated overnight at 55 °C with continuous shaking. Proteinase K was inactivated at 95 °C and RNase (5 μg μl^{-1}) was then added for 30 min at 60 °C, followed by phenol:chloroform:isoamyl-alcohol extraction. DNA was finally precipitated with absolute ethanol.

Real-time PCRs were performed in a thermocycler ABI Prism 7000 PCR Detection System (Applied Biosystem, Foster City, CA, USA) using iQ SYBR Green Supermix (BioRad, Hercules, CA, USA). The vector copy number was determined by amplification of a 127 bp fragment from cDNA encompassing exons 2 and 3 from the *CD40L* gene. The primers were F-Exon2-CD40L (5′-GATACAGAGATGCAACACAGGA-3′) and R-Exon3-CD40L (5′-GCTGTTTTCTTTCTTCGTCTCC-3′). The parameters for the PCR were 1×(95 °C, 2 min) and 40×(95 °C, 20 s/55 °C, 30 s/72 °C, 30 s).

The vector copy number per cell in eGFP vectors was determined by amplification of the *eGFP* gene using primers F-GFP (5′-GCCCGACAACCACTACCT-3′) and R-GFP (5′-CGTCCATGCCGAGAGTGA-3′). The parameters for the PCR were 1×(95 °C, 2 min); 40×(95 °C, 15 s/63 °C, 30 s/72 °C, 30 s); 1×(72 °C, 2 min). The number of vector copies per cell was calculated by

interpolating the results in a standard curve constructed with 10-fold-increasing quantities of plasmid DNA (S-CD40L or pCD40L-GFP plasmids). Quantitative analysis of CD40L mRNA was carried out by retrotranscription of total RNA of the cell lines, followed by amplification using primers F-exon –CD40L (5′-CCAGGGTTACCAAGTTGTTGCTCA-3′) and R-exon –CD40L (5′-GCGG CACATGTCATAAGTGAGGC-3′). Amplification conditions were 1×(50 °C, 2 min); 1×(95 °C, 10 min); 40×(95 °C, 15 s; 60 °C, 1 min); and 1×(95 °C, 15 s).

Immunostaining and flow cytometry

Transduced cells were collected 7 days after transduction, unless otherwise indicated, washed, blocked and stained with the anti-CD40L monoclonal antibody 24–31 (Calbiochem, Darmstadt, Germany), followed by a phycoerythrin-labeled goat antimouse IgG antibody (Caltag Laboratories, Burlingame, CA, USA). For double fluorescence experiments, an allophycocyanine-labeled second antibody was used (BD-Pharmingen, San Diego, CA, USA). Cells transduced with the pCD40L-eGFP vector were washed and analyzed on a BD FACSCanto II flow cytometer (Becton Dickinson, San Jose, CA, USA).

CONFLICT OF INTEREST

The authors declare no conflict of interest.

ACKNOWLEDGEMENTS

We are grateful to Dr Maria Cruz Garcia (La Paz University Hospital, Madrid, Spain), Dr Jorge Gómez-Sirvent (N.S. Candelaria University Hospital, Tenerife, Spain) and to Dr Graham Davies (Great Ormond Street Hospital London, UK) for their invaluable help in providing blood samples from their patients. We thank our colleague, Dr J Trout, for revising the English text. We acknowledge the continuous and generous supply of rIL-2 provided by the National Institutes of Health AIDS Research and Reference Reagent Program (Rockville, MD, USA). This work was supported by grants SAF2009/09818 (to IJM) and PS09/00340 (to FM) from the Spanish Ministry for Science and Innovation and P06-CTS-02112 from the Department of Innovation and Science, Regional Government of Andalusia (to IJM).

1 Thrasher AJ. Gene therapy for primary immunodeficiencies. *Immunol Allergy Clin North Am* 2008; **28**: 457–471, xi.
2 Aiuti A, Roncarolo MG. Ten years of gene therapy for primary immune deficiencies. *Hematology Am Soc Hematol Educ Program* 2009: 682–689.
3 Hacein-Bey-Abina S, Von Kalle C, Schmidt M, McCormack MP, Wulffraat N, Leboulch P *et al.* LMO2-associated clonal T cell proliferation in two patients after gene therapy for SCID-X1. *Science* 2003; **302**: 415–419.
4 Howe SJ, Mansour MR, Schwarzwaelder K, Bartholomae C, Hubank M, Kempski H *et al.* Insertional mutagenesis combined with acquired somatic mutations causes leukemogenesis following gene therapy of SCID-X1 patients. *J Clin Invest* 2008; **118**: 3143–3150.
5 Prioleau MN, Nony P, Simpson M, Felsenfeld G. An insulator element and condensed chromatin region separate the chicken beta-globin locus from an independently regulated erythroid-specific folate receptor gene. *EMBO J* 1999; **18**: 4035–4048.
6 Rincon-Arano H, Furlan-Magaril M, Recillas-Targa F. Protection against telomeric position effects by the chicken cHS4 beta-globin insulator. *Proc Natl Acad Sci USA* 2007; **104**: 14044–14049.
7 Werner M, Kraunus J, Baum C, Brocker T. B-cell-specific transgene expression using a self-inactivating retroviral vector with human CD19 promoter and viral post-transcriptional regulatory element. *Gene Ther* 2004; **11**: 992–1000.
8 Marodon G, Mouly E, Blair EJ, Frisen C, Lemoine FM, Klatzmann D. Specific transgene expression in human and mouse CD4+ cells using lentiviral vectors with regulatory sequences from the CD4 gene. *Blood* 2003; **101**: 3416–3423.
9 Martin F, Toscano MG, Blundell M, Frecha C, Srivastava GK, Santamaria M *et al.* Lentiviral vectors transcriptionally targeted to hematopoietic cells by WASP gene proximal promoter sequences. *Gene Ther* 2005; **12**: 715–723.
10 Frecha C, Toscano MG, Costa C, Saez-Lara MJ, Cosset FL, Verhoeyen E *et al.* Improved lentiviral vectors for Wiskott-Aldrich syndrome gene therapy mimic endogenous expression profiles throughout haematopoiesis. *Gene Ther* 2008; **15**: 930–941.
11 Lagasse E, Connors H, Al Dhalimy M, Reitsma M, Dohse M, Osborne L *et al.* Purified hematopoietic stem cells can differentiate into hepatocytes *in vivo*. *Nat Med* 2000; **6**: 1229–1234.
12 Camargo FD, Green R, Capetanaki Y, Jackson KA, Goodell MA. Single hematopoietic stem cells generate skeletal muscle through myeloid intermediates. *Nat Med* 2003; **9**: 1520–1527.
13 Jang YY, Collector MI, Baylin SB, Diehl AM, Sharkis SJ. Hematopoietic stem cells convert into liver cells within days without fusion. *Nat Cell Biol* 2004; **6**: 532–539.
14 Toscano MG, Frecha C, Benabdellah K, Cobo M, Blundell M, Thrasher AJ *et al.* Hematopoietic-specific lentiviral vectors circumvent cellular toxicity due to ectopic expression of Wiskott-Aldrich syndrome protein. *Hum Gene Ther* 2008; **19**: 179–197.
15 Fuleihan R, Ramesh N, Loh R, Jabara H, Rosen RS, Chatila T *et al.* Defective expression of the CD40 ligand in X chromosome-linked immunoglobulin deficiency with normal or elevated IgM. *Proc Natl Acad Sci USA* 1993; **90**: 2170–2173.
16 Winkelstein JA, Marino MC, Ochs H, Fuleihan R, Scholl PR, Geha R *et al.* The X-linked hyper-IgM syndrome: clinical and immunologic features of 79 patients. *Medicine (Baltimore)* 2003; **82**: 373–384.
17 Lane P, Traunecker A, Hubele S, Inui S, Lanzavecchia A, Gray D. Activated human T cells express a ligand for the human B cell-associated antigen CD40 which participates in T cell-dependent activation of B lymphocytes. *Eur J Immunol* 1992; **22**: 2573–2578.
18 Castle BE, Kishimoto K, Stearns C, Brown ML, Kehry MR. Regulation of expression of the ligand for CD40 on T helper lymphocytes. *J Immunol* 1993; **151**: 1777–1788.
19 Foy TM, Aruffo A, Bajorath J, Buhlmann JE, Noelle RJ. Immune regulation by CD40 and its ligand GP39. *Annu Rev Immunol* 1996; **14**: 591–617.
20 Jain A, Atkinson TP, Lipsky PE, Slater JE, Nelson DL, Strober W. Defects of T-cell effector function and post-thymic maturation in X-linked hyper-IgM syndrome. *J Clin Invest* 1999; **103**: 1151–1158.
21 Brown MP, Topham DJ, Sangster MY, Zhao J, Flynn KJ, Surman SL *et al.* Thymic lymphoproliferative disease after successful correction of CD40 ligand deficiency by gene transfer in mice. *Nat Med* 1998; **4**: 1253–1260.
22 Sacco MG, Ungari M, Cato EM, Villa A, Strina D, Notarangelo LD *et al.* Lymphoid abnormalities in CD40 ligand transgenic mice suggest the need for tight regulation in gene therapy approaches to hyper immunoglobulin M (IgM) syndrome. *Cancer Gene Ther* 2000; **7**: 1299–1306.
23 Tsytsykova AV, Tsitsikov EN, Geha RS. The CD40L promoter contains nuclear factor of activated T cells-binding motifs which require AP-1 binding for activation of transcription. *J Biol Chem* 1996; **271**: 3763–3770.
24 Cron RQ. CD154 transcriptional regulation in primary human CD4T cells. *Immunol Res* 2003; **27**: 185–202.
25 Schubert LA, Cron RQ, Cleary AM, Brunner M, Song A, Lu LS *et al.* A T cell-specific enhancer of the human CD40 ligand gene. *J Biol Chem* 2002; **277**: 7386–7395.
26 Brunner M, Zhang M, Genin A, Ho IC, Cron RQ A. T-cell-specific CD154 transcriptional enhancer located just upstream of the promoter. *Genes Immun* 2008; **9**: 640–649.
27 Ford GS, Barnhart B, Shone S, Covey LR. Regulation of CD154 (CD40 ligand) mRNA stability during T cell activation. *J Immunol* 1999; **162**: 4037–4044.
28 Tahara M, Pergolizzi RG, Kobayashi H, Krause A, Luettich K, Lesser ML *et al.* Trans-splicing repair of CD40 ligand deficiency results in naturally regulated correction of a mouse model of hyper-IgM X-linked immunodeficiency. *Nat Med* 2004; **10**: 835–841.
29 Dunn RJ, Luedecker CJ, Haugen HS, Clegg CH, Farr AG. Thymic overexpression of CD40 ligand disrupts normal thymic epithelial organization. *J Histochem Cytochem* 1997; **45**: 129–141.
30 Molina IJ, Kenney DM, Rosen FS, Remold-O'Donnell E. T cell lines characterize events in the pathogenesis of the Wiskott-Aldrich syndrome. *J Exp Med* 1992; **176**: 867–874.
31 Demaison C, Parsley K, Brouns G, Scherr M, Battmer K, Kinnon C *et al.* High-level transduction and gene expression in hematopoietic repopulating cells using a human immunodeficiency virus type 1-based lentiviral vector containing an internal spleen focus forming virus promoter. *Hum Gene Ther* 2002; **13**: 803–813.
32 Schubert LA, King G, Cron RQ, Lewis DB, Aruffo A, Hollenbaugh D. The human gp39 promoter. Two distinct nuclear factors of activated T cell protein-binding elements contribute independently to transcriptional activation. *J Biol Chem* 1995; **270**: 29624–29627.

OPEN ACCESS Freely available online

PLoS one

Development of an All-in-One Lentiviral Vector System Based on the Original *TetR* for the Easy Generation of Tet-ON Cell Lines

Karim Benabdellah¤, Marién Cobo¤, Pilar Muñoz¤, Miguel G. Toscano¤, Francisco Martin*¤

Andalusian Stem Cell Bank, Centro de Investigaciones Biomédicas, Universidad de Granada, Parque Tecnológico Ciencias de la Salud, Granada, Spain

Abstract

Lentiviral vectors (LVs) are considered one of the most promising vehicles to efficiently deliver genetic information for basic research and gene therapy approaches. Combining LVs with drug-inducible expression systems should allow tight control of transgene expression with minimal side effect on relevant target cells. A new doxycycline-regulated system based on the original *TetR* repressor was developed in 1998 as an alternative to the *TetR-VP16* chimeras (*tTA* and *rtTA*) to avoid secondary effects due to the expression of transactivator domains. However, previously described *TetR*-based systems required cell cloning and/or antibiotic selection of tetracycline-responsive cells in order to achieve good regulation. In the present manuscript we have constructed a dual Tet-ON system based on two lentiviral vectors, one expressing the *TetR* through the spleen focus forming virus (SFFV) promoter (STetR) and a second expressing *eGFP* through the regulatable CMV-TetO promoter (CTetOE). Using these vectors we have demonstrated that the *TetR* repressor, contrary to the reverse transactivator (*rtTA)*, can be expressed in excess to bind and modulate a high number of TetO operons. We have also showed that this dual vector system can generate regulatable bulk cell lines (expressing high levels of *TetR*) that are able to modulate transgene expression either by varying doxycycline concentration and/or by varying the amount of CTetOE vector genomes per cell. Based on these results we have developed a new all-in-one lentiviral vector (CEST) driving the expression of *TetR* through the SFFV promoter and the expression of *eGFP* through the doxycycline-responsive CMV-TetO operon. This vector efficiently produced Tet-ON regulatable immortalized (293T) and primary (human mesenchymal stem cells and human primary fibroblasts) cells. Bulk doxycycline-responsive cell lines express high levels of the transgene with low amount of doxycycline and are phenotypically indistinct from its parental cells.

Citation: Benabdellah K, Cobo M, Muñoz P, Toscano MG, Martin F (2011) Development of an All-in-One Lentiviral Vector System Based on the Original *TetR* for the Easy Generation of Tet-ON Cell Lines. PLoS ONE 6(8): e23734. doi:10.1371/journal.pone.0023734

Editor: Andre Van Wijnen, University of Massachusetts Medical School, United States of America

Received May 19, 2011; **Accepted** July 23, 2011; **Published** August 18, 2011

Funding: Fondo de Investigaciones Sanitarias (FIS) grant: PS09/00340. Junta de Andalucia grants: P09-CTS-04532 and PI0001/2009. The funders had no role in study design, data collection and analysis, decision to publish, or preparation of the manuscript.

Competing Interests: The authors have applied for an european patent on the development of the highly inducible Tet-ON vector system: European Application number: EP11166754.9, Applicant: Fundación Progreso y Salud, Date of receipt: 19-May-2011. This patent application does not alter the authors' adherence to all the Plos ONE policies on sharing data and materials. Therefore all materials presented in the manuscript will be freely available to the scientific community although not for commercial purposes.

* E-mail: francisco.martin.molina@juntadeandalucia.es

¤ Current address: GENYO (Pfizer-University of Granada-Andalusian Government Centre for Genomics and Oncological Research), Parque Tecnológico Ciencias de la Salud, Granada, Spain

Introduction

Inducible gene expression systems based on antibiotics or hormones are a potent research tools and are constantly developed for their use in basic research and/or clinical application. Among the existing inducible transcriptional gene regulatory systems, the reverse Tet transactivator (*rtTA*)-regulatable system is the most widely exploited tool for inducible gene expression. This system, described for the first time by Gossen and Bujard [1] is based on a chimeric transcription factor (the *tTA* transactivator), resulting of the fusion of the bacterial *Tet* repressor (*TetR*) with the activating domain of the herpes virus simplex viral protein 16 (*VP-16*). Random mutagenesis of *tTA* resulted in the *rtTA* (reverse tetracycline controlled *trans*-activator) protein that, contrary to *tTA*, requires the tetracycline to bind the TetO (For review see [2]). The *rtTA*-based system requires the addition of tetracycline to activate transcription (TET-ON system) by allowing the binding of the *rtTA* to the TetO-CMV promoter. Several improvements of the *rtTA* have been done that get better inducibility and reduced background [3,4,5,6]. However, all these tetracycline-inducible systems require a tetracycline-dependant-transactivator to activate the regulated promoter. The requirement of a transactivator for transcriptional activity has several undesired consequences: 1- The regulated promoters are activated by the transactivator and therefore, its natural activity can be altered. 2- Binding of the transactivator to *pseudo-TetO* sites can activate cellular genes. 3- The presence of a transactivating domain makes these proteins very toxic [7,8,9,10]. In fact, several studies have demonstrated that the *rtTA*-based systems can give rise to data misinterpretation due to the toxicity of the transactivator [9,10,11].

A new doxycycline-regulated system based on the original *TetR* repressor was developed in 1998, by Yao and colleagues [12]. The original *TetR* do not contain any transactivation domain and

rely on blocking the activity of endogenous promoters. These characteristics should allow the design of a less-toxic Tet-inducible expression cassette [12] that maintain the endogenous characteristics of the regulated-promoters and do not transactivate other cellular genes. Using this system, several groups have achieved good results in terms of low leakiness and high induction levels [13,14,15,16,17]. However, most of these systems are based on two vector systems and are reproducible only if the doxycycline-responsive cells are selected either by cloning [15,16,18] or antibiotic selection [17]. One of the potential reasons for this is the high concentrations of *TetR* required to block promoter activity [12,19]. In spite of the potential advantages of the *TetR over rtTA* to modulate transcription, the development of regulatable vector systems based on *TetR* harbouring all the elements required for doxycycline modulation (all-in-one vectors) has not been explored in detail. Only three all-in-one vectors have been described so far, one system based on herpesvirus simplex (HSV) [19] and two system based on plasmids and/or lentiviral vectors [17,20]. The use of HSV based vectors has been mainly limited to neural and cancer cells due to their tropism and their toxicity.

Lentiviral vectors are one of the most promising vectors for gene transfer in primary human cells [21,22]. They are highly efficient and do not express any viral gene that could alter normal cellular physiology. The generation of a highly efficient lentiviral system for easy generation of doxycycline-responsive primary cell lines based on the *TetR* repressor will certainly be of use not only for basic research but also for gene therapy applications [23]. Wiederschain at al described recently a useful all-in-one lentiviral vector able to regulate RNAi. However this system required selection with antibiotics of the doxycycline-responsive cells [17]. In 2001, Ogueta el al. developed an autoregulatable lentiviral vector without the requirement of antibiotic selection [20]. This autoregulatable vector express the *TetR* repressor through an internal ribosomal entry site (IRES) located downstream of the CMVTetO2 promoter. Although this lentiviral system could be of use for several applications, there have been no further publications based on this vector module since 2001. In fact, the same authors observed several potential drawbacks of the system that could limit the use of the vector: 1- The *TetR* repressor and the regulated transgen are expressed through the CMVTetO promoter. Therefore, the steady-state *TetR* concentration that is required to block CMV expression will always allow expression of the transgene. 2- The efficiency of the IRES (from the EMCV) is cell-type specific and this can lead to the lost of doxycycline regulation in important target cells [24].

We have developed a novel two-vector lentiviral system based on the efficient production of two vectors; one expressing the *TetR* repressor through the highly efficient Spleen-Focus-Forming-Virus (SFFV) promoter (STetR vector) and other harbouring the CMVTetO2 doxycycline-regulated expression cassette driving *eGFP*. This dual system allow the easy generation of doxycycline-regulatable cell lines able to express various amounts of transgenes by increasing the multiplicity of infection (MOI) of the regulatable vector. No cloning or antibiotic selection is required to obtain highly responsive cell lines with this system. In addition we have combined all the elements required for Tet-ON regulation into a single lentiviral vector named CEST. CEST contain the doxycycline-responsive cassette (CMVTetO) driving the expression of the transgene (*eGFP*) and the SFFV promoter expressing high amounts of the *TetR* protein. This vector efficiently produced doxycycline-regulated cell lines, including primary human fibroblasts (HFF) and human mesenchymal stem cells (hMSCs).

Results

The binary Lentiviral vector system based on the original *TetR* repressor achieves high induction and low background in bulk populations

In order to develop a Tet-ON lentiviral system without transactivator domains (such as those based on tTA and rtTA) we used the two expression vectors of the T-Rex Expression System from Invitrogen (pcDNA4/TO-E and pcDNA/TR, Invitrogen). We first constructed an alternative two lentiviral vector system based on pHRSIN-WPRE lentiviral vector [25] (Figure 1A). The first vector, STetR drives the expression of the original *TetR* repressor through the spleen focus forming virus (SFFV) promoter and the second vector, CTetOE, express *eGFP* through the regulatable CMV-TetO promoter (see M&M). The titre (number of transducing units (tu) per millilitre(ml)) obtained with both vectors was above 10.000.000 tu/ml before concentration (data not shown). We used these vectors to generate doxycycline-regulatable 293 T, K562 and primary human fibroblasts (HFF) cell lines. We first transduced the different cell lines with the STetR vector at a MOI of 10 and 7 days later with the CTetOE vectors at a MOI of 2. Seven days later, the different cell lines were incubated in the presence or absence of doxycycline for 48 hours and analyzed for *eGFP* expression by flow cytometry (Figure 1B) and fluorescence microscopy (Figure 1C). All cells kept *eGFP* expression tightly controlled in the absence of doxycycline although with significant differences in terms of regulation efficacy. Tet-ON 293T and HFF cells presented the tightest repression of *eGFP* expression in the absence of doxycycline while Tet-ON K562 cells showed the higher leakiness (*eGFP* expression levels in the absence of doxycycline)(Figure 2C).

We next studied the responsiveness of our dual Tet-ON system to different doxycycline concentrations. Tet-ON HFFs were incubated with increasing doses of doxycycline, from 0.001 μg/ml to 0.1 μg/ml, to determine the minimal dose required for maximal induction. As can be observed in Figure 2, the addition of 0.01 μg/ml of doxycycline was enough to achieved maximal expression, although 0.001 μg/ml already increased *eGFP* expression significantly (Figure 2D). These results showed that the high titre of the STeR lentiviral vector allowed the easy generation of stable bulk cell lines, including primary cells, which are highly responsive to doxycycline after transduction with the regulatable lentiviral vector CTetOE.

High induction and low leakiness of the *TetR*-based system is dependent on high *TetR* concentration but independent on CMVTetO target sites

Transactivator-containing repressor (*tTA* and *rtTA*) are quite toxic for most cells and must be kept at low concentration. In order to achieve good regulation, the concentration of TetO binding sites must be kept low to equal low transactivator concentrations[26]. We therefore studied whether this was also the case for the unmodified *TetR*-based systems by using STetR and CTetOE lentiviral vectors. We used increasing amounts of STetR to obtain 293 T cell lines with increasing amounts of *TetR* repressor (Figure 2A; from left to right). All these 293T-$TetR^{+}$ cell lines were transduced with increasing amounts of the CTetOE to obtain increasing concentrations of CMVTetO targets (Figure 2A: from top to bottom). We showed that only those cells expressing high levels of *TetR* repressor have good induction and low leakiness (Figure 2A right panels). A minimum of 2 vector genomes per cell (v.g.c.) of the STetR are required in order to achieve good regulation and over 3–4 v.g.c. give minimal background and

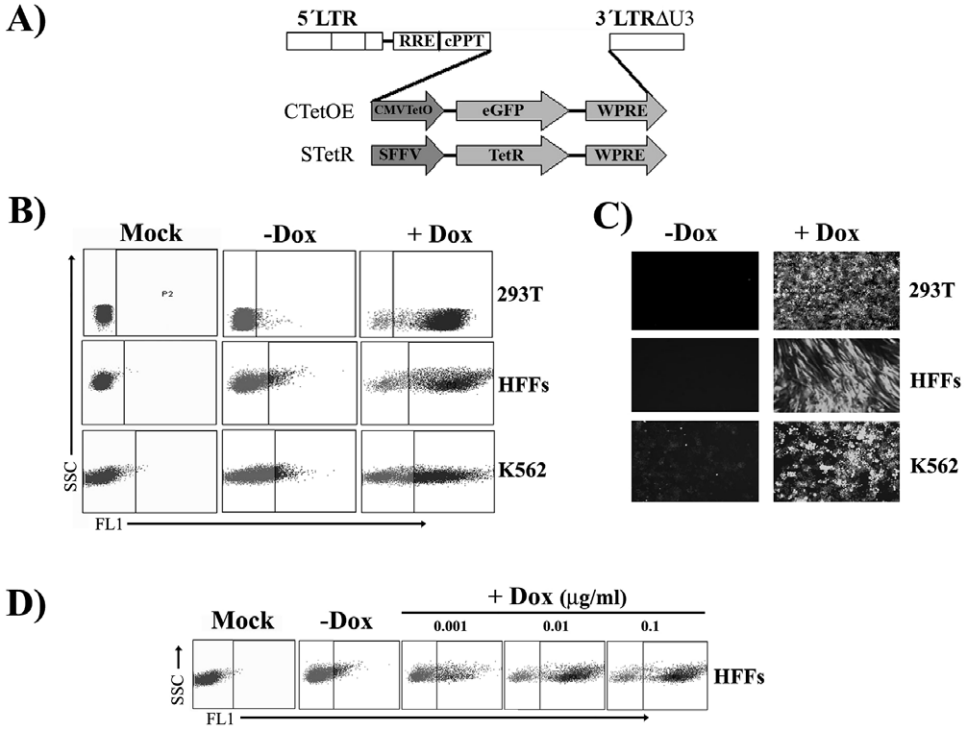

Figure 1. *TetR*-based two-vector system for efficient generation of dose-responsive Tet-On cell lines. A) Maps of the two lentiviral vectors required for doxycycline-dependant transgene regulation. The *TetR* repressor is expressed through the constitutive SFFV promoter, highly active in most cell types, including hematopoietic cells. The second lentiviral vector contain the doxycycline-responsive CMV-TetO promoter(Yao et al. 1998) driving the expression of *eGFP*. 293T, primary human fibroblasts (HFFs) and K562 cells were co-transduced with STetR and CTetOE lentiviral vectors at high MOI and analyzed by fluorescence microscopy **(B)** or flow cytometry **(C)** in the absence (–Dox) or presence (+Dox) of 10 ng/ml of doxycycline. **D)** Doxycycline responsiveness (0.001 μg/ml, 0.01 μg/ml and 0.1 μg/ml as indicated) of the Tet-ON HFF cell line derived by cotransduction with STetR and CTetOE LVs.
doi:10.1371/journal.pone.0023734.g001

maximal induction (Figure 2A; second right graphs). Interestingly, there was a direct correlation between the CTetOE v.g.c. and the fold induction index (Figure 2B). We reached around 1000 fold induction in bulk populations containing 4–9 v.g.c. of the STetR vector and 10 v.g.c. of the CTetOE vector (Figure 2A and 2B) This indicates that the *TetR* repressor, contrary to the *rtTA* transactivator, can be expressed in excess to modulate a high number of TetO operons. This dual vector system can therefore generate regulatable cell lines expressing different transgene amounts by incubating the $TetR^+$ cells with different amounts of the regulatable vector (CTetOE) (see Figure 2A right plots, top to bottom). Each of the different cell lines generated can additionally be modulated by adjusting doxycycline concentrations (as can be observed in Figure 1D for HFF cells).

Development of *TetR*-based all-in-one LV that efficiently regulates transgene expression

Although a two vector system has several applications in basic research, single vectors able to deliver the *TetR* repressor and the regulatable expression cassette (i.e. CMVTetO) are highly desirable for the easy generation of doxycycline-responsive primary cell lines and for gene therapy strategies. We therefore constructed an all-in-one dual-promoter lentiviral vector named CEST containing both, the doxycycline-responsive cassette (CMVTetO) expressing *eGFP* transgene and the *TetR* expressing casset (SFFV-TetR)(Figure 3A). We tested the CEST vector in immortalized cells (293 T) and primary cells (hMSCs and HFF). We incubated the different cell lines with increasing MOIs of the CEST vector. Two weeks later, the different cell lines harbouring increasing amounts of the CEST vector were analysed for responsiveness to doxycycline (Figure 3B, only shows for 293 T cells), leakiness (Figure 3C right graphs) and fold induction index (Figure 3C, left graphs). Tet-On cells responded to 0.001 μg/ml in cells harbouring 1–4 v.g.c. of CEST and to 0.01 μg/ml in cells harbouring 10–20 v.g.c. of CEST (Figure 3B and data not shown). Interestingly, as occur for the two-vector system, CEST-Tet-ON cells also requires also several copies of the CEST vector (four or more v.g.c.) to achieve good regulation (Figure 3B and 3C). To analyse this results in detail, leakiness and fold induction index of the different CEST-Tet-ON cell lines were determined and plotted in function of the amount of integrated CEST vector per cell. In all cells analysed we found the same results: cells harbouring the highest amounts of CEST vectors integrated presented the lowest leakiness (Figure 3C right graphs) and the highest fold induction index (Figure 3C, left graphs). We reached up to 400, 180 and 100 fold induction in 293 T (with 20 v.g.c.), HFF (with 10 v.g.c.) and hMSCs (with 2 v.g.c.) respectively. These data corroborate the hypothesis that high concentrations of the *TetR* repressor is the main factor required to get good doxycycline regulation and not the number of TetO target sites. Increased numbers of TetO targets (up to 20 times in 293 T cells; Figure 2B and 2C top graphs) do not preclude *TetR* repression but it does augment transgene expression and therefore increase total fold induction. This property allowed us to control transgene expression not only by adjusting doxycycline concentrations but also by controlling the MOI used for transduction of the target

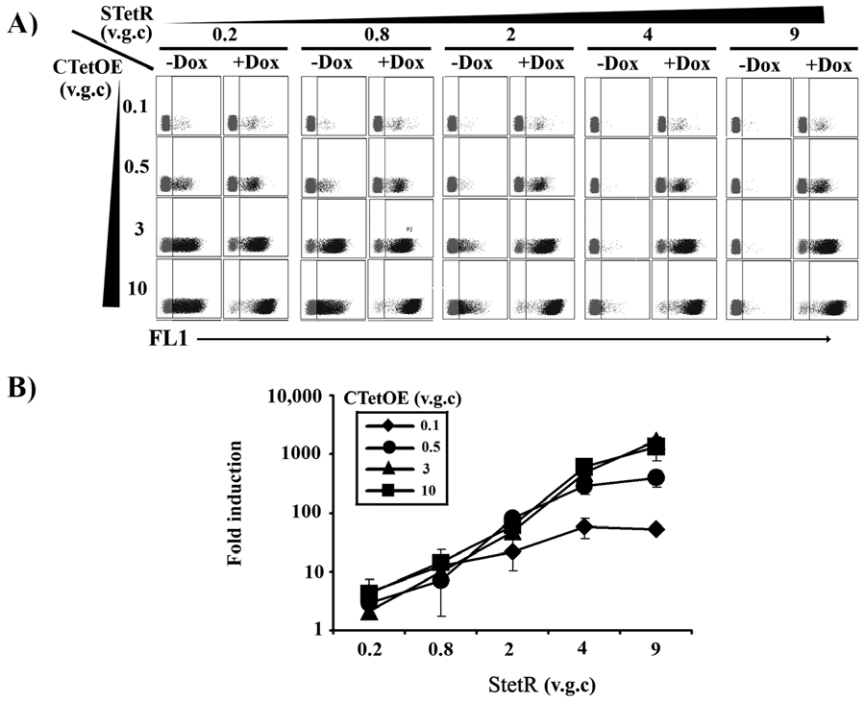

Figure 2. GFP induction level using binary lentiviral vectors. A) 293T cells were stably transduced with increasing amount of STetR lentiviral vector. Different *TetR*-expressing 293 T cell lines were generated each harbouring an average of 0.2, 0.8, 2, 4 and 9 vector genomes per cell (v.g.c.) (indicated on the top of Figure A). Each of these *TetR*-expressing 293 T cell lines where later transduced with increasing amount of CTetOE vectors (average of 0.5, 3, 6 and 10 v.g.c.)(indicated on the left of Figure A). Plots show *eGFP* expression of the different cell lines in the absence (-Dox) or presence (+Dox) of 1 μg of doxycycline. **B)**. Graph showing the increment in fold induction of transduced 293 T cells after the addition of 100 ng/ml of doxycycline. The highest induction levels are achieved when the cells contain multiple copies of both StetR (7-9 v.g.c.) and CTetOE vectors (6–10 v.g.c.).
doi:10.1371/journal.pone.0023734.g002

cells (Figure 3B and 3C). The highest transgene expression and the highest inducibility were always obtained with the highest MOIs. CEST-transduced-293T, -HEF and -hMSC expression levels go from a MFI of 179, 260 and 872 in the absence of doxycycline to a MFI of 47956, 46211 and 20265 in the presence of doxycycline respectively (Figure 3B and data not shown).

The *TetR* protein efficiently localize to the nucleus

Theoretically, if the amount of *TetR* repressor expressed by one copy of the CEST vector is not enough to control one TetO operon (as demonstrated by the absence of modulation at low MOI), cells containing multiple copies of the CEST should have even higher leakiness. One possible explanation could be an inefficient nuclear transport of the *TetR* repressor and the subsequent requirement of hight *TetR* concentrations in the cytoplasm to get *TetR* into the nuclei. To test this hypothesis, we analysed *TetR* content in the cytoplasmic and nuclear fractions of 293 T cells transduced at different MOIs. The results showed that up to 80% of the *TetR* localize in the nuclei even at low MOI (Figure 4A; 0.06 v.g.c.). In addition, the percentage of *TetR* repressor present in the nuclear versus the cytoplasmic fractions was very similar independently of the concentration of the *TetR* (Figure 4B). These data indicate that *TetR* is transported to the nuclei quite efficiently independently of the total *TetR* cell content.

We further analyzed the level of correlation between *eGFP* expression and *TetR* concentration and/or nuclear localization. We performed immunostaining of CEST-transduced hMSCs containing an average of 2 v.g.c. (Figure 4 C). These bulk CEST-hMSCs contained highly-responsive cells (as observed in Figure 3C middle graphs and data not shown) but they also contained a percentage of cells that were inadequately regulated (cells that are $eGFP^+$ in the absence of doxycycline). Due to the low eGFP expression levels of some cells, the pictures taken with the fluorescence microscopy were further enhanced to visualize any residual *eGFP* expression. The aim was to correlate eGFP expression levels (Figure 4C left panels) with *TetR* expression (Figure 4C middle panels). Cells expressing higher amounts of *TetR* (white arrows) were completely negative for *eGFP* expression. In these cells, a significant part of the *TetR* was located in the nuclei as indicated by the purple colour of their nucleus as result of the co-localization of red (*TetR*) and blue (DAPI) colours (Figure 4C white arrows, middle panel). On the contrary, cells expressing *eGFP* were negative for *TetR* expression (Figure 4C, yellow arrows, middle panel) as demonstrated by the absence of colocalization of the green and red colours (Figure 4C right panels).

Doxycycline-responsive primary cell lines maintain the main properties of parental cells

MSCs are an important target for cell-gene therapy applications. Their role in regeneration, immunomodulation as well as their migratory capabilities to inflammatory locations makes them an attractive target for gene manipulation. The development of an efficient doxycycline-responsive gene transfer system to achieve high levels of transgene expression in MSCs (without affecting its phenotype) is of special interest for the field. We therefore studied potential changes on doxycycline-responsive hMSCs compared with parental hMSCs. We compared control hMSCs (MOCK) with hMSCs containing increasing amounts of

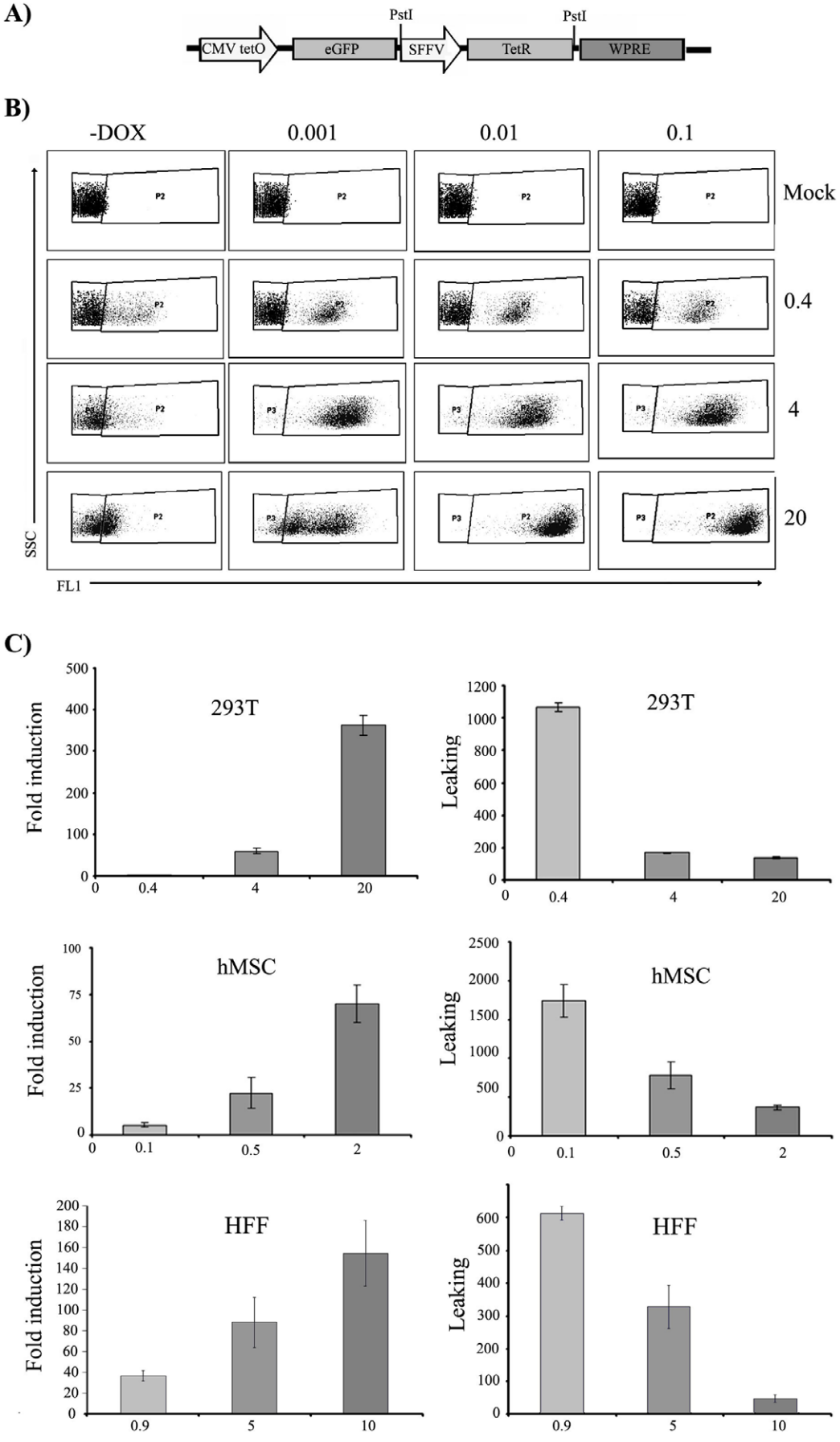
A)
PstI
PstI
CMV tetO
eGFP
SFFV
TetR
WPRE
B)
-DOX
0.001
0.01
0.1
Mock
0.4
4
20
SSC
FL1
C)
293T
Fold induction
Leaking
hMSC
HFF

Figure 3. Easy generation of highly responsive cell lines with the all-in-one doxycline-controlable lentiviral vector CEST. A). Schematic representation of the CEST. *eGFP* transgene is expressed from a Tetracycline –responsive CMV-TetO promoter and the *TetR* repressor is expressed from the SFFV promoter. **B**) Doxycycline responsiveness of 293 T containing different amounts of CEST vector copy per cell (0 (Mock), 0.4, 4 and 20 v.g.c. as indicated on the left hand side). The different cell lines were incubated in the absence of doxycycline (-Dox), and with 0.001 μg/ml, 0.01 μg /ml and 0.1 μg /ml as indicated on the top. The leaking in the absence of doxycycline decrease as the vector copy number increase (left graphs from top to bottom) **C**) Fold induction (left panels) and leaking (right panels) in 293 T (top panels) and human mesenchymal stem cells (hMSC) (bottom panels) transduced with increasing MOIs of the CEST vector. The average CEST v.g.c. of the different cell lines analyzed are indicated at the bottom of the graphs. The best regulation in terms of higher inducibility and lower leaking is achieved in the cells that contain the highest number of CEST vector integrated.
doi:10.1371/journal.pone.0023734.g003

integrated CEST vectors. We study potential variations in the expression of positive (CD73, CD90, CD105, CD166) and negative (CD19, CD34, CD45, and HLA-DR) surface markers. We also studied potential alteration in proliferation and/or apoptosis in hMSCs containing 2 v.g.c. by analyzing cell cycle status with Propidium Iodide. We did not detect any changes on neither the expression of the main surface markers (Figure 5A) nor in the cell cycle status (Figure 5B).

Another important characteristic of MSCs is their ability to differentiate toward different cell types. We therefore studied whether vector transduction affect the ability of MSCs to differentiate to adipocytes, osteocytes and chondriocytes. As can be observed in Figure 5C, neither CE (expressing only eGFP) nor CEST (expressing eGFP and *TetR*) transduction of MSCs had any detectable impact on the differentiation potential of MSCs.

Discussion

In the present work we have developed a *TetR*-based dual and all-in-one lentiviral system that efficiently generate doxycycline-responsive cell lines without the requirements of cloning and/or antibiotic selection. Most of the doxycycline-responsive systems are based on the TetR-VP16 chymeras (tTA and rtTA) [2,3,4,5,6]. In these systems, the promoter is only active when the tTA or the rtTA transactivators bind the regulated promoter. The expression of the VP16 transactivators in the regulated cells can have several

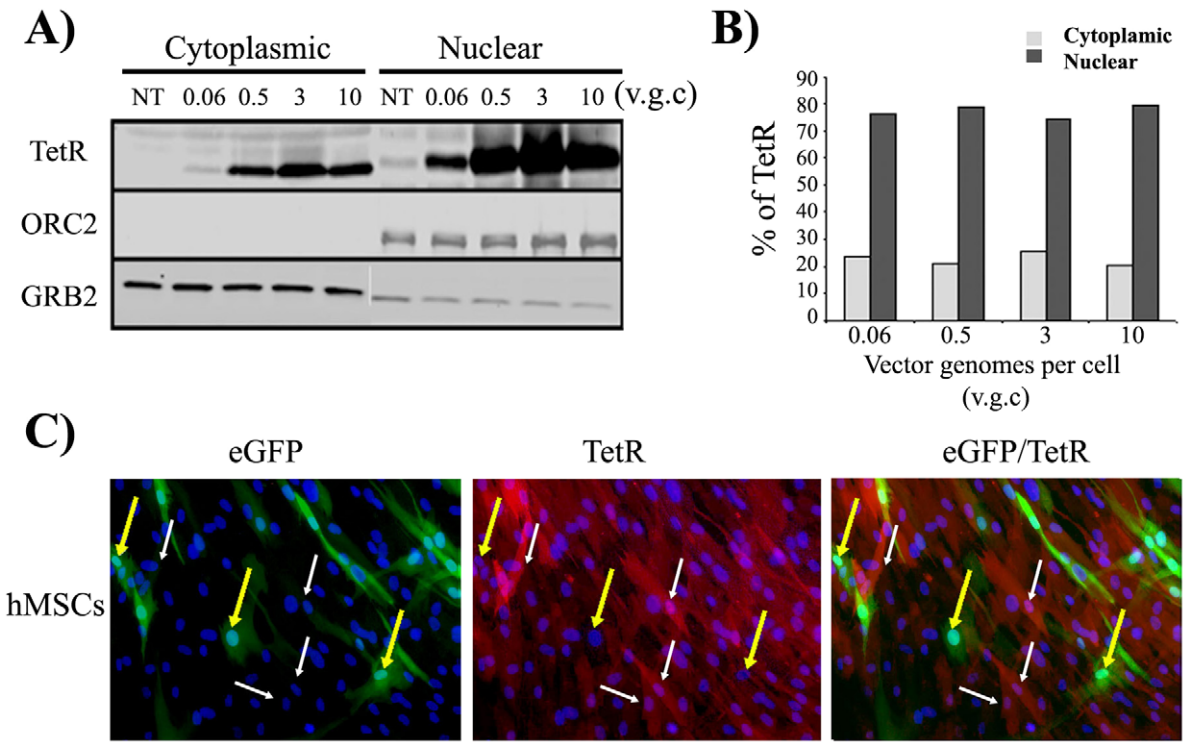

Figure 4. Nuclear localization of *TetR* repressor in CEST-transduced cells correlates with complete repression of CMV promoter. A). Quantitative Western blot analysis showing *TetR* expression in cytoplasmic and nuclear fraction of 293 T cells transduced with increasing CEST MOIs. Cell fractionation was carried out as indicated in M&M. ORC2 and GRB2 were used as markers for the nuclear and cytoplasmic fraction respectively, and as a loading control. **B)**. Graph showing percentage of *TetR* repressor that is present in the cytoplasmic (gray bars) and nuclear (black bars) fractions as determined by densitometry analysis of the Western blot (A). Note that the *TetR* protein is mainly localized within the nucleus, independently of the *TetR* concentration. **C)**. Immunofluorescence staining of *TetR* in CEST transduced hMSCs (2 v.g.c.). Cells were fixed and incubated with monoclonal IgG1 against *TetR* amino acid 84-98 and incubated with DAPI (marking nuclei in blue) as indicated in M&M. Left panel shows a picture that has been manually enhanced to visualize minimally expressed eGFP. Middle and right pictures show *TetR* expression and *eGFP/TetR* merge images respectively. White arrows indicate cells which are completely negative for eGFP expression. Note the purple colour of these cells (middle and right panels) as consequence of the co-localization of DAPI (Blue) and red (*TetR*). Yellow arrows indicates cell expressing low levels of *TetR* repressor and, therefore expressing eGFP (left and right panels). The nuclei of these cells are intense blue (middle panel) indicating the absence of *TetR* expression. v.g.c.; vector genomes per cell. NT; not transduced.
doi:10.1371/journal.pone.0023734.g004

A)

		CEST (v.g.c)		
	MOCK	0.1	0.5	2
CD73	++	++	++	++
CD45	-	-	-	-
CD34	-	-	-	-
CD90	++	++	++	++
CD166	++	++	++	++
HLA-DR	-	-	-	-
CD19	-	-	-	-
CD105	++	++	++	++

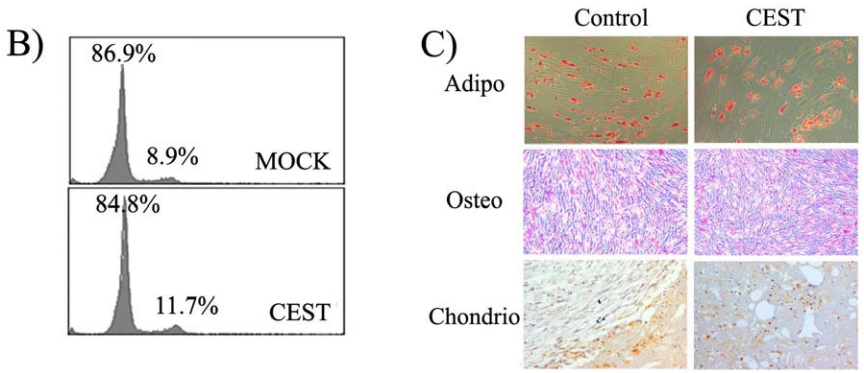

Figure 5. Doxycycline-responsive human mesenchymal stem cells (hMSCs) maintain the main properties of parental hMSCs. **A**) Different doxycycline-responsive hMSCs were generated with increasing MOIs of the CEST vector to obtain an average of 0.1, 0.5, and 2 v.g.c. (indicated on the top). Expression of the different surface markers were analyzed by flow cytometry and compared to the expression by a parental (MOCK-transduced) hMSCs. The hMSCs containing 2 v.g.c. of the CEST vector was further analyzed to test the influence of vector expression on cell cycle status **B**) and on differentiation potential toward adipogenesis (top panels), osteogenesis (middle) and chondriogenesis (bottom panles) **C**). No significant differences were observed between the parental and the CEST-transduced hMSCs.
doi:10.1371/journal.pone.0023734.g005

undesired consequences such as alteration of the promoter natural activity, activation of cellular genes and toxicity [7,8,9,10,11]. We based our studies in a new doxycycline-regulated system based on the original *TetR* repressor developed in 1998 by Yao et al. [12] as an alternative to the *TetR-VP16* chimeras (*tTA* and *rtTA*).

We first developed two lentiviral vectors; one driving the expression of the original *TetR* repressor through the SFFV promoter (STetR) and a second one harbouring the CMVTetO cassette expressing eGFP. We used the SFFV promoter to drive *TetR* expression for its well-known characteristic as a strong promoter in several cell types, including important targets for gene therapy [25,27,28]. The STetR lentiviral vector was used to generate different cell lines expressing variable levels of *TetR* repressor by increasing the MOI. These cell lines allowed us to study the minimal requirement of *TetR* concentration needed for the regulation of the CMVTetO operon. Previous studies are somehow contradictory regarding the *TetR* repressor concentrations required to achieve tetracycline regulation. While Yao et al. propose that *TetR* concentration must be kept high to obtain good tetracycline responsiveness[12,19], other authors argue that minimal amounts of *TetR* could be sufficient to shut off the TetO-regulatable CMV promoter[20]. The fact that most (if not all) recent publications using the *TetR* repressor system required cloning selection or antibiotic selection [15,16,17,18] to generate regulatable cell lines favour the theory of Yao et al. In this direction we have done a systematic study demonstrating that in order to achieve good inducibility and low leakiness, the cells must contain al least 2 copies of the StetR vector integrated. For maximal responsiveness, the cells must have over 4 vectors genomes of STetR per cell that, as shown by Western blot analysis (Figure 4B), produce very high concentrations of *TetR* repressor.

The different TetR-293T cell lines were further used to study if the TetO concentrations are a limiting factor as occur for the rtTA system. Transactivator-containing repressors (rtTA) are quite toxic for most of the cells and must be kept at a low concentration. Therefore, the concentration of TetO binding sites must be kept low to equal low repressor concentrations[7,11,26]. Contrary to rtTA-based systems, *TetR* concentrations inside the regulated cells were able to modulate high amounts of TetO sequences (present in the CTetOE vector). Since the leaking was similar in cells harbouring increasing copies of the CTetOE (in cells harbouring over 4 StetR v.g.c.) and the expression levels in the presence of doxycycline augmented proportionally to the amount of CTetOE v.g.c, the final fold induction index was always better for cells containing multiple copies of the CTetOE vector. This vector module can therefore be used to generate regulatable cell lines expressing increasing amount of the transgene simply by increasing the MOI of the CTetOE vector. Each of the different cell lines generated can additionally be modulated by adjusting doxycycline concentrations.

Although a two vector system has important applications both in basic research and cell-gene therapy therapeutic approaches, the availability of all-in-one vector harbouring all the necessary elements to regulate a transgene is highly desirable for several applications including *in vivo* application and the generation of regulatable human primary cells. All-in-one vectors have the additional advantage of minimising the amount of integrative vectors required for transgene modulation and therefore reduce

the potential alteration of regulatable cell lines We have therefore generated an all-in-one *TetR*-based lentiviral vector (CEST) module for the generation of immortalized and primary human doxycycline-responsive cell lines. The CEST vector produce over 10.000.000 tu/ml and one transduction with concentrated vector were able to generate highly-responsive immortalized (293T) and primary (hMSCs and HEF) cells.

The necessity of multiple copies of the CEST vector to regulate the transgene confirm the requirement of high levels of the *TetR* repressor and, at the same time, also confirms that once this levels are achieved, they can modulate high amounts of CMVTeO expression cassettes. Indeed, in CEST-transduced cells, the cells expressing higher levels of *TetR* repressor have also higher levels of CMVTetO to regulate. Still the leakiness drop and the fold induction increased proportionally to CEST vector genomes per cell (Figure 3). These data support the hypothesis that high concentrations of the *TetR* repressor is the main factor required to get good doxycycline regulation. In fact increasing the numbers of TetO targets up to 20 times with the CEST do not preclude significantly *TetR* repression but it does augment transgene expression and therefore increase total fold induction. This property allowed us to control transgene expression not only by adjusting doxycycline concentrations but also by controlling the MOI used for transduction of the target cells. We also showed that the system is highly responsive to low doses of doxycycline with 1 ng/ml being sufficient to reach peak expression in cells containing up to 4 v.g.c. However in cell lines with very high amounts of CEST vector integrated (20 v.g.c.), the maximum inducibility was achieved with 10 ng/ml of doxycycline. The fact that high MOIs of the CEST showed lower leakiness than low MOIs was surprising and probably reflects some way of *TetR* cooperation to achieve promoter shut down. We have shown that in 293 T and MSCs, the *TetR* repressor is transported inside the nucleus quite efficiently (up to 80% of the total cell content) and independently of the *TetR* concentration eliminating the possibility of *TetR* cooperation to reach the nucleus as a factor involved in this phenomenon. Therefore, we favour the hypothesis of a requirement of high concentration of *TetR* to cooperate for the formation of *TetR* homodimers required for promoter shut down. At low MOIs, the *TetR* concentration does not reach the minimum required and are therefore unable to modulate transgene expression.

An important factor related to the use of the original *TetR* repressor is the absence of toxic effects. We analyzed the potential alteration of *TetR* overexpression in hMSC, an important target for cell-gene therapy applications because of its role in regeneration and immunomodulation. We did not found any alteration on the phenotype, cell cycle status or differentiation potential on hMSCs that were transduced at high MOI with the CEST vector and that were highly-responsive to doxycycline. However, the fold induction index of the CEST-transduced MSCs was slightly lower than CEST-transduced 293 T and HEF cells, probably due to the differences in CEST vector genome per cell achieved (293 T and HEF cells are 8–4 times more permissive than hMSCs).

Although both, the dual (StetR and CTetOE) and the all-in-one-based (CEST) vectors described in this manuscript, are highly efficient for the development of doxycycline-regulated cell lines, the requirement of multiple v.g.c. to achieve regulation is an important drawback of the system. Indeed multiple integrations are more likely to alter physiology of the doxycycline-regulated cells and the system work poorly in highly restrictive cells such as CD34+ cells (data not shown). The ideal vector should allow complete CMVTetO promoter inhibition with only one vector integration. We are at the moment trying to improve the system by comparing various nuclear localization signals on the *TetR* repressor, by insulating the all-in one vector and by using alternate vector modules to increase *TetR* production. We have evidences that different cell lines behave differently in term of nuclear localization of the original *TetR* and that these differences correlate with differences in doxycycline regulation (our unpublished data). Therefore, the use of nuclear localization signal together with further improvements in the vector should improve not only the amount of cell lines that can be modulated but also will open the window to its use for *in vivo* applications.

Materials and Methods

Cells and reagents

293 T cells (Chantret *et al.* 1994) were maintained in Dulbecco's Modified Eagle's Medium (DMEM, Invitrogen) supplemented with 10% Fetal Bovine Serum (FBS, Invitrogen), 1% essential amino-acids and antibiotics. Human mesenchymal stem cells (hMSCs) were obtained from Inbiobank (www.inbiobank.org; San Sebastian, Spain), and were cultured in Advanced-DMEM (Gibco) plus 10% FBS. When cell cultures achieved over 85% of density, adherent cells were trypsinized, washed in PBS and re-plated at a concentration of 5×10^3 cells/cm^2. HFFs were purchased from ATCC (SCD-1112SK). During routine maintenance, HFFs were grown in IMDM, plus 10% FCS and 2 mM L-glutamine and split in the ratio 1:2 when they reached 80-90% confluence. K562 were obtained from the ATCC (CCL-243) and maintained in RPMI media (Invitrogen), supplemented with 10% Fetal Bovine Serum (Invitrogen).

Plasmids construction

Dual system. StetR and CTetOE. The StetR vector plasmid was obtained by replacing *EGFP* cDNA from the pHRSIN-CSEW [25] plasmid (using BamHI and NotI excision) with a *TetR* cDNA obtained by PCR using pcDNA6TR (Invitrogene) as a template and the BamH1-TetR Fw (5′ GGATCCATGTCTAGATTAGATAAAAG) and Not-TetR reverse (5′ GCGGCCGCTTAATAAGATCTGAATTCCCGGG). Primers to include the BamHI NotI sites at both ends. To construct the CTetOE vector plasmid, we used pHRSIN-CSEW vector as backbone, excising the SFFV promoter using EcoRI/BamHI restriction enzymes. A PCR fragment containing CMVTetO cassette was obtained by PCR using the EcoR1 forward (CCGGAATTCGTTGACATTGATTATTGACTA) and BamH1 reverse (CGCGGATCCCGGAAGATGGATCGGTCC) primers and the pcDNA4/TO plasmid (Invitrogene) as template.

All-in-one CEST lentiviral vector. The CEST vector plasmid harbouring the CMV-TetO regulatable cassette driving the expression of *GFP* as well as the spleen focus-forming virus promoter driving the expression of the *TetR* repressor gene was constructed by cloning the SFFV-TetR PstI fragment from the STetR vector into the unique Pst1 restriction site of the CTetOE vector.

Vector production and titration

The HIV packing plasmid (pCMVDR 8.9) and VSG-G plasmid (pMD.G) are described elsewhere (Naldini et al., 1996; Zufferey et al., 1998). Vector production was performed as described previously (Toscano et al., 2004). Briefly, 293 T cells, were plated, and the vector, packaging, and envelope plasmids (plasmid proportion 3:2:1) were resuspended in 1.5 ml of Opti-MEM (GIBCO) mixed with 60 µl of Lipofectamine 2000 (Invitrogen, Carlsbad, CA) and diluted in 1.5 ml of Opti-MEM (GIBCO). The mixture was added to the 293 T cells, which were incubated for 6–

8 h, washed and cultured for an additional 48 h. Viral supernants were collected and filtered through a 0.45 μm (pore size) filter (Nalgene, Rochester, NY) aliquoted and immediately frozen at −80°C. For the titration of vectors, transduced cells were lysed and DNA extracted after 7–10 days, and vector copy number per genome (v.c.g) was determined using quantitative PCR as described below.

DNA extraction and quantitative real-time PCR

Genomic DNA was isolated by adding 1 ml per 10^6 cells of SNET extraction buffer (20 mM Tris-HCl [pH 8], 5 mM EDTA [pH 8], 400 mM NaCl, 1% SDS) containing proteinase K (100 mg/ml; Sigma- Aldrich). DNA samples were incubated at 55°C for 2 hr, proteinase K was inactivated by incubating at 98°C for 10 min, and RNase (1 mg/ml) was finally added for 30 min at 37°C. Proteins were extracted twice with phenol–chloroform, and DNA was then precipitated and its concentration determined by spectrophotometry. Quantitative real-time PCR were performed with an Mx3005P system (Agilent). The real time PCRs were performed using the QuantiTect^{TM} SYBR Green PCR Kit (from Qiagen). To quantitate CEST lentiviral integration we used primers for the WPRE sequence; WPRE-F: 5′- CACCACCTGTCAGCTCCTTT and WPRE-R: 5′- ACAACACCACGGAATTGTCA. For the STetR vector we used primers for *TetR* sequence, TetR–F: 5′ GGGATCCTAGTGAT-TATGTCT and TetR-R: 5′ TTACGGGTTGTTAAACCTTC and for the CTetOE vector we used primers for the eGFP sequence, GFP-F: 5′GTTCATCTGCACCACCGGCAAG and GFP-R TTCGGGCATGGCGGACTTGA. The parameters for the PCR were 1× (95°C, 2 min); 40×(95°C, 15 sec / 55°C, 30 sec / 72°C, 30 sec); 1×(72°C 2 min). We calculated the vector copy number per genome by interpolation in the standard curve made with 10-fold increasing amounts of plasmid DNA (CTetOE)) from 10^3 to 10^7 v.g.c. and by starting with 0.6 μg genomic DNA (about 100.000 genomes).

Cell extraction and Western blotting.

Cytosolic and nuclear fractions of transduced and controls cells were obtained using the Qproteome nuclear protein Kit (Qiagen) following the manufacturer's instruction. Proteins were resolved by sodium dodecyl sulfate– polyacrylamide gel electrophoresis (SDS–PAGE; 10% polyacrylamide gels, reducing conditions), and electrotransferred to Hybond-P polyvinylidene difluoride (PVDF) membranes (GE Healthcare Life Sciences, Buckinghamshire, UK). Membranes were blocked with 5% nonfat milk and probed for 1 hr at room temperature with rabbit anti-GRB2 (BD pharmingen; no 559266), rabbit anti-ORC (BD Pharmigen, no 559166) and mouse anti-Tet-repressor (Mobitec; no TET02). Combination of IRDye 680LT Goat anti-Rabbit IgG (Licors: no 26-68021) and IRDye 800CW Goat anti-Mouse IgG (Licors: no 926-32210) were use at 1:10.000 dilutions to analyzed *TetR* protein in combination with either ORC or GRB2. After washing the membranes, detection and quantification of protein were performed using Odyssey Image Scanner System (Licor Biosciences, Cambridge, UK) using IRdye-conjugated secondary antibodies (Licor) and the Odyssey quantification software.

Inmunostaining

For immunofluorescence analysis of cultured cells, cells were fixed in 4% paraformaldehyde-PBS for 20 min, permeabilized with 0.1–1% Triton X-100-PBS for 15 min, and blocked with 5% PBS for 45 min at room temperature (RT). Fixed cells were incubated with 2 μg/ml anti-Tet-repressor (Mobitec; TET02) and then with a secondary Texas-red-conjugated anti-mouse IgG (Becton Dickinson (BD)). Stained cells were then mounted in Vectashield mounting medium with DAPI (H-1500, vector laboratories) to stain the nuclei and examined using an Olympus AX60 fluorescence microscope.

Phenotype of hMSCs

MSCs were collected, washed and pre-incubated in a PBS-blocking solution containing 3% of fetal bovine serum (FBS) and 0,2% sodium azide for 15 minutes at 4°C. The following antibodies were used to fully characterize expression pattern of transduced and untransduced MSCs: anti human CD90-FITC, CD73-PE, CD105-FITC, CD166-PE, CD106-PE, CD45-PerCP, CD34-APC, HLA-DR- PerCP, CD19-APC all from Becton Dickinson (BD). Antibodies were diluted in PBS 0,3% of FBS and 0,02% sodium azide. Cells were incubated with 100 μl of the different antibodies (1/100), for 1 h at 4°C and agitation and washed in PBS 0,3% of FBS and 0,02% sodium azide followed by a final wash in PBS alone. Cells were analyzed on FACS Canto Flow Cytometer.

Adipocyte, Osteocyte and chondriocyte differentiation

Differentiation potential of hMSCs was studied by incubating the different cell lines in specific differentiation inductive media (Lonza, Basel, Switzerland). For adipogenic differentiation, cells were cultured in Adipogenic MSCs differentiation BulletKit (Lonza, Basel, Switzerland) and stained with Oil Red O (Amresco, Solon, OH). For osteogenic differentiation, cells were cultured in Osteogenic MSCs differentiation BulletKit (Lonza, Basel, Switzerland) and stained with Alizarin Red S (Sigma). For chondrogenic differentiation, cells were cultured in chondrogenic MSCs differentiation BulletKit (Lonza, Basel, Switzerland), differentiated cells were include in paraffin block, and chondrocyte-like cells were inmunodetected with Anti-S100 (*Dako*, polyclonal rabbit *anti-S100*, code Z0311).

Fold induction index and leakiness determination.

Transduced cells incubated in the presence or absence of different concentrations of doxycycline were analyzed by flow cytometry to determine the percentage of eGFP positive cells and the Mean fluorescence intensity (MFI) of either, the eGFP+ population or the entire population.

The *Fold induction index* was estimated as arbitrary units obtained by following formula:

[% eGFP$^+$ (+Dox) / %eGFP$^+$(-Dox)] x [MFI eGFP$^+$ cells (+Dox) / MFI eGFP$^+$ cells (-Dox)]

Leakiness of the system was determined by using the following formula:

[% eGFP$^+$ (-Dox) / %eGFP$^+$(+Dox)] x MFI eGFP$^+$ cells (-Dox)

Cell cycle analysis

Cell cycle assays were performed as previously described[29]. Briefly, the trypsinized cells were fixed in 70% ethanol, washed with PBS, and then incubated with Propidium Iodide (20 mg/ml) in PBS containing RNase A for 30 min at 37^{a}C. After washing, cells were analyzed by flow cytometry (FACS Canto, Becton Dickenson).

Acknowledgments

We would like to thank Dr Per Anderson for useful comments and English grammar correction and Dr René Rodríguez for help on cell cycle analysis.

Author Contributions

Conceived and designed the experiments: FM KB. Performed the experiments: KB. Analyzed the data: FM KB. Contributed reagents/materials/analysis tools: FM KB MC MGT PM. Wrote the paper: FM KB.

References

1. Gossen M, Bujard H (1992) Tight control of gene expression in mammalian cells by tetracycline-responsive promoters. Proc Natl Acad Sci U S A 89: 5547–5551.
2. Toniatti C, Bujard H, Cortese R, Ciliberto G (2004) Gene therapy progress and prospects: transcription regulatory systems. Gene Ther 11: 649–657.
3. Wells KD, Foster JA, Moore K, Pursel VG, Wall RJ (1999) Codon optimization, genetic insulation, and an rtTA reporter improve performance of the tetracycline switch. Transgenic Res 8: 371–381.
4. Urlinger S, Baron U, Thellmann M, Hasan MT, Bujard H, et al. (2000) Exploring the sequence space for tetracycline-dependent transcriptional activators: novel mutations yield expanded range and sensitivity. Proc Natl Acad Sci U S A 97: 7963–7968.
5. Vieyra DS, Goodell MA (2007) Pluripotentiality and conditional transgene regulation in human embryonic stem cells expressing insulated tetracycline-ON transactivator. Stem Cells 25: 2559–2566.
6. Barde I, Zanta-Boussif MA, Paisant S, Leboeuf M, Rameau P, et al. (2005) Efficient control of gene expression in the hematopoietic system using a single Tet-on inducible lentiviral vector. Mol Ther.
7. Judelson HS, Narayan R, Fong AM, Tani S, Kim KS (2007) Performance of a tetracycline-responsive transactivator system for regulating transgenes in the oomycete Phytophthora infestans. Curr Genet 51: 297–307.
8. Sisson TH, Hansen JM, Shah M, Hanson KE, Du M, et al. (2006) Expression of the reverse tetracycline-transactivator gene causes emphysema-like changes in mice. Am J Respir Cell Mol Biol 34: 552–560.
9. Perl AK, Zhang L, Whitsett JA (2009) Conditional expression of genes in the respiratory epithelium in transgenic mice: cautionary notes and toward building a better mouse trap. Am J Respir Cell Mol Biol 40: 1–3.
10. Whitsett JA, Perl AK (2006) Conditional control of gene expression in the respiratory epithelium: A cautionary note. Am J Respir Cell Mol Biol 34: 519–520.
11. Morimoto M, Kopan R (2009) rtTA toxicity limits the usefulness of the SP-C-rtTA transgenic mouse. Dev Biol 325: 171–178.
12. Yao F, Svensjo T, Winkler T, Lu M, Eriksson C, et al. (1998) Tetracycline repressor, tetR, rather than the tetR-mammalian cell transcription factor fusion derivatives, regulates inducible gene expression in mammalian cells. Hum Gene Ther 9: 1939–1950.
13. Nghiem P, Park PK, Kim Y, Vaziri C, Schreiber SL (2001) ATR inhibition selectively sensitizes G1 checkpoint-deficient cells to lethal premature chromatin condensation. Proc Natl Acad Sci U S A 98: 9092–9097.
14. Trapani JG, Korn SJ (2003) Control of ion channel expression for patch clamp recordings using an inducible expression system in mammalian cell lines. BMC Neurosci 4: 15.
15. Reeves PJ, Callewaert N, Contreras R, Khorana HG (2002) Structure and function in rhodopsin: high-level expression of rhodopsin with restricted and homogeneous N-glycosylation by a tetracycline-inducible N-acetylglucosaminyltransferase I-negative HEK293S stable mammalian cell line. Proc Natl Acad Sci U S A 99: 13419–13424.
16. van de Wetering M, Oving I, Muncan V, Pon Fong MT, Brantjes H, et al. (2003) Specific inhibition of gene expression using a stably integrated, inducible small-interfering-RNA vector. EMBO Rep 4: 609–615.
17. Wiederschain D, Wee S, Chen L, Loo A, Yang G, et al. (2009) Single-vector inducible lentiviral RNAi system for oncology target validation. Cell Cycle 8: 498–504.
18. Abu-Hamad S, Sivan S, Shoshan-Barmatz V (2006) The expression level of the voltage-dependent anion channel controls life and death of the cell. Proc Natl Acad Sci U S A 103: 5787–5792.
19. Yao F, Theopold C, Hoeller D, Bleiziffer O, Lu Z (2006) Highly efficient regulation of gene expression by tetracycline in a replication-defective herpes simplex viral vector. Mol Ther 13: 1133–1141.
20. Ogueta SB, Yao F, Marasco WA (2001) Design and in vitro characterization of a single regulatory module for efficient control of gene expression in both plasmid DNA and a self-inactivating lentiviral vector. Mol Med 7: 569–579.
21. Cockrell AS, Kafri T (2007) Gene delivery by lentivirus vectors. Mol Biotechnol 36: 184–204.
22. Escors D, Breckpot K (2010) Lentiviral vectors in gene therapy: their current status and future potential. Arch Immunol Ther Exp (Warsz) 58: 107–119.
23. Kafri T, van Praag H, Gage FH, Verma IM (2000) Lentiviral vectors: regulated gene expression. Mol Ther 1: 516–521.
24. Licursi M, Christian SL, Pongnopparat T, Hirasawa K (2011) In vitro and in vivo comparison of viral and cellular internal ribosome entry sites for bicistronic vector expression. Gene Ther 18: 631–636.
25. Demaison C, Parsley K, Brouns G, Scherr M, Battmer K, et al. (2002) High-level transduction and gene expression in hematopoietic repopulating cells using a human immunodeficiency [correction of imunodeficiency] virus type 1-based lentiviral vector containing an internal spleen focus forming virus promoter. Hum Gene Ther 13: 803–813.
26. Haack K, Cockrell AS, Ma H, Israeli D, Ho SN, et al. (2004) Transactivator and structurally optimized inducible lentiviral vectors. Mol Ther 10: 585–596.
27. Toscano MG, Benabdellah K, Munoz P, Frecha C, Cobo M, et al. (2009) Was cDNA sequences modulate transgene expression of was promoter-driven lentiviral vectors. Hum Gene Ther 20: 1279–1290.
28. Toscano MG, Frecha C, Ortega C, Santamaria M, Martin F, et al. (2004) Efficient lentiviral transduction of Herpesvirus saimiri immortalized T cells as a model for gene therapy in primary immunodeficiencies. Gene Ther 11: 956–961.
29. Rodriguez R, Meuth M (2006) Chk1 and p21 cooperate to prevent apoptosis during DNA replication fork stress. Mol Biol Cell 17: 402–412.

ARTÍCULO ENVIADO

CELL TRANSPLANTATION
The Regenerative Medicine Journal

Mesenchymal stem cells expressing vasoactive intestinal peptide ameliorate symptoms in a model of chronic multiple sclerosis

Journal:	*Cell Transplantation*
Manuscript ID:	Draft
Manuscript Type:	Original Article
Date Submitted by the Author:	n/a
Complete List of Authors:	Cobo, Marien; GENYO (Pfizer-University of Granada-Andalusian Government Centre for Genomic, Genomic variability Anderson, Per; GENYO (Pfizer-University of Granada-Andalusian Government Centre for Genomic, Genomic variability Benabdellah, Karim; GENYO (Pfizer-University of Granada-Andalusian Government Centre for Genomic, Genomic variability Toscano, Miguel; GENYO (Pfizer-University of Granada-Andalusian Government Centre for Genomic, Genomic variability Muñoz, Pilar; GENYO (Pfizer-University of Granada-Andalusian Government Centre for Genomic, Genomic variability Gutierrez, Iván; Biobanco-CIBM- Consejería de Salud Delgado, Mario; IPB Lopez Neyra (CSIC), Immunology Martin, Francisco; GENYO (Pfizer-University of Granada-Andalusian Government Centre for Genomics, Genomic variability
Keywords:	Mesenchymal stem cell, cell and gene therapy, lentiviral vectors, vasoactive intestinal petide, experimental autoimmune encephalomyelitis(EAE)
Abstract:	Multiple sclerosis (MS) is a severe debilitating disorder characterised by progressive demyelination and axonal damage of the central nervous system (CNS). Current therapies for MS inhibit the immune response and demonstrate reasonable benefits if applied during the early phase of relapsing-remitting MS while there are no treatments for patients that progress neither to the chronic phase nor for the primary progressive form of the disease. In this manuscript we study the therapeutic efficacy of a cell & gene therapy strategy for the treatment of a mouse model of chronic MS (MOG-induced experimental autoimmune encephalomyelitis (EAE)). We used mesenchymal stem cells (MSCs) as a therapeutic tool and also as vehicle to deliver vasoactive intestinal peptide (VIP) to the peripheral immune organs and to the inflamed central nervous system. Intra-peritoneal administrations of MSCs expressing VIP stopped progression and reduced symptoms when administered at peak of disease. The improvement in clinical score correlated with diminished peripheral T cell responses against MOG as well as lower inflammation, lower demyelination and higher neuronal integrity at the CNS. Interestingly, neither lentiviral vectors expressing VIP nor unmodified MSCs were therapeutic when

	administer at peak of disease. The increased therapeutic effect of MSC expressing VIP over unmodified MSC requires the immunoregulatory and neuroprotective roles of both VIP and MSCs and the ability of the MSCs to migrate to peripheral lymph organs and the inflamed CNS. Abstract.doc

Mesenchymal stem cells expressing vasoactive intestinal peptide ameliorate symptoms in a model of chronic multiple sclerosis.

Marién Cobo[1,*], Per Anderson[1,*], Karim Benabdellah[1], Miguel G. Toscano[1], Pilar Muñoz[1], Iván Gutierrez[2], Mario Delgado[3] and Francisco Martin[1,$].

[1] GENYO (Pfizer-University of Granada-Andalusian Government Centre for Genomics and Oncological Research), Avd de la Ilustración 114. Parque Tecnológico Salud (PTS), Granada 18007, Spain

[2] Biobanco. Parque Tecnológico Salud (PTS). Armilla 18100. Universidad de Granada, Spain

[3] IPB Lopez Neyra. CSIC. Parque Tecnológico Salud (PTS). Armilla 18100, Granada. Spain

* Authors share first authorship

[$] Correspondence should be addressed to F.M. (francisco.martin@genyo.es). GENYO (Pfizer-University of Granada-Andalusian Government Centre for Genomics and Oncological Research), Avd de la Ilustración 114. Parque Tecnológico Salud (PTS), Granada 18007, Spain. Telephone: 34958637103. FAX: 34958637071

Abstract

Multiple sclerosis (MS) is a severe debilitating disorder characterised by progressive demyelination and axonal damage of the central nervous system (CNS). Current therapies for MS inhibit the immune response and demonstrate reasonable benefits if applied during the early phase of relapsing-remitting MS while there are no treatments for patients that progress neither to the chronic phase nor for the primary progressive form of the disease. In this manuscript we have studied the therapeutic efficacy of a cell & gene therapy strategy for the treatment of a mouse model of chronic MS (MOG-induced experimental autoimmune encephalomyelitis (EAE)). We used mesenchymal stem cells (MSC) as a therapeutic tool and also as vehicle to deliver vasoactive intestinal peptide (VIP) to the peripheral immune organs and to the inflamed central nervous system. Intra-peritoneal administrations of MSC expressing VIP stopped progression and reduced symptoms when administered at peak of disease. The improvement in clinical score correlated with diminished peripheral T cell responses against MOG as well as lower inflammation, lower demyelination and higher neuronal integrity in the CNS. Interestingly, neither lentiviral vectors expressing VIP nor unmodified MSC were therapeutic when administer at the peak of disease. The increased therapeutic effect of MSC expressing VIP over unmodified MSC requires the immunoregulatory and neuroprotective roles of both VIP and MSC and the ability of the MSC to migrate to peripheral lymph organs and the inflamed CNS.

Key words

Mesenchymal stem cell, cell and gene therapy, lentiviral vectors, vasoactive intestinal petide, experimental autoimmune encephalomyelitis (EAE), multiple sclerosis.

Introduction

Multiple sclerosis (MS) is a severe debilitating disorder characterised by progressive demyelination and axonal damage of the central nervous system (CNS). Although the exact causes that trigger disease development are not known, it is generally accepted that MS starts when autoreactive T cells infiltrate the CNS and mount a demyelinating immune attack. MS usually begins as a relapsing-remitting (RRMS) disease which in about 65% of the cases, develops into secondary-progressive MS (SPMS). RRMS is characterized by periods of acute disability followed by periods of functional recovery. In this form of the disease, the resolution of inflammation is followed by remyelination of damaged axons and partial or complete recovery of the symptoms. However, the SPMS is associated with chronic microglia activation and a steady disease progression due to heavy axonal loss and neurodegeneration. In general, the currently approved MS therapies (e.g. IFN-beta, glatiramer acetate and mitoxantrone), inhibit the immune response and demonstrate thus greater benefits on RRMS compared to SPMS, postponing the secondary progressive phase. Approved therapies of MS are also associated with side effects including depression, multifocal leukoencephalopathy and hypersensitivity reactions warranting the development of safer and more effective therapies, especially for SPMS.

Mesenchymal stromal cells (MSC) have emerged as a promising therapy of MS because of their ability to migrate into sites of inflammation, suppress the immune response and protect neuronal cell death through the release of neuroprotective factors or possibly through transdifferentiation of MSC into neurons or oligondendrocytes (see (16) and (42) for review). Bone marrow derived MSC (BM-MSC) have traditionally been used in most

preclinical and clinical trials, although other potential sources are umbilical cord, endometrial polyps, menses blood, peripheral blood and adipose tissue. (13). Adipose tissue-derived MSC (ASC) are emerging as an attractive replacement because of their promising therapeutic effects and readily available, non-invasive source in using lipoaspirates (21). ASCs resemble their bone marrow derived counterpart but some differences in gene expression profile, phenotype and proliferative capacity exist. Importantly, ASCs possess an equal or more potent immunosuppressive capacity compared to BM-MSC (39) and inhibit pathologies in several animal models of autoimmunity and inflammation (18).

Experimental autoimmune encephalomyelitis (EAE) is a clinically relevant model of MS which has given rise to several approved MS therapies, including IFN-beta (reviewed in (46)). Systemic administration of MSC has shown to ameliorate EAE by inhibiting the expansion and cytokine production by autoreactive T-helper (Th)1 and Th17 cells resulting in a decrease in CNS demyelination (4). However, whereas MSC administration readily ameliorates disease symptoms in murine EAE, human trials for the treatment of MS have given less impressive results. The number of MSC injected is most likely an important factor contributing to the discrepancy. In animal studies the normal dose is 40-80 x 10^6 cells/kg whereas in human trials the cell number has averaged 2 x 10^6 cells/kg due to limitations in the expansion potential of MSC in vitro. Increasing the potency of MSC through forced expression of therapeutic genes could be a step in the right direction towards a successful MSC-based therapy of MS.

Several groups have attempted to increase therapeutic potential of MSC by expressing different genes (see (33) and (31) for review). The aim is to enhance the homing

capacity and increase the immunomodulatory and neuroregenerative potential of MSC by delivering new therapeutic agents to areas of inflammation. In this strategy MSC have two roles, 1- to deliver the therapeutic transgene to peripheral immune tissues and to the damaged CNS and 2- to make use of its natural immunomodulatory and neuroprotective capabilities to protect the damaged CNS. For instance, MSC/interleukin-10 (IL-10) prevent lung ischemia-reperfusion injury (30), MSC/neurotrophin-3, MSC/bone morphogenetic protein (BMP)-9 and MSC/BMP-2 all improved spinal fusion (14,32,49), MSC/angiopoietin-1 + vascular endothelial growth factor (VEGF) and MSC/placental growth factor (PlGF) improved cerebral ischemia (27,44), MSC/CXCR4 improved post-infarction myocardial repair (6), MSC/transforming growth factor beta1 (TGFbeta1) and MSC/BMP-2 improves cartilage repair (35,36) and MSC/brain-derived neurotrophic factor (BDNF) promote functional recovery and reduce infarct size (26).

Vasoactive intestinal peptide (VIP) is a neuropeptide of 28 amino acids with a broad spectrum of biological activities including immunoregulation (dampening T cell responses and lowering inflammation) and neuroprotection (through blocking microglial activation and induction of ADNF and ADNP neuroprotective factors). We and others have demonstrated important therapeutic effects of systemic delivery of synthetic VIP in several animal models of autoimmune diseases (see (9) for review). In addition, a recent phase I/II clinical trial in patients with sarcoidosis demonstrated that inhalation of VIP decreased the levels of inflammatory markers in lung and increased the number of suppressive regulatory T cells (38). However, multiple doses of high concentration of the peptide are required to obtain the beneficial effects. In addition, the instability of the peptide makes this strategy difficult to perform and highly variable, especially when VIP is systemically administered.

In order to improve delivery of VIP into target organs we have previously developed a lentiviral vector expressing VIP cDNA (LentiVIP) (12). A single injection of LentiVIP in a mouse model of severe rheumatoid arthritis (RA) provided a highly effective treatment with complete regressions in established disease associated with reduction of the autoimmune and inflammatory responses. In another study we developed tolerogenic dendritic cells (DC) by transducing DCs with LentiVIP during differentiation from bone marrow cells (43). A single administration of LentiVIP-DC proved therapeutic when administered before onset of EAE by reducing IL-1β, TNF-α and IL-6 and increasing IL-10. However, in spite of their potential, the difficulties to scale up DCs/LentiVIP production could be a serious limitation for future clinical applications of this strategy. In addition, while allogeneic cells are a very interesting alternative when considering cell therapies as potential medicaments, the use of allogeneic DC/LentiVIP is not an alternative due to their potential side effects. We have therefore looked for alternative therapeutic strategies aiming to treat MS.

In the present manuscript we have studied the therapeutic efficiency of MSC expressing VIP (MSC/LentiVIP) for the treatment of a mouse model of chronic MS (MOG-induced EAE in C57Bl/6 mice) and compare it with the effects of direct injection of LentiVIP particles and unmodified MSC. We obtained routinely over 10^8 MSC/LentiVIP cells secreting VIP. We showed that direct injection of LentiVIP particles did not result in LentiVIP expression in CNS and was not effective for the treatment of chronic EAE. In contrast, injection of MSC/LentiVIP (but not unmodified MSC) into mice with severe established disease ameliorated disease symptoms. The therapeutic efficacy of MSC/LentiVIP treatment correlated with a stronger suppression of the autoimmune T cell

response and less CNS inflammation/damage compared to treatment with MSC or with unmodified MSC.

Results

Direct injection of LentiVIP particles into mice with established chronic EAE lack therapeutic effect

Repetitive administration of exogenous VIP has shown to inhibit disease in both relapsing/remitting and chronic models of EAE in mouse (20). However, VIP is rapidly subjected to proteolytic degradation in vivo substantially lowering potency and clinical applicability of exogenous peptide administration (17). In order to improve therapeutic efficiency of VIP for the treatment of autoimmune diseases we have previously developed a lentiviral vector driving the expression of preproVIP cDNA (LentiVIP) (12) (Figure S1). A single injection of LentiVIP particles enhanced the therapeutic benefits achieved by VIP peptide in a collagen-induced arthritis (CIA) mice model of RA (12). We hypothesized that a similar strategy could also be applied to improve therapeutic strategies for MS. We induced chronic EAE in C57Bl/6 mice using the myelin oligodendrocyte glycoprotein (MOG)35-55 peptide and the animals were intraperitoneally inoculated with an average of 10^8 tu (transduction units) of LentiVIP at the peak of disease (mice with an EAE score of 3-4, see scoring in materials and methods). Contrary to what we found in the CIA model, we could not observe any significant therapeutic effect when the LentiVIP particles were administered at the peak of disease (**Fig. 1**). We detected vector genomes and vector-derived VIP expression in spleen, draining lymph nodes (DLN) and liver (Table 1) but we were unable to detect the vector neither in the brain nor in spinal cord.

MSC/LentiVIP secrete a more stable form of VIP while maintaining the main properties of MSC.

In order to achieve an improved MS therapy we designed a combined gene-cell therapy strategy in which we wanted to combine the anti-inflammatory and neuroprotective properties of VIP with two main characteristics of MSC: (1) the migratory potential of MSC toward inflamed tissues (acting as a vehicle to deliver VIP to the damaged CNS), and (2) the immunoregulatory and neuroprotective properties. Non-transduced MSC did not express nor secrete VIP, neither under resting conditions nor after stimulation with LPS or inflammatory cytokines (Figure S2, Figure S3 and data not shown). However, transduction of MSC at an early passage with LentiVIP (MSC/LentiVIP) resulted in the stable expression of VIP transgene for at least 15 passages in vitro (**Fig. 2a**). MSC/LentiVIP cell lines secreted high levels of VIP protein as evidenced by the detection of VIP and/or preproVIP (the unprocessed polypeptide resulting from VIP gene expression) in the supernatant (**Fig. 2b** and Figure S3). Expression levels varied from 1-2 ng/ml (**Fig. 2b,** right graph, 0h). Importantly the MSC-secreted VIP was more stable than the synthetic VIP peptide at 37ºC (**Fig. 2b,** left versus right graph). We have previously shown that supernatant from LentiVIP-transduced 293T cells induced cAMP and decreased LPS-induced TNF-alpha production in macrophages, showing that the lentivirally produced VIP is biologically active (12). Independently of the expression levels, the MSC/LentiVIP cell lines maintained their main phenotypic characteristics in terms of morphology, differentiation potential and membrane expression markers (Figure S4 and data not shown).

All MSC populations expressed similar levels of Sca-1, CD29 and CD44 while lacking expression of CD45 and MHC class II.

MSC inhibit T cell proliferation induced by anti-CD3/CD28 antibodies, concanavalin A (ConA) and mixed leukocyte reactions (MLR) (50). VIP has also been shown to inhibit the proliferation and cytokine production by murine T cells (34) and to inhibit the maturation of dendritic cells (11). In order to assess a possible contribution of VIP to the MSC-mediated suppression we activated splenocytes with ConA in the presence or absence of increasing numbers of non-transduced MSC, MSC/LentiGFP or MSC/LentiVIP. All MSC populations inhibited splenocyte proliferation to the same extent in a dose dependent manner (**Fig. 2c**). We did observe a small but consistent increase in suppressive activity in MSC expressing VIP but the difference did not reach statistical significance.

A single dose of MSC/LentiVIP at the peak of disease improves survival and reduces EAE severity.

Next, we wanted to assess the potential of VIP-expressing MSC on established disease in which both immunomodulation and neuroprotection would be beneficial. Most studies on the therapeutic effect of MSC on EAE have administered the MSC before or early after disease onset (40). However, once the disease is approaching its peak many therapies lose their beneficial effects as have been seen in both mouse studies and with human MS drugs (15,45). We therefore explored the therapeutic potential of MSC/LentiVIP in the MOG-induced EAE model of chronic MS at peak of disease (average score 3.3; complete paralysis of back legs and partial paralysis of front legs). We selected cell lines secreting

about 2 ng/ml of VIP and expanded them for 4-5 passages. EAE mice were injected intraperitoneally with 10^6 MSC/LentiVIP, MSC/LentiGFP or non-transduced MSC. Only MSC/LentiVIP were able to significantly reduce EAE severity (**Fig. 3a** and Table 2), while most of the mice treated with MSC alone or MSC/LentiGFP progressed from moderate to severe EAE. This was corroborated when the cumulative disease index (CDI) was determined: MSC/LentiVIP decreased CDI to 131±32 (p=0,001) in comparison to untreated (245±60), MSC- (226±65) and MSC/LentiGFP-treated mice (227±74) (Table 2). The differences in EAE score between MSC- and MSC/LentiVIP-treated mice started to be significant from day 4 after treatment. The MSC/LentiVIP-treated mice recovered from complete hind leg paralysis toward a moderate hind leg paresis whereas the remaining groups developed a more aggressive disease (**Fig. 3a** and Table 2). Of note, none of the MSC/LentiVIP treated mice required to be sacrificed by the disease, while 50%, 60% and 70% of the mice treated with MSC, MSC/LentiGFP and PBS respectively were sacrificed or died from EAE severity (Table 2). MSC-derived VIP could be detected in spleen, liver, kidney and peripheral LNs. Importantly, in contrast to the LentiVIP particles, MSC-derived VIP could be detected in both brain and spinal cord (Table 1) suggesting that MSC/LentiVIP have the capacity to migrate into the inflamed CNS. No difference between MSC/lentiGFP and non-transduced MSC were found in the in vivo experiments prompting us to use non-transduced MSC for the further mechanistic studies in vivo.

MSC/LentiVIP significantly reduce MOG-specific T cell proliferation but do not induce Foxp3+ Tregs

An important event in EAE and MS is the activation and expansion of autoreactive T cells secreting either IFN-gamma (Th1) or IL-17 (Th17) in peripheral lymphoid organs followed by their infiltration into the brain. Thus, to find an explanation for the improved therapeutic effect of MSC/LentiVIP compared to nontransduced MSC we set out to analyze the MOG35-55 specific recall response in draining LNs of immunized mice.

We found that MOG-specific proliferation of lymph node cells from MSC/LentiVIP treated mice was significantly lower compared to MSC-treated or untreated control mice suggesting that the secretion of VIP increases the immunosuppressive capacity of MSC in vivo (**Fig. 3b,** left). The effect was antigen specific since activation of total T cells with anti-CD3 resulted in similar proliferation in all three groups (**Fig. 3b**, right).

MSC have been shown to induce or expand the population of regulatory T cells (Treg) expressing Foxp3 in models of allergy driven airway inflammation and arthritis (25) (22). However, the case is less clear in EAE with only few studies analyzing the frequency of these cells with contradictory results (48) (28). In contrast, VIP has been demonstrated to induce Foxp3 expressing T cells in draining LNs with immunosuppressive capacity in many models of autoimmune disease (19). We thus assessed the possible induction of Foxp3-expressing T-cells in response to MSC or MSC/LentiVIP in EAE. As can be seen in **Fig. 3c** we did not observe a significant increase in $CD4^{+}Foxp3^{+}$ T cells in either draining LNs or spleen. Apart from the Foxp3+ Tregs there exist several Foxp3-negative T cell populations with regulatory function which suppress T cell responses through the secretion of IL-10 (1). However, we did not detect increased levels of IL-10 or IL-4 in ex vivo cultures of splenocytes or cells from draining LNs stimulated with MOG suggesting that

MSC/LentiVIP did not induce IL-10 producing Tregs or a skewing towards a Th2 response (data not shown).

MSC/LentiVIP administration reduced inflammation, increased expression of neuroprotective factors and reduced neuronal degeneration in the inflamed CNS.

In addition to autoreactive T cells, monocytes enter the CNS where they, along with activated astrocytes and microglia, secrete high levels of proinflammatory cytokines and nitric oxide (NO) resulting in axonal damage and neuronal degeneration. In the progressive stage the innate immunity predominates and any treatment for the chronic stage of MS needs to inactivate the diffuse inflammation that drives the axonal degeneration and subsequent neuronal cell death. We therefore studied the effect of MSC/LentiVIP on CNS inflammation and on neurodegeneration. EAE mice were injected with either non-transduced MSC or with MSC/LentiVIP at the peak of disease and five days later sacrificed to obtain brain and spinal cord samples. The different samples were analyzed by RT-Q-PCR and immunohistochemistry for expression of markers of inflammation (IL-17, inducible nitric oxide synthase (iNOS), TNF-α, IL-6, glial fibrillary acidic protein (GFAP) and CD11b), immune regulation (IL-10, Foxp3), neuroprotection (activity-dependent neuroprotective protein (ADNP), BDNF and neurodegeneration (β-amyloid, β-tubulin). We found a significant decrease in the transcript levels of the proinflammatory cytokines IL-17, TNF-alpha, IL-6 and iNOS in the spinal cords of both MSC- and MSC/LentiVIP- treated mice (**Fig. 4**). In contrast, IL-10 was increased in both groups compared to untreated mice, although significance was only reached in the MSC/LentiVIP group. In addition, we

observed increased *Foxp3* mRNA in the MSC/LentiVIP group compared with the MSC and untreated groups but the differences were not significant.

VIP has been shown to induce the secretion of the neuroprotective factors BDNF-1,-3, -5 (41) and ADNP by astrocytes (24). However, we observed significant increases in BDNF and ADNP mRNA levels in both MSC- and MSC/LentiVIP-treated mice (**Fig. 4**). Although the Q-PCR data indicates a role of lowering inflammation and increasing neuroprotection in the therapeutic effect of MSC/LentiVIP administration, it does not reveal the differential mechanism that could explain the increased therapeutic benefits of MSC/LentiVIP over MSC.

In contrast, immunohistochemical analysis of CNS tissue from control, MSC- or MSC/LentiVIP-treated mice showed that MSC/LentiVIP were more efficient compared to nontransduced MSC in decreasing both astrogliosis (GFAP) and number of macrophages/activated microglia in the parenchyma (CD11b) (**Figs. 5a,b**). Immunohistochemical analysis of beta-amyloid protein expression, which is a marker for neuronal degeneration, showed that MSC/LentiVIP, but not nontransduced MSC, significantly decreased beta-amyloid expression in the inflamed brain. This correlated with significantly higher levels of the neuronal marker beta-tubulin in the MSC/LentiVIP treated group compared with the untreated or MSC-treated groups. These results were confirmed by the analysis performed at day 50 after treatment. At this stage, MSC/LentiVIP treated mice showed higher levels of beta-tubulin, increased myelin integrity and lower numbers of beta-amyloid bodies compared with MSC-treated or untreated mice (Figure S5). Taken together, these data suggest that although both MSC and MSC/LentiVIP-treatment decrease

CNS levels of proinflammatory cytokines (**Fig. 4**), MSC/LentiVIP are more efficient in limiting the immune-mediated damage to the CNS (**Fig. 5**).

Discussion

In the present manuscript we have developed a new gene-cell therapy strategy for chronic EAE that combines the therapeutic benefits of VIP and MSC. We have previously reported that a single injection of LentiVIP in a mouse model of severe RA resulted in a systemic expression of LentiVIP (spleen, lung, DLN and joints) and provided a highly effective treatment with complete regression of established disease associated with reduction of the autoimmune and inflammatory responses (12). However, in the present study we have shown that the same strategy had no effect on established disease in a model of chronic EAE.

The reason for this discrepancy could be two-fold. Firstly, in the RA model we observed LentiVIP expression both in peripheral lymphoid organs and at the site of inflammation and tissue destruction, i.e. the joints, whereas in the EAE model we could not detect VIP expression in the CNS, the target of the autoimmune attack. Secondly, in the RA model LentiVIP increased the number of Foxp3+ Tregs both in peripheral LNs and in the joints whereas in the EAE model we could not detect an increase in Foxp3+ Tregs (data not shown). This suggests that, although the LentiVIP particles do reach peripheral lymphoid organs, the treatment fails because the virus particles cannot reach the inflamed CNS.

Thus, new therapies for chronic MS must attempt not only the inhibition of the peripheral autoimmune response against CNS antigens but also stop the ongoing CNS inflammation and induce remyelination and/or neuroprotection of damaged neurons. Recently, MSC have emerged as a promising tool for the delivery of therapeutic molecules to the CNS for several reasons(42,45). Firstly, MSC have been shown to home to secondary

lymphoid organ and to sites of tissue injury where they inhibit inflammation/immune responses and might contribute to tissue regeneration (reviewed in (5) (47)). Secondly, administration of MSC per se has been shown to infiltrate the CNS and ameliorate chronic and relapsing/remitting EAE (4). Thirdly, MSC can easily be isolated from different sources such as bone marrow, cord blood or adipose tissue and expanded in vitro. We therefore used MSC, transduced with LentiVIP (MSC/LentiVIP), with the aim of (1) achieve VIP expression in the damaged CNS and (2) implement the MSC own immunoregulatory and neuroprotective properties thereby reinforcing the therapeutic potential of both agents on chronic EAE/MS.

We first showed that transduction of MSC with LentiVIP resulted in a high and sustained expression of stable VIP which did not significantly affect the biological properties of MSC, including their ability to suppress T cell responses in vitro. We then studied the therapeutic effect of intraperitoneal MSC/LentiVIP administration in chronic EAE. Contrary to direct injection of LentiVIP particles, systemic injection of MSC/LentiVIP to mice with severe EAE (complete paralysis of back legs and partial paralysis of front legs) significantly reduced EAE symptoms. Treated mice regained their ability to walk with their hind legs although they still exhibited partial paresis. In contrast to direct injection of Lentiviral particles encoding for VIP, administration of MSC/LentiVIP resulted in the detection of LentiVIP transcripts in the CNS. In our hands, neither MSC nor MSC/LentiGFP reached any significant therapeutic activity at this stage of disease suggesting that the combination of the biological effects of both VIP and MSC are necessary to achieve therapeutic benefits in chronic disease.

The innate immune response predominates in chronic MS and T cell infiltration into the CNS gray and white matter is low in both primary and secondary progressive MS. However, larger numbers of T cells have been found in the meninges where they produce IFN-gamma and are thought to interact with inflammatory macrophages (3). In addition IL-17 transcripts are upregulated in chronic MS lesions (29) highlighting the involvement of T cells in chronic MS. Functional studies demonstrated that MSC/LentiVIP administration was more potent compared to MSC alone in inhibiting the in vivo antigen-specific T cell autoimmune responses in peripheral LNs. Both MSC (50) and VIP(8) have been shown to induce DCs with lower expression of costimulatory molecules that are defective in inducing T cell responses. Importantly, VIP can directly induce cell cycle arrest at multiple levels and anergy in activated human T cells (2,37). Thus, we suspect that MSC/LentiVIP could induce a state of unresponsiveness/anergy in T cells both during their initial activation in the LNs but also in activated T cells present in the periphery or in the CNS.

The inhibition of the T cell response did not correlate with increased numbers of $Foxp3^+$ Tregs nor higher IL-10 expression levels in draining LNs or spleens in MSC/LentiVIP-treated mice compared to MSC alone. The role of Foxp3+ Tregs is MS is not well known. Tregs appear to have impaired function in RRMS, and they are not readily detected in MS lesions (reviewed in (23)). Whether or not MSC induce functional Tregs in EAE is also not clear (48). Our results showed that MSC/LentiVIP did not increase the frequency of CD4+Foxp3+ T cells in the draining LNs, despite the expression of VIP. We did detect a small increase in of *Foxp3* mRNA in the CNS of mice treated with MSC/LentiVIP compared with those treated with MSC but these differences were not significant.

In the CNS both MSC/LentiVIP and MSC significantly inhibited the expression of proinflammatory cytokines and iNOS compared to control mice. However, at day 50, myelin immunoreactivity in the CNS from MSC/LentiVIP-treated mice was significantly higher compared to MSC-treated or control mice showing that the MSC/LentiVIP cells were more efficient in inhibiting the demyelinating immune attack and/or increasing remyelination in the CNS. Brain tissue sections from MSC/LentiVIP-treated mice showed lower GFAP (a marker of astrocyte activation) staining compared to both MSC- or PBS-treated mice. The reduction in astrocyte activation could be the consequence of the reduced neuronal cell death in MSC/LentiVIP-treated mice which was evidenced by the lower accumulation of beta-amyloid deposits and higher levels of beta-tubulin immunoreactivity in the CNS. The decrease in neurodegeneration could also be explained by the potent neuroprotective effects of VIP through the inactivation of microglia (10) or modulation of astrocyte activity (7). VIP induces BDNF and ADNP which are growth factors involved in neuroprotection (41), therefore it is reasonable to hypothesize that the enhanced effect observed with MSC/LentiVIP could be due to enhanced BDNF and/or ADNP production. However, we observed similar BDNF and ADNP increments in MSC/LentiVIP- and MSC-treated mice, although the levels were increased in both groups compared to untreated controls. Although the specific mechanism explaining the MSC/LentiVIP-mediated effects remain elusive we propose the following events as instrumental in achieving the therapeutic effect observed by intraperitoneal administration of MSC/LentiVIP: (1) the increased inhibition of autoimmune T cells, (2) the reduction in astrogliosis that results in a reduced infiltration of $CD11b^{+}$ cells and (3) the increased neuronal survival.

In summary, we have demonstrated the therapeutic potential of gene-cell based strategies for treatment of chronic EAE, an animal model for multiple sclerosis. In particular we have demonstrated that MSC can be used to deliver VIP and that this combination is far more efficient than the use of MSC or Lentiviral vectors expressing VIP alone. The easy growth of MSC and the integration of Lentiviral vectors allow the design of easy protocols to scale up the number of MSC/LentiVIP for the potential application in human patients. In addition the possibility of using allogeneic MSC opens up the possibility of banking gene-modified cells for in detail analyses before clinical use.

Materials and Methods

Plasmids and lentiviral constructs

The HIV packaging (pCMVΔR8.91) and VSV-G (pMD.G) plasmids were kindly provided by D. Trono (University of Geneva, Geneva, Switzerland).. The packaging plasmid pCMVΔR8.91 encodes *gag*, *pol*, *tat* and *rev* genes. The pMD.G plasmid encodes the vesicular stomatitis virus G (VSVg) glycoprotein. The LentiGFP (CEWP) and LentiVIP lentiviral vectors express eGFP and VIP, respectively, through the strong CMVTetO promoter. They were constructed as previously described (12).

Isolation and culture of MSC

Mesenchymal stem cells (MSC) were isolated from abdominal fat from male Balb/c mice (Charles River, Barcelona, Spain). The fat was aseptically removed and washed twice in HBSS. The fat tissue was weighed, cut into small pieces (≤ 2 mm^3) and resuspended in 2,5 ml of Hank´s balanced salt solution (HBSS; GIBCO, Invitrogen, Carlsbad, CA) containing 2 mg/ml collagenase type I (Sigma Aldrich, St.Louis, MO) per gram fat tissue and incubated for 30 minutes at 37°C, swirling the tube every 5 minutes. The digest was washed twice with 10 ml HBSS and filtered each time through a 100 μm cell strainer. The cells were washed with HBSS again and filtered through a 40 μm cell strainer. Finally, cells were resuspended in complete MesenCult (Stem Cell, Grenoble, France) medium

containing 100 units/ml penicillin/ streptomycin (Gibco, Invitrogen) and 20% mouse mesenchymal supplements (Stem Cell) and plated at a density of 15-30000 cells/cm^2 and cultured at 5% O_2. Non-adherent cells were removed after 24 hours in culture. Subsequent passages were plated at 5-10000 cells/cm^2 in complete MesenCult media. MSC/LentiVIP and MSC/lentiGFP were done by transduction with LentiVIP and LentiGFP vectors respectively.

Immunophenotypic analysis and Foxp3 staining

MSC, MSC/LentiVIP and MSC/LentiGFP were stained with APC-labeled antibodies against CD45, CD44, SCA1**,** MHCII and CD29 (eBioscience, San Diego, CA). For Foxp3 staining, cells from DLN and spleens were isolated from mice 5 days post-treatment and incubated with 7AAD (Sigma-Aldrich) and 24G2 (eBioscience) and stained with the FoxP3 staining kit (eBioscence) according to the manufacturer´s instructions. Cells were and acquired and analyzed on a BD FACS Canto II using the FACS Diva software (BD).

Vector production and titration

Lentiviral vectors were produced by co-transfection of 293T kidney cells with three plasmids: 1- Vector plasmid (CEWP or LentiVIP), 2- Packaging plasmid pCMVΔR8.9 and 3- Envelope plasmid pMD.G, as previously described using Lipofectamine 2000 (Invitrogen). Viral supernatants were collected and filtered through a 0.45 μm filter and immediately frozen at -80ºC or used to transduce MSC. Vector particles were concentrated

by ultrafiltration at 2000xg and 4ºC, using 100Kd Centrifugal filter devices (Amicon Ultra-15, Millipore, Billerica, MA). Vector titration was performed in 293T cells. CEWP vector titration was determined by the percentage of eGFP positive cells by FACS analysis 7 days post-transduction. For titration of LentiVIP vectors, transduced cells were lysed and DNA extracted after 7-10 days. Vector copy number per cell was determined using Q-PCR. Q-PCR was performed with MX3005Pro sequence detection system (Stratagene, Santa Clara, CA). Primer pairs: VIP: FW 5'-CCA CGC TGT TTT GAC CTC CAT, RV 5'-GGG CCT TAT TTC TGG TGT CCA T.

Determination of secreted VIP

MSC/LentiVIP, MSC/LentiGFP and MSC cells (4 x 10^5 cells/well in 2 ml) were seeded in 6-well plates and cultured for 48h before harvesting the supernatants. VIP levels were determined with an ELISA kit from Phoenix Pharmaceuticals (Phoenix Pharmaceuticals,Karlsruhe, Germany).

EAE induction and treatment

C57Bl/6 mice (5-7 weeks-old from Charles River) were injected subcutaneously (s.c.) with 100 µg of MOG_{35-55} (Genescript, Hong Kong, China) emulsified in complete Freund´s adjuvant (CFA) (Difco, Detroit, MI) containing 0.5 mg of *M. Tuberculosis* (Difco). Mice were injected intraperitoneal (i.p.) with 100 ng of pertussis toxin (Sigma-Aldrich), at the same day of immunization and 48h later. Lentiviral treatment consisted of a single i.p.

administration of $2x10^8$ copies of LentiVIP per mouse. As control, mice were injected with PBS or LentiGFP ($2x10^8$ copies/mouse). MSC treatment consisted in a single i.p. administration of 10^6 MSC, MSC/LentiGFP or MSC/LentiVIP per mouse when mice showed established disease (clinical score = 2.5-3.5). Clinical scores used: grade 0, no clinical signs; grade 1, complete loss of tail tonicity; grade 2, flaccid tail and abnormal gait; grade 3, hind leg paralysis; grade 4, hind leg paralysis with hind body paresis; grade 5, hind and fore leg paralysis; and grade 6, death. Mice that were in between the clear-cut gradations of clinical signs were scored intermediate in increments of 0.5.

Proliferation assays

To study the effect of MSC on T cell proliferation, MSC were irradiated at 42 Gy and plated in triplicates in 96-wells plates at 40000, 20000, 10000, 5000 and 0 cells/well. Splenocytes were isolated (erythrocytes were lysed) and added to the wells at 200.000 cells/well, and stimulated with concanavalin A (2.5 µg/ml) (Sigma-Aldrich). For the *in vitro* analysis of the MOG-specific recall responses cell suspensions were obtained from DLN of mice 4 days post-immunization. The cells were plated at $4x10^5$ cells/well in triplicates, and stimulate with MOG_{35-55} (50 µg/ml) and anti-CD3 (1 µg/ml) (eBioscience). In both cases, after 3 days cells were pulsed with 0,5 µCi/well [3H]-thymidine (Perkin Elmer, Waltham, MA) for 6 hours and harvested onto glass fiber filters using an LKB 96 well-harvester (Wallac Oy, Turku, Finland). Uptake of [3H]-thymidine was measured on a 1450 microbeta Trilux scintillation counter (Wallac).

Vector and cell distribution

The distribution of LentiVIP and MSC/LentiVIP was studied by Q-PCR. Primer pair: VIP: FW 5´-CAC CAC CTG TCA GCT CCT TT-3´; RV 5'-AAG CAG CGT ATC CAC ATA GCG-3´ PCR was performed by using QuantiTect SYBRGreen PCR kit (Qiagen, Hilden Germany) with MX3005Pro sequence detection system (Stratagene).

RNA extraction and quantification of transcripts

The RNA from mouse tissues was obtained using trizol reagent (Invitrogen). RNA samples were reverse-transcribed into cDNA using Superscript first-strand (Invitrogen). Q-PCR was performed by using the QuantiTect SYBRGreen PCR kit (Qiagen) in a Stratagene MX3005P system. Primer pairs: *IL17:* FW 5'-TTT AAC TCC CTT GGC GCA AAA-3', RV 5'-CTT TCC CTC CGC ATT GAC AC-3'; *iNOS:* FW 5'-GTT CTC AGC CCA ACA ATA CAA GA-3', RV 5'-GTG GAC GGG TCG ATG TC AC-3'; *TNFα*: FW 5´-GGC AGG TCT ACT TTG GAG TCA TTG C-3´, RV 5'-ACA TTC GAG GCT CCA GTG AAT TCG G-3´; *IL10*: FW 5'-CTG GAC AAC ATA CTG CTA ACC G-3', RV 5'-GGG CAT CAC TTC TAC CAG GTA A-3'; *IL6:* FW 5'-TAG TCC TTC CTA CCC CAA TTT CC-3', RV 5'-TTG GTC CTT AGC CAC TCC TTC-3'; *FoxP3:* FW 5'-CCC ATC CCC AGG AGT CTT G-3', RV 5'-ACC ATG ACT AGG GGC ACT GTA-3'; *ADNP:* FW 5´-AGA AAA GCC CGG AAA ACT GT-3´, RV 5´-AAG CAC TGC AGC AAA AAG GT-3´; *BDNF*: FW 5´-CCC TCC CCC TTT TAA CTG AA-3´, RV 5´-GCC TTC ATG CAA CCG AAG TA-3´.

Immunohistochemistry and staining quantification

Mice were sacrificed 7 or 50 days after treatment and brain and spinal cord were removed and immersed in OCT and frozen in chilled 2-methylbutane, and stored at -80ºC. Sections were cut at 4 µm and stained with antibodies against GFAP (Dako, Glostrup, Denmark), CD11b (Millipore), beta-amyloid (Sigma-Aldrich), beta-tubulin (Millipore), MBP (Millipore) and DAPI (Vectashield, Vector, Peterborough, UK). Histological examination was done using a Nikon Eclipse fluorescence microscope. An average of 10 different images per section was captured using a Nikon digital sight controller with the NIS-element BR 3.10 program. The acquisition conditions were always set up to background levels related to staining samples with isotype controls. Each image was then analyzed to measure number of spots/cells. For each antibody, the appropriate isotype control was used to set up the object count to zero. Sections from healthy and EAE mice were used to set up the conditions to measure the numbers of the desire spots. For that, both the area (px^2) and circularity parameters of the spots were restricted with the NIS element program to focus the quantification to the desired spots. Once the settings were established, all images (taken form tissue sections from the different treatments) were processed equally to determine number of spots.

Statistical Analysis

Results are expressed as mean ± SEM. The Mann-Whitney *U*-test to compare nonparametric data for statistical significance was applied on all results and cell-culture experiments.

Acknowledgments

This work has been supported by the Fondo de Investigaciones Sanitarias (FIS) grant PS09/00340 and Junta de Andalucia / FEDER grants (operative programme FEDER de Andalucia 2007-2013) P09-CTS-04532 and PAIDI-Bio-326 and PI0001/2009 to Francisco Martín. M.C. and F.M. are financed by Fundación Progreso y Salud (Consejería de Salud - Junta de Andalucía). K.B and M.G.T. are financed by P09-CTS-04532 and PI0001/2009 grants respectively. P.A. and P.M. have a Miguel Servet and Sara Borrell contracts respectively (Fondo de Investigaciones Sanitarias (FIS) - Institute of health Carlos III). There are no conflicts of Interest.

References

1. Anderson, C. F.; Oukka, M.; Kuchroo, V. J.; Sacks, D. CD4(+)CD25(-)Foxp3(-) Th1 cells are the source of IL-10-mediated immune suppression in chronic cutaneous leishmaniasis. J Exp Med 204(2):285-297; 2007.
2. Anderson, P.; Gonzalez-Rey, E. Vasoactive intestinal peptide induces cell cycle arrest and regulatory functions in human T cells at multiple levels. Mol Cell Biol 30(10):2537-2551; 2010.
3. Androdias, G.; Reynolds, R.; Chanal, M.; Ritleng, C.; Confavreux, C.; Nataf, S. Meningeal T cells associate with diffuse axonal loss in multiple sclerosis spinal cords. Annals of neurology 68(4):465-476; 2010.
4. Constantin, G.; Marconi, S.; Rossi, B.; Angiari, S.; Calderan, L.; Anghileri, E.; Gini, B.; Bach, S. D.; Martinello, M.; Bifari, F.; Galie, M.; Turano, E.; Budui, S.; Sbarbati, A.; Krampera, M.; Bonetti, B. Adipose-derived mesenchymal stem cells ameliorate chronic experimental autoimmune encephalomyelitis. Stem Cells 27(10):2624-2635; 2009.
5. Chamberlain, G.; Fox, J.; Ashton, B.; Middleton, J. Concise review: mesenchymal stem cells: their phenotype, differentiation capacity, immunological features, and potential for homing. Stem Cells 25(11):2739-2749; 2007.

6. Cheng, Z.; Ou, L.; Zhou, X.; Li, F.; Jia, X.; Zhang, Y.; Liu, X.; Li, Y.; Ward, C. A.; Melo, L. G.; Kong, D. Targeted migration of mesenchymal stem cells modified with CXCR4 gene to infarcted myocardium improves cardiac performance. Mol Ther 16(3):571-579; 2008.
7. Dejda, A.; Sokolowska, P.; Nowak, J. Z. Neuroprotective potential of three neuropeptides PACAP, VIP and PHI. Pharmacol Rep 57(3):307-320; 2005.
8. Delgado, M.; Chorny, A.; Ganea, D.; Gonzalez-Rey, E. Vasoactive intestinal polypeptide induces regulatory dendritic cells that prevent acute graft versus host disease and leukemia relapse after bone marrow transplantation. Ann N Y Acad Sci 1070:226-232; 2006.
9. Delgado, M.; Ganea, D. Anti-inflammatory neuropeptides: a new class of endogenous immunoregulatory agents. Brain Behav Immun 22(8):1146-1151; 2008.
10. Delgado, M.; Ganea, D. Vasoactive intestinal peptide prevents activated microglia-induced neurodegeneration under inflammatory conditions: potential therapeutic role in brain trauma. FASEB J 17(13):1922-1924; 2003.
11. Delgado, M.; Gonzalez-Rey, E.; Ganea, D. The neuropeptide vasoactive intestinal peptide generates tolerogenic dendritic cells. J Immunol 175(11):7311-7324; 2005.
12. Delgado, M.; Toscano, M. G.; Benabdellah, K.; Cobo, M.; O'Valle, F.; Gonzalez-Rey, E.; Martin, F. In vivo delivery of lentiviral vectors expressing vasoactive intestinal peptide complementary DNA as gene therapy for collagen-induced arthritis. Arthritis Rheum 58(4):1026-1037; 2008.
13. Ding, D. C.; Shyu, W. C.; Lin, S. Z. Mesenchymal stem cells. Cell Transplant 20(1):5-14; 2011.
14. Dumont, R. J.; Dayoub, H.; Li, J. Z.; Dumont, A. S.; Kallmes, D. F.; Hankins, G. R.; Helm, G. A. Ex vivo bone morphogenetic protein-9 gene therapy using human mesenchymal stem cells induces spinal fusion in rodents. Neurosurgery 51(5):1239-1244; discussion 1244-1235; 2002.
15. Freedman, M. S.; Bar-Or, A.; Atkins, H. L.; Karussis, D.; Frassoni, F.; Lazarus, H.; Scolding, N.; Slavin, S.; Le Blanc, K.; Uccelli, A. The therapeutic potential of mesenchymal stem cell transplantation as a treatment for multiple sclerosis: consensus report of the International MSCT Study Group. Mult Scler 16(4):503-510; 2010.
16. Garcia-Gomez, I.; Elvira, G.; Zapata, A. G.; Lamana, M. L.; Ramirez, M.; Castro, J. G.; Arranz, M. G.; Vicente, A.; Bueren, J.; Garcia-Olmo, D. Mesenchymal stem cells: biological properties and clinical applications. Expert Opin Biol Ther 10(10):1453-1468; 2010.
17. Goetzl, E. J.; Sreedharan, S. P.; Turck, C. W.; Bridenbaugh, R.; Malfroy, B. Preferential cleavage of amino- and carboxyl-terminal oligopeptides from vasoactive intestinal polypeptide by human recombinant enkephalinase (neutral endopeptidase, EC 3.4.24.11). Biochem Biophys Res Commun 158(3):850-854; 1989.
18. Gonzalez-Rey, E.; Anderson, P.; Gonzalez, M. A.; Rico, L.; Buscher, D.; Delgado, M. Human adult stem cells derived from adipose tissue protect against experimental colitis and sepsis. Gut 58(7):929-939; 2009.

19. Gonzalez-Rey, E.; Fernandez-Martin, A.; Chorny, A.; Delgado, M. Vasoactive intestinal peptide induces CD4+,CD25+ T regulatory cells with therapeutic effect in collagen-induced arthritis. Arthritis Rheum 54(3):864-876; 2006.
20. Gonzalez-Rey, E.; Fernandez-Martin, A.; Chorny, A.; Martin, J.; Pozo, D.; Ganea, D.; Delgado, M. Therapeutic effect of vasoactive intestinal peptide on experimental autoimmune encephalomyelitis: down-regulation of inflammatory and autoimmune responses. Am J Pathol 168(4):1179-1188; 2006.
21. Gonzalez-Rey, E.; Gonzalez, M. A.; Varela, N.; O'Valle, F.; Hernandez-Cortes, P.; Rico, L.; Buscher, D.; Delgado, M. Human adipose-derived mesenchymal stem cells reduce inflammatory and T cell responses and induce regulatory T cells in vitro in rheumatoid arthritis. Ann Rheum Dis 69(1):241-248; 2010.
22. Gonzalez, M. A.; Gonzalez-Rey, E.; Rico, L.; Buscher, D.; Delgado, M. Treatment of experimental arthritis by inducing immune tolerance with human adipose-derived mesenchymal stem cells. Arthritis Rheum 60(4):1006-1019; 2009.
23. Goverman, J. Autoimmune T cell responses in the central nervous system. Nat Rev Immunol 9(6):393-407; 2009.
24. Gozes, I.; Divinsky, I.; Pilzer, I.; Fridkin, M.; Brenneman, D. E.; Spier, A. D. From vasoactive intestinal peptide (VIP) through activity-dependent neuroprotective protein (ADNP) to NAP: a view of neuroprotection and cell division. J Mol Neurosci 20(3):315-322; 2003.
25. Kavanagh, H.; Mahon, B. P. Allogeneic mesenchymal stem cells prevent allergic airway inflammation by inducing murine regulatory T cells. Allergy 66(4):523-531; 2011.
26. Kurozumi, K.; Nakamura, K.; Tamiya, T.; Kawano, Y.; Kobune, M.; Hirai, S.; Uchida, H.; Sasaki, K.; Ito, Y.; Kato, K.; Honmou, O.; Houkin, K.; Date, I.; Hamada, H. BDNF gene-modified mesenchymal stem cells promote functional recovery and reduce infarct size in the rat middle cerebral artery occlusion model. Mol Ther 9(2):189-197; 2004.
27. Liu, H.; Honmou, O.; Harada, K.; Nakamura, K.; Houkin, K.; Hamada, H.; Kocsis, J. D. Neuroprotection by PlGF gene-modified human mesenchymal stem cells after cerebral ischaemia. Brain 129(Pt 10):2734-2745; 2006.
28. Liu, X. J.; Zhang, J. F.; Sun, B.; Peng, H. S.; Kong, Q. F.; Bai, S. S.; Liu, Y. M.; Wang, G. Y.; Wang, J. H.; Li, H. L. Reciprocal effect of mesenchymal stem cell on experimental autoimmune encephalomyelitis is mediated by transforming growth factor-beta and interleukin-6. Clin Exp Immunol 158(1):37-44; 2009.
29. Lock, C.; Hermans, G.; Pedotti, R.; Brendolan, A.; Schadt, E.; Garren, H.; Langer-Gould, A.; Strober, S.; Cannella, B.; Allard, J.; Klonowski, P.; Austin, A.; Lad, N.; Kaminski, N.; Galli, S. J.; Oksenberg, J. R.; Raine, C. S.; Heller, R.; Steinman, L. Gene-microarray analysis of multiple sclerosis lesions yields new targets validated in autoimmune encephalomyelitis. Nat Med 8(5):500-508; 2002.
30. Manning, E.; Pham, S.; Li, S.; Vazquez-Padron, R. I.; Mathew, J.; Ruiz, P.; Salgar, S. K. Interleukin-10 delivery via mesenchymal stem cells: a novel gene therapy approach to prevent lung ischemia-reperfusion injury. Hum Gene Ther 21(6):713-727; 2010.

31. Mejia-Toiber, J.; Castillo, C. G.; Giordano, M. Strategies for the Development of Cell Lines for Ex Vivo Gene Therapy in the Central Nervous System. Cell Transplant. Epub ahead of print; Dec 22 2010.
32. Miyazaki, M.; Zuk, P. A.; Zou, J.; Yoon, S. H.; Wei, F.; Morishita, Y.; Sintuu, C.; Wang, J. C. Comparison of human mesenchymal stem cells derived from adipose tissue and bone marrow for ex vivo gene therapy in rat spinal fusion model. Spine (Phila Pa 1976) 33(8):863-869; 2008.
33. Myers, T. J.; Granero-Molto, F.; Longobardi, L.; Li, T.; Yan, Y.; Spagnoli, A. Mesenchymal stem cells at the intersection of cell and gene therapy. Expert Opin Biol Ther 10(12):1663-1679; 2010.
34. Ottaway, C. A. Selective effects of vasoactive intestinal peptide on the mitogenic response of murine T cells. Immunology 62(2):291-297; 1987.
35. Pagnotto, M. R.; Wang, Z.; Karpie, J. C.; Ferretti, M.; Xiao, X.; Chu, C. R. Adeno-associated viral gene transfer of transforming growth factor-beta1 to human mesenchymal stem cells improves cartilage repair. Gene Ther 14(10):804-813; 2007.
36. Palmer, G. D.; Steinert, A.; Pascher, A.; Gouze, E.; Gouze, J. N.; Betz, O.; Johnstone, B.; Evans, C. H.; Ghivizzani, S. C. Gene-induced chondrogenesis of primary mesenchymal stem cells in vitro. Mol Ther 12(2):219-228; 2005.
37. Pozo, D.; Anderson, P.; Gonzalez-Rey, E. Induction of alloantigen-specific human T regulatory cells by vasoactive intestinal peptide. J Immunol 183(7):4346-4359; 2009.
38. Prasse, A.; Zissel, G.; Lutzen, N.; Schupp, J.; Schmiedlin, R.; Gonzalez-Rey, E.; Rensing-Ehl, A.; Bacher, G.; Cavalli, V.; Bevec, D.; Delgado, M.; Muller-Quernheim, J. Inhaled vasoactive intestinal peptide exerts immunoregulatory effects in sarcoidosis. Am J Respir Crit Care Med 182(4):540-548; 2010.
39. Puissant, B.; Barreau, C.; Bourin, P.; Clavel, C.; Corre, J.; Bousquet, C.; Taureau, C.; Cousin, B.; Abbal, M.; Laharrague, P.; Penicaud, L.; Casteilla, L.; Blancher, A. Immunomodulatory effect of human adipose tissue-derived adult stem cells: comparison with bone marrow mesenchymal stem cells. Br J Haematol 129(1):118-129; 2005.
40. Rafei, M.; Campeau, P. M.; Aguilar-Mahecha, A.; Buchanan, M.; Williams, P.; Birman, E.; Yuan, S.; Young, Y. K.; Boivin, M. N.; Forner, K.; Basik, M.; Galipeau, J. Mesenchymal stromal cells ameliorate experimental autoimmune encephalomyelitis by inhibiting CD4 Th17 T cells in a CC chemokine ligand 2-dependent manner. J Immunol 182(10):5994-6002; 2009.
41. Rangon, C. M.; Dicou, E.; Goursaud, S.; Mounien, L.; Jegou, S.; Janet, T.; Muller, J. M.; Lelievre, V.; Gressens, P. Mechanisms of VIP-induced neuroprotection against neonatal excitotoxicity. Ann N Y Acad Sci 1070:512-517; 2006.
42. Sanberg, P. R.; Eve, D. J.; Willing, A. E.; Garbuzova-Davis, S.; Tan, J.; Sanberg, C. D.; Allickson, J. G.; Cruz, L. E.; Borlongan, C. V. The treatment of neurodegenerative disorders using umbilical cord blood and menstrual blood-derived stem cells. Cell Transplant 20(1):85-94; 2011.

43. Toscano, M. G.; Delgado, M.; Kong, W.; Martin, F.; Skarica, M.; Ganea, D. Dendritic cells transduced with lentiviral vectors expressing VIP differentiate into VIP-secreting tolerogenic-like DCs. Mol Ther 18(5):1035-1045; 2010.
44. Toyama, K.; Honmou, O.; Harada, K.; Suzuki, J.; Houkin, K.; Hamada, H.; Kocsis, J. D. Therapeutic benefits of angiogenetic gene-modified human mesenchymal stem cells after cerebral ischemia. Experimental neurology 216(1):47-55; 2009.
45. Uccelli, A.; Laroni, A.; Freedman, M. S. Mesenchymal stem cells for the treatment of multiple sclerosis and other neurological diseases. Lancet neurology 10(7):649-656; 2011.
46. Vesterinen, H. M.; Sena, E. S.; ffrench-Constant, C.; Williams, A.; Chandran, S.; Macleod, M. R. Improving the translational hit of experimental treatments in multiple sclerosis. Mult Scler 16(9):1044-1055; 2010.
47. Yagi, H.; Soto-Gutierrez, A.; Parekkadan, B.; Kitagawa, Y.; Tompkins, R. G.; Kobayashi, N.; Yarmush, M. L. Mesenchymal stem cells: Mechanisms of immunomodulation and homing. Cell Transplant 19(6):667-679; 2010.
48. Zappia, E.; Casazza, S.; Pedemonte, E.; Benvenuto, F.; Bonanni, I.; Gerdoni, E.; Giunti, D.; Ceravolo, A.; Cazzanti, F.; Frassoni, F.; Mancardi, G.; Uccelli, A. Mesenchymal stem cells ameliorate experimental autoimmune encephalomyelitis inducing T-cell anergy. Blood 106(5):1755-1761; 2005.
49. Zhang, W.; Yan, Q.; Zeng, Y. S.; Zhang, X. B.; Xiong, Y.; Wang, J. M.; Chen, S. J.; Li, Y.; Bruce, I. C.; Wu, W. Implantation of adult bone marrow-derived mesenchymal stem cells transfected with the neurotrophin-3 gene and pretreated with retinoic acid in completely transected spinal cord. Brain Res 1359:256-271; 2010.
50. Zhao, S.; Wehner, R.; Bornhauser, M.; Wassmuth, R.; Bachmann, M.; Schmitz, M. Immunomodulatory properties of mesenchymal stromal cells and their therapeutic consequences for immune-mediated disorders. Stem Cells Dev 19(5):607-614; 2010.

Supplementary Material

Figure S1. Diagram of the lentiviral vectors used in EAE treatment. Self-inactivated human immunodeficiency virus type 1-derived vectors expressing enhanced green fluorescent protein (LentiGFP) or vasoactive intestinal peptide (LentiVIP) has been previously described (12) . LTR=long terminal repeat; RRE= Rev-responsive element; cPPT=central polypurine tract; WPRE= woodchuck hepatitis posttranscriptional regulatory element.

Figure S2. Western blot analysis showed preproVIP protein in cell lysates of MSC/LentiVIP but not in non-transduced MSC.

Figure S3. Graph showing the concentration of VIP in supernatants of MSC, MSC/LentiVIP and MSC/LentiGFP.

Figure S4. Graph showing the surface expression levels of CD29, CD44, CD45, MHC-II and sca-1 in MSC, MSCLentiVIP and MSCLentiGFP. All cells were analyzed between 4-8 passages (n≥3).

Figure S5. Quantification of beta-tubulin, myelin, GFAP and beta-amyloid bodies at day 50 post-treatment. EAE mice with a clinical score of 3-3.5 were treated with MSC or MSC/LentiVIP or left untreated (Control EAE). 50 days later mice were sacrificed and the brains included in OCT resin. OCT-included brains were sectioned and stained for myelin, beta-tubulin, GFAP and beta-amyloid. Quantification was performed using the NIS-element BR 3.10 program (see materials and methods for details).

Supplementary Material and Methods

Detection of VIP protein by Western Blotting

MSC were lysed with 1% Nonidet P40 lysis buffer containing protease inhibitor cocktail (Sigma,St Louis, MO), resolved by sodium dodecyl sulphate polyacrylamide gel electrophoresis (15% polyacrylamide gels under reducing conditions), and electrotransferred to Hybond P polyvinylidene difluoride membranes (Amersham Biosciences,Little Chalfont, UK). Membranes were blocked with 5% nonfat milk and probed for 1 hour at room temperature with 2 μg/ml of anti-VIP monoclonal antibody (mAb) (clone H16; Santa Cruz Biotechnology, Santa Cruz, CA), and 0.05μg/ml anti-ERK polyclonal antibody (Upstate, Chicago, IL), followed by incubation with horseradish peroxidase–labelled goat anti-mouse antibody (1:10000 dilution, Caltag, Burlingame, CA). Analysis was performed using the ECL Advanced Western Blotting Detection Kit (Amersham Biosciences).

Figure Legends

Figure 1. Direct injection of Lentiviral particles expressing VIP has no effect on established EAE. Graph showing EAE progression after injection of 10^8 LentiVIP particles (filled squares) at peak of disease (3-3.5). Untreated mice (open squares) and mice treated with LentiGFP (open triangles) showed identical EAE progression, indicating the failure of LentiVIP administration for EAE therapy at this stage of disease. Data are shown as mean ± SEM. 10 animals per group.

Figure 2. LentiVIP-transduced mesenchymal stem cells (MSC/LentiVIP) stably express and secrete VIP and maintain the T cell inhibitory potential of non-transduced MSC. **a**) Analysis of VIP transgene expression over time in MSC/LentiVIP cell lines. MSC cell lines transduced with LentiVIP at high multiplicity of infection (MOI) (left panels) or low MOI (right panel) were analyzed with RT-Q-PCR at passages 5, 8 and 15 (5p, 8p and 15p respectively). Data represent arbitrary units relative to untransduced MSC. **b**) Graph showing stability of synthetic VIP peptide (left panels) versus MSC/LentiVIP-secreted VIP (right panels). VIP peptide (added to the conditioned medium of non transduced cells) (left panel) and conditioned medium of MSC/LentiVIP (right panel) were incubated at 37ºC for up to 48 hours. The concentration of VIP was measured at different time points by aVIP specific ELISA (Phoenix Pharmaceuticals). Data shown

are mean ± SEM. **c**) MSC/LentiVIP inhibit T cell proliferation at similar level to non-transduced MSC. Different numbers (0-40.000 cells) of irradiated MSC (diamonds), MSC/LentiVIP (squares) and MSC/LentiGFP (filled triangles) were added to a fixed amount (200000 cells) of concanavalin A (2.5 μg/ml) stimulated splenocytes. Proliferation was measured by thymidine incorporation (see materials and methods). (NS:snon stimulated splenocytes (open triangles).

Figure 3. Intraperitoneal administration of MSC/LentiVIP cells stops progression and reduce severity of EAE when administered at the peak of disease. a) Therapeutic effect of intraperitoneal administration of MSC/LentiVIP cells. MOG35-55 immunized mice were scored and stratified in 4 groups (untreated, MSC, MSC/LentiGFP and MSC/LentiVIP) of 10 animals per group with an average clinical score of 3±0.36. At this point 0,2 ml of PBS (open squares) or $1x10^6$ cells of MSC (filled squares), MSC/LentiGFP (open triangles) and MSC/LentiVIP (filled triangles) were inoculated intraperitoneally. After administration of the cells, the EAE clinical score were followed for over 50 days. Values are the mean ± SEM of 10 mice/group, **p<0.01, ***p<0.001. **b**) MSC/LentiVIP administration reduces MOG-specific T cell responses in DLN. Proliferation data are related to untreated controls. Cells were isolated from mice 4 (or 7 days?) days post-treatment and restimulated with MOG35-55 (50 μg/ml) or anti-CD3 (1 μg/ml). Values are expressed as mean ± SEM of 9 mice/group, *p<0.05. **c**) Graph showing percentage of CD4+Foxp3+ Tregs in spleen (left) and DLN (DLN, right) of untreated EAE mice (white bars), MSC-treated (gray bars) or MSC/LentiVIP-treated mice (Black bars). The percentages of CD4+Foxp3+ were analyzed

by flow cytometry as discussed in materials and methods section. Values are the mean ± SEM of 8 mice/group.

Figure 4. MSC- and MSC/LentiVIP- treated mice have reduced levels of proinflammatory cytokines and increased levels of neuroprotective factors in the CNS. RT-Q-PCRs were performed on RNA extracted from spinal cords of untreated mice (control, G3.5), MSC-treated (MSC) and MSC/lentiVIP-treated mice (MSC/LentiVIP) that were sacrificed seven days after treatment. Expression levels of pro-inflammatory (IL-17, TNF-alpha, IL-6) and anti-inflammatory cytokines (IL-10), Tregs (Foxp3+), oxidative burst (iNOS) and neuroprotective factors (ADNP and BDNF) were determined for all groups as described in materials and methods. Data are shown as mean ± SEM. (*p<0.05, ** p<0.01, ***p<0.001)

Figure 5. ***MSC/LentiVIP administration reduces astrogliosis and neurodegeneration in the CNS of EAE mice.*** EAE mice with a clinical score of 3-3.5 were treated with MSC or MSC/LentiVIP or left untreated (control EAE). Seven days later mice were sacrificed and the brains included in OCT resin. The brains were sectioned and stained for markers of astrogliosis (GFAP), macrophage/microglia (CD11b), neuronal degeneration (beta-amyloid) and neuronal markers (beta-Tubulin) as described in materials and methods. All samples were simultaneously stained with DAPI (blue) to visualize the cell nucleus. **a**) Representative images of the untreated (left column), MSC-treated (centre column) and

MSC/LentiVIP (right column) stained for the different markers (labels at the right) with phycoerythrin (PE), in red. **b**) Quantification of the signals obtained with the different markers (see materials and methods). (*p<0.05, ** p<0.01, ***p<0.001)

Tables

Table 1. LentiVIP transcripts are detected at the CNS of EAE mice only when MSC/LentiVIP are inoculated.

	Liver	Spleen	DLN	Brain	Spinal Cord	Kidney	Lung
LentiVIP particles	+	+	+	-	-	-	ND
MSC/LentiVIP cells	+	+	+	+	+	+	-

Presence (+) or absence (-) of VIP mRNA sequences derived from LentiVIP was determined using standard PCR techniques (see materials and methods). Mice were inoculated with 10^8 LentiVIP particles or 10^6 MSC/LentiVIP cells and sacrificed 7 days later for analysis. (ND= not determined).

Table 2. Summary of MSC/LentiVIP therapeutic efficiency compared to MSC and MSC/LentiGFP.

Day after treatment EAE Score	Day 0			Day 50			CDI (Cumulative Disease Index)
	mild	moderate	severe	mild	moderate	severe	
Untreated	30%	50%	20%	0%	20%	80%	245.45±60.31
MSC	20%	70%	10%	0%	0%	100%	226.25±64.65
MSC/LentiGFP	40%	50%	10%	30%	0%	70%	227.25±73.95
MSC/LentiVIP	30%	60%	10%	70%	20%	10%	130.75±32.32

EAE clinical scores were separated into mild (1-2.5), moderate (3-3.5) and severe (4-6). Day 0 represents the day of treatment. At day 0 EAE scores ranked from 2.5 to 4. All groups (untreated, MSC, MSC/LentiGFP and MSC/lentiVIP) had similar average score at day 0. CDI is equal to the sum of the daily disease scores from each animal over 50 days. Data are mean ± SEM (n=10).

Mesenchymal stem cells expressing vasoactive intestinal peptide ameliorate symptoms in a model of chronic multiple sclerosis.

Marién Cobo[1,*], Per Anderson[1,*], Karim Benabdellah[1], Miguel G. Toscano[1], Pilar Muñoz[1], Iván Gutierrez[2], Mario Delgado[3] and Francisco Martin[1,$].

[1] GENYO (Pfizer-University of Granada-Andalusian Government Centre for Genomics and Oncological Research), Avd de la Ilustración 114. Parque Tecnológico Salud (PTS), Granada 18007, Spain

[2] Biobanco. Parque Tecnológico Salud (PTS). Armilla 18100. Universidad de Granada, Spain

[3] IPB Lopez Neyra. CSIC. Parque Tecnológico Salud (PTS). Armilla 18100, Granada. Spain

* Authors share first authorship

[$] Correspondence should be addressed to F.M. (francisco.martin@genyo.es). GENYO (Pfizer-University of Granada-Andalusian Government Centre for Genomics and Oncological Research), Avd de la Ilustración 114. Parque Tecnológico Salud (PTS), Granada 18007, Spain. Telephone: 34958637103. FAX: 34958637071

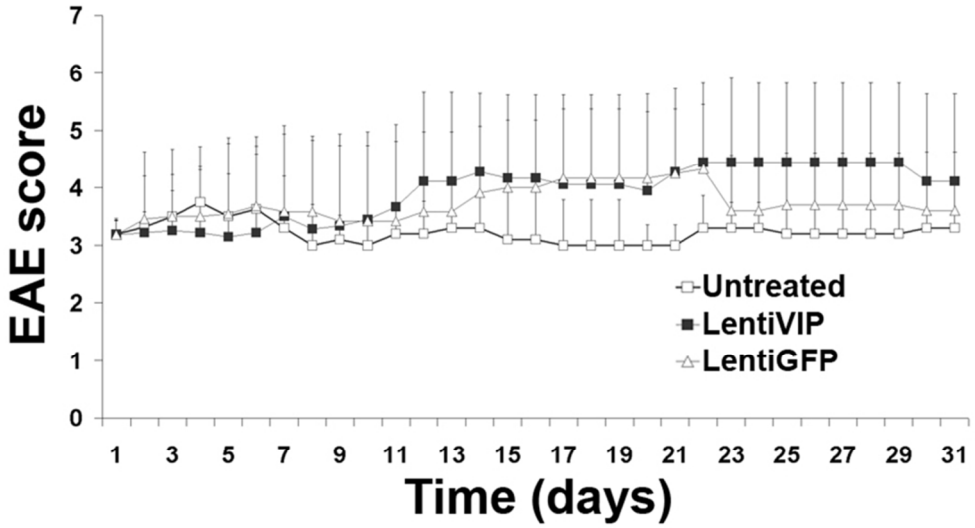

45x26mm (600 x 600 DPI)

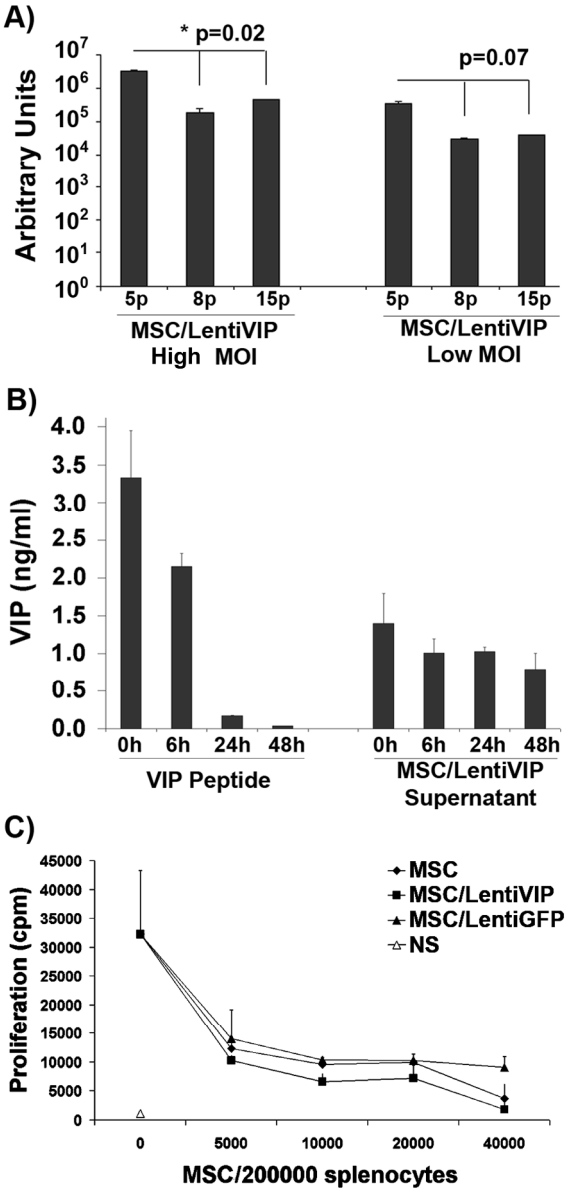

168x353mm (600 x 600 DPI)

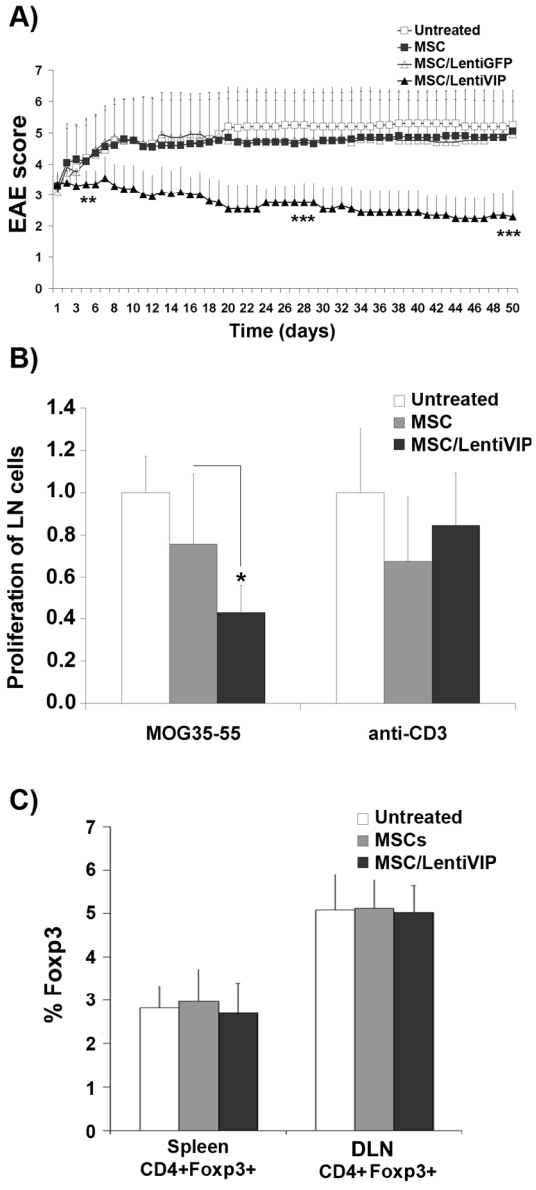

181x410mm (600 x 600 DPI)

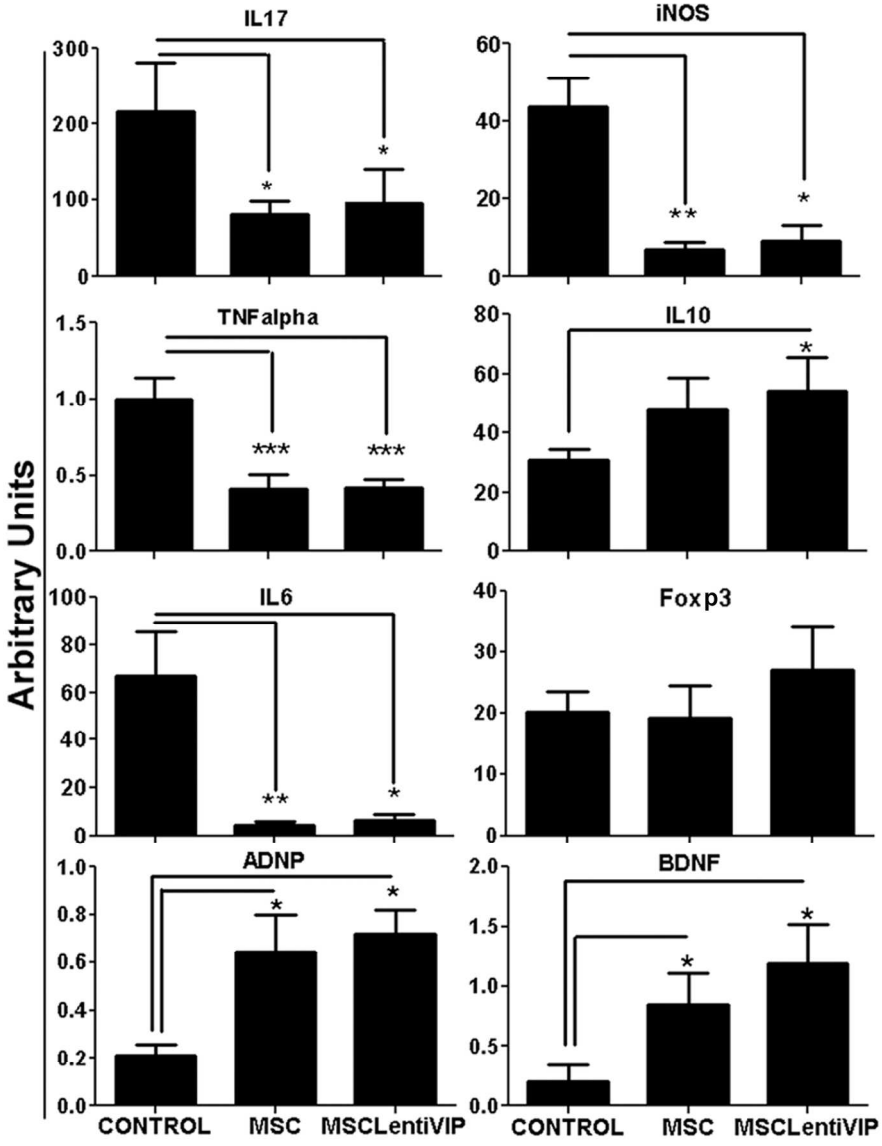

Figure 4
106x140mm (600 x 600 DPI)

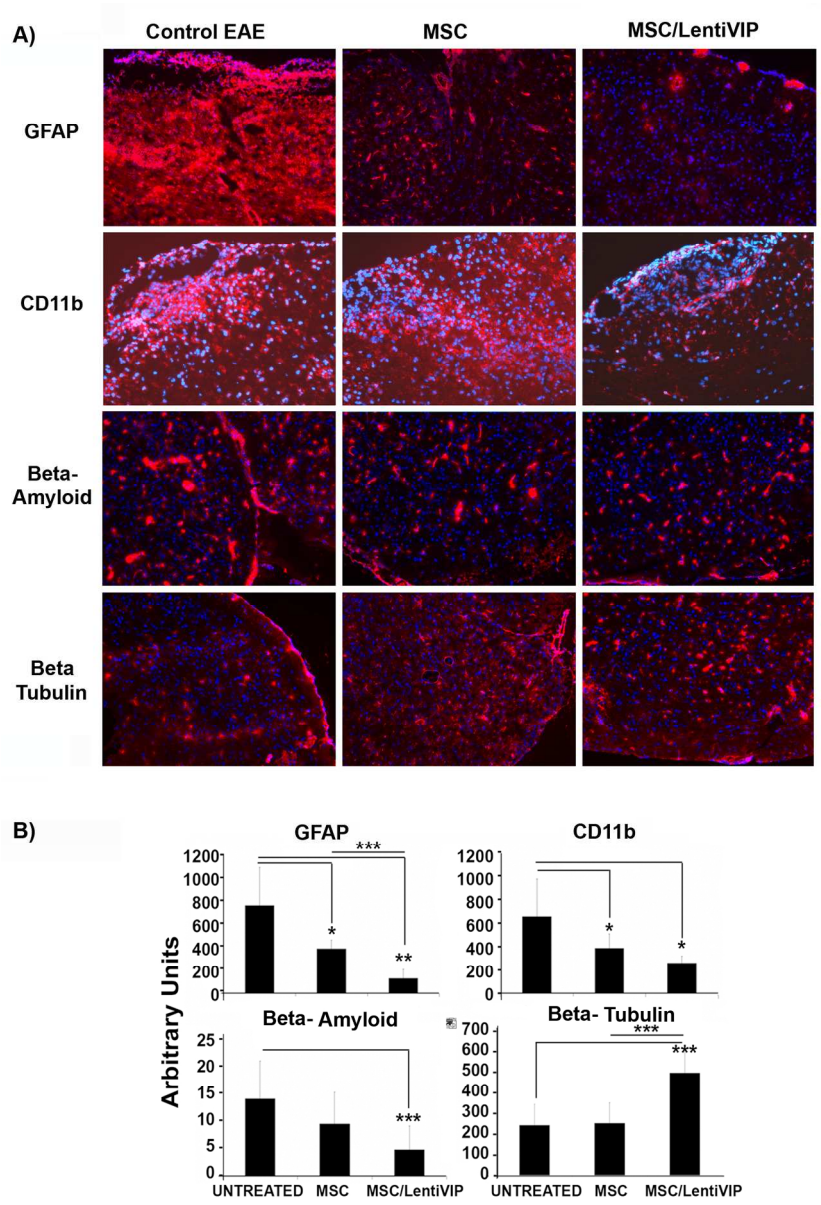

160x230mm (300 x 300 DPI)

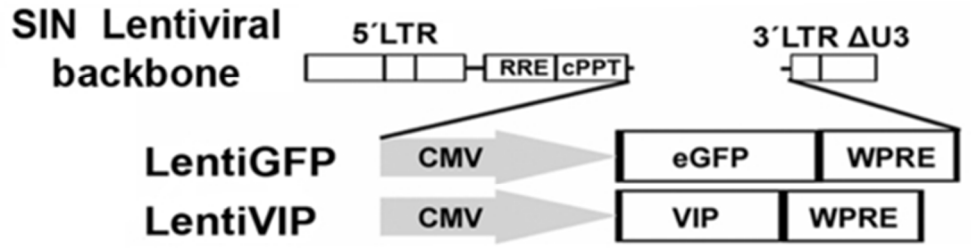

Supplementary Figure 1
22x7mm (600 x 600 DPI)

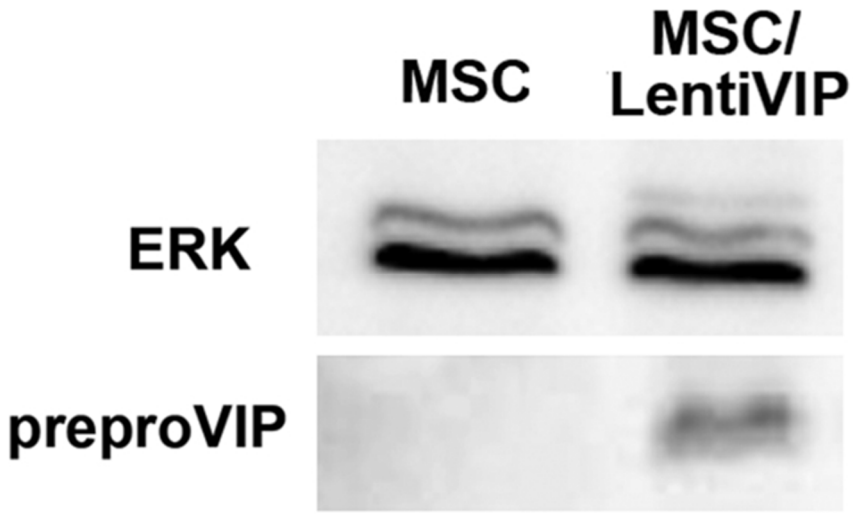

Supplementary Figure 2
32x19mm (600 x 600 DPI)

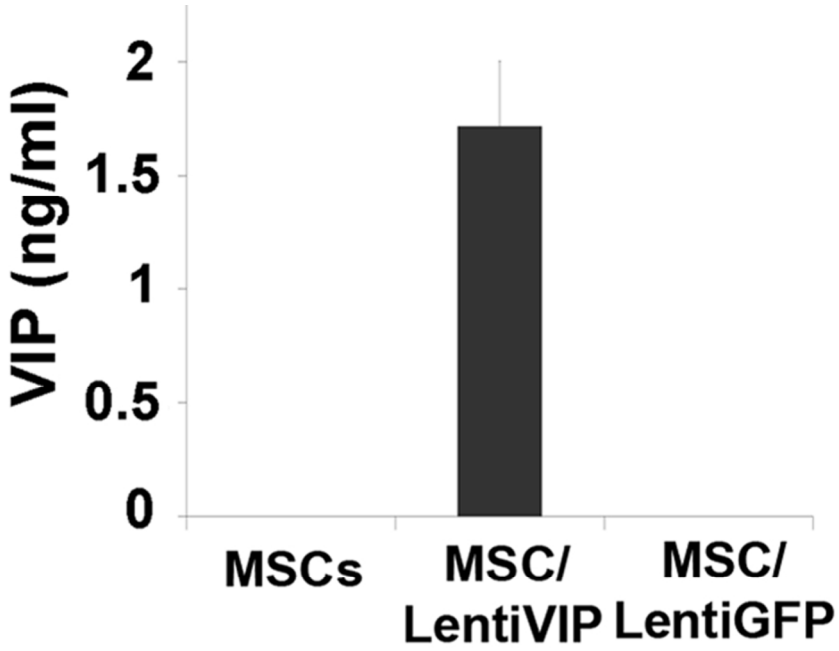

Supplementary Figure 3
53x35mm (600 x 600 DPI)

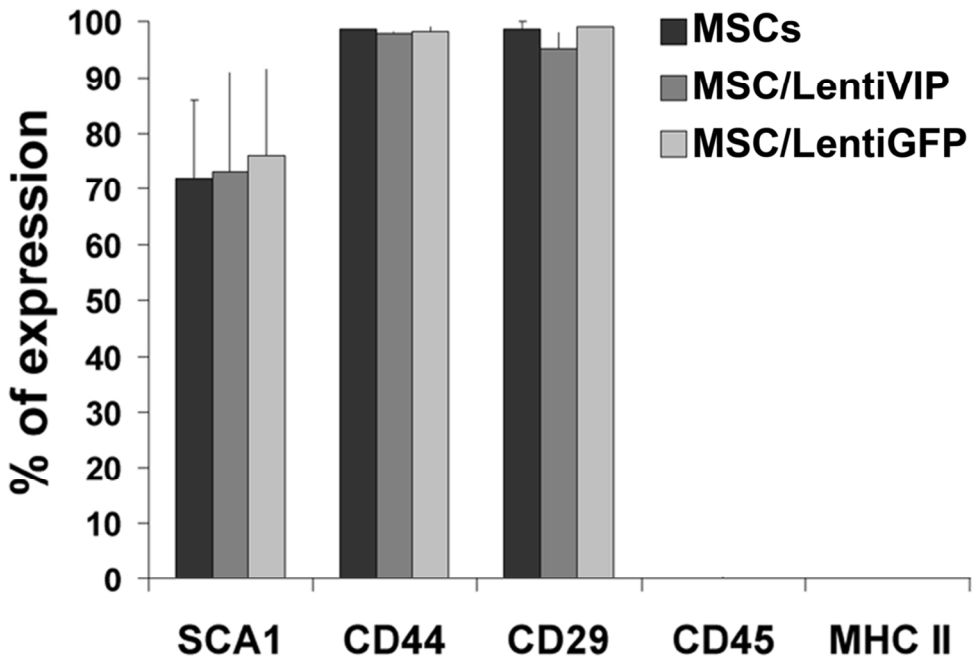

Supplementary Figure 4
55x38mm (600 x 600 DPI)

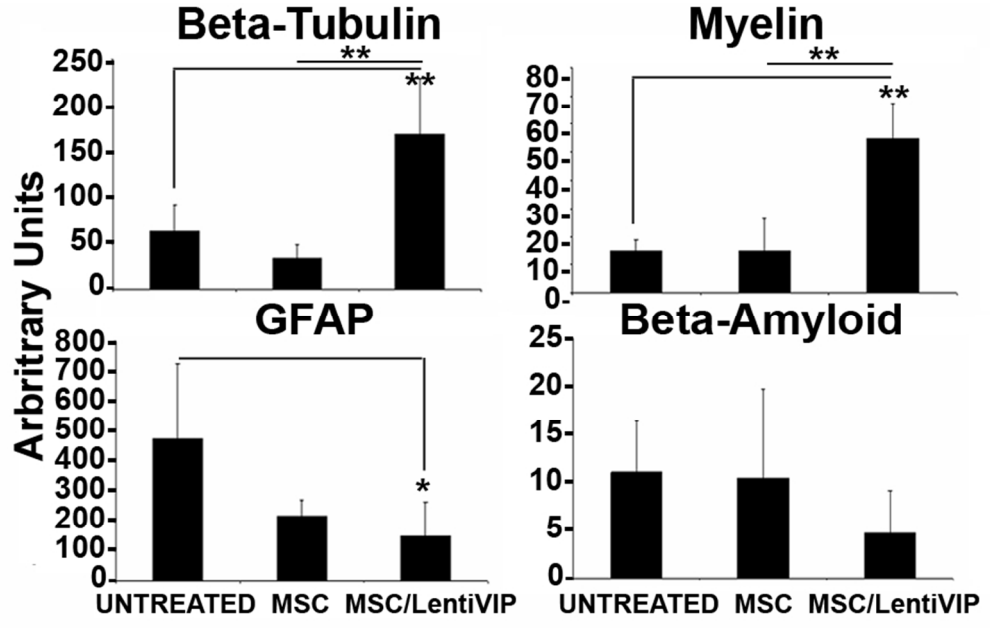

Supplementary Figure 5
80x50mm (300 x 300 DPI)